University of Alberta

From the basic understanding of N-myristoylation during apoptosis to a potential personalized medical treatment of B cell lymphomas

by

Conganige Maneka Perinpanayagam

A thesis submitted to the Faculty of Graduate Studies and Research

in partial fulfillment of the requirements for the degree of

Doctor of Philosophy

Department of Cell Biology

Fall 2013

Edmonton, Alberta

Dedication

For my daughter, Raya

May this remind you that none of your dreams are impossible to achieve.

Abstract

Myristoylation is a type of fatty acylation that involves the irreversible attachment of myristate (C14) to an amino-terminal glycine of a protein via an amide bond by N-myristoyltransferase (NMT). The two human N-myristoyltransferases (NMT1 and NMT2) typically play a pro-survival role in cells and their expression levels are increased in various cancers. Myristoylation occurs both co-translationally during protein synthesis and post-translationally during apoptosis. Our laboratory and others have identified several caspase-cleaved post-translationally myristoylated proteins during apoptosis and demonstrated the existence of numerous others. Hence, we hypothesized that myristoylation plays critical roles in both the survival and death of the cell by regulating apoptosis. Therefore, we were compelled to investigate the regulation of NMTs during apoptosis.

Herein, we demonstrate an elegant interplay between caspases and NMTs during apoptosis whereby caspases not only cleave substrates for post-translational myristoylation but also the NMTs themselves. Caspase-3 and -8 cleave NMT1 while only caspase-3 cleaves NMT2. Interestingly, the cleavages of NMTs did not abrogate their activity, actually caspase-cleavage increased NMT2 activity while that of NMT1 remained unchanged. Furthermore, the cleavages of the N-termini of both enzymes removed electrostatically charged domains resulting in a change of subcellular localization, potentially affecting NMTs' substrate

specificities as the cell switches from co- to post-translational myristoylation.

Our data and those of others suggest that NMTs are emerging as novel regulators of apoptosis. Because the regulation of the apoptotic process is usually defective in cancer cells, we further hypothesized that the regulation of the co- and post-translational myristoylation processes could also be defective in cancer cells. Our search for potential myristoylation “abnormalities” in cancer cells surprisingly revealed that NMT2 levels were down-regulated in Burkitt lymphomas, indicating that NMT2 could also play a pro-apoptotic role in hematologic cancers. We then exploited this unique molecular context by using low concentrations of a highly selective NMT inhibitor to preferentially kill malignant Burkitt lymphoma cells that only express one NMT (NMT1) and spare “normal” immortalized B lymphocytes that have both NMTs. This synthetically lethal approach could represent a novel personalized medical treatment option with minimized side-effects for lymphomas and perhaps other cancers devoid of NMT2.

Acknowledgements

I would like to express my gratitude to my supervisor, Luc, for giving me a chance and taking me into his lab, although I had no previous lab experience. I am grateful for everything he's taught me. In addition to that he's also been a good friend and supported me through every decision I made during my graduate studies.

I've been privileged to be a part of a great lab during my graduate studies. The Berthiaume lab has been my home away from home for many reasons and I'd like to thank everyone who contributed to the great dynamic that we had going on in the lab. First, I'd like to thank Dale Martin, an extremely smart previous graduate student, who took me under his wing and taught me so many lab techniques. He was a very good teacher and an even better friend. I am also indebted to "Super Megan" Yap, our lab technician, who offered a great deal of guidance when I was a newbie getting my hands wet in the lab. I thank her for being ever ready to help with my projects and for being one of my closest and most encouraging friends. I will miss her a great deal. I'd also like to thank Ryan Heit, who just knows everything. Ryan is an incredibly kind person and I value his advice and friendship through my grad school years. I'd like to thank Erwan Beauchamp, a previous post-doctoral fellow and a great friend, who was a part of the "NMT situation". I've learnt so much from him and I appreciate his help in my projects. I'd also like to thank past lab members, Aleksandra Janowicz (Ola), Veronic Provencher, Morris Kostiuk

and Greg Plummer for all their help during my time in the lab. Finally, I'd like to thank the best undergraduate student I've ever taught, Jacky Sim, who was incredibly helpful. He taught me patience and kept me laughing, even on the bad days, and I appreciate that.

I'd like to thank all the amazing people I met at the Department of Cell Biology. There are so many professors and students who have offered me a great deal of advice when I've run into problems with my projects and I'm grateful that I had such a great support system. I'd like to express my gratitude to the Cell Biology office staff, namely, Kendall, Claire, Blair, Sylvia, Nikki, Carl, Colleen and Deborah, who made my life in graduate school so much easier. I'd like to thank all the friends I've made here in Cell Biology, especially Sue-Ann, Bao, Alicia, Carolina, Valeria, Caro, Emily, Ola, Katie and Zackie, who have made my time in grad school truly memorable and fun.

I am indebted to my supervisory committee members, Dr. Shairaz Baksh and Dr. Thomas Simmen. They've always had my best interest at heart and helped direct my projects forward by offering great ideas and reagents. I'd also like thank Dr. John Mackey, Cheryl Santos and Dr. W. Dong at the Cross Cancer Institute who helped us a great deal with the Burkitt lymphoma project.

I'd like to thank my family here in Edmonton, especially Susan, who has been an incredible friend and kept my mental health in-check. I'd also like to thank Alora, who recently lost her battle to cancer but taught me to

“only fear a life unlived”. I thank her for helping me realize what is truly important in life.

I am thankful for having an amazing family and I’d especially like to thank my mother-in-law, Indri and my mom, who helped us out with Raya when I was busy finishing up my thesis work. I am deeply grateful for my brother Rehan and sister Shehara for always being encouraging and supportive. I especially thank my parents who have always been supportive of every dream I wanted to follow. They have sacrificed so much so that I could be where I am today, and I am so grateful for their love, support and encouragement.

I’d like to thank my beautiful daughter Raya for being so patient with me while I was busy with my thesis work. She is the light of my life and has made my life complete. She is my most challenging project and I am glad she’s mine. Finally, I am deeply grateful for my husband, Andrew. He decided to embark on this adventure with me almost 7 years ago and I know that I would not have completed this Ph.D. program if not for his love, understanding, encouragement and incredible patience. He has shared all the ups and downs of graduate school with me and supported me though it all. I’m really glad he’s mine too!

Table of Contents

CHAPTER 3 – Characterization of the roles of N-myristoytransferases in co- and post-translational myristoylation

List of Tables

List of Figures

List of Abbreviations

2-BP	2-bromo palmitate
^{3}H	Tritium
Abl	Abelson murine leukemia viral oncogene homolog 1
AID	Activation induced cytidine deaminase
AIDS	Acquired immunodeficiency syndrome
AIF	Apoptosis inducing factor
Ala	Alanine
ALCL	Anaplastic large cell lymphoma
Alk-C14	ω-alkynyl myristic acid
Apaf-1	Apoptosis protease activating factor-1
APT	Acyl protein thioesterase
Arf	ADP-ribosylation factor
ATCC	American type culture collection
Avr	Avirulence
Bcl-2	B cell lymphoma-2
Bid	BH3 interacting-domain death agonist
Bim	Bcl-2 interacting mediator of cell death
BL	Burkitt lymphoma
C8DN	Caspase 8 dominant negative
CaNMT	*Candida albicans* NMT
Caspases	Cysteine aspartyl proteases

CCLE	Cancer cell line encyclopedia
CD20	Cluster of differentiation 20
CDC42	Cell division control protein 42
CDC6	Cell division control protein 6
CD-IC2A	Cytoplasmic dynein-intermediate chain 2A
CRD	Cysteine rich domain
ct-	Caspase truncated
C-terminus	Carboxy-terminus
Cys	Cysteine
DD	Death domains
DED	Death effector domains
DISC	Death inducing signaling complex
DLBCL	Diffuse large B cell lymphoma
DNA	Deoxyribonucleic acid
EC_{50}	Half maximal effective concentration
EGF	Epidermal growth factor
EL	Extra-long
eNOS	Endothelial nitric oxide synthase
ER	Endoplasmic reticulum
Erk	Extracellular-signal-regulated kinases
FADD	Fas associated protein with death domain
FAK	Focal adhesion kinase
FL	Follicular lymphoma

FTase	Farnesyltransferase
FTI	Farnesyltransferase inhibitors
G2A	Glycine to Alanine
GAP-43	Growth associated protein 43
GFP	Green fluorescent protein
GGTase	Geranylgeranyltransferase
GH	Growth hormone
GHS-R	G-protein coupled growth hormone secretagogue receptor
Gln	Glutamine
Gly	Glycine
GNAT	Gcn5-related N-acetyltransferases
GOAT	Ghrelin O-acyltransferase
GPI	Glycophosphatidylinositol
G-proteins	Guanosine nucleotide-binding proteins
HAT	Histone acetylase
HDAC	Histone deacetylase
HDACi	Histone deacetylase inhibitor
Hh	Hedgehog
His	Hexa his
HIV-1	Human immunodeficiency virus-1
HL	Hodgkin’s lymphoma
HMA	2-hydroxy myristic acid

hNMT	Human NMT
HSC70	Heat shock cognate protein 70
Htt	Huntingtin
IAP	Inhibitors of apoptosis
IC_{50}	Inhibitory concentration 50
ICAD	Inhibitor of caspase activated DNAse
Ig	Immunoglobulin
IHC	Immunohistochemistry
IPP	Isopentenydiphosphate
JNK	c-Jun N-terminal kinase
K-box	Lysine box
Leu	Leucine
MACF1	Microtubule actin cross-linking factor 1
MAPK	Mitogen-activated protein kinases
MARCKS	Myristoylated alanine rich C kinase
MBOAT	Membrane bound O-Acyl transferase
MEKK	Mitogen activate protein kinase kinase kinase
Met	Methionine
MetAP	Methionine aminopeptidase
Mst-1	Macrophage stimulating-1
MVA	Mevalonate
MW	Molecular weight
Myristoylome	Myristoylated proteome

NCBI	National Center for Biotechnology Information
NHL	Non-hodgkin’s lymphoma
NIP71	NMT inhibitor protein 71
NK	Natural killer
NMT	N-myristoyltransferase
NOD	Non-obese diabetic
NSG	NOD *scid* gamma
N-terminus	Amino-terminus
P_{100}	Membrane fraction
PAK2	p21 activated kinase 2
PARP-1	Poly(ADP-ribose) polymerase 1
PAT	Protein acyl transferase
PDX	Patient derived xenograft
Phe	Phenylalanine
PKA	Protein kinase A
PKC	Protein kinase C
PM	Plasma membrane
PNS	Post-nuclear supernatant
qRT-PCR	Quantitative reverse transcriptase polymerase chain reaction
Rac	Ras-related C3 botulinum toxin substrate
REP	Rab escort proteins
RGGTase	Rab geranylgeranyltransferase

RIP	Receptor interaction protein kinase
RSV	Rous sarcoma virus
S_{100}	Cytosolic fraction
S2G	Serine to glycine
SAHA	Suberoylanilide hydroxamic acid
SCID	Severe Combined Immunodeficiency
ScNMT	*Saccharomyces cerevisiae* NMT
Ser	Serine
SMAC	Second mitochondria derived activator of caspases
STS	Staurosporine
Tb NMT	*Trypanosoma brucei* NMT
Thr	Threonine
TNFR-1	Tumor necrosis factor receptor-1
TNFα	Tumor necrosis factor α
TRAMPP	Tandem reporter assay for the identification of myristoylated proteins post-translationally
Tris DBA	Tris(dibenzylideneacetone)dipalladium
UV	Ultra-violet
WB	Western blotting
YTHDF2	YTH domain family protein 2
z-DHHC	(z)Asp-His-His-Cys

Chapter 1

Introduction

1.1 Protein Lipidation – Modification of Proteins with Lipids

Protein lipidation is an important type of post-translational modification that is essential for directing a host of cellular proteins to their various subcellular membranes and membrane compartments. There are hundreds of proteins which have been demonstrated to be covalently modified by a variety of lipid groups. Protein lipidation plays key roles in signal transduction, protein trafficking and protein-protein interactions. It is therefore vital for the proper functioning and survival of the cell. There are four main types of protein lipidation; namely, cholesteroylation, isoprenylation, glypiation and fatty acylation which will be discussed in detail below.

1.1.1 Cholesteroylation

Cholesteroylation is an autocatalytic process which leads to the attachment of cholesterol to a protein. Hedgehog (Hh) proteins which are essential for embryonic patterning and development are the only known proteins to undergo cholesteroylation to date (Mann and Beachy, 2004). Once the Hh precursor peptide enters the lumen of the endoplasmic reticulum (ER), an internal cholesterol-dependent autocatalytic processing reaction that results in a cleavage between conserved Gly-Cys residues takes place (Mann and Beachy, 2004). Next, a cholesterol adduct is formed at the carboxy(C)-terminal end of the amino(N)-terminal product (Hh-N), which results in the internal cleavage of the cholesteroylated protein from the catalytic domain (Porter et al., 1996; Ryan and Chiang, 2012). This N-terminal fragment is further modified in the secretory pathway by the attachment of a palmitate group to the N-terminal cysteine via an amide bond, which results in the fully processed mature Hh protein that is active in signaling (Mann and Beachy, 2004; Buglino and Resh, 2008; Ryan and Chiang, 2012). Recently, a chemical probe that enables the bioorthogonal tagging of cholesteroylated proteins in live cells was developed and it could be used to identify *de novo* cholesteroylated proteins (Heal et al., 2011).

1.1.2 Isoprenylation

Protein isoprenylation is the post-translational attachment of either a 15-carbon (farnesyl) or 20-carbon (geranylgeranyl) isoprenoid to the cysteine residues at or near the C-terminus of a protein. Isoprenoids are derived from the five-carbon (C_5) unit of isopentenyl diphosphate (IPP), which are synthesized through the mevalonate (MVA) pathway in animals and are essential intermediates in cholesterol synthesis (McTaggart, 2006). In isoprenylation, an isoprenoid (farnesyl or geranylgeranyl) is linked to a protein via a thioether bond to one or more cysteine residues located at or near the C-terminus of the protein (Resh, 2006).

Many of the prenylated proteins have a signature 'CAAX' (Cys-aliphatic-aliphatic-X) box located on their C-terminus and the 'X' determines whether the cysteine located within the CAAX box is farnesylated by farnesyltransferase (FTase) (if X is Ala, Ser, Cys, Met or Gln) or geranylgeranylated by geranylgeranyltransferase I (GGTase-I) (if X is Leu or Phe) (Maurer-Stroh and Eisenhaber, 2005; Hannoush and Sun, 2010). FTase and GGTase-I are characterized as enzymes which are heterodimers that share an α-subunit but have distinct β-subunits (Zhang and Casey, 1996) .

Once a protein is isoprenylated, the AAX residues are proteolytically removed by the endoprotease Ras converting enzyme 1 (Rce-1), and the resulting α-carboxyl group on the C-terminal prenylated

cysteine is carboxymethylated by the *s*-adenosylmethionine-dependent protein carboxymethyltransferase in the ER (McTaggart, 2006; Resh, 2006).

GGTase-1 substrates include the small GTPases Rac1, Rho A, Rho B and CDC42 (Roskoski, 2003). Interestingly, the gernaylgeranylation of Rab GTPase protein family, which are involved in vesicular trafficking are performed by GGTase-II (also known as RGGTase), in the presence of Rab escort proteins (REP) (Gutkowska and Swiezewska, 2012). In this case, RGGTase, which is exclusively responsible for the isoprenylation of Rab GTPases, recognizes the following motifs –CXCX, -CCXX or –XXCC (Gutkowska and Swiezewska, 2012). Hence, Rab proteins are dually geranylgeranylated and this regulates their role in membrane trafficking (Gutkowska and Swiezewska, 2012). Conversely, Rabs that fail to undergo geranylgeranylation are localized in the cytosol and are unable to perform their normal functions including vesicle budding, transport and fusion (Gutkowska and Swiezewska, 2012).

Some examples of farnesylated proteins are the proto-oncogenic Ras family of GTPases (H-Ras, K-Ras and N-Ras) and RhoB GTPase as well as the nuclear lamins (Lamin A and B) (Resh, 1996; Novelli and D'Apice, 2012). Notably, the potential of the inhibition of protein prenylation has been investigated by some researchers as a strategy for developing novel chemotherapies as the oncogenic Ras proteins require farnesylation for their proper biological function (Berndt et al., 2011).

Although farnesyltransferase inhibitors (FTIs) seemed promising at first because of their low toxicity, obtaining clinical efficacy has been an issue, potentially because GGTase-I can compensate for the loss of FTase with FTIs (Zverina et al., 2012). However, depleting levels of both FTase and GGTase by genetically knocking out the enzymes or inhibiting both prenylating activities by FTase and GGTase inhibitors has proven to be a more promising therapeutic approach to treat various cancers (Liu et al., 2010; Sjogren et al., 2011; Morgan et al., 2012).

1.1.3 Glypiation

Glypiation is characterized as the post-translational addition of a glycosylphosphatidylinositol (GPI) anchor to the C-terminus of proteins in the lumen of the ER and this modification anchors the glypiated protein to the outer leaflet of the plasma membrane in the cell. The structure of the GPI anchor is more complex in nature as it contains a phosphoethanolamine linker, glycan core and a phospholipid tail (Paulick and Bertozzi, 2008). The attachment of the GPI anchor to proteins is facilitated by GPI-transamidase, which cleaves the peptide bond at the GPI-anchor attachment site (ω site), found at the C-terminal end of select proteins, and attaches the GPI to the newly generated carboxyl group at the C-terminus of the cleaved protein by an amide bond (Mayor and Riezman, 2004). One of the most interesting features of the GPI anchored

proteins is that they are functionally diverse and have roles in signal transduction, immune response and cancer progression (Tsai et al., 2012).

1.1.4. Fatty Acylation – The modification of proteins with fatty acids

Fatty acylation describes the covalent attachment of the saturated 14-carbon (C14) myristic acid (myristoylation) or 16-carbon (C16) palmitic acid (palmitoylation) to proteins. While some proteins are modified by either myristate or palmitate alone, there are others which are modified by both types of modifications. These modifications are further described in the sections below. The key features of palmitoylation and myristoylation are highlighted in **table 1.1**. It is important to note that there are rare types of fatty acylation which are further described in the section entitled atypical fatty acylation.

	Palmitoylation	Myristoylation
Fatty Acid	C-16	C-14
Modification	Post-translational	Co-translational Post-translational (during apoptosis)
Linkage	Thioester (dynamic)	Amide (stable)
Enzyme	Palmitoyl-Acyltransferases (zDHHC-CRD PAT, MBOAT)	N-myristoyltransferase (NMT1, NMT2)
Modified Residue	Cysteine	Glycine (Amino-terminal)
Examples	H-Ras, N-Ras, Wnt Proteins	Src family kinases HIV-1 Gag

Table 1.1: Comparison of key features of palmitoylation and myristoylation. (zDHHC-CRD PAT: (z)Asp-His-His-Cys-cysteine rich domain protein acyl transferase, MBOAT: Membrane bound O-acyl transferase)

1.1.4.1 S-Palmitoylation and N-Palmitoylation

S-Palmitoylation or palmitoylation generally refers to the attachment of a palmitoyl moiety to one or more cysteine residues within a protein via a reversible thioester bond. This reaction is known to occur post-translationally. Palmitoylation is the general term that is commonly used to define S-acylation, because other medium- and long-chain fatty acids could also be attached to “palmitoylated” proteins such as growth associated protein-43 (GAP-43) and Fyn (Liang et al., 2002; Liang et al., 2004). Because palmitic acid is the most abundant fatty acid in cells and is the most frequently found attached to cysteine residues of proteins, the term palmitoylation is routinely and preferentially used in the literature.

It is known that palmitic acid attached to proteins usually have a short turnover rate on most proteins (Fukata and Fukata, 2010). Various extracellular signals regulate the palmitoylation–depalmitoylation cycles and allows proteins to shuttle between various subcellular compartments; indeed, proteins such as H-Ras and N-Ras shuttle between the plasma membrane and the Golgi by employing the palmitoylation–depalmitoylation cycle (Rocks et al., 2005; Fukata and Fukata, 2010).

Palmitoylation plays diverse roles in the cellular environment such as membrane association, trafficking of palmitoylated proteins from the secretory pathway to the plasma membrane and even facilitating the direct targeting of certain lipidated proteins to plasma membrane or plasma membrane subdomains such as lipid rafts (Smotrys and Linder, 2004).

The discovery that palmitoylation can occur spontaneously when a palmitoyl group is attached to peptides and proteins via a thioester bond *in vitro* at a neutral pH in the presence of palmitoyl-CoA, lead to the suggestion that palmitoylation occurs via a non-enzymatic mechanism *in vivo* (Mitchell et al., 2006). This concept was challenged with the discovery that *Saccharomyces cerevisiae* Ras2 was palmitoylated by the Ras protein acyltransferase complex, Erf2-Erf4 (Lobo et al., 2002). Since then two classes of enzymes that are responsible for the palmitoylation of proteins have been identified; namely the zinc-finger-like (z)-Asp-His-His-Cys-cysteine rich domain (CRD) protein acyltransferases (PAT) (z-DHHC-CRD PATs) and the membrane bound O-acyltransferases (MBOATs).

There are 23 human z-DHHC-PATs which are encoded by the *zDHHC* genes that have been identified (Korycka et al., 2012). In addition to having DHHC-cysteine rich domain, these multi-pass proteins have four to six transmembrane domains and a majority of these enzymes localize to the Golgi apparatus and/or ER, whereas a few localize to the plasma membrane (Ohno et al., 2006; Greaves and Chamberlain, 2011; Korycka et al., 2012). One of the more commonly used chemical inhibitors of palmitoylation is the palmitate analog, 2-bromopalmitate (2-BP), which typically acts as a broad inhibitor of palmitate incorporation, but does not appear to selectively inhibit the palmitoylation of specific palmitoylation substrates (Webb et al., 2000; Draper and Smith, 2009).

Acyl-protein thioesterase 1 (APT1) is the first de-palmitoylating enzyme that was identified and it could remove the palmitoyl group in proteins such as Giα proteins, H-Ras and eNOS *in vivo* (Smotrys and Linder, 2004; Dekker et al., 2010). More recently, APT2 was identified as the depalmitoylating enzyme involved in the palmitoylation/depalmitoylation cycle of GAP-43, hence, affecting its subcellular distribution (Tomatis et al., 2010). Recently, the small-molecule APT1 inhibitor palmostatin B was found to perturb the acylation cycle at the level of depalmitoylation and therefore affect the epidermal growth factor (EGF)-induced Ras activity (Dekker et al., 2010). Additionally, palmostatin B was also shown to cause partial phenotypic reversion of the oncogenic HRasG12V-transformed fibroblasts (Dekker et al., 2010).

N-palmitoylation occurs when proteins are linked to palmitate by an amide bond and this reaction is catalyzed by MBOATs (Resh, 2006). Interestingly, MBOATs are also multi-pass membrane proteins which are responsible for the palmitoylation of the secreted proteins Hh, Spitz and Wnt (Resh, 2006; Buglino and Resh, 2012).

1.1.4.2 Atypical fatty acylation

In addition to palmitoylation and myristoylation, other forms of fatty acylation have also been reported; the term ‘atypical fatty acylation’ is used to describe these additional forms.

One such protein that is atypically fatty acylated is ghrelin, a ligand that binds to the G protein coupled growth hormone secretagogue receptor (GHS-R), that is responsible for regulating the release of growth hormone (GH) from the pituitary gland (Kojima et al., 1999). Kojima et al. describe ghrelin to be n-octanoylated on the Ser3 residue and acylation of ghrelin is required for GH release, both *in vitro* and *in vivo* (Kojima et al., 1999). Recently, ghrelin O-acyltransferase (GOAT) which belongs to the MBOAT family of acyltransferases, was identified as enzyme that facilitates the octanoylation of Ghrelin (Yang et al., 2008). Ghrelin has gained much attention in the recent years for its implications as an appetite stimulant and its role in promoting weight gain, regulating glucose metabolism and insulin secretion (Al Massadi et al., 2011).

The Wnt family of secreted proteins plays a major role in embroyogenesis and cancer, and Wnt is known to be palmitoylated at a conserved cysteine residue. Wnt-3a is further modified by the attachment of monosaturated palmitoleic acid at a conserved serine residue (Ser209), and it is evident that this type of acylation is required for its secretion (Takada et al., 2006). Furthermore, oleic acid was shown to be attached to

a lysine residue of the lens membrane protein, Aquaporin 0, by an amide bond, and this modification is thought to play a role in targeting this protein to the lipid rafts (Schey et al., 2010).

1.1.4.3 N-myristoylation

N-myristoylation refers to the irreversible attachment of myristic acid (C14) to the amino-terminal glycine residue of a protein via an amide bond and this reaction is catalyzed by N-myristoyltransferase (NMT) (Boutin, 1997). The saturated 14-carbon myristic acid is considered to be a rare fatty acid in living matter and represents less than 1% of total fatty acids present in cells (Boutin, 1997). Previously, it was approximated that 0.5% of all eukaryotic proteins are myristoylated (Maurer-Stroh et al., 2002b; Maurer-Stroh et al., 2002a). Recent work by Utsumi's group using a cell-free assay demonstrated that 1.4% proteins of 1929 proteins queried were myristoylated, indicating that the myristoylome (proteome of myristoylated proteins) may be larger than previously predicted (Suzuki et al., 2010). Myristoylation was first discovered when an unusual N-terminal blocking group prevented the sequencing of the catalytic subunit of bovine cardiac muscle cyclic AMP-dependent protein kinase by Edman degradation, and later this blocking group was identified as an amide-linked myristic acid by mass spectrometry (Carr et al., 1982). Soon after, Aitken et al. reported that the N-terminal blocking group of the Ca^{2+}- binding β-subunit of calcineurin

was also myristic acid that was attached to the N-terminal glycine of the calcineurin B via an amide bond (Aitken et al., 1982). Furthermore, myristic acid was shown to be attached to the very first oncoprotein identified, $p60^{v\text{-}src}$, the transforming protein of the Rous sarcoma virus (RSV) and $p60^{c\text{-}src}$, it's cellular homolog (Buss et al., 1984).

Although myristoylation often occurs on the N-terminal glycine residues of proteins, there has been reports of myristic acid being attached to lysine residues through an amide bond (Lin et al., 2012). These include the insulin receptor, TNFα and interleukin-1α (Hedo et al., 1987; Stevenson et al., 1992; Stevenson et al., 1993; Lin et al., 2012). However, the enzyme that facilitates lysine myristoylation has not been identified to date.

It has been determined that the binding energy required for a myristoylated peptide to bind the phospholipid bilayer (K_d = ~10^{-4}M) is insufficient to provide stable membrane anchoring (Peitzsch and McLaughlin, 1993; Resh, 2006). For myristoylated proteins to achieve stable membrane binding, they require a second signal in the form of a palmitoylated cysteine residue or a polybasic domain, this forms the basis of the "two-signal" hypothesis (Peitzsch and McLaughlin, 1993; Resh, 2006). Many myristoylated proteins such as Src family kinases (including Fyn, Lck, Yes), endothelial nitric oxide synthase (eNOS) and Gα subunits of the heteromeric guanine nucleotide binding proteins (G proteins) use a myristate and a palmitate modification for stable membrane anchoring (Resh, 2006). In addition, Src, myristoylated alanine-rich C kinase substrate (MARCKS) and

retroviral Gag proteins utilize a myristoyl group together with a polybasic amino acid cluster which attach to the negatively charged plasma membrane, to confer stable membrane attachment (Resh, 2006). Of note, some prenylated proteins also adhere to the "two-signal" hypothesis when forming stable membrane attachments [i.e. N-and H-Ras (palmitoyl + isoprenyl moieties) as well as K-Ras 4B and Lamin B3 (polybasic domain and isoprenyl moiety)] (Resh, 2006).

Structural studies have demonstrated that certain myristoylated proteins can have two distinct conformations; one conformation exposes the myristoyl moiety and promotes membrane interactions and the other sequesters the myristoyl moiety inside a hydrophobic binding pocket within the myristoylated protein (Resh, 2006). This phenomenon is referred to as a 'myristoyl switch' and is usually triggered by ligand binding, which induces a conformational change that causes the myristoyl group to flip outside the myristoyl binding pocket and promote membrane binding (**Fig. 1.1**). Conversely, upon loss of the ligand, the myristoyl-moiety returns to the hydrophobic binding pocket and the protein is released from the membrane (Resh, 2006). Some myristoylated proteins that utilize the 'myristoyl switch' mechanism are recoverin (neuronal calcium binding protein primarily found in the photoreceptor cells in the eye), Arf, c-Abl and the PKA catalytic subunit (Resh, 2006).

A variation of the 'myristoyl switch' proteins is referred to as the 'myristoyl-electrostatic' switch. MARCKS is a classic example of such a

protein, as the phosphorylation of the myristoylated MARCKS protein by protein kinase C (PKC) imparts a negative charge within the positively charged polybasic cluster, and reduces its electrostatic attraction to the negatively charged inner leaflet of the plasma membrane (McLaughlin and Aderem, 1995; Resh, 2006). Hence, phosphorylation causes the release of myristoylated MARCKS from the plasma membrane (**Fig. 1.1**).

Furthermore, by using green fluorescent protein (GFP) tagged with various fatty acylated N-terminal sequences, our lab demonstrated that myristoylation plays a key role in differential targeting of proteins to various subcellular membranes, including the targeting of certain proteins to sub-membrane domains commonly referred to as lipid rafts (McCabe and Berthiaume, 1999; McCabe and Berthiaume, 2001). One of our most important findings was that myristoylation was sufficient by itself to exclude GFP from the nucleus and associate with intracellular membranes such as endosomes and ER, however, plasma membrane localization required a second signal in the form of a palmitoylated cysteine residue or a polybasic domain (McCabe and Berthiaume, 1999).

Historically, myristoylation was known as a strictly co-translational process (Wilcox et al., 1987; Deichaite et al., 1988), but myristoylation is now known to occur either co-translationally during protein synthesis or post-translationally after caspase-cleavage during apoptosis (**Fig. 1.2**).

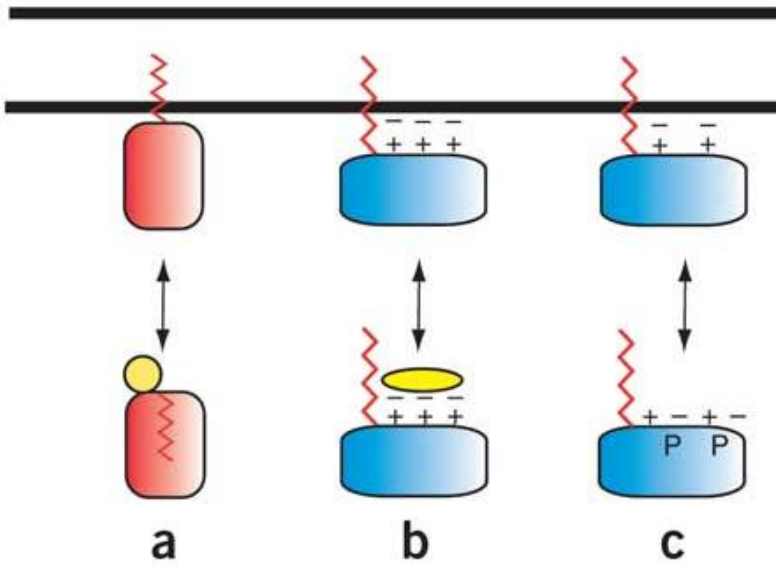

Figure 1.1: Three different strategies for lipidated proteins to associate and dissociate from a lipid bilayer. Fatty acyl groups are red. (**a**) A myristoyl switch is induced by the binding of a ligand (yellow) to an N-myristoylated protein (red). (**b**) An electrostatic switch is induced by the binding of a ligand (yellow) to the basic motif of a myristate + basic–containing protein (blue) (**c**) An electrostatic switch is also induced by the phosphorylation within the basic motif. **[Modified from (Resh, 2006)]**

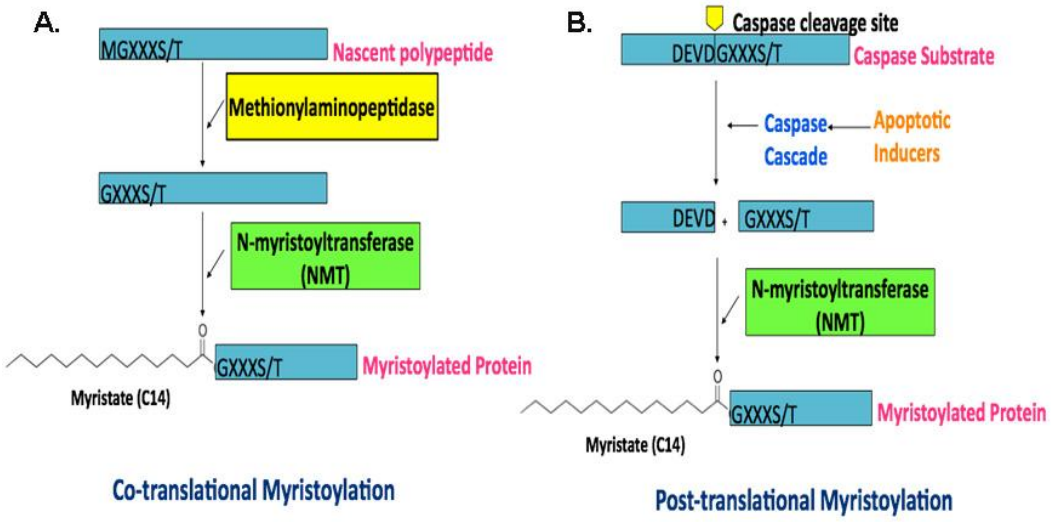

Figure 1.2: Co- and Post- translational myristoylation of proteins. Myristoylation involves the addition of the 14-carbon fatty acid myristate to the amino terminal glycine of a protein via an amide bond. **A. *Co-translational myristoylation*** proceeds when the initiatior methionine of a nascent polypeptide is removed by methionlyaminopeptidase. Whereas, **B. *Post-translational myristoylation*** occurs when the caspase cleavage of a protein during apoptosis reveals an amino-terminal glycine with a myristoylation consensus sequence. Both forms of myristoylation are catalyzed by the action of N-myristoyltransferases (NMTs)**.**

1.1.4.3.1 Co-translational myristoylation of nascent proteins

Wilcox et al. first identified that myristoylation occurred co-translationally on nascent polypeptides and this was confirmed by another group (Deichaite et al., 1988) who added that their data suggested that the myristoylation of proteins occured even before the first 100 amino acids of the nascent polypeptide were polymerized (Wilcox et al., 1987; Deichaite et al., 1988). Co-translational myristoylation occurs upon the cleavage of the initiator methionine on the nascent polypeptide by methionine aminopeptidase (MetAP) and the exposure of the N-terminal glycine residue part of a myristoylation consensus sequence (discussed in NMT section). Next, the polypeptide with an exposed glycine residue is subjected to the action of NMT, which catalyses the transfer of a myristoyl moiety from myristoyl-CoA to the glycine residue resulting in the formation a stable amide bond (**Fig. 1.2**) (Martin et al., 2011).

Notably, the cleavage of the initiator methionine is a common modification in many proteins, as it occurs in up to 80% of proteins present in cells (Matheson et al., 1975; Martin et al., 2011). Interestingly, a study on *Escherichia coli* (*E.coli*) MetAP-1 substrate specificity revealed that the MetAP-1 catalysis was more efficient when glycine followed the initiator methionine in the amino acid sequence (Frottin et al., 2006). There are many co-translationally myristoylated proteins which have been identified

and characterized. Among them, perhaps the most studied myristoylated protein is the Src tyrosine kinase.

The RSV was found to transform cultured chicken embryo fibroblasts in to tumors in chickens as a result of the expression of the *src* gene ($p60^{v\text{-}src}$) and later, its cellular homolog $p60^{c\text{-}src}$ (now commonly referred to as Src or c-Src) was also discovered (Cross et al., 1984). Since then, many members of the Src family of tyrosine kinases (i.e.: Src, Lyn, Fyn, Yes, Lck), that also participate in cellular transformation and signal transduction have been shown to be modified at their N-terminus by a myristoyl group (Resh, 1994). The newly synthesized myristoylated Src family of proteins has a tendency to bind to membranes post-translationally. Various studies using $p60^{v\text{-}src}$ have established that myristoylation is required for membrane association and that myristoylation-deficient $p60^{v\text{-}src}$ mutants do not bind to membranes as efficiently as their myristoylated counterparts, as they remain in the cytosol and fail to transform cells (Cross et al., 1984; Kamps et al., 1985; Resh, 1996).

Additionally, many of the myristoylated Src family members are also palmitoylated proteins and addition of a palmitoyl-moiety increases hydrophobicity thereby facilitating interaction with lipid bilayers (i.e.: Yes, Fyn, Lyn, Lck) (Resh, 1994; Resh, 1999). Other members like Src and Blk utilize a polybasic domain as second signal adjacent to the myristoylated glycine residue to facilitate electrostatic interaction with the negatively

charged phospholipids enriched on the inner leaflet of the plasma membrane (Sigal et al., 1994; Resh, 2006).

Of note, guanine nucleotide binding proteins such as Gα proteins and some ADP-ribosylation factors (Arfs) are also myristoylated and/or palmitoylated and these lipid modifications seem to play an important role in membrane targeting and also in the interaction between Gα subunits with other subunits of the heteromeric G protein (Chen and Manning, 2001). It seems apparent that the membrane binding of Gαi subunit conforms to a two-signal (lipid) membrane trapping model, which involves the transient membrane binding of the myristoylated $G_{\alpha i}$ subunit, which would in turn allow palmitoylation to proceed, as palmitoyl-CoA and some PATs are enriched in the plasma membrane (Chen and Manning, 2001; Ohno et al., 2006).

There are many more co-translationally myristoylated proteins that have considerable roles in the regulation of the cellular environment. Some examples of co-translationally myristoylated proteins are shown in **table 1.2**. Typically, the addition of a myristoyl moiety contributes to various protein functions such as subcellular targeting, mediating protein-protein interactions and also protein-membrane interactions required for the proper functioning of those proteins (Resh, 2006; Wright et al., 2010)

Function	Myristoylated Protein
Protein Kinases	Src family protein tyrosine kinases • Src • Yes • Fyn • Lyn • Lck Abl tyrosine kinases • C-Abl • Arg Ser/Thr kinases and anchoring proteins • cAMP-dependent protein kinase, catalytic subunit α and β-1
Phosphatases	• Calcineurin B • Yeast phosphatase, PP-Z2
Guanine nucleotide binding proteins	Gα proteins • Gαi1, Gαo, Gαt, Gαx ADP-ribosylation factors(Arf) • Arf-1, -3, -5, -6
Ca^{2+} binding proteins	• Recoverin • Neurocalcin
Membrane and cytoskeletal bound structural proteins	• MARCKS • Annexin XIII • Rapsyn
Viral proteins	• Gag proteins [Human Immunodeficiency Virus-1 (HIV-1), Maloney murine sarcoma virus, mouse mammary tumor virus] • HIV-1 Nef, • Herpes simplex virus UI 11
Miscellaneous	• NADH cytochrome $b_5$reductase • Nitric oxide synthase • BASP-1

Table 1.2: Some co-translationally myristoylated proteins and their function. Modified from (Resh, 1999)

1.1.4.3.2 Post-translational myristoylation of caspase-cleaved proteins during cell death

Post-translational myristoylation, also referred to as 'morbid myristoylation' (Mishkind, 2001; Resh, 2006), takes place when the caspase cleavage of a protein during apoptosis reveals an amino-terminal glycine part of a myristoylation consensus sequence that is recognized by NMT (discussed in the NMT section) (**Fig. 1.2**). Up until 2000, myristoylation was thought to be a strictly co-translational process that occurred upon the removal of the initiator methionine by MetAP while the protein was still being translated on the ribosome. This established dogma changed when the Korsmeyer group discovered that the pro-apoptotic Bcl-2 family member Bid was myristoylated on an internal glycine residue that was exposed after caspase cleavage during apoptosis (Zha et al., 2000).

When the 21 kDa Bid is cleaved by caspase-8 during apoptosis, two fragments are generated; 7 kDa N-terminal fragment and 15 kDa C-terminal fragment which remain hydrophobically associated (Zha et al., 2000; Mishkind, 2001). As a result of this cleavage, an internal myristoylation motif bearing an N-terminal glycine residue becomes exposed at the N-terminus of the C-terminal 15 kDa fragment of caspase-truncated Bid (ctBid), allowing NMT to utilize ctBid as a substrate for post-translational myristoylation (Zha et al., 2000). Myristoylated ctBid while still associated to the 7 kDa N-terminal fragment is translocated to the mitochondria, where this complex induces the release of cytochrome c

and cell death (Zha et al., 2000). When the authors substituted the glycine residue which is essential for myristoylation to an alanine (G60A) in ctBid, mitochondrial association of mutant ctBid was severely reduced (<30%) when compared to wild-type myristoylated (myr) ctBid (Zha et al., 2000). Furthermore, using an *in vitro* system using purified mitochondria, the authors demonstrated that myr-ctBid was approximately 350 times more effective than its non-myristoylated form at eliciting mitochondrial cytochrome c release (Zha et al., 2000). The release of cytochrome c is an important event as it affects many downstream events in the intrinsic apoptotic pathway (discussed later in the apoptosis section). Hence, it is apparent that myr-ctBid plays a key role in the induction of apoptosis.

Since the initial discovery of myr-ctBid, many other proteins have also emerged as substrates for post-translational myristoylation. The 15 kDa fragment of caspase cleaved cytoskeletal Actin (ctActin), is one such example that was found to be post-translationally myristoylated (Utsumi et al., 2003). Actin plays a structural role in the cytoskeleton by forming microfilaments (polymers of actin subunits) and is vital for the regulation of cell structure, division, organelle movement and motility. In this study, the authors found that C-terminally FLAG tagged myr-ctActin co-localized with mitochondria, similar to myr-ctBid, however, myr-ctActin did not seem to affect apoptosis nor cause any changes to cellular morphology (Utsumi et al., 2003).

The same group performed a subsequent study where they showed that the C-terminal fragment of the actin-severing protein, Gelsolin (ctGelsolin) was post-translationally myristoylated (Sakurai and Utsumi, 2006). Interestingly, exogenously expressed ctGelsolin-HA was shown to be primarily cytosolic regardless of its myristoylation status as assessed by both subcellular fractionation and immunofluorescence staining experiments (Sakurai and Utsumi, 2006). Furthermore, cells overexpressing myr-ctGelsolin were more resistant to apoptosis induced by etoposide (topoisomerase inhibitor), when compared to cells over-expressing the glycine to alanine (G2A) mutant of ctGelsolin (Sakurai and Utsumi, 2006). Hence, the addition of a myristoyl group to ctGelsolin post-translationally does not appear to play a role in membrane targeting as it does not target ctGelsolin to the mitochondria as seen with myr-ctBid and myr-ctActin, but this modification rather seems to be implicated in the anti-apoptotic activity of ctGelsolin.

In parallel, our laboratory had also started to investigate the existence of other post-translationally myristoylated proteins and reported the post-translational myristoylation of caspase cleaved p21-activated protein kinase 2 (PAK2) in 2006 (Vilas et al., 2006). PAK2 is a serine/threonine kinase whose activity is stimulated by the binding of the small GTPases Rac and CDC42 (Bokoch, 2003). It is known to regulate cell growth, cell motility and even membrane blebbing during apoptosis (Bokoch, 2003). Notably, PAK2 is cleaved by caspase-3 during apoptosis,

which leads to the generation of a pro-apoptotic C-terminal kinase domain that is constitutively active (Rudel and Bokoch, 1997). Interestingly, more than 50% apoptotic cells were observed after merely 12 hours of transient transfection with a vector expressing WT-ctPAK2-Myc, when only 23% apoptotic cells were observed in cells transfected with the vector control and vector expressing G213A-ctPAK2-Myc (Vilas et al., 2006). This indicates that myr-ctPAK2-Myc is a more potent activator of apoptosis when compared to its mutant (G213A-ctPAK2-Myc). We also observed an increase (5 fold) in phosphorylation of the stress-activated c-Jun N-terminal kinase (JNK) in cells expressing myr-ctPAK2 when compared to the cells expressing vector alone. When indirect immunofluoresence was used to study the localization of myr-ctPAK2-Myc, we found that the myristoylated form of ctPAK2 localized to plasma membrane ruffles and early endosomes. Conversely, its non-myristoylated counterpart G213A-ctPAK2-Myc was largely cytosolic, suggesting that myristoylation is crucial for the proper localization of ctPAK2.

Interestingly, myr-ctPAK2 mediated cell death without releasing cytochrome c, without loss of mitochondrial membrane potential and also without the exposure of phosphatidylserine at the cell surface, as often observed during the cell death process (Vilas et al., 2006). Consequently, the data suggests that myr-ctPAK2 was able to induce cell death through the increased signaling of the stress activated JNK pathway, and it does

so by circumventing several hallmarks of apoptosis that lead to compromised mitochondrial integrity.

A recent publication by our laboratory also shows that caspase-cleaved ctPKCε-HA is myristoylated at its N-terminal glycine residue and it localized to various membranes, including membrane ruffles, whereas non-myristoylatable G2A-ctPKCε-HA was predominantly cytosolic (Martin et al., 2012). When exogenously expressed in HeLa cells, myr-ctPKCε-HA led to an increase in MAPK signaling through the Erk1/2 cell-survival pathway when compared to cells that expressed the non-myristoylatable form of ctPKCε (Martin et al., 2012). Interestingly, this also resulted in a simultaneous phosphorylation of the pro-apoptotic Bcl-2 family member, Bcl-2 interacting mediator of cell death (Bim), as well as an overall decrease in Bim protein levels. Indeed, Erk1/2 activation leads to the phosphorylation of the pro-apoptotic Bim [Bim-extra long (EL)] at Ser69, targets it for ubiquitination and subsequently, its proteosomal degradation (Luciano et al., 2003). Hence, the pro-apoptotic activity of Bim is inhibited following its phosphorylation by Erk 1/2.

Interestingly, myr-ctPKCε-HA prevented a major loss of mitochondrial potential (17% over non-myristoylatable G2A-ctPKCε-HA) in HeLa cells in the presence of apoptotic stimuli (Martin et al., 2012). In conclusion, these observations suggest that myr-ctPKCε may have an anti-apoptotic role in cells, similar to what was observed with myr-ctGelsolin.

The above mentioned proteins represent the only few post-translationally myristoylated proteins which have been characterized, but it is apparent that these proteins play a role in cell death (**Fig. 1.3**). Recent studies by Martin et al. and Yap et al. demonstrated the existence of more than 15 post-translationally myristoylated proteins in apoptotic Jurkat T cells, using novel non-radioactive labeling methods developed by our laboratory to label fatty-acylated proteins (Martin et al., 2008; Yap et al., 2010). Many of these proteins need to be identified and further characterized.

In Martin et al. (2012), we developed a tandem reporter assay for the identification of myristoylated proteins post-translationally (TRAMPP). The use of this vector circumvents issues possibly encountered when we used a co-translational assay to identify post-translationally myristoylated proteins in our earlier experiments (Martin et al., 2008; Martin et al., 2012). The TRAMPP vector was used to identify more putative substrates for post-translationally myristoylated proteins; these include cell division control protein 6 homologue (Cdc6), microtubule-actin cross-linking factor 1 (MACF1), the apoptotic regulator-induced myeloid leukemia cell differentiation protein (Mcl-1), the causative agent for Huntington's disease, Huntingtin (Htt), isoform 1 of YTH domain family protein 2 (YTHDF2) and cytoplasmic dynein-intermediate chain 2A (CD-IC2A) (Martin et al., 2012).

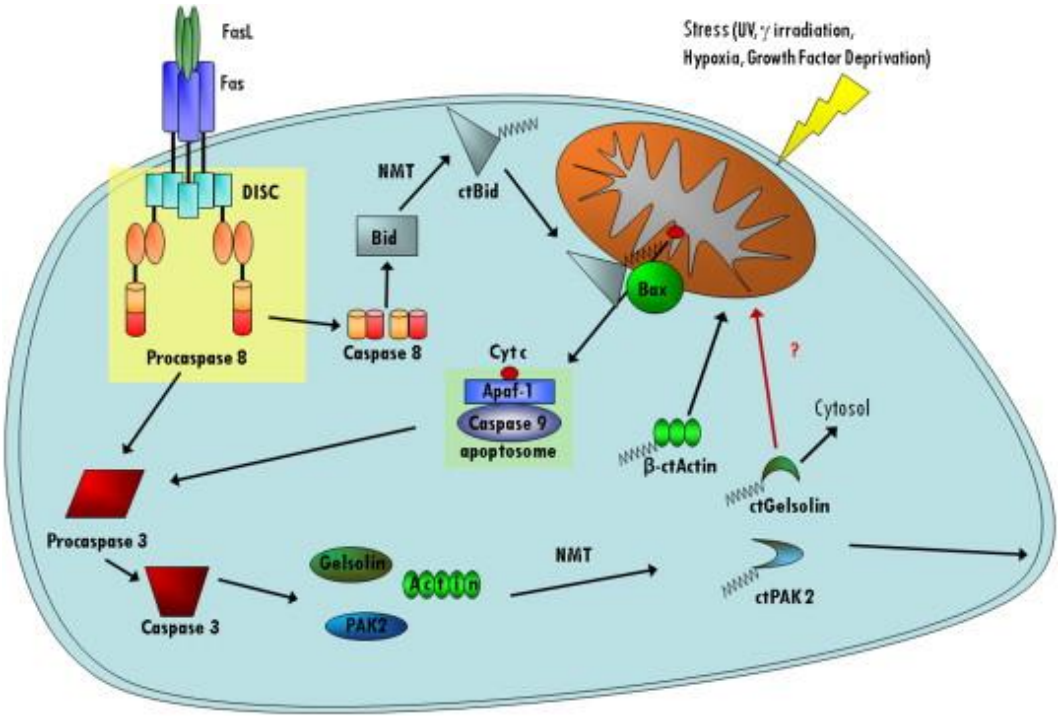

Figure 1.3: Post-translational myristoylation of proteins during cell death. The extrinsic apoptotic pathway is activated with the binding of a death ligand [e.g. Fas ligand (FasL)] to its corresponding death receptor (i.e. Fas). Subsequent binding of adaptor proteins leads to the formation of the death inducing signaling complex (DISC) and caspase-8 activation. Caspase-8 cleaves the pro-apoptotic protein Bid, which is then post-translationally myristoylated by NMT at the exposed amino-terminal glycine of the C-terminal fragment, which is essential for ctBid's translocation to the mitochondria and progression of apoptosis by the release of cytochrome c. β-Actin, Gelsolin and p21-activated kinase 2 (PAK2) are all proteins which are cleaved by caspase-3 to yield caspase-truncated (ct) products: ctActin, ctGelsolin and ctPAK2, which are subsequently post-translationally myristoylated. The post-translationally myristoylated caspase-truncated products move to their new respective membrane locales to affect apoptosis. **(Published in Martin et al., 2011)**

1.1.4.3.3 Aberrant myristoylation in disease

For the first time Cordeddu et al. showed that a spontaneous genetic mutation leading to aberrant myristoylation caused a disease phenotype named Noonan-like syndrome with loose anagen hair (Cordeddu et al., 2009). This rare developmental disorder is associated with reduced growth, facial dysmorphism and cognitive defects (Cordeddu et al., 2009). In this case, 25 patients exhibiting the Noonan-like syndrome with loose anagen hair phenotype had a missense mutation (S2G amino acid substitution) in the SHOC2 protein, that introduced a myristoylation site which would lead to the aberrant myristoylation of the protein (Cordeddu et al., 2009). They reported that the $SHOC2^{S2G}$ mutant was myristoylated and this modification targeted the mutant form of SHOC2 to the plasma membrane instead of the nucleus and this lead to an inappropriate increased activation of Ras and the MAPK pathway (Cordeddu et al., 2009).

1.1.4.4 Innovative, non-radioactive methods to detect fatty acylation of proteins

Traditionally, myristoylated proteins were detected by metabolically radiolabelling cells or purified proteins with [^{3}H]-myristate or [^{3}H]-myristoyl-CoA and detection by fluorography (McCabe and Berthiaume, 1999; Vilas et al., 2006) However, this is a very labor-intensive process that often took weeks or even months of film exposure to obtain a result. The hazardous γ - emitter containing iodo-fatty acid analogs which contain [^{125}I] has improved detection times and sensitivity (Peseckis et al., 1993; Berthiaume et al., 1995), however, having to work with large quantities of radioactive material is certainly a drawback to using this method to detect fatty acylation (Wright et al., 2010). Mass spectrometry is yet another method used to detect fatty acylation, but using this method could be problematic because fatty acylated proteins could be lost in sample preparation (Wright et al., 2010). Because of the above mentioned limitations, developing more sensitive and efficient techniques to label fatty acylated proteins is of utmost importance.

Recently, our laboratory along with others, have developed various non-radioactive techniques for the labeling of myristoylated proteins with bio-orthogonal analogs of fatty acids that can be incorporated into proteins and detected using probes that exclusively react with these fatty acid analogs (**Fig. 1.4**) (Martin et al., 2011).

Originally, the modified Staudinger ligation was utilized to facilitate the detection of myristoylated proteins (Hang et al., 2007; Martin et al., 2008). The Staudinger ligation refers to the very exclusive reaction between an alkyl-azide and a phosphine. In this method, the bio-orthogonal analog of myristate, termed azido-myristate (Az-C12), can be specifically incorporated into the N-terminal glycine of proteins undergoing co- or post-translational myristoylation (**Fig. 1.4C**) (Hang et al., 2007; Martin et al., 2008). Consequently, the azido moiety of the Az-C12 analog is chemoselectively ligated via Staudinger ligation to triarylphosphines linked to a biotin or FLAG tag and detected by western blotting with short exposure times (Hang et al., 2007; Martin et al., 2008). Our publication reported that the signal emitted by a myristoylated protein labeled with our methodology is amplified by at least a million-fold signal when compared to myristoylated proteins labeled with tritiated radioactive fatty acids (Martin et al., 2008). This method was used to demonstrate the existence of at least 15 post-translationally myristoylated proteins in Jurkat T cells undergoing apoptosis (Martin et al., 2008).

Another type of chemical ligation method, the Cu (I) – catalyzed [3 + 2] Huisgen cycloaddition reaction (Rostovtsev et al., 2002; Wang et al., 2003), often referred to as click chemistry, was used by our laboratory and others to label fatty acylated proteins with alkynyl-fatty acid analogues followed by reaction with various azido-probes (Charron et al., 2009; Hannoush and Arenas-Ramirez, 2009; Martin and Cravatt, 2009; Yap et

al., 2010). In the context of myristoylation, the click reaction performed refers to the reaction that of a bio-orthogonal fatty acid analog, ω-alkynyl-myristate (Alk-C14) and various azido-probes. In this case, we showed that Alk-C14 is readily incorporated into myristoylatable proteins and click chemistry is utilized to covalently link the alkynyl moiety of the fatty acid analog Alk-C14 to an azido-probe that would be used as a detection tool. The probe could be biotin, a fluorescent molecule such as rhodamine or a fluorogenic molecule such as coumarine (**Fig. 1.4 A and B**) (Charron et al., 2009; Hannoush and Arenas-Ramirez, 2009; Martin and Cravatt, 2009; Yap et al., 2010). The various probes used in this method allow for some versatility in detection modes utilized (i.e. western blotting, in-gel fluorescence detection and even the affinity purification of some palmitoylated proteins) (Charron et al., 2009; Hannoush and Arenas-Ramirez, 2009; Martin and Cravatt, 2009; Yap et al., 2010). Additionally, I confirmed the existence of numerous post-translationally myristoylated proteins (>15) in cells undergoing apoptosis by using the above mentioned click chemistry methodology in this original publication (Yap et al., 2010). The presence of numerous post-translationally myristoylated proteins in apoptotic cells suggests an important and understudied role for myristoylation in the regulation of apoptosis.

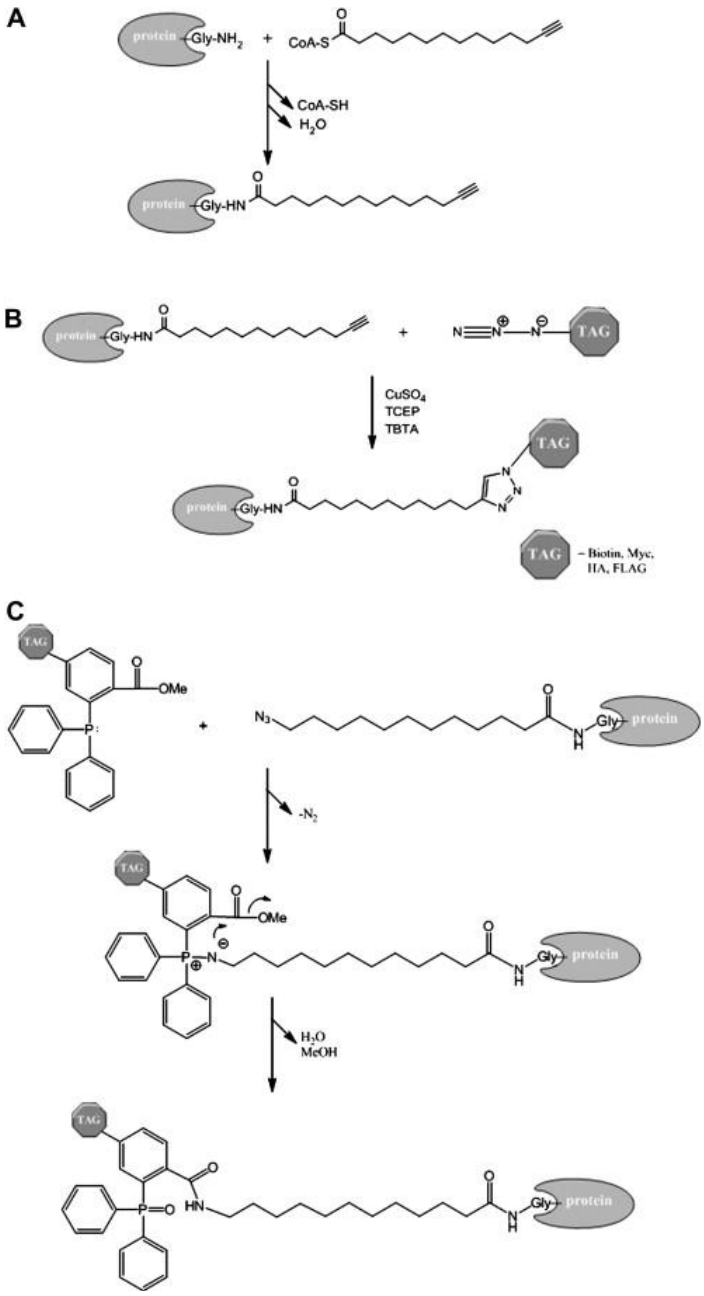

Figure 1.4: Schematic of the copper (I)-catalyzed azide-alkyne cycloaddition and the Staudinger ligation which is used to detect myristoylation of proteins. (A) ω-alkynyl-myristate is added to the cells, which leads to its activation to the CoA ester and its NMT dependent addition to the N-terminal glycine residue of a protein. ω-alkynyl-myristoylated proteins are reacted to a variety of tags using the Copper (I)-catalyzed azide-alkyne cycloaddition which is more commonly referred to as "Click" reaction (**B**). Likewise, an azido-myristate analog (ω-azido-dodecanoate, Az-C12) can be incorporated into cellular proteins and ligated to a variety of tagged-phosphine probes by the Staudinger ligation (**C**). **(Published in Martin et al., 2011)**

1.1.4.5 N-Myristoyltransferases (NMTs)

As mentioned before, NMTs are the enzymes that catalyze the attachment of myristate to the N-terminal glycine of a protein using myristoyl-CoA as a fatty acid donor [reviewed in (Boutin, 1997; Selvakumar et al., 2007; Wright et al., 2010; Martin et al., 2011)]

1.1.4.5.1 A comparison between NMT1 and NMT2

NMTs are structurally related to the GCN5 acetyltransferase (GNAT) superfamily of acetyltransferases (Dyda et al., 2000). A NCBI search by Martin et al. revealed that over 50 species from various taxa such as fungi, yeast, apicomplexan parasites (i.e. *Plasmodium* sp.), plants and mammals possess the gene that encodes for NMT, and of those, 16 species contain genes that encode for both NMT1 and NMT2 (Martin et al., 2011). Vertebrates possess both NMT1 and NMT2 proteins.

The existence of NMT was first demonstrated in the yeast strain *Sachcharomyces cerevisiae* (also known as NMT1p). Soon after its discovery, it was purified and characterized extensively (Towler and Glaser, 1986; Towler et al., 1987a; Towler et al., 1987b). The characterization of *S. cerevisiae* NMT1p has provided a great deal of information on the enzymology of NMT. In addition to yeast NMT, NMT(s) have also been purified from various organisms such as pathogenic fungi

(*Candida albicans, Cryptococcus neoformans, Histoplasma capsulatum*), the fruit fly *Drosophila malanogaster* and mammals (mouse, rat, bovine and human) and characterized (Duronio et al., 1992; McIlhinney et al., 1993; Lodge et al., 1994b; Ntwasa et al., 1997; Giang and Cravatt, 1998; Rioux et al., 2006).

The cloning and the characterization of the second mammalian N-myristoyltransferase (NMT2) revealed key differences between the two isoenzymes (NMT1 and NMT2) (Giang and Cravatt, 1998). Comparisons between mouse or human NMT1 and NMT2 revealed that these enzymes shared 76-77% sequence identity and the sequence divergence was more prevalent at the N-termini of the enzymes (**Fig. 1.5**) (Giang and Cravatt, 1998). Interestingly, the mouse and the human versions of each NMT (NMT1 and NMT2) were highly homologous as they were found to have over 95% sequence identity (Giang and Cravatt, 1998). When substrate specificity between hNMT1 and hNMT2 were compared, the authors found that these enzymes had similar but distinct substrate specificities and interestingly hNMT2 showed a preference for the c-Src peptide substrate (Giang and Cravatt, 1998). However, Smith's group reported c-Src phosphorylation was reduced in HT-29 cells which were depleted of NMT1 but not NMT2 (using siRNA) (Ducker et al., 2005). The authors also report that the phosphorylation of focal adhesion kinase (FAK), a substrate of c-Src was also reduced in the cells depleted of NMT1, indicating that NMT1

may preferentially myristoylate c-Src in a cellular environment (Ducker et al., 2005).

NMT has been shown to be essential for the survival of some organisms that encode for only one NMT such as *S. cerevisiae*, *Drosophila* and *C. albicans* (Duronio et al., 1989; Weinberg et al., 1995; Ntwasa et al., 2001). Studies indicate that NMT1 plays a vital role in early mouse development, as $NMT1^{-/-}$ mice died during embryogenesis suggesting that NMT2 is not able to fully substitute for NMT1 when it comes to the myristoylation of proteins required for the development of mice embryos (Yang et al., 2005). This indicates that although NMTs may have some overlapping substrate specificity, they also must have their own unique substrate subsets.

When investigating the subcellular localization of NMTs, McIlhinney's group performed immunofluoresence staining of NMT in HeLa cells and showed NMT1 was predominantly cytosolic (McIlhinney and McGlone, 1996). Interestingly, they also reported that although a substantial amount of NMT1 activity is cytosolic, there is a significant amount of NMT1 activity (>20%) that remains associated with membranes or organelles (McIlhinney and McGlone, 1996). Later on, it was reported that the N-terminal domain of NMT1 was involved in targeting the enzyme to the ribosome enriched subcellular fraction, where co-translational myristoylation takes place (Glover et al., 1997). Recently these results were confirmed by a separate study that demonstrated that the basic-

amino-acid-rich cluster sequence [named the lysine (K) box] (**figure 1.5**), found within the N-terminal region of both enzymes (NMT1 and 2) is essential for the binding of the enzymes to the ribosomes (Takamune et al., 2010).

Additionally, Ducker et al. conducted a study to elucidate the roles that the two NMT isoenzymes play in cells (Ducker et al., 2005). In their study, they used siRNA directed against NMT1 or NMT2 and found that depleting either of the NMTs induced apoptosis (Ducker et al., 2005). Interestingly, the depletion of NMT2 had a 2.5-fold greater effect in inducing apoptosis than depleting NMT1, indicating that NMT2 may have a more prominent role in cell survival when compared to NMT1 (Ducker et al., 2005). Furthermore, when they conducted an *in vivo* study which consisted of intratumoral injections of NMT1 or NMT2 siRNA into female BALB/c mice with tumors xenografts (formed after injecting mice with mammary adenocarcinoma cells), they found that pharmacological reduction of NMT1 lead to anti-tumor activity (Ducker et al., 2005).

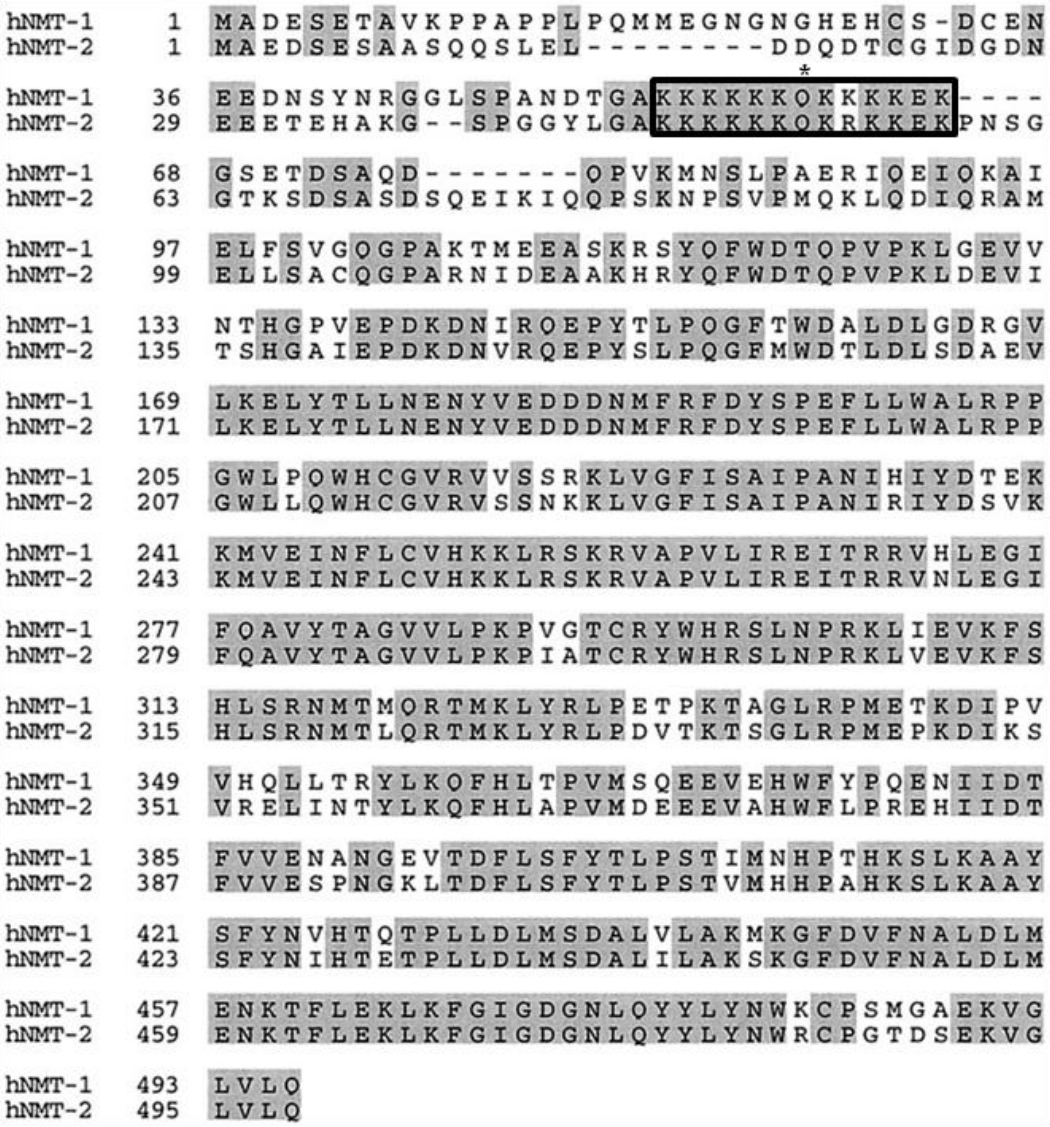

Figure 1.5: Comparison of the amino acid sequences from human NMT1 and NMT2 cDNAs Shared sequence identities between NMT1 and NMT2 are shaded in grey. Location of lysine box (K-box) is indicated by asterisk (*) (Modified from **Giang and Cravatt, 1998**).

1.1.4.5.2 Substrate specificity of NMTs

The N-terminal glycine residue is an absolute requirement for myristoylation to proceed and the substitution of this glycine residue with any other amino acid abrogates this process (Towler et al., 1987b; Farazi et al., 2001). In addition, NMT has also some preferred amino acid sequences at the N-termini of proteins that form a loose consensus. NMTs amino-acid consensus sequence is: Gly_2-X_3-X_4-X_5-$(Ser/Thr/Cys)_6$ where X represents most amino acids, however, proline, aromatic or charged residues are typically not tolerated in position X_3 (Farazi et al., 2001).

While NMT preferentially myristoylates proteins that have Ser, Thr, or Cys at position X_6, various studies have found that other amino acids such as Ala and Gly are also tolerated at this position (Jackson and Baltimore, 1989; Turnay et al., 2005). Furthermore, it is apparent that the combination of amino acids located at position 3, 6 and 7, plays and an important role in the myristoylation of a candidate protein (Silverman and Resh, 1992; Utsumi et al., 2004). When designing a myristoylation prediction method, Maurer-Stroh et al. identified that the first 17 amino acids following the initiator methionine was important for the predicting if a protein is indeed myristoylated (Maurer-Stroh et al., 2002b). There are various computer algorithms that have been designed over the years to predict if a protein is myristoylated. Importantly, these computer algorithms have been used to predict that at least 0.5 to 3% proteins of the mammalian and plant proteomes respectively are putative

substrates for myristoylation (Maurer-Stroh et al., 2002b; Boisson et al., 2003; Podell and Gribskov, 2004; Sugii et al., 2007).

Although the above mentioned computer algorithms have led to the discovery of many myristoylated proteins, there have been many proteins that have been falsely predicted to be myristoylated (Traverso et al., 2013). Therefore, it is important that the rules of substrate specificity to be established for each organism to enhance the accuracy of these algorithms, which are designed to predict protein myristoylation. To circumvent this problem, Traverso et al. has developed a high-throughput screening method with a large number of peptides which identifies the common features of the myristoylomes of various organisms (Traverso et al., 2013).

1.1.4.5.3 Enzymology of N-myristoyltransferases

The purification and characterization of the *S. cerevisiae* NMT has helped uncover their enzymatic mechanism. Rudnick et al. reported that *S. cerevisiae* NMT follows a sequential ordered bi bi mechanism when catalyzing the myristoylation reaction (**Fig. 1.6**) (Rudnick et al., 1991). This mechanism entails the binding of myristoyl-CoA to the apo-enzyme (NMT) and inducing a conformational change that allows the peptide substrate to bind (Rudnick et al., 1991). Once the peptide substrate binds NMT, a chemical transformation takes place via nucleophilic substitution when the N-terminal glycine amine attacks the myristoyl-CoA thioester bond (Rudnick et al., 1991; Wright et al., 2010). Following this transformation, the release of CoA occurs prior to the release of the myristoylated peptide (**Fig. 1.6**) (Rudnick et al., 1991) .

The crystal structures of *C. albicans* NMT (CaNMT) and *S. cerevisiae* NMT (ScNMT/ NMT1p) has been solved and these studies indicate that NMT is a monomeric enzyme with a compact globular structure. The enzyme has a large saddle-shaped β-sheet which is located in the core of the structure and is surrounded by several α-helices (Weston et al., 1998; Bhatnagar et al., 1999; Wright et al., 2010). Interestingly, NMT comprises of two distinct but structurally similar regions, which correspond to the N- and C-terminal halves of the enzyme that leads to NMT having internal pseudo two-fold symmetry, forming a

unique ‘NMT fold’ (Weston et al., 1998; Bhatnagar et al., 1999). Furthermore, these studies revealed that the N-terminal half forms the myristoyl-CoA binding site, whereas the C-terminal half forms most of the peptide binding site, but there are important contact sites on the N-terminal half which facilitate peptide binding (**Fig. 1.7**) (Bhatnagar et al., 1999).

Recently, the crystal structure of the full-length *S. cerevisiae* was solved and this together with NMT mutation experiments carried out by the authors suggests that N-terminal region of NMT plays a pivotal role in the binding of myristoyl-CoA and the peptide substrate, but is not involved in the catalytic process (Wu et al., 2007). These results are concomitant with an earlier mutagenesis study using *S. cerevisiae* NMT (ScNMT) which demonstrates that the first 34 amino acid residues located in the N-terminal region has no significant effect on NMTs enzymatic activity (Rudnick et al., 1992a). A glycine residue that is located five amino acid residues from the C-terminus of the yeast (Gly^{451}) and human (Gly^{412}) NMTs seem to play an important role in catalysis, as mutating these Gly residues to Asp or Lys seemed to markedly reduce NMT activity (Duronio et al., 1992). Importantly, the structure of full length hNMTs is yet to be solved and the only hNMT structures solved so far used truncated NMTs missing 108 residues at their N-terminal domain (Protein Data Bank ID: 3IWE, 3JTK, 3IU1, 3IU2; all solved by Dr. Paul Wyatt’s group, University of Dundee, Scotland).

Various *in vitro* enzymatic assays have determined that myristoyl-CoA is the preferred substrate for NMT, and this is concomitant with the data obtained by studying the crystal structure of NMT, which shows that acyl chain of myristoyl-CoA binds the NMT active site in a bent conformation and the active site cavity could optimally accommodate this myristoyl moiety (Kishore et al., 1991; Bhatnagar et al., 1994; Bhatnagar et al., 1999). Although myristoyl-CoA is the preferred substrate for NMT, it has been reported that NMT can catalyze the linkage of other fatty acids (i.e. lauric, tridecanoic, pentadecanoic and palmitic acid) to a peptide that mimics the N-terminal region of a protein, although at a reduced efficiency when compared to myristoyl-CoA (Rudnick et al., 1992b). Since palmitoyl-CoA can be used *in vitro* in place of myristoyl-CoA in the myristoylation reaction and because palmitic acid is more widely available in the cell when compared to the rare myristic acid (5nM in animal cells), it is crucial for NMT to gain access to myristoyl-CoA pools within the cell (Martin et al., 2011).

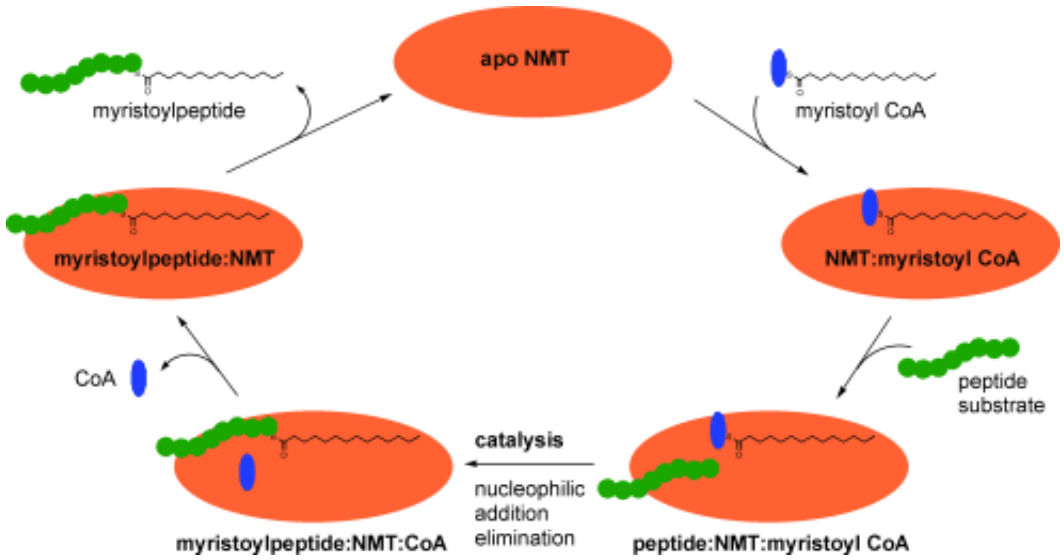

Figure 1.6: Schematic of the sequential ordered Bi–Bi mechanism of NMT action. The enzyme first binds myristoyl-CoA to cause a structural rearrangement that allows the binding of the N terminus of the peptide/protein substrate. The nucleophilic addition–elimination reaction is catalyzed by stabilizing interactions from the protein which leads to formation of products that then dissociate in a stepwise manner. [**Published in (Bowyer et al., 2008)**]

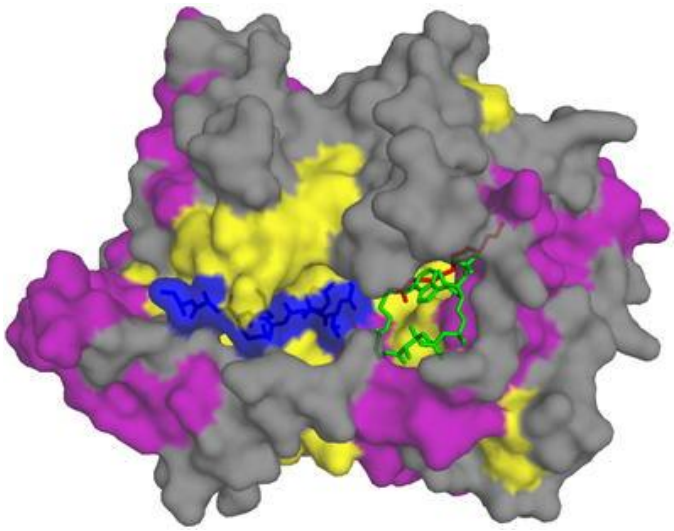

Figure 1.7: The crystal Structure of Saccharomyces cerevisiae NMT and bound myristoyl-CoA (PDB: 1IID) The helical structure is in *purple*, β-sheet in *yellow*, a peptide substrate in *blue*, myristate in *red* and CoA in *green*. Image was generated with PyMol (2008, DeLano Scientific). **(Published in Wright et al., 2010)**

1.1.4.5.4 Biological and chemical inhibitors of NMT

There is evidence of endogenous proteins acting as inhibitors of NMT within the cell. The Sharma group first isolated an NMT inhibitor named NMT inhibitor protein 71 (NIP71) from bovine brain using an *in vitro* NMT assay (King and Sharma, 1993). Interestingly, NIP71 shares 43% sequence homology with the heat shock cognate protein 70 (HSC70) and both purified particulate NIP71 and cytosolic HSC70 inhibited NMT in a dose-dependent manner (Selvakumar et al., 2007). The Sharma group also identified that the glycolytic enzyme enolase was a potent inhibitor of NMT *in vitro* (Shrivastav et al., 2003). As for now, it is unknown whether these inhibitors play a key role in the regulation of myristoylation in a cellular environment.

Since NMT is required for the survival of several human pathogens it has become an attractive therapeutic target and various chemical inhibitors that inhibit NMT activity have been developed mainly for therapeutic reasons (Farazi et al., 2001; Selvakumar et al., 2007). These chemical inhibitors can be divided mainly into three classes; myristate and myristoyl-CoA derivatives, myristoylpeptide derivatives and histidine analogs (Farazi et al., 2001; Selvakumar et al., 2007). Of these, the myristic acid derivative and competitive inhibitor 2-hydroxymyristic acid (HMA; IC_{50}~1mM), which inhibits myristoylation but not palmitoylation, was first used to study myristoylation (Paige et al., 1990; Yap et al., 2010).

Interestingly, several NMT inhibitors which are myristic acid or myristoyl-CoA derivatives have been found to negatively affect the replication of certain viruses such as HIV, varicella-zoster and Junin (Devadas et al., 1992; Harper et al., 1993; Cordo et al., 1999). Other notable NMT inhibitors include Tris dibutylbenzinylidene acetone palladium (TrisDBA, EC_{50}~1-10μM) (Bhandarkar et al., 2008) and DDD85646 (EC_{50}~1-10nM), a lead compound to treat African sleeping sickness (Frearson et al., 2010).

1.1.4.5.5. N-myristoyltransferase and disease

Many myristoylated proteins are crucial components of many signaling pathways and myristoylation is required to ensure the proper localization of many of these proteins so that they function optimally in the cellular environment. NMTs are ubiquitous enzymes in eukaryotes that have been shown to be essential to the survival of several organisms (i.e. yeast, drosophila, mice) (Duronio et al., 1992; Ntwasa et al., 2001; Yang et al., 2005). There are many proteins which are involved in the propagation of several infectious diseases and carcinogenesis that are myristoylated and this modification is required for their function. Therefore NMTs become attractive drug targets that could be exploited when developing therapeutics to combat these diseases (Sikorski et al., 1997; French et al., 2004; Wright et al., 2010; Tate et al., 2013).

1.1.4.5.5.1 The role of NMTs in infectious diseases

Myristoylation has been linked to the survival and the propagation of several human infectious pathogens. NMT was first shown to be essential for the vegetative growth of the human pathogenic fungus *C. Albicans* (Weinberg et al., 1995). In that study, the authors infected immunosuppressed mice with a strain of *C. Albicans* that produced a mutant form of NMT with greatly reduced activity, the mice with the mutant NMT survived, while the mice infected with wild-type fungus were killed (Weinberg et al., 1995). Likewise, NMT activity was shown to be critical for the virulence of *Cryptococcus neoformans*, yet another fungal human pathogen known to cause chronic meningitis in immunosuppressed patients (Lodge et al., 1994a). Interestingly, when compared, yeast and human NMTs seem to have many distinct and overlapping substrate specificities (Rocque et al., 1993). The differences in substrate specificity between the two organisms are significant enough to be exploited when developing NMT inhibitors that target pathogenic fungi, such as *C. albicans*, *C. neoformans* and *H. capsulatum* (Rocque et al., 1993; Lodge et al., 1994a; Lodge et al., 1994b; Devadas et al., 1997).

It is evident that several disease causing parasitic protozoa such as *Leishmania major* and *Leishmania donovani* (leishmaniasis), *Plasmodium falciparum* (malaria), and *Trypanosoma brucei* (African sleeping sickness) retain their own NMT, and it seems to be essential for the survival of these

organisms (Price et al., 2003; Panethymitaki et al., 2006; Brannigan et al., 2010). Various NMT inhibitors that target the above mentioned parasitic protozoa are currently being tested and validated (Bowyer et al., 2008; Sheng et al., 2009). Recently, a novel treatment for African sleeping sickness, in the form of a pyrazole sulfonamide based inhibitor that specifically targets *T. brucei* NMT has been identified (Frearson et al., 2010). Frearson et al. show that this high-affinity inhibitor (DDD85646) binds the peptide binding pocket of NMT and inihibits myristoylation in trypanosomes. Interestingly, its selectivity for TbNMT is 100 fold over its selectivity for hNMT. Besides killing *T. brucei* both *in vitro* and *in vivo*, this drug has also cured mice infected with *T. brucei* in a mouse model of human African trypanosomiasis. Hence, this NMT inhibitor shows much promise as a potential therapeutic drug that could be used to treat African sleeping sickness.

Certain bacteria such as *Pseudomonas syringae* use a type III delivery system to inject myristoylatable avirulence (Avr) effector proteins that have a N-terminal glycine residue in to the cytosol of the host cell (Nimchuk et al., 2000). The injected Avr proteins are then myristoylated by the host NMT which aids in the relocalization of these proteins to the plasma membrane (Nimchuk et al., 2000). The authors demonstrate that certain Avr proteins of *P. syringae* have to be myristoylated in order to gain access to the plasma membrane where they function optimally by contributing to pathogenic virulence (Nimchuk et al., 2000).

Developing NMT inhibitors that target human immunodeficiency virus type 1 (HIV-1) viral proteins Gag and Nef has taken precedence in the recent years. Both Gag and Nef have to be myristoylated by NMT during viral processing that takes place in the host cell in order to execute their roles in HIV-1 replication and virulence (Seaton and Smith, 2008; Wright et al., 2010). Gag is a structural protein that is relocalized to the plasma membrane upon myristoylation and where it initiates the recruitment of RNA and other viral proteins that participate in the budding of newly formed viral particles (Seaton and Smith, 2008). Interestingly, non-myristoylated Gag proteins are unable to facilitate the assembly of active viral particles or to initiate viral budding (Bryant and Ratner, 1990).

Nef is an HIV-1 accessory protein that plays an important role in HIV-1 pathogenesis and myristoylation is essential for its role in viral infectivity (Seaton and Smith, 2008). In this context, a drug that targets HIV-1 Gag or Nef myristoylation would have to be one that is directed against the human form of NMT, but this may be problematic as it could potentially be toxic to human cells. Seaton et al. examined the substrate specificities of the NMT isozymes and reported that both NMTs preferred Gag over Nef, but NMT2 showed greater affinity to Nef than NMT1, both *in vitro* and *in vivo* (Seaton and Smith, 2008). Therefore, it is possible that a drug may be developed that exploits the substrate specificities of the two human NMTs. However, there have been publications that report results that conflict with the substrate specificity results reported by Seaton et al.

(Wright et al., 2010). This indicates that methods currently used to predict substrate specificity have their limitations and also that either hNMTs (NMT1 or NMT2) may be able to compensate for the loss of the other when myristoylating putative substrates. Hence, better understanding of NMT substrate specificity is required to develop new NMT inhibitors.

1.1.4.5.5.2 The role of NMTs in Cancer

There are many myristoylated proteins that are involved in signaling processes that regulate cell proliferation, cell growth and even cell death. Therefore, Felsted, Glover and Hartman, first proposed that myristoylation should be considered as a chemotherapeutic target when developing drugs that treat cancer (Felsted et al., 1995). Their proposal was mainly fueled by the study done by Magnuson et al., who reported increased NMT activity in both human and rat models of colonic tumors when compared to normal colonic tissue (Magnuson et al., 1995). Felsted et al., reported that there may be a correlation between increased oncogenic c-src activity and the parallel increase of NMT activity, and as mentioned earlier, myristoylation is required for the proper function of c-src (Felsted et al., 1995).

Since then, Sharma and co-workers have shown that NMT1 is over-expressed in a variety of cancer types thereby providing evidence that warrant further investigation of NMT as a chemotherapeutic target

(Selvakumar et al., 2007), especially in human colorectal tumors and colorectal adenocarcinomas (Magnuson et al., 1995; Raju et al., 1997b; Selvakumar et al., 2006). The same laboratory has shown increased levels of NMT1 in gallbladder cancer, brain tumors and breast cancer (Rajala et al., 2000; Lu et al., 2005; Selvakumar et al., 2007; Shrivastav et al., 2009). Altogether, the fact that NMT1 is over-expressed in a large variety of cancers, make it an attractive therapeutic target.

1.2 Apoptosis

Apoptosis is an essential mechanism used by eukaryotic organisms to remove unnecessary or superfluous cells and is a tightly regulated process. Cellular alterations leading to the up or down regulation of apoptosis can lead to disease, including Alzheimer's disease and cancer respectively. Apoptotic cells are characterized by several hallmarks such as nuclear condensation, membrane blebbing and the formation of apoptotic bodies [reviewed in (Cohen, 1997; Solary et al., 1998; Bratton and Cohen, 2001; Liston et al., 2003; Moffitt et al., 2010)].

Cysteine-aspartyl proteases, known as caspases are responsible for the cleavage of a myriad of proteins during apoptosis and are typically known to be the executioners of apoptotic process. Caspases are subdivided into two classes; initiator caspases (caspase-8 and caspase-9) and effector caspases (caspases-3, -6 and -7). Initiator caspases have long prodomains,

which facilitate their interactions with other 'adapter' proteins (Bratton and Cohen, 2001). During apoptotic activation, 'adapter' proteins cluster and bring initiator caspases in close proximity with each other inducing the trans-catalytic activation of initiator caspases (Bratton and Cohen, 2001). Initiator caspases in turn cleave other effector caspases, which contain a short prodomain. Importantly, caspases cleave proteins almost exclusively after an aspartate residue once they recognize various tetra- or penta-peptide motifs (i.e. DEVD, IETD) which are located on their substrate proteins including other caspases (Bratton and Cohen, 2001). Consequently, 'Effector' caspases cleave many structural and regulatory proteins, resulting in cell death. Generally, caspase cleavage leads to the activation of pro-apoptotic proteins and the inactivation of anti-apoptotic proteins. Inhibitors of apoptosis (IAPs) are intrinsic regulators of the caspase cascade that bind and inhibit caspases, therefore playing a role in deciding cell fate (Liston et al., 2003).

B-cell lymphoma-2 (Bcl-2) family proteins are also key regulators of apoptosis. These proteins can be divided into three classes; inhibitors of apoptosis (Bcl-2, Bcl-XL, Mcl-1), activators of apoptosis (Bax, Bak, Bok) and BH3 only proteins (Bad, Bik, Bid, Bim), that have a conserved BH3 domain that allows them to bind to and regulate the Bcl-2 members that inhibit apoptosis (Youle and Strasser, 2008).

Apoptosis is generally executed through two distinct but overlapping pathways, the extrinsic and intrinsic apoptotic pathways (**Fig. 1.3**).

1.2.1 Extrinsic apoptotic pathway

The extrinsic apoptotic pathway is initiated by the extracellular binding of signaling molecules to transmembrane death receptors such as Fas/CD95 and tumor necrosis factor receptor-1 (TNFR-1) which are located on the plasma membrane (Moffitt et al., 2010). Death receptors contain amino acid motifs such as death domains (DD) and death effector domains (DED) that are capable of forming homotypic interactions with other proteins bearing similar domains (Fadeel and Orrenius, 2005). Once ligated, death receptors such as Fas aggregate on the cell surface and recruits Fas-associated death domain (FADD) protein which also has the DD and DED domains that form homotypic interactions with the DD on Fas (Moffitt et al., 2010). Consequently, FADD recruits initiator pro-caspase-8 via its DED domain and this leads to the formation of the death-inducing signal complex (DISC). Once DISC is formed, the autocatalytic processing and activation of pro-caspase-8 takes place, because of its high local concentration and caspase-8 in turn cleaves and activates the downstream effector caspase, caspase-3. Consequently, caspase-3 cleaves downstream substrates such as poly(ADP-ribose) polymerase 1 (PARP1), PAK2, Actin and gelsolin and stimulates apoptosis (Cohen, 1997; Martin et al., 2011). Inhibitor of caspase activated DNAse (ICAD) is yet another important substrate of caspase-3. The cleavage of ICAD by caspase-3, releases the inhibition from CAD and this leads to DNA

fragmentation, which is one of the key features of a cell that is undergoing apoptosis (Nagata, 2000).

Importantly, Fas/CD95 expressing cells are classified as type I or type II based on the fact whether the intrinsic pathway contributes to the amplification of the caspase cascade or not (Hao and Mak, 2010). Briefly, in type I cells, the activation of caspase-8 is mediated by DISC and this leads to the activation of the executioner caspases (i.e.: caspase-3 and -7), without the involvement of the intrinsic apoptotic pathway (Hao and Mak, 2010). In type II cells, activated caspase-8 is also able to cleave Bid to produce the c-terminal product (ct-Bid), which is myristoylated and relocalized to the mitochondria where myr-ctBid facilitates the release of cytochrome c as discussed earlier (Zha et al., 2000; Moffitt et al., 2010). In type II cells, the release of cytochrome c through the action of Bax/Bak contributes to the formation of the apoptosome and thereby amplifies the caspase cascade through the activation of the intrinsic apoptotic pathway as discussed in the following section (Hao and Mak, 2010).

1.2.2 Intrinsic apoptotic pathway

The intrinsic apoptotic pathway is commonly referred to as the mitochondrial apoptotic pathway. This pathway is initiated when the mitochondria is perturbed by various cellular stressors, chemicals (i.e.: chemotherapeutic drugs, oxidizers) and even by the activation of the

extrinsic apoptotic pathway (cytochrome c release by myr-ctBID) (Inoue et al., 2009). This pathway is characterized by the loss of mitochondrial membrane potential, the release of cytochrome c, apoptosis inducing factor (AIF) and second mitochondria derived activator of caspases (Smac/Diablo) (Moffitt et al., 2010).

Once cytochrome c is released from the mitochondria, it binds with apoptosis protease activating factor-1 (Apaf-1), which leads to the formation of an oligomeric complex that recruits and binds procaspase-9 (Moffitt et al., 2010). This oligomeric complex can only be formed in the presence of ATP or dATP and is called the 'apoptosome'. Subsequently, the cleavage and activation of procaspase-9 takes place and caspase-9 can in turn activate effector caspases such as caspase-3 and caspase-7, which cleave a variety of apoptotic substrates (Inoue et al., 2009; Moffitt et al., 2010).

Importantly, anti-apoptotic Bcl-2 family members (Bcl-2, Bcl-XL) work to prevent the formation of the apoptosome by impeding the release of cytochrome c, which is vital for the formation of the apoptosome (Bratton and Cohen, 2001). On the other hand, pro-apoptotic family members such as Bax, Bak and myr-ctBid, promote apoptosis by stimulating cytochrome c release and consequently triggering the formation of the apoptosome, which leads to the dismantling of cellular components (Bratton and Cohen, 2001).

1.2.3 Alternative forms of cell death

There are many alternative forms of cell death which are employed to get rid of unwanted cells. Necrosis is one of the main alternative forms of cell death that is not as tightly controlled as apoptosis and occurs upon mechnical injuries and sometimes leads to the random killing of cells (Moffitt et al., 2010; Wu et al., 2012). In necrosis, cells swell and lyse, releasing their cytosolic and nuclear content into extracellular space, thus causing inflammation and damage to neighboring tissues (Moffitt et al., 2010).

Another form of cell death termed necroptosis is induced by stimulating death receptors (TNF, Fas) with their respective ligands (Wu et al., 2012). Necroptosis is a regulated, caspase-independent alternative cell death mechanism that exhibits the morphological features of a cell undergoing necrosis and it requires the involvement of receptor interaction protein kinase 1 and 3 (RIP1 and RIP3) (Wu et al., 2012). Parapoptosis is also another form of apoptosis that is mediated by caspase-9, but is Apaf-1 independent and the cells do not exhibit DNA fragmentation as seen with cells undergoing apoptosis (Sperandio et al., 2000). Parapoptotic cells exhibit swelling, has enlarged ER and mitochondria, and ultimately resemble cells undergoing necrosis (Sperandio et al., 2000).

Autophagy represents yet another mechanism used by the cell to induce cell death, although the primary role of autophagy is to protect the

cell from stressful conditions such as starvation (Chen and Klionsky, 2011). When cells are undergoing starvation, autophagy is used to breakdown non-essential cellular components in order to produce amino acids, lipids and sugars that can be utilized to produce energy and synthesize new proteins which are essential for survival (Chen and Klionsky, 2011). During autophagy, cytoplasmic material including cytosol, organelles and vacuoles are sequestered and targeted for degradation by lysosomes (Moffitt et al., 2010; Chen and Klionsky, 2011). When the autophagic process is excessive, it induces cell death. This type of autophagic cell death, although different from apoptosis, is also negatively regulated by Bcl-2 and Bcl-XL (Chen and Klionsky, 2011).

1.3 B cell lymphomas

Hematological malignancies are cancers that affect blood, bone marrow and lymph nodes. There are four main types of hematological malignancies, namely, lymphomas, leukemias, myeloma and myelodysplastic syndrome.

Blood cancers that develop in the lymphatic system are referred to as lymphomas and about 95% of lymphomas are of B cell origin, while the rest are of T cell or natural killer (NK) cell origin (Kuppers, 2005; Jaffe, 2009). Additionally, the World Health Organization has classified approximately 50 different types of lymphomas, which highlights the complex nature of this disease (Jaffe, 2009). B-cell lymphomas are

typically present as nodal or extra-nodal malignant masses. Nodal malignant masses are present in the lymph nodes and extra-nodal malignant masses are present in the bone marrow, skin, gut, brain and liver.

Importantly, lymphomas are further subdivided into 2 main types, namely Hodgkin's (HL) and Non Hodgkin's (NHL) lymphomas. Hodgkin's lymphoma is typically defined by the presence of abnormal cells called Reed-Sternberg cells and is typically a cancer that carries a good prognosis. Importantly, the Leukemia and Lymphoma society reports that over 500,000 people in United States are living with or are in remission from NHL and over 70,000 people are estimated to be newly diagnosed with NHL in 2012, making it the 7th most common cancer in the United States (www.lls.org).

Often, reciprocal chromosomal translocations that involve immunoglobulin loci and an oncogene are the hallmark of many types of B cell lymphomas (Kuppers, 2005). As a result of such translocation, the oncogene falls under the control of a strong active immunoglobulin promoter, and this causes deregulated, constitutive expression of the oncogene (Kuppers, 2005). NHL is often treated with chemotherapy and radiotherapy. More recently, NHL treatment has been revolutionized by the addition of rituximab (a monoclonal antibody directed at CD20 surface antigen) to standard chemotherapies and these treatments have improved

the overall survival of NHL patients subjected to such treatments (Saini et al., 2011; Miles et al., 2012).

Diffuse large B cell lymphomas (DLBCL) and especially Burkitt lymphoma (BL) are the most relevant forms of lymphomas to our study, and because of this will be discussed further.

1.3.1 Diffuse Large B Cell Lymphoma (DLBCL)

DLBCLs are the most prevalent type of aggressive lymphomas, which are of B cell origin (B cell lymphomas), accounting for almost 40% of newly diagnosed lymphomas (Lenz and Staudt, 2010). Furthermore, DLBCL are categorized into several sub-types and because of its heterogeneous nature, the 5-year survival rates of patients with DLBCL range from 26%-73% (Sehn and Connors, 2005). The current treatment of DLBCL involves the combination of chemotherapy (cyclophosphamide, doxorubicin, vincristine and prednisone; CHOP) together with the monoclonal antibody rituximab (R-CHOP regimen) and this form of chemoimmunotherapy has good prognosis with recovery rates as high as 70% (Ferrara and Ravasio, 2008). However, the survival rates following chemotherapy seem to be heavily dependent on the DLBCL sub-type treated, as some sub-types are more aggressive than others (Foon et al., 2012). Disease recurrence, particularly after rituximab exposure has been a cause for concern, because early relapse in patients given rituximab in

their first-line of therapy seem to have a poor prognosis (Gisselbrecht et al., 2010).

1.3.2 Burkitt Lymphoma

In 1958, Dennis Burkitt first described BL as an obscure tumor involving the jaws of African children (Burkitt, 1958). This particular B-cell malignancy was also the very first cancer whose pathogenesis was linked to an oncogenic virus, Epstein-Barr virus (EBV) and also to the activation of the oncogene, c-myc (Kelly and Rickinson, 2007). BL tumors have a doubling time of 24-48 hours and is therefore has one of the highest cell proliferation rates of any human tumor (Iversen et al., 1972).

All forms of BL tumors are histologically similar, as they contain round monomorphic cells with round nuclei which are intermingled with macrophages that phagocytose apoptotic debris in the tumor environment (Brady et al., 2007; Kelly and Rickinson, 2007). These scattered macrophages give BL tumors their signature “starry sky” pattern (Brady et al., 2007). BL tumor cells typically express IgM and B cell markers (CD19, CD20 and CD22) (Brady et al., 2007). Interestingly, BL tumor cells also express markers (CD10, CD38 and BCL6), that are characteristic of the germinal center where mature naïve B cells are activated through the germinal center reaction (Kelly and Rickinson, 2007; Lenz and Staudt, 2010).

The germinal center reaction is the foundation of T-cell dependent humoral immunity against foreign pathogens in the adaptive immune response and it occurs when mature naïve B cells are stimulated with a T-cell dependent antigen (Gatto and Brink, 2010; Lenz and Staudt, 2010). Accordingly, the B cell receptor is modified in the germinal center, through the altering of B cell DNA by somatic hypermutation and class-switch recombination that is initiated by activation-induced cytidine deaminase (AID) (Lenz and Staudt, 2010). Somatic hypermutation leads to mutations in immunoglobulin variable regions that leads to generating a B cell population that has an increased or decreased affinity to a specific antigen, while the class-switch recombination results in the changing of immunoglobulin (Ig) heavy chain class from IgM to IgG, IgE or IgA (Lenz and Staudt, 2010). Importantly, although these genetic changes are required for the adaptive immune response, they are also thought to be the source of DNA damage that leads to mutations that cause B-cell lymphomas (Lenz and Staudt, 2010).

There are three main epidemiologically distinct forms of BL; namely endemic BL, Sporadic BL and AIDS-associated BL (Kelly and Rickinson, 2007). Endemic BL presents itself as a EBV-positive, jaw, kidney or abdominal tumor in children in areas where malaria (*Plasmodium falciparum*) is holoendemic, such as equatorial Africa or Papua New Guinea (Kelly and Rickinson, 2007). It is thought that the polymicrobial effect induced by the EBV infection together with a malarial infection

causes immune system deregulation, therefore allowing EBV-positive B cells to evade the immune system and propagate (Rasti et al., 2005; Yustein and Dang, 2007). Importantly, endemic EBV-associated BL accounts for up to 74% of childhood malignancies in the African equatorial belt (van den Bosch, 2004).

In comparison, Sporadic BL ioccurs worldwide, although western countries have low incidence rates and has different degrees of EBV association, depending on the area (Kelly and Rickinson, 2007). Similar to endemic BL, sporadic BL is more commonly expressed in children and accounts for 40-50% of childhood NHL (Aitken et al., 1982; Kelly and Rickinson, 2007; Yustein and Dang, 2007; Miles et al., 2012). Conversely, sporadic BL in adults accounts for only 1-2% of all lymphomas in North America and Western Europe (Yustein and Dang, 2007). Tumors of sporadic BL which is more common in developed countries usually arise from the lymphoid tissues in the gut and upper respiratory tract (Yustein and Dang, 2007). AIDS associated BL, is found commonly in HIV infected individuals who are chronically immunosuppressed and only 30-40% of these tumors are EBV associated (Kelly and Rickinson, 2007).

C-myc is a tightly regulated transcription factor that controls cellular processes such as growth, proliferation and apoptosis and deregulation of c-myc has been implicated in many cancers (Dang, 1999). In BL, the deregulation of c-myc is typically a result of one of the following reciprocal translocations involving the *MYC* gene (at 8q24.21) and one of the

following three immunoglobulin genes, immunoglobulin heavy chain gene (IgH, 14q32.33), kappa (IgK, 2p11.2) or lambda (IgL, 22q11.2) (Brady et al., 2007; Miles et al., 2012). The most common translocation (80% of cases) occurs between the IgH and MYC genes [t(8;14)] and the remainder (20%) occurs between the MYC gene and IgK [t(2;8)] or IgL [t(8;22)] (Brady et al., 2007; Miles et al., 2012).

BL tumors are typically treated with short, high intensity chemotherapy because of their high proliferative rates and the introduction of this type of highly intensive treatment has improved prognosis of many BL patients (Yustein and Dang, 2007; Molyneux et al., 2012). Current BL treatment regimens include cyclical intensive chemotherapy coupled with aggressive intrathecal prophylaxis (chemotherapeutic drugs are delivered into the space under the arachnoid membrane which covers the brain and spinal cord) and are reported to routinely achieve 80%-90% response rates (Kenkre and Stock, 2009). More recently, the addition of rituximab to these intensive regimens has greatly improved the survival rate in BL patients (Griffin et al., 2009; Kenkre and Stock, 2009; Molyneux et al., 2012). Regrettably, the benefits of these treatments are somewhat outweighed by the severity of the side effects of these treatments, which include neurotoxicities from intrathecal therapy, severe mucositis and hematological toxicities (Yustein and Dang, 2007).

Recently, focus has been placed on the development of efficacious treatments that are low in toxicity, because of the highly cytotoxic

chemotherapy regimens which are currently used (Yustein and Dang, 2007). Finally, microarray technology has been used to profile the differential gene expression of BL tumors when compared to other aggressive B cell lymphomas, such as DLBCL, in order to identify predictive BL markers, as it is thought that BL patients may benefit from more individualized treatments (Alizadeh et al., 2000; Dave et al., 2006; Hummel et al., 2006; Foon et al., 2012; Love et al., 2012).

1.4 Thesis Objectives

The objective of this thesis is to characterize the roles that NMT1 and NMT2 play during cell death and to investigate the potential of NMTs as an effective chemotherapeutic target in the personalized medical treatment of select B-lymphomas.

Chapter 2

Materials and Methods

2.1 Materials

The following reagents and supplies were utilized in the experiments described in this thesis. Unless otherwise indicated, the products were used according to manufacturer's instructions.

Table 2.1: Reagents used in experiments

Reagent Name	Source
[9,10(n)-^{3}H]-Myristic acid	GE Healthcare
1 kb DNA ladder (#N32325)	New England Biolabs
2-hydroxy-myristic acid (HMA)	Sigma-Aldrich
3-[3-Cholamidopropyl)dimethylammonio]-1-propanesulfonate (CHAPS)	Sigma-Aldrich
4-(2-hydroxyethyl)-1-piperazineethanesulfonic acid (HEPES)	Life Technologies
Acrylamide	Bio-Rad
Adenosine 5'-triphosphate (ATP) disodium salt hydrate	Sigma-Aldrich
Agar	Life Technologies
Agarose (electrophoresis grade)	Rose Scientific
Albumin	Pierce
Alkyne-myristate (13-tetradecynoic acid, Alk-Myr, Alk-C14)	Custom synthesis by OMM Scientific
Amicon Ultra-15 centrifugal filter	Millipore
Ammonium chloride (NH_4Cl)	Sigma-Aldrich
Ammonium persulphate	Bio-Rad
Azido-Biotin	Custom synthesis by OMM Scientific (originally synthesized in Dr. Bertozzi's laboratory, UC Berkeley)
Azido-myristate (12-azidododecanoic acid, Az-C12, Az-Myr)	Dr. John Falck Laboratory (UT Southwestern, Dallas)
Bacto-tryptone	Difco
Bacto-yeast extract	Difco
Bicinchoninic acid (BCA) protein assay reagent	Pierce
Bis-acrylamide (N-N'-Methylene-bis-Acrylamide)	Bio-Rad
Bovine serum albumin (BSA) fatty acid free	Sigma-Aldrich
Bovine serum albumin (BSA) fraction V	Sigma-Aldrich
Branson Sonifier 450	Branson

Reagent Name	Source
Bromophenol blue	BDH
Calf intestinal phosphatase (CIP)	NEB
Cell Titer® AQ_{ueous} non-radiactive cell proliferation assay	Promega
Complete™ protease inhibitors	Roche
Coomassie Brilliant Blue R-250	ICN
Copper(II)Sulphate ($CuSO_4$)	Sigma-Aldrich
Cycloheximide (CHX)	Sigma-Aldrich
Dako® antibody diluent buffer	Agilent Technologies
Dako® EnVison+System-HRP labeled polymer (anti-rabbit)	Agilent Technologies
Dako® Liquid DAB+substrate chromogen	Agilent Technologies
DDD73226	Drs. David Gray and Paul Wyatt, Dundee Drug Discovery Unit, University of Dundee
DDD85646	Drs. David Gray and Paul Wyatt, Dundee Drug Discovery Unit, University of Dundee
DDD86481	Drs. David Gray and Paul Wyatt, Dundee Drug Discovery Unit, University of Dundee
Deoxyribonucleotide triphosphate (dNTP)	Fermentas
DH5α competent *E.coli* cells	Life Technologies
Dimethyl sulphoxide (DMSO)	Sigma-Aldrich
Dithiothreitol (DTT)	Sigma-Aldrich
Dulbecco's modified Eagle's medium (DMEM)	Life Technologies
ECL Plus	GE Healthcare
ECL Prime	GE Heathcare
Ethanol	Commercial Alcohols
ethylene glycol tetraacetic acid (EGTA)	Sigma
Ethylenediaminetetraacetic acid (EDTA)	Sigma-Aldrich
Fetal bovine serum (FBS)	Life Technologies
Fluorochem FC imaging system	Alpha Innotech Coorporation
Fugene 6 transfection reagent	Roche Applied Sciences
GeneClean® Turbo PCR purification kit	Q-Biogene
GENECLEAN® Turbo PCR purification kit	Q-Biogene
Glacial acetic acid	Fisher
Glycerol	BDH

Reagent Name	Source
Glycine	Bio-Rad
Haematoxylin	Sigma-Aldrich
Hank's Balanced Salt Solution (HBSS)	Life Technologies
High capacity cDNA reverse transcription kit	Life Technologies
High-capacity DNA reverse transcription kit	Applied Biosciences
His-Pure Ni NTA agarose beads	Thermo Fisher Scientific
Hydrachloric acid	Fisher
Hydrogen peroxide (H_2O_2)	Sigma-Aldrich
Imidazole	Sigma-Aldrich
Immunobilon-P Polyvinylidene fluoride (PVDF) membrane	Millipore
Isopropanol	Fisher Scientific
Isopropyl β-D-1-thiogalactopyranoside (IPTG)	Fisher Scientific
Lemo21(DE3)pLysS competent cells	New England Biolabs
L-Glutamine	Life Technologies
LiCoA	Sigma
Lithium Carbonate(Li_2CO_3)	Sigma-Aldrich
LR Clonase II	Life Technologies
LS6500 scintillation counter	Beckman Coulter
Magnesium Chloride ($MgCl_2$)	Fisher
Mannitol	Sigma-Aldrich
Mastercycler I thermocycler	Eppendorf
Mastercycler® ep realplex thermocylcer	Eppendorf
Methanol	Fisher
MG-132	Enzo Life Sciences
Microwave pressure cooker	Nordicware
Monosodium Phosphate (NaH_2PO_4)	Sigma
N,N,N',N',-tetramethylenediamine (TEMED)	Life Technologies
NeutrAvidin™-HRP	Pierce
Nikon Eclipse 80i microscope	Nikon
Nitrocellulose membrane (0.45 micron pore)	Bio-Rad
Nonidet P-40 (NP40)/IGEPAL CA-630	Sigma-Aldrich
Nuclease-free water	Fermentas
Odyssey® fluorescence imaging system	LI-COR
One Shot® ccdB Survival™ 2 T1R Competent cells	Life Technologies
p81 phosphocellulose paper discs	Whatman
PAP pen	Sigma-Aldrich
Pfu Turbo DNA polymerase	Agilent Technologies
Phosphorimager screen	GE Healthcare
Piperazine-N,N′-bis(2-ethanesulfonic acid) (PIPES)	Sigma
Plasmid mini or midi kits	Qiagen

Reagent Name	Source
Platinum Pfx® DNA polymerase	Life Technologies
Potassium Hydroxide (KOH)	Sigma-Aldrich
Potassium phosphate monobasic (KH_2PO_4)	Sigma-Aldrich
Proteinase K	Life Technologies
Pseudomonas Acyl-CoA synthase	Sigma-Aldrich
QIAquick PCR purification kit	Qiagen
QImaging scientific camera	QImaging
Quickchange® site-directed mutagenesis kit	Agilent Technologies
Realplex® software	Eppendorf
Recombinant purified active caspase-3	BD Biosciences
Recombinant purified active caspase-8	BD Biosciences
Restriction Endonucleases, Fast Digest	New England Biolabs, Fermentas
Skim milk	Carnation
Sodium bicarbonate (Na_2CO_3)	Sigma-Aldrich
Sodium chloride (NaCl)	Sigma-Aldrich
Citric acid monohydrate	Sigma-Aldrich
Sodium deoxycholate	Sigma-Aldrich
Sodium dodecyl sulphate (SDS)	Bio-Rad
Sodium hydroxide (NaOH)	Sigma-Aldrich
Sodium myristate	Sigma
Spectra/Por2 dialysis tubing	Spectrum Laboratories
Staurosporine	Sigma-Aldrich
Suberoylanilide hydroxamic acid (SAHA)	Sigma-Aldrich
Sucrose	BDH
Superfrost® plus slides	Fisher Scientific
SYBRsafe® DNA gel stain	Life Technologies
T4 DNA ligase	New England Biolabs, Fermentas
Taqman® probes	Life Technologies
TaqMan® universal master mix II	Life Technologies
TC10™ automated cell counter	Bio-rad
TC10™ trypan blue dye	Bio-rad
Transblot® apparatus	Bio-rad
Transblot® turbo transfer system	Bio-rad
Trichloroacetic acid (TCA)	Sigma-Aldrich
Tricine	Bio-Rad
Tris base [Tris(hydroxymethyl)aminomethane]	Roche
Tris(benzytrazolylmethyl)amine (TBTA)	Sigma-Aldrich
Tris-carboxyethylphosphine (TCEP)	Sigma-Aldrich
Tris-DBA	Dr. Jack Arbiser (Emory University)
Tris-HCl	Sigma-Aldrich

Reagent Name	Source
Triton X-100	BDH
TRIzol® reagent	Life Technologies
Trypsin (0.25% w/v)	Life Technologies
Tween 20 (polyoxyethylenesorbitan monolaureate)	Caledon
Ultra-violet gel transilluminator	Fisher Biotech
XtremeGENE9 transfection reagent	Roche
Xylene	Fisher Scientific
Yeast extract	Difco
z-DEVD-FMK (caspase-3 inhibitor)	EMD chemicals
z-FA-FMK (negative control inhibitor)	EMD chemicals
z-IETD-FMK (caspase-8 inhibitor)	EMD chemicals
z-LEHD-FMK (caspase-9 inhibitor)	EMD chemicals
z-VAD-FMK (general caspase inhibitor	EMD chemicals
β-mercaptoethanol	Sigma-Aldrich

Table 2.2: Commonly Used Media and Buffers

Media/Buffer	Composition
1X Blotto Solution	0.1% Tween 20, 150 mM NaCl, 50 mM Tris-HCl pH 7.5
2.5X Homogenization Buffer	625 mM sucrose, 25 mM HEPES, pH 7.4 with EDTA-free complete protease inhibitors
Bacterial Lysis Buffer	300 mM NaCl, 20% glycerol, 0.5% Triton X-100, 50 mM NaH_2PO_4, pH 8.0
Citrate buffer (IHC)	10 mM Citric Acid, 0.05% Tween-20, pH 6.0 (pH adjusted with 1N NaOH)
Coomassie Blue gel destaining solution	10% glacial acetic acid, 45% methanol in milliQ (MQ) water
Coomassie Blue gel staining solution	0.25% Coomassie Brilliant Blue R-250, 10% glacial acetic acid, 45% methanol in MQ water
Dialysis buffer	50 mM Tris-HCl, 150 mM NaCl, 20% glycerol
Laemmli 5X SDS-PAGE loading buffer	300 mM Tris-HCl pH 6.8, 50% glycerol, 10% SDS, 0.1% Bromophenol blue, 1 mM DTT or 5% β-mercaptoethanol
Laemmli Running Buffer	1% SDS, 0.025 M Tris pH 8.8, 0.2 M Glycine
Laemmli Separating Gel Buffer	0.4% SDS, 1.5 M Tris-HCl pH 8.3
Laemmli Stacking Gel Buffer	0.4% SDS, 0.5 M Tris-HCl pH6.8
LB	1% tryptone, 0.5% yeast extract, 1% NaCl
Mg Resuspension Hypotonic Buffer	10 mM NaCl, 1.5 mM $MgCl_2$, 10 mM HEPES, pH 7.4 with EDTA-free complete protease inhibitors
Myristoyl-CoA generation buffer	38.6mM Tris-HCl pH 7.4, 1.93 mM DTT, 19.3 mM $MgCl_2$, 1.93 mM EGTA
Ni-NTA Agarose Column Buffer	300 mM NaCl, 20% glycerol, 50 mM NaH_2PO_4, pH 8.0
NMT cleavage assay buffer	20 mM PIPES, 100 mM NaCl, 1 mM EDTA, 0.1% CHAPS, 10% Sucrose, 10 mM DTT, pH 7.2
Phosphate Buffered Saline (PBS)	1.4 M NaCl, 30 mM KCl, 10 mM Na_2HPO_4-$7H_2O$, 14 mM KH_2PO_4
Radioactive NMT assay buffer	0.26M Tris-HCl pH 7.4, 3.25 mM EGTA, 2.92 mM EDTA and 29.25 mM 2-mercaptoethanol, 1% Triton X-100
Radioactive NMT assay wash buffer	0.025M Tris-HCl pH 7.4

*Table 2.2 Commonly Used Media and Buffers (continued***)**

Media/Buffer	**Composition**
RIPA buffer	50 mM Tris-HCl pH 8.0, 150 mM NaCl, 1% NP-40, 0.5% sodium deoxycholate, 2 mM $MgCl_2$, 2 mM EDTA, and complete protease inhibitor
RIPA-HEPES buffer	0.1% SDS, 50 mM HEPES, pH 7.4, 150 mM NaCl, 1% Igepal CA-630, 0.5% sodium-deoxycholate, 2 mM $MgCl_2$, EDTA-free complete protease inhibitor
SOC Media	2% w/v bacto-tryptone, 0.5% w/v bacto-yeast, 8.56 mM NaCl, 2.5 mM KCl, 10 mM $MgCl_2$, 20 mM glucose
TAE	40 mM Tris-acetate pH 8.0, 1 mM EDTA
TE buffer	10 mM Tris-HCl pH 8.0, 1 mM EDTA
Transfer buffer	0.04 M Glycine, 0.05 M Tris, 20% Methanol
Tris buffered saline (TBS)	140 mM NaCl, 25 mM Tris-HCl pH 7.5

Table 2.3: Selective Antibiotics

Antibiotic	**Source**
Ampicillin	Calbiochem
Carbenicillin	Calbiochem
Kanamycin	Calbiochem
Penicillin G (sodium salt)	Life Technologies
Streptomycin sulfate	Life Technologies

Table 2.4: Antibodies used in experiments

WB: Western blot, IHC: Immunohistochemistry

Antibody	Species	Use	Source	Catalog number
Alexafluor® 680 goat anti-rabbit IgG	Rabbit	LICOR	Life Technologies	A-21109
Anti-cleaved caspase 8 (Asp 391)	Rabbit	WB	Cell Signaling	9496
Anti-cleaved caspase 9	Rabbit	WB	Cell Signaling	9502
Anti-cleaved caspase-3 (Asp175)	Rabbit	WB	Cell Signaling	9664
Anti-cleaved PAK2	Rabbit	WB	Eusera*	N/A
Anti-GAPDH	Rabbit	WB	Eusera*	N/A
Anti-GFP	Rabbit	WB	Eusera*	EU1
Anti-His	Mouse	WB	Qiagen	34660
Anti-MCL1	Mouse	WB	Sigma	M8423
Anti-NMT1	Rabbit	WB	Proteintech	11546-1-AP
Anti-NMT1 (clone 14)	Mouse	WB	BD Biosciences	611301
Anti-NMT2 (clone 30)	Mouse	WB	BD Biosciences	611310
Anti-NMT2	Rabbit	IHC	Origene	TA504177
Anti-p21/WAF1	Mouse	WB	Abcam	AB16767
Anti-PARP-1	Rabbit	WB	Eusera*	N/A
Anti-V5	Rabbit	WB	Sigma Aldrich	V8137
Anti-α-tubulin	Mouse	WB	Sigma Aldrich	T5168

*****Eusera is a company founded by Dr. Berthiaume that sells antibody online (www.eusera.com).

Table 2.5: Plasmids used in this study

Plasmid	Source
NMT1 ORF-Express shuttle clone (entry clone)	Genecopoeia
NMT2 ORF-Express shuttle clone (entry clone)	Genecopoeia
pcDNA-DEST^{TM}53 (GFP)	Life Technologies
pcDNA-DEST^{TM}17 (Hexa histidine)	Life Technologies
pcDNA3.1/nV5DEST (V5)	Life Technologies
pET-19b (Hexa histidine)	Novagen, Life Technologies
GFP-NMT1	This work
GFP-NMT2	This work
V5-NMT1	This work
V5-NMT2	This work
His-NMT1	This work
His-NMT2	This work
V5-NMT1 (D72E)	This work
V5-NMT2 (D25E)	This work
V5-NMT2 (D67E)	This work
His-73NMT1	This work
His-26NMT2	This work
His-68NMT2	This work

Table 2.6: Oligonucleotide primers used in this study

Primer	Primer Sequence 5' to 3'	Engineered restriction site	Use
V5-NMT1 (D72E) forward	GCAGTGAGACAGAATCAGCCCAGGATC	N/A	Site-directed mutagenesis
V5-NMT1 (D72E) reverse	GATCCTGGGCTGATTCTGTCTCACTGC	N/A	Site-directed mutagenesis
V5-NMT2 (D25E) forward	CGTGCGGGATAGAAGGGGACAATGAG	N/A	Site-directed mutagenesis
V5-NMT2 (D25E) reverse	CTCATTGTCCCCTTCTATCCCGCACG	N/A	Site-directed mutagenesis
V5-NMT2 (D67E) forward	GGCACCAAGTCAGAATCGGCATCTGATTC	N/A	Site-directed mutagenesis
V5-NMT2 (D67E) reverse	GAATCAGATGCCGATTCTGACTTGGTGCC	N/A	Site-directed mutagenesis
His-D73 NMT1 forward	AAAAAA<u>CATATG</u>ATGTCAGCCCAGGATCAGCCT	NdeI	NMT1 caspase cleaved truncated vector
His-D73 NMT1 reverse	AAAAAA<u>CTCGAG</u>CTATTGTAGCACCAGTCCAAC	XhoI	NMT1 caspase cleaved truncated vector

Table 2.6 Oligonucleotide primers used in this study (continued)

Primer	Primer Sequence 5' to 3'	Engineered restriction site	Use
His-D26 NMT2 forward	AAAAAACATATGATGGGGGACAATGAGGAG	NdeI	NMT2 caspase cleaved truncated vector
His-D26 NMT2 reverse	AAAAAAGGATCCCTATTGTAGTACTAGTCCAAC	BamHI	NMT2 caspase cleaved truncated vector
His-D68 NMT2 forward	AAAAAACATATGATGTCGGCATCTGATTCCCAG	NdeI	NMT2 caspase cleaved truncated vector
His-D68 NMT2 reverse	AAAAAAGGATCCCTATTGTAGTACTAGTCCAAC	BamHI	NMT2 caspase cleaved truncated vector

Table 2.7: Cell lines used in this study

HL: Hodgkin's Lymphoma, ALCL: Anaplastic Large cell Lymphoma, ATCC: American type culture collection

Cell	Description	Source
BL2	Human, B lymphocyte, Burkitt lymphoma	Dr. Robert Ingham (University of Alberta)
CEM	Human, T lymphoblast, Leukemia	Dr. Karl Riabowol (University of Calgary)
COS-7	African green monkey, kidney cell	ATCC
Daudi	Human, B lymphocyte, Burkitt lymphoma	Dr. Robert Ingham (University of Alberta)
HD-MYZ	Human, B lymphocyte, HL	Dr. Robert Ingham (University of Alberta)
HeLa	Human, cervical cell, adenocarcinoma	ATCC
IM9	Human, B lymphoblast, Epstein-Barr virus (EBV) transformed	ATCC
Jurkat T	Human, peripheral blood, T lymphocyte (leukemia)	Dr. Michele Barry (University of Alberta)
Jurkat T caspase 8 dominant negative (Jurkat T - C8DN)	Human, peripheral blood, T lymphocyte (leukemia), caspase 8 dominant negative. First used in (Juo et al., 1998)	Dr. Shairaz Baksh (University of Alberta)
Karpas 299	Human, T lymphoblast, Lymphoma	Dr. Robert Ingham (University of Alberta)
KMH2	Human, B lymphocyte, HL	Dr. Robert Ingham (University of Alberta)
L0	Human, B lymphoblast, Epstein-Barr virus (EBV) transformed	Dr. Karl Riabowol (University of Calgary)
L428	Human, B lymphocyte, HL	Dr. Robert Ingham (University of Alberta)

Table 2.7 Cell lines used in this study *(continued)*

Cell	Description	Source
MCF-7	Human, mammary gland/breast, derived from metastatic site pleural effusion	Dr. Shairaz Baksh (University of Alberta)
MCF-7 / caspase 3	Human, mammary gland/breast, derived from metastatic site pleural effusion. First used in (Kagawa et al., 2001)	Dr. Shairaz Baksh (University of Alberta)
Ramos	Human, B lymphocyte, Burkitt lymphoma	Dr. Robert Ingham (University of Alberta)
Sup-M2	Human, T lymphoblast, ALCL	Dr. Robert Ingham (University of Alberta)
UCONN	Human, T lymphoblast, ALCL	Dr. Robert Ingham (University of Alberta)
VDS	Human, B lymphoblast, Epstein-Barr virus (EBV) transformed	Dr. Robert Ingham (University of Alberta)

2.2 Methodology

2.2.1 Molecular cloning

2.2.1.1 Gateway cloning: Engineering of V5-, GFP- and His-tagged NMTs

NMT1 and NMT2 entry clones (ORFEXPRESS^{TM}-Shuttle clones) compatible with the Gateway^{TM} cloning system (Life Technologies, Grand Island, N.Y.) were purchased from Genecopoeia (Rockville, MD). The full-length human NMT1 and NMT2 genes were incorporated into the destination vector pcDNA-DEST^{TM} 53 (GFP-tagged), pcDNA3.1/nV5 DEST(V5-tagged) or pcDNA-DEST^{TM} 17 [Hexa histidine (His)-tagged] (Life Technologies) using the LR clonase II enzyme (Life Technologies) according to the manufacturer's instructions.

Typically, 75 ng of Gateway entry clone (NMT1 and NMT2) was incubated with 75 ng of Gateway destination vector and the reaction volume brought up to 4 μL with TE buffer, pH 8.0. 1 μL of Gateway LR clonase II enzyme mix was added to the mixture and reactions were incubated at room temperature for 1h. Subsequently, 0.5 μL of Proteinase K (2 μg/ μL) solution was added to each sample, vortexed and incubated at 37^{o}C to terminate the reaction. Next, 1 μL of each LR clonase reaction was transformed into 50 μL chemically competent DH5α cells as

described below. Gateway cloning was used to generate the following N-terminally-tagged NMTs: GFP-NMT1, GFP-NMT2, His-NMT1, His-NMT2, V5-NMT1 and V5-NMT2. The GFP- and V5-tagged NMT constructs were used for mammalian cell expression, whereas His-NMT constructs were used for bacterial expression. The cloning products were confirmed by DNA sequencing (Eurofins MWG Operon).

2.2.1.2 Mutation of caspase cleavage sites in V5-NMT by site-directed mutagenesis

The NMT1 and NMT2 caspase cleavage sites identified by Edman degradation sequencing (Alphalyse) were mutated by site-directed mutagenesis. Therefore, we used previously cloned V5-NMT1 and V5-NMT2 gateway vectors to mutate the identified caspase cleavage sites. Hence, the Asp-72 residue of V5-NMT1 and Asp-25, Asp-67 and both Asp-25,67 (double mutant) residues of V5-NMT2 were mutated using the Quickchange® site-directed mutagenesis kit (Agilent Technologies) according to manufacturer's instructions.

Briefly, site-directed mutagenesis was performed using 5 to 50 ng of dsDNA (vector), 5 μL of 10x reaction buffer, 125 ng of primers dissolved in nuclease-free water and was brought up to a final reaction volume of 50 μL with nuclease-free water. 2.5 U of *PfuTurbo* DNA polymerase (Agilent Technologies) was added to the mix prior to starting the reaction, which

was performed for 18 cycles in the Eppendorf Mastercycler 1 thermocycler. Subsequently, the parental dsDNA was digested by adding 10 U of *Dpn* I restriction enzyme to each reaction and incubating for 1 h at 37^{o}C. Additionally, the primers for site-directed mutagenesis were designed using the PrimerX program (http://www.bioinformatics.org/primerx/) (listed in **table 2.6**). Importantly, the aspartate (D) residues of the caspase cleavage sites were mutated into glutamate (E) residues to generate the following vectors; V5-NMT1 (D72E), V5-NMT2 (D25E), V5-NMT2 (D67E) and V5-NMT2 (D25,67E). The mutations were confirmed by automated DNA sequencing (Eurofins MWG Operon).

2.2.1.3 Generation of His-tagged caspase-cleaved, truncated NMT vectors

The following caspase cleaved, truncated NMTs were generated by molecular cloning; His-73NMT1, His-26NMT2 and His-68NMT2. The truncated DNA sequences were cloned into the pET-19b (Novagen®) vector, which has an N-terminal hexa histidine (His)-tag sequence.

Previously cloned gateway vectors, GFP-NMT1 and GFP-NMT2 were used as templates for these PCR reactions. PCR reactions were performed using Platinum Pfx® DNA polymerase (Life Technologies) and PCR reactions were set up as per manufacturer's guidelines. Each PCR

reaction was prepared as follows; 200ng DNA template, 5 μL 10X Pfx amplification buffer, 5 μL 10X PCR enhancer solution, 1 mM $MgSO_4$, 0.3 mM dNTP mixture, 0.5 μM each of forward and reverse primers (listed in table **2.6**), 1 U Platinum Pfx® DNA polymerase and nuclease free water upto 50 μL. The reaction was set up in the Eppendorf Mastercycler 1 Thermocycler as per guidelines provided in the Platinum Pfx® DNA polymerase kit and the reactions were performed in 30 cycles.

2.2.2 Methodology used for molecular cloning

2.2.2.1 Purification of PCR products and restriction enzyme digestion

QIAquick® PCR purification kit from Qiagen was used to purify PCR products from other contaminating PCR components as per manufacturer's instructions. Nuclease free water was used to elute purified PCR products and 13-15 μL of PCR product was used for restriction enzyme digestion. The digestion was performed in a reaction volume of 20 μL, with PCR products, 1 U of specified restriction enzymes and when required 0.1 mg/mL of BSA was added to the reaction.

2.2.2.2 Use of agarose gel electrophoresis to isolate DNA fragments

Agarose gels were made by dissolving 1%-2% (w/v) electrophoresis grade agarose in TAE buffer by heating. Next, 1X SYBR® safe DNA stain was added when the agarose was slightly cooled and gels were poured. Next, DNA samples were mixed with 6X DNA gel loading dye, loaded on to the agarose gel and separated by gel electrophoresis. Accordingly, DNA was visualized using a FluorChem FC imaging system (Alpha Innotech Corporation) or a ultra-violet gel transilluminator (Fisher Biotech electrophoresis system). DNA extraction from agarose gels was done using the GENECLEAN® Turbo PCR purification kit (Q-BIOgene) as per manufacturer's instructions and DNAs were eluted using 30 – 50 μL nuclease-free water.

2.2.2.3 DNA ligation

Once extracted from agarose gels and purified, the DNA inserts and vectors were combined at approximately 3:1 (v/v) ratio. Next, T4 DNA ligase was used to ligate the DNA in the buffer supplied by the manufacturer for 2 h at room temperature

2.2.2.4 Bacterial transformation and extraction of DNA plasmids

Prior to bacterial transformation, 50-500 ng of DNA was added to 25-50 μL of chemically competent DH5α, gently mixed and incubate on ice for 30 min. For the transformation of ligated DNA, 5 μL of ligation mixture was added to 50 μL of chemically component DH5α. Next, the DNA-bacterial mixture was heat shocked by placing the mixture at 42^{o}C for 45 seconds. This was followed by a 5 min recovery incubation on ice. Subsequently, 950 μL of SOC was added and the mixture was shaken in an incubator set at 37^{o}C for 1 h. Following the incubation, the transformed DH5α was spread on pre-warmed LB agar plates that have the suitable selective antibiotic. DNA plasmids were purified from bacteria using the QIAGEN plasmid mini or midi kits according to manufacturer's instructions.

2.2.3 Cell Culture and Maintenance

COS-7 and HeLa cells were maintained in DMEM supplemented with 10% fetal bovine serum (FBS), 100 U/mL penicillin, 0.1 mg/mL streptomycin and 2mM L-Glutamine. MCF7, VDS, L0, IM9, Ramos, BL2, Daudi, BJAB, KMH2, Jurkat T and CEM cell lines were maintained in RPMI medium supplemented with 10% FBS, 100 U/ml penicillin, 0.1 mg/ ml

streptomycin, 1 mM sodium pyruvate and 2mM L-Glutamine. All cells used were maintained at 37°C and 5% CO_2 in a humidified incubator.

2.2.4 Cellular transfection with plasmid DNA

Cells were transiently transfected with the indicated constructs using FuGene 6 or X-tremeGENE 9 DNA transfection reagents according to manufacturer's protocols. Cells were maintained in DMEM supplemented with 10% fetal bovine serum (FBS), 100 U/mL penicillin, 0.1 mg/mL streptomycin and 2mM L-glutamine. The DNA complexes in transfection reagent were left in the medium for 22 hours.

2.2.5 Inhibition of caspases

Cells were pre-treated with 10 μM of established caspase inhibitors purchased from EMD Chemicals, 1 hour prior to the induction of apoptosis. The caspase inhibitors used were general caspase inhibitor (z-VAD-FMK), caspase-3 (z-DEVD-FMK), caspase-8 (z-IETD-FMK), caspase-9 (z-LEHD-FMK) and negative control (z-FA-FMK). The control cells were treated with DMSO (1:1000).

2.2.6 Treatment of cells with MG-132

IM9, KMH2, BL2 and Ramos cells were plated ($3x10^6$ cells per well in a 6-well dish) and treated with 10 μM MG-132 for 5 hours. Equal amount of DMSO was added to the control samples. Cells were then lysed and subjected to SDS-PAGE/Western blot analyses.

2.2.7 Treatment of cells with suberoylanilide hydroxamic acid (SAHA)

IM9, BL2 and Ramos cells were plated at $3x10^6$ cells per well in a 6-well dish and treated with 1 μM suberoylanilide hydroxamic acid (SAHA), which is a reversible inhibitor of class I and class II histone deacetylases (HDACs), for 24 hours. Equal amount of DMSO was added to cells as a control. Cells were lysed and subjected to SDS-PAGE/Western blot analyses.

2.2.8 Apoptosis Induction

150 or 300 ng/mL mouse anti-Fas antibody was used to stimulate apoptosis through the extrinsic pathway and 2.5 μM staurosporine (STS) was used to stimulate apoptosis through the intrinsic pathway. Where indicated, cycloheximide (5 μg/mL) was used to inhibit protein translation and to further promote cell death.

2.2.9 Treatment of cells with NMT inhibitor, 2-hydroxymyristic acid (HMA)

HMA was saponified and conjugated to bovine serum albumin (BSA) prior to addition to cells to facilitate its cellular uptake as described previously (Yap et al., 2010). Briefly, HMA was incubated with a 20% molar excess of potassium hydroxide (KOH) at 65°C for 15 min. Subsequently, a 20X solution was made by dissolving the KOH saponified HMA in serum-free RPMI media containing 20% fatty acid-free BSA at 37°C, followed by an additional 15 min incubation at 37°C. Since sodium myristate was used as a control, it was also incubated in serum-free RPMI media containing 20% fatty acid-free BSA at 37°C prior to addition to cells.

Subsequently, Jurkat T cells (1×10^7 cells) were incubated with either 1mM HMA or 1mM sodium myristate conjugated to fatty-acid free BSA (final concentration in cell culture 1%) for 1 h at 37^oC in RPMI media (without FBS, supplements or antibiotics). After incubation, apoptosis was induced using anti-Fas (150 ng/mL) or STS (2.5 μM) with cycloheximide (5 μg/mL) or vehicle alone (DMSO). Samples were collected every 2 h for an 8 h period, washed with cold PBS and lysed with 0.3 mL of 1% sodium dodecyl sulfate (SDS)-radio-immuno-precipitation assay (RIPA) buffer and subjected to 2 rounds of sonication for 15 seconds at an output of 5.5-6.5 on a Branson Sonifier and placed on ice for 2 min in between each cycle.

2.2.10 Treatment of lymphocytic cell lines with NMT inhibitor, Tris DBA

2 x 10^6 cells (CEM, L0, BL2 and Ramos) were grown in 6 well plates and incubated with increasing amounts (0, 1, 2 and 5 μg/ml) of Tris (dibenzylideneacetone) dipalladium (Tris DBA) (Bhandarkar et al., 2008). The viability of cells treated with Tris DBA was measured with a trypan blue exclusion assay (Hudson, 1976).

2.2.11 Treatment of lymphocytic cell lines with NMT inhibitors, DDD85646 and DDD73226

1 x 10^5 cells [KMH2 (Hodgkins lymphoma), IM9 ("normal" EBV immortalized B cell), BL2, Ramos] (100 μL/well) were plated in 96-well plates and treated with increasing amounts of the pyrazole sulfonamide based NMT inhibitor DDD85646 [Molecular weight (MW) 495.43] (Frearson et al., 2010) and a less potent pyrazole sulfonamide based analog DDD73228 (MW=362.5) for 24, 48 and 72 hours. The drugs were dissolved in DMSO to make 100X stock solutions for each concentration tested, so that the final volume of DMSO in each well was 1%. The viability of cells treated with these inhibitors was measured with a trypan blue exclusion assay (Hudson, 1976).

2.2.12 Treatment of lymphocytic cell lines with NMT inhibitor, DDD86481

1 x 10^5 cells [KMH2 (Hodgkin's lymphoma), IM9 ("normal" EBV immortalized B cell), BL2, Ramos] (100 μL/well) were plated in 96-well plates and treated with increasing amounts of DDD86481 [MW 610.5]. The drugs were dissolved in DMSO to make 100X stock solutions for each concentration tested, so that the final volume of DMSO in each well was 1%. MTS [(3-(4,5-dimethylthiazol-2-yl)-5-(3-carboxymethoxyphenyl)-2-(4-sulfophenyl)-2H-tetrazolium)] assay was used to measure the cytotoxicity of the drug (Cory et al., 1991).

2.2.13 Cell lysis

Typically, cells were washed in cold PBS, harvested, lysed in 0.1% SDS-RIPA buffer or 0.1% SDS-RIPA-HEPES buffer (when cells were labeled with alkyne-fatty acids) that was supplemented with 1X complete protease inhibitor. The cell suspension was rocked for 15 min at 4^{o}C. Cell lysates were then centrifuged at 16,000 *g* for 10 min at 4^{o}C and the post-nuclear supernatant was collected. Protein concentrations were measured using Pierce^{TM} bicinchoninic acid (BCA) protein assay kit (Thermo Fisher Scientific, Waltham, MA).

2.2.14 Lysis of Lymophoma tissue samples

Human diffuse large B-cell lymphoma (DLBCL) and follicular lymphoma (FL) tissues were kind gifts from Dr. Raymond Lai (Cross Cancer Institute, Alberta, Canada). The frozen tumor tissues were cut into small (~1 mm^3) pieces and mixed with 1% SDS-RIPA with 1X complete protease inhibitor. Samples were homogenized using a small Dounce homogenizer and then sonicated repeatedly for 2 min with 1 min intervals (on ice) in between at an output of 6.0 (Branson Sonifier 450) until the tumor tissues dissolved in the lysis buffer. The samples were then centrifuged at 16,000 *g* for 10 min at 4^oC and the post-nuclear supernatant was collected for western blotting analyses.

2.2.15 Sodium dodecyl sulphate polyacrylamide gel electrophoresis (SDS-PAGE) and western blotting

Typically, protein samples were prepared in 1X SDS-PAGE sample loading buffer and samples were heated at 95^oC for 5 min. Laemmli SDS-PAGE gels (percentages ranging from 8 – 15%) (Laemmli, 1970) were used to separate proteins, based on the separation requirements of the experiments. Following electrophoresis, proteins were proteins were transferred onto nitrocellulose or Immobilon-P PVDF membranes by using either the Bio-Rad Trans Blot apparatus (100V for 2 h) or the Bio-Rad

Trans-Blot turbo transfer system (25V for 30 min) apparatus. Following protein transfer, membranes were blocked in either 5% BSA or 5% non-fat skim milk (NFM) in Tris-buffered saline (TBS) containing 0.1% Tween 20 for 1 h at room temperature or at 4^{o}C overnight with gentle rocking. Subsequently, the membranes were incubated with the indicated primary antibodies and the membranes were subjected to 6 wash cycles, lasting 5 min each; 2 washes in PBS, 2 washes in PBS with 0.1% Tween 20, and finally 2 washes in PBS. Following the washes, the membranes were incubated with the corresponding HRP-conjugated secondary antibodies, washes were repeated as before and the membranes were processed for ECL detection as per manufacturer's instructions.

2.2.16 Western blotting using Odyssey scanner

(*Note: This method was only used for the cleaved caspase-3 blot provided in* ***figure 4.14****, all other western blotting was done using the standard procedure described in 2.2.15 in the materials and methods section*)

Following electrophoresis, gels were transferred onto a nitrocellulose membrane and blocked in 5% NFM in PBS with 0.1% Tween 20 (PBS-T) for 1 hour. The primary antibody (rabbit anti-cleaved caspase-3; Cell Signaling) was also diluted at 1:2000 in 5%NFM in PBS-T, added to the membrane and incubated for 24 h. Next, the membranes

were subjected to 6 wash cycles, lasting 5 min each; 2 washes in PBS, 2 washes in PBS-T, and finally 2 washes in PBS. The secondary antibody (Alexa Fluor 680 goat-anti-rabbit; Life Technologies) was added after diluting in PBS-T (1:5000) and the blots were covered in aluminum foil and incubated with the secondary antibody for 1h and subjected to the same 6X wash cycle with PBS and PBS-T as before. Blots were scanned on Odyssey ® fluorescence imaging system from LI-COR Inc. at a scanning resolution of 84 μm (Intensity: 5 to 7) on channel 700 (for rabbit).

2.2.17 Subcellular fractionation

HeLa cells were grown to confluency in 150 mm plates and were induced to undergo apoptosis with anti-Fas (300 ng/mL) (extrinsic) or STS (intrinsic) for a period of 5 h. Cells were then metabolically labeled with alkyne-C14 (described in detail in the section below) (Yap et al., 2010) and subjected to hypotonic lysis.

Briefly, cells were washed with cold PBS buffer, scraped off the plates using a cell lifter, and collected. Samples were then centrifuged at 2000 *g* for 5 min, the supernatant was aspirated and cells were resuspended in 600 μL of hypotonic buffer that causes cells to swell (Mg resuspension buffer) and incubated on ice for 20 min. The cell suspension was transferred to a Dounce homogenizer and homogenized with 45 strokes using the tight pestle. Consequently, 400 μL of EDTA-free 2.5X

homogenization buffer (HB) was added to the homogenate and the cells were homogenized with 15 strokes in the Dounce homogenizer using the loose pestle. The homogenate was then centrifuged at 1000 *g* for 5 min and the post-nuclear supernatant (PNS) was collected. Next, 200 μL of PNS was saved and remainder (~750 μL) was centrifuged at 100,000 *g* for 45 min in a Beckman TLA 120.2 rotor, which resulted in a cytosolic fraction (S100) and a light membrane pellet (P100).

The P100 pellet was washed once with 1X HB and the P100 fractions were adjusted to the volume of the cognate S100 fraction using 1X HB. Following this, the resulting post-nuclear supernatant (PNS), cytosolic fractions (S100) and membrane fractions (P100) fractions were adjusted to contain 1% SDS. Consequently, the same fraction volume was subjected to western blot analysis and protein levels were quantified using Image J software (http://rsbweb.nih.gov/ij/).

2.2.18 Metabolic labeling of cells using bio-orthogonal ω-alkynyl myristic acid and click chemistry

2.2.18.1 Metabolic labeling of cells using ω-alkynyl myristic acid

Cells were labeled with 100 to 25 μM ω-alkynyl myristic acid 30 min prior to harvesting the cells and lysed in 0.1%SDS-RIPA-HEPES buffer. Protein (50 - 30 μg) from the resulting cell lysates were reacted with 100

μM azido-biotin using click chemistry and processed as described previously (Yap et al., 2010). Briefly, cells were starved of fatty acids by incubating in media (RPMI or DMEM) which were supplemented with 5% dextran-coated charcoal-treated FBS (DCC-FBS) for 1 h prior to labeling. Next, ω-alkynyl-myristic acid was dissolved in DMSO to generate 25 or 100 mM stock solutions. Typically, the cellular uptake of ω-alkynyl myristic acid typically was improved with saponification and conjugation to BSA. Therefore, prior to labeling, ω-alkynyl myristic acid was saponified with 20% molar excess of potassium hydroxide at 65°C for 15 min. Next, serum-free culture media (pre-warmed) containing 20% fatty acid-free BSA at 37°C was added to the saponified ω-alkynyl myristic acid and incubated for an additional 15 min at 37°C.

Subsequently, cells deprived of fatty acids were washed once with warm PBS and incubated in fresh RPMI or DMEM without any supplements. Next, the appropriate volume of 20X fatty acid-BSA conjugate in serum-free media was added to the cells, to ensure that the final concentration of BSA was 1% and ω-alkynyl myristic acid was at the indicated concentration (25 μM or 100 μM) for each respective experiment. DMSO or unlabeled fatty acids conjugated to BSA were used as controls for the experiments performed. Cells were labeled with ω-alkynyl myristic acid for 30 min at 37°C in a 5% CO_2 humidified incubator prior to harvesting. Cells were harvested in 0.1% SDS-RIPA-HEPES

buffer that was supplemented with 1X complete protease inhibitor (EDTA-free).

2.2.18.2 Click chemistry

After labeling cells with ω-alkynyl myristic acid, the resulting lysates were subjected to click chemistry with azido-biotin to enable the detection of the myristoylated proteins by ECL as described previously (Yap et al., 2010). Typically, cell lysates (30 – 50 μg of protein) were adjusted to to contain 1% SDS and incubated with 100 μM Tris-(benzyltriazolylmethyl)amine (TBTA), 1 mM $CuSO_4$, 1 mM Tris-carboxyethylphosphine (TCEP), and 100 μM azido-biotin at 37°C for 30 min in darkness, in order for the click reaction to proceed. Next, 10 volumes of ice-cold acetone was added to stop the click reaction and proteins were precipitated at −20°C overnight. Subsequently, the acetone precipitated proteins were centrifuged at 16,000 *g* for 10 min, resuspended in 1X SDS-PAGE sample buffer with 20 mM DTT. Samples were then heated at 95^{o}C for 5 min and subjected to SDS-PAGE, and transferred on to PVDF membranes for western blot analysis.

2.2.18.3 Treatment of PVDF membranes with neutral Tris-HCl or KOH

Protein samples were loaded on duplicate SDS-PAGE gels for the experiments where PVDF membranes were treated with KOH or neutral Tris-HCl. After electrophoresis, the KOH treated PVDF membranes were incubated in 100 ml of 0.1 N KOH in methanol [1 N KOH in H_2O: methanol 1:9 (v/v)], whereas the other was incubated in 0.1 N Tris-HCl pH 7.0 in methanol [1 N Tris-HCl, pH 7.0:methanol 1:9 (v/v)] at room temperature for 45 min with gentle shaking. Subsequently, the treated membranes were washed thoroughly with PBS, probed with Streptavidin-HRP or Neutravidin-HRP and detected with ECL.

2.2.19 Radioactive NMT activity assay in cells undergoing apoptosis

NMT activity was measured by adapting a protocol developed by the Sharma laboratory (King and Sharma, 1991; Raju and Sharma, 1999). A stock solution of [^{3}H]-myristoyl-CoA was prepared freshly and synthesized as described previously (Towler and Glaser, 1986). To make a 200 μL stock solution of [^{3}H]-myristoyl-CoA, 97 μL of myristoyl-CoA generation buffer was combined with 20 μL of 50 mM ATP, 10 μL of 20 mM LiCoA, 60 μL of *pseudomonas* acyl-CoA synthetase and 13 μL of [9,10 – ^{3}H]-myristic acid. The solution was mixed gently and incubated at 37^{o}C for 30 min.

For this assay, COS-7 cells transiently transfected with plasmids encoding for V5-NMT1 and V5-NMT2 were induced to undergo apoptosis with STS (2.5 μM) and cycloheximide (5 μg/ml) or not, and, harvested at 0, 1, 2, 4 and 8 h time points. The cells were sonicated using a Branson sonifier 450 and ~20 μg of lysate (lysed in 50 mM NaH_2PO_4 pH 7.4, 0.25M sucrose buffer) was used for each reaction. For each NMT assay reaction, 3.85 μL of NMT assay buffer, 1.25 μL 20% Triton X-100 and 2.5 μL (0.1 mM) myristoylatable (**BID_G**: **G**NRSSHSRLG) or non-myristoylatable (**BID_A**: **A**NRSSHSRLG) decapeptide (purchased from Peptide 2.0 Inc.) corresponding to the N-terminal sequence of ct-Bid (1mM stock in ethanol) was added to a microcentrifuge tube and kept on ice before the start of the reaction. At the start of the reaction, 7.4 μL (10 pMol) of freshly synthesized of [^{3}H] myristoyl-CoA was added to each microcentrifuge tube containing the NMT assay mixture at 15 second intervals and 25 μL reactions were incubated for 15 min at 30^{o}C. The reaction was terminated by spotting 15 μL of the reaction mixture onto a P81 phosphocellulose paper disc (Whatman) at 15 second intervals and dried with a hair dryer for 30 seconds.

Next, the p81 phosphocellulose paper discs were transferred to the washing unit and washed 3 times, 30 min each, with NMT assay wash buffer for a total period of 90 min. Subsequently, the radioactivity remaining on the phosphocellulose (which corresponds to the myristoylated peptide) was quantified in 5 mL of liquid scintillation mixture

using a Beckman Coulter LS6500 scintillation counter. The NMT activity was calculated as fmol/min/μg of protein.

2.2.20 Use of a radioactive assay to measure NMT activity in purified His-tagged NMTs

The NMT activity of full length and truncated His-tagged NMTs were measured using the same protocol as described above. However, only 1 μg of purified protein (volume was brought up to 10 μL in NMT assay buffer) was used in this assay. The NMT activity was calculated as fmol/min/nanomole (nmol) of protein.

2.2.21 *In vitro* NMT cleavage assay

The *in vitro* NMT cleavage assay was performed by incubating 10 μg of purified His-NMT1 and His-NMT2 with 1 μg of recombinant human active caspase-3 or -8 in caspase cleavage assay buffer in 100 μL reactions for 1 hour at 37 ^{o}C. Reaction was terminated with the addition of 10 μM general caspase inhibitor z-VAD-FMK and subsequently 5X sample loading buffer were added. Reacted samples were separated on a 10% SDS-PAGE gel and transferred onto a PVDF membrane. The bands were visualized by Coomassie blue staining and cleavage fragments were

excised from the membrane and sent for Edman degradation to Alphalyse in Palo Alto, CA.

2.2.22 Protein purification of recombinant His-NMTs

Lemo21(DE3) pLysS competent cells (New England Biolabs) were transformed with His-NMT1 and His-NMT2 vectors according to manufacturer's protocol. NMT1 and NMT2 proteins were prepared as follows: a 3 mL starter culture was grown in LB broth (1% tryptone, 0.5% yeast extract, 0.5% NaCl, 100 μg/mL ampicillin and 34 μg/mL Chloramphenicol) for 4 h at 37^{o}C, while shaking at 225 rpm. The entire culture was used to inoculate a 50 mL culture which was grown at 37^{o}C for 16 h. Next, the bacterial cells were pelleted by centrifugation at 6000 x g for 10 min at room temperature. The bacterial pellet was resuspended in 10 mL LB and 5 mL of the resuspension was used to inoculate 500 mL of LB that was incubated at 37^{o}C with vigorous shaking (225 rpm) until an OD_{600} of 0.5-0.6 was reached.

Next, protein expression was induced by 0.5 mM Isopropyl β-D-1-thiogalactopyranoside (IPTG) addition at 30^{o}C with vigorous shaking (225 rpm) for 4 h. The suspension was centrifuged at 6000 x g at 4^{o}C for 20 min and the bacterial pellet was frozen overnight. Subsequently, the thawed bacterial pellet was resuspended in 25 mL bacterial lysis buffer supplemented with complete protease inhibitor (CPI) from Roche and

incubated on ice for 30 min. Samples were then sonicated 3 times for 1 min with 1 min intervals in between at an output of 5.0 (Branson Sonfier 450) and incubated at 37^{o}C for 30 min prior to centrifugation at 15,000 x g for 1 h at 4^{o}C.

Meanwhile, Ni-NTA agarose beads (His-Pure Ni-NTA resin from Thermo Fisher Scientific) were packed into columns according to manufacturer's instructions and washed with column buffer three times. The clear supernatant obtained from the previous centrifugation was then loaded into the column and incubated with gentle shaking at 4^{o}C for 1 h. The sample was then eluted from the column by gravity flow and the column was washed twice with 5 mL wash buffer (column buffer with 20 mM imidazole, pH 8.0). Next, 2 x 5 mL of elution buffer 1 (column buffer with 75 mM imidazole, pH 8.0) was used to elute the first two fractions and 2 x 5 mL of elution buffer 2 (column buffer with 150 mM imidazole, pH 8.0) was used to elute the next two fractions. The last fraction was eluted with elution buffer 3 (column buffer with 250 mM imidazole, pH 8.0). Finally, 20% glycerol was added to each of the fractions collected before freezing at -80^{o}C. Samples from each step of the protein purification process was collected, run on a 12.5% SDS-PAGE gel and stained with Coomassie blue in order to determine which fraction(s) had the highest concentration of protein.

Since samples from the first four elutions had the highest protein concentration, they were pooled and dialysed to remove any imidazole

present. Hence, the pooled samples were loaded on to Spectra/Por 2 (Spectrum Laboratories) dialysis tubing with a molecular weight cut off (MWCO) 12 – 14 kDa to remove any small degraded protein fragments. Protein samples were then dialyzed in 4 L of chilled dialysis buffer for 2 h at 4^{o}C with gentle stirring, followed by overnight dialysis with the same buffer at 4^{o}C with another 4 L of fresh, chilled buffer. Dialyzed protein samples were concentrated by spinning in Amicon Ultra-15 centrifugal filter with MWCO 30 kDa (Millipore) at 5,000 g, 4^{o}C until desired volumes were achieved.

2.2.23 qRT-PCR of B cell lymphoma cell lines

RNA was isolated from IM9, KMH2, Ramos and BL2 cells using TRIzol® reagent according to manufacturer's protocols. Next, the High Capacity cDNA Reverse Transcription kit with a random primer scheme from Applied Biosciences was used to synthesize cDNA from the isolated RNA according to manufacturer’s instructions. Quantitative real time PCR (qRT PCR) reactions were set-up using the TaqMan® Universal Master Mix II and NMT1, NMT2 and 18 Taqman® probes purchased from Life Technologies (Carlsbad, CA) and three replicates of each reaction were set up according to supplier’s guidelines. qRT PCR was performed using a Mastercycler® ep *realplex* thermocycler (Eppendorf) and results were analyzed using the *Realplex* software (Eppendorf).

2.2.24 Trypan Blue Exclusion Assay

The viability of cells treated with Tris DBA, DDD73228, and DDD85646 was measured by incubating cells with TC10^{TM} Trypan Blue Dye (Biorad) (Hudson, 1976), according to manufacturer's instructions. Cell viability was then quantified using the TC10^{TM} automated cell counter (Biorad).

2.2.25 MTS [(3-(4,5-dimethylthiazol-2-yl)-5-(3-carboxymethoxyphenyl) -2-(4-sulfophenyl)-2H-tetrazolium)] Assay

The viability of cells treated with DDD86481 was measured using the CellTiter 96 AQ_{ueous} Non-Radioactive cell proliferation assay (MTS) (Cory et al., 1991) from Promega according to manufacturer's instructions.

2.2.26 Immunohistochemistry

B cell lymphoma tumors were fixed in formalin and embedded in paraffin and cut on a microtome to desired thickness (~5 microns or μm) and affixed onto a Superfrost® plus positively charged slide (Fisher Scientific). Before staining the slides containing tumor tissues were deparaffinized by dipping in xylene 3 times for 10 min each, a series of washes in ethanol [20 dips in 100% ethanol (repeat 4 times), 20 dips in

80% ethanol, and 20 dips in 50% ethanol] and a final wash in running cold water for 10 min.

For antigen retrieval, slides were loaded in a slide holder and placed in a Nordicware® microwave pressure cooker and 800 mL of 10 mM citrate buffer pH 6.0 was added to it. The pressure cooker was tightly closed, placed in a microwave and microwaved on high for 20 min. Next, slides were washed in cold running water for 10 min. Peroxidase blocking was performed by soaking slides in 3% H_2O_2 in methanol for 10 min and washing with warm running water for 10 min before washing in PBS for 3 min.

Next, excess PBS was removed and a hydrophobic circle was drawn around the sample with a PAP pen (Sigma-Aldrich). Rabbit anti-NMT1 (Proteintech) or rabbit anti-NMT2 (Origene) were diluted with Dako antibody diluent buffer (Dako, Agilent Technologies) at 1:50 dilution and added with a Pasteur pipette (~400 μL per slide) and incubated in a humidity chamber overnight at 4^{o}C. Subsequently, slides were washed in PBS twice for 5 min each and ~4 drops of DAKO EnVision+System-HRP labeled polymer (anti-Rabbit) (Dako, Agilent Technologies) was added to each slide and incubated at room temperature for 30 min. Slides were washed again in PBS twice for 5 min each, 4 drops of Liquid DAB (diaminobenzidine) + substrate chromogen (prepared according to manufacturer's instructions; Dako, Agilent Technologies) was added, developed for 5 mins and rinsed under running cold water for 10 min.

The slides were then soaked in 1% $CuSO_4$ for 5 min, rinsed briefly with running cold water, counter stained with haematoxylin for 60 sec and rinsed with running cold water until water ran clear. Next, slides were dipped in lithium carbonate 3 times and rinsed with running tap water briefly. Slides were then dehydrated in a series of steps; 20 dips in 50% ethanol, 20 dips in 80% ethanol and 20 dips in 100% ethanol (repeat 4 times) and finally in xylene (3 times for 10 min each). Coverslips were then added to the slides and microscopy of the tumor samples were performed using a Nikon eclipse 80i microscope. Images were created using a QImaging scientific camera (Qimaging).

Chapter 3

Characterization of the roles of N-myristoyltransferases in co- and post-translational myristoylation

A version of this chapter has been published in **Perinpanayagam, M.A.**, Beauchamp, E., Martin, D.D.O., Sim, J.Y.W., Yap, M.C., Berthiaume, L.G. The regulation of co- and post-translational myristoylation of proteins during apoptosis: interplay of N-myristoyltransferases and caspases. *FASEB J.* (2013) **27**(2), 811-21

3.1 Overview

Protein lipidation plays a major role in targeting proteins to various membranes, membrane domains and organelles within cells. Examples of lipid modifications of proteins include isoprenylation, glypiation, cholesteroylation and fatty acylation (Magee and Seabra, 2005). Fatty acylation primarily encompasses palmitoylation and myristoylation. Palmitoylation typically represents the attachment of the 16-carbon fatty acid (palmitic acid) to cysteine residues of proteins via a labile thioester bond. Myristoylation involves the co- or post-translational addition of the saturated 14-carbon fatty acid, myristic acid, to the amino (N) -terminal glycine of a protein via an amide bond.

The consensus sequence required for co-translational N-myristoylation of a protein is Gly_2-X_3-X_4-X_5-$(Ser/Thr/Cys)_6$ where "X" represents most amino acids except proline, aromatic or charged residues at X_3 [reviewed in (Wright et al., 2010; Martin et al., 2011)]. While Ser, Thr, or Cys are preferred at X_6, other amino acids, such as Ala and Gly, are also tolerated at this position. Co-translational myristoylation requires the removal of the initiator methionine by methionine amino peptidase (MetAP), while **c**ysteinyl **asp**artic prote**ases** (caspases), and presumably yet to be identified proteases, are required to expose an N-terminal glycine residue to the action of NMT in post-translational myristoylation. A glycine residue is an absolute requirement at position 2; the substitution of this glycine reside to any other amino acid residue abrogates myristoylation.

The enzymes responsible for myristoylation are N-myristoyltransferases (NMTs) 1 and 2 and human NMTs (hNMT1 and hNMT2) have been identified, cloned and characterized (Duronio et al., 1992; Giang and Cravatt, 1998). They exhibit 77% amino acid sequence identity with most of the divergence occurring at their N-terminal domains (Giang and Cravatt, 1998). In NMT1, the N-terminal sequence was shown to be important for targeting the enzyme to ribosome enriched fractions (Glover et al., 1997), while the carboxy-terminal domain contains the catalytic active site (Rudnick et al., 1992a; Bhatnagar et al., 1998). A separate study confirmed that the basic-amino-acid-rich cluster sequence [named the lysine (K) box], located within the N-terminal region of both enzymes is essential for the binding of NMT1 and 2 to the ribosome enriched fractions (Takamune et al., 2010). Different studies have demonstrated that the two NMTs exhibit both overlapping and different substrate specificities (Giang and Cravatt, 1998; Ducker et al., 2005). This was exemplified by the simple depletion of NMT2 by siRNA in SKOV-3 cells, which led to a 2.5-fold greater effect in inducing apoptosis (19% of cell death) when compared to cells depleted of NMT1(7.8% cell death), indicating that NMT2 in particular plays a more prominent role in a cell survival (Ducker et al., 2005).

For many years, myristoylation was thought to occur only co-translationally, until the C-terminal fragment of caspase truncated Bid (ct-Bid) was demonstrated to be post-translationally myristoylated during

apoptosis (Zha et al., 2000). Since then, work done by the laboratories of Utsumi and ours have identified the caspase cleaved C-terminal products of actin (Utsumi et al., 2003), gelsolin (Sakurai and Utsumi, 2006), p21-activated kinase 2 (PAK2) (Vilas et al., 2006) and PKCε (Martin et al., 2012) to be post-translationally myristoylated. Furthermore, in Martin *et al*. (Martin et al., 2008) and Yap *et al.* (Yap et al., 2010), we demonstrated the existence of several proteins (>15), which are post-translationally myristoylated in apoptotic Jurkat T cells. Recently, our laboratory developed a method named tandem reporter assay for myristoylated proteins post-translationally (TRAMPP) in order to identify new post-translationally myristoylated proteins (Martin et al., 2012). By utilizing this method, we have been successful in identifying 5 more potential caspase-cleaved substrates for post-translational myristoylation, which include a key anti-apoptotic regulator, the apoptotic regulator-induced myeloid leukemia cell differentiation protein (Mcl-1) and the causal agent of Huntington's disease, huntingtin (Htt) (Martin et al., 2012).

Apoptosis is the tightly regulated process used by eukaryotic organisms to remove superfluous or defective cells. Apoptosis is stimulated by extrinsic (e.g. Fas ligand, anti-Fas antibody, TNFα) or intrinsic [e.g. UV irradiation, DNA damage, staurosporine (STS)] stimuli and is launched by the activation of the caspase cascade. Apoptotic stimuli cause the cleavage and the activation of initiator caspases (i.e.: caspase-8 – extrinsic pathway, caspase-9 – intrinsic pathway), which

sequentially cleave and activate effector caspases (e.g. caspase-3, caspase-7). Effector caspases are responsible for the cleavage and the activation or inactivation of a myriad of substrates including poly-ADP-ribose-polymerase 1 (PARP-1) and PAK2 (Solary et al., 1998) leading to dismantling of the cell and death. Notably, caspase-9 can also be activated through the extrinsic cell death pathway. More specifically, the binding of external apoptotic stimuli such as Fas ligand to its cognate receptor or cross-linking of Fas using anti-Fas antibodies leads to activation of caspase-8 and the cleavage of Bid. The resulting caspase cleaved C-terminal Bid (ctBid) is myristoylated and directed to the mitochondria, where it causes the release of cytochrome c, the formation of the apoptosome and activation of caspase-9 (Zha et al., 2000; Shawgo et al., 2009).

Because of the opposing roles of post-translationally myristoylated proteins wherein ctBid and ctPAK2, have been shown to be pro-apoptotic while post-translationally myristoylated ctGelsolin and ctPKCε are anti-apoptotic (Zha et al., 2000; Utsumi et al., 2003; Sakurai and Utsumi, 2006; Vilas et al., 2006; Martin et al., 2012), we think post-translational myristoylation could play an important role in the regulation of the balance between cell death and cell survival. The existence of numerous post-translationally myristoylated proteins in various apoptotic cells (Hang et al., 2007; Martin et al., 2008; Charron et al., 2009; Hannoush and Arenas-Ramirez, 2009; Martin and Cravatt, 2009; Yap et al., 2010; Heal et al.,

2011), combined with the potential regulatory role for post-translational myristoylation in dying cells, has prompted us to investigate the regulation of N-myristoyltransferases during apoptosis.

Our results indicate that NMT1 is a substrate of caspase-3 and caspase-8, whereas, NMT2 is a substrate of caspase-3 and we have identified the cleavage site located at the N-termini of both NMTs. The cleavages of NMTs during apoptosis resulted in a change of subcellular localization like it is often the case for other proteins participating in apoptosis regulation [e.g. Bid, PAK2, Inhibitor of Caspase Activated DNAse (ICAD) and the protein kinases Mst-1 and MEKK] (Enari et al., 1998; Zha et al., 2000; Jakobi, 2004; Vilas et al., 2006). Concomitantly, we observed a change in the myristoylation profile as the cells switched from co-translational to post-translational myristoylation during apoptosis. Overall, our results suggest caspases play a key role in post-translational myristoylation by not only regulating the rate of substrate production, but also by controlling the localization of the NMTs themselves. Since apoptosis is often suppressed in cancer, the reduced caspase activity seen in cancer cells might also explain the high NMT activity and/ or NMT1 levels observed in many cancers (Magnuson et al., 1995; Raju et al., 1997b; Rajala et al., 2000; Shrivastav et al., 2003; Lu et al., 2005; Selvakumar et al., 2007; Shrivastav et al., 2009).

3.2 Results

3.2.1 NMT cleavage on the induction of apoptosis

Because of the large number of post-translationally myristoylated proteins in apoptotic cells (Martin et al., 2011) and the fact that NMTs catalyze both co- and post-translational myristoylation, we sought to investigate the role(s) of NMTs in living and dying cells. To do this, Jurkat T cells induced to undergo programmed cell death with anti-Fas or STS were analyzed for their content in NMTs. The treatment of Jurkat T cells with either anti-Fas or STS resulted in the time dependent cleavage of both NMT1 and NMT2 (**Fig. 3.1**). The cleavage of NMT1 began 2 h after the induction of cell death, while that of NMT2 was only detectable after 4 h of apoptosis. This observation was consistent in both the anti-Fas and STS treated cells. The fact that NMT1 cleavage precedes that of NMT2 can also be seen in **figure 3.10**. Although it is possible that the NMT1 and NMT2 antibodies exhibit different affinities towards the proteins, therefore NMT1 could appear to be cleaved earlier than NMT2 if the sensitivity of the NMT1 antibody were to be greater than that of the NMT2 antibody. The cleavage of NMT1 migrating at an apparent 67 kDa protein (predicted M.W. = 56.8 kDa) resulted in an apparent ~46 kDa fragment (**Fig. 3.1**). The cleavage of NMT2 migrating as an apparent 65 kDa protein (predicted M.W. = 56.9) produced an apparent ~55 kDa fragment at early time

points, which was converted into a shorter fragment migrating at or below ~46 kDa at later time points (4 and 8 h) (**Fig. 3.1**). This shorter NMT2 fragment was seen overlapping with a non-specific protein band in figure **3.1**. However, it was more visible in the Fas-treated Jurkat cell lysates in figures **3.2** (8h) and **3.4 A** (4h and 8h). Thus, the cleavages of NMT1 and NMT2 result primarily and initially in the loss of ~11 kDa and ~10kDa fragments, respectively. The reason for the discrepancies between the apparent migrations and predicted molecular weights of NMTs is not known. The timing of the cleavage of NMTs paralleled that of the apoptotic marker PARP-1 suggesting it is due to the action of caspases.

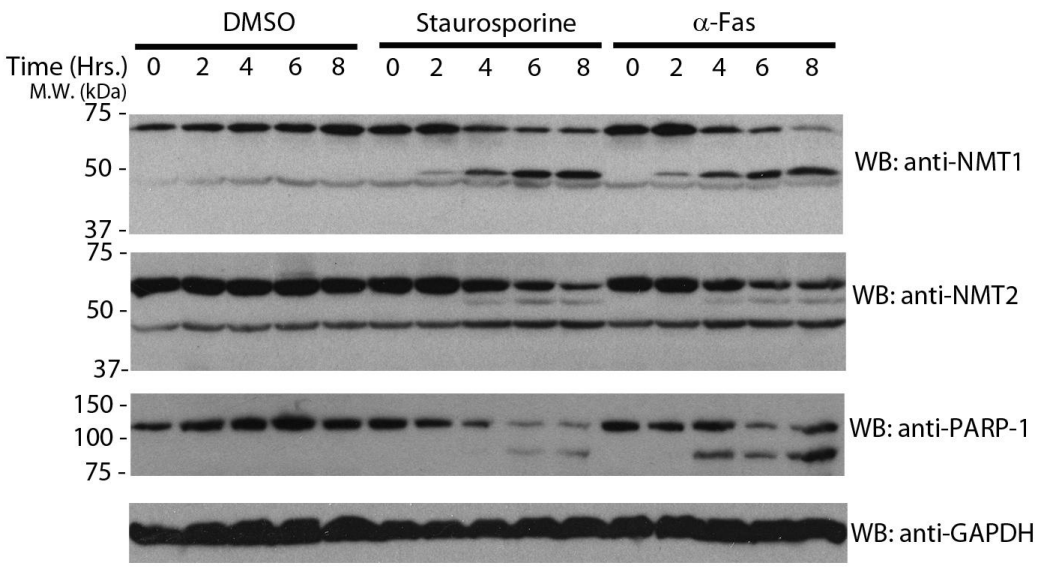

Figure 3.1: NMT cleavage upon induction of apoptosis. Jurkat T cells were treated with DMSO, staurosporine (2.5 μM) or anti-Fas (300 ng/ml) with cycloheximide (5 μg/mL) and samples were collected at 0, 2, 4, 6 and 8 h time points. Cells were lysed and the presence of NMT1, NMT2, PARP-1 and GAPDH was assessed by western blotting using ECL

3.2.2 NMT1 is a substrate of caspases-3 or -8, and NMT2 is a substrate of caspase-3

To investigate whether caspases are involved in the cleavage of NMTs, we induced anti-Fas mediated apoptosis in Jurkat T cells in the presence or absence of well-characterized irreversible inhibitors of caspases-3, -8, and -9 along with a general inhibitor of caspases and analyzed the cellular contents for both NMTs. The cleavage of NMT1 was abrogated by the general and caspase-8-specific inhibitors, whereas it was only partially blocked by the caspase-3-specific inhibitor (**Fig. 3. 2**), which suggests that NMT1 is a substrate of caspases-3 or -8. In contrast, NMT2 cleavage was noticeably inhibited by all caspase inhibitors used (**Fig.3.2**). This suggests that NMT2 is likely a substrate of caspase-3 since the inhibition of the initiator caspases-8 or -9, would in turn inhibit the cleavage and activation of the effector caspase-3 (please refer to **Fig. 3.3** for the caspase activation cascade). The progression of apoptosis induced by anti-Fas was verified by western blotting with anti-PARP-1 antibody (**Fig. 3.2**). The extent of PARP-1 cleavage was concomitant with and commensurate to that of NMT1 and NMT2. Of note, the effectiveness of the caspase inhibitors used in this study was optimized and validated in Jurkat T and COS-7 cells with a variety of known caspase targets by western blotting (unpublished data).

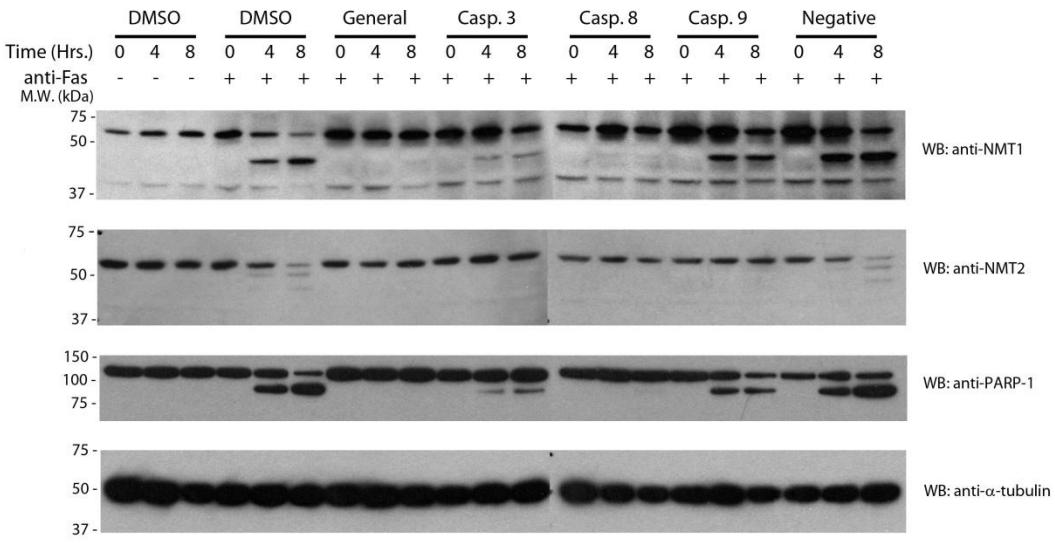

Figure 3.2: Cleavage of NMT1 and NMT2 in Jurkat T cells undergoing apoptosis in the presence of caspase inhibitors. A. Jurkat T cells were treated with 10 μM caspase inhibitors for one hour and then treated with anti-Fas (300 ng/mL) and cycloheximide (5 μg/mL) to induce apoptosis. Samples were collected at 0, 4, and 8 h time points. Cells were lysed and the presence of NMT1, NMT2 and PARP-1 was assessed by western blotting using ECL. The blots were then stripped and reprobed with anti-tubulin (loading control) (composite gels).

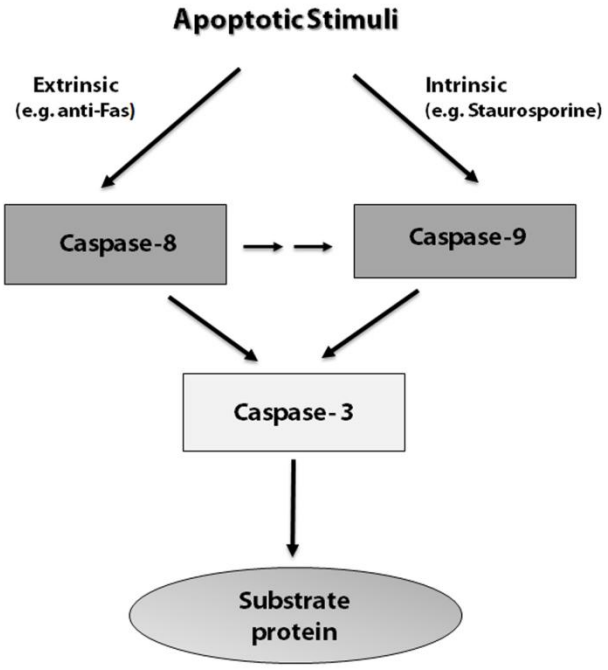

Figure 3.3: Schematic of the extrinsic and intrinsic apoptotic pathways highlighting the caspase activation cascade.

In order to validate the NMT1 cleavage by caspase-8, the cleavage of NMT1 was investigated in wild-type Jurkat T and Jurkat T cells expressing a caspase-8 dominant negative mutant (C8DN) (Juo et al., 1998). The expression of C8DN in apoptotic Jurkat T cells severely abrogated the cleavage of NMT1 when compared to levels seen in the wild-type Jurkat T cells (**Figs. 3.4A and B**). Furthermore, we observed a minimal amount of NMT2 cleavage in Jurkat-C8DN cells after 8 h of apoptosis induction (**Fig. 3.4B**). Since we did not see a significant cleavage of NMT2 in Jurkat C8DN cells undergoing apoptosis, we rationalized that the inactivation of caspase 8 (which is cleaved and activated during Fas-induced apoptosis) in Jurkat C8DN cells would in turn abrogate the cleavage of caspase 3, which we have shown to be responsible for NMT2 cleavage (**Fig. 3.2**). As demonstrated in Figure **3.4B**, the cleavage of PARP-1 and caspase-8 was also inhibited in the Jurkat T-C8DN cells. This further confirmed that NMT1 is indeed a likely substrate of caspase-8. Of note, NMT1 appears occasionally as a doublet on western blots. The presence of the doublet was not due to phosphorylation and appeared to vary with the lot/batch/age of the monoclonal antibody used (unpublished data).

The potential NMT2 cleavage by caspase-3 was re-assessed in MCF-7 cells known to be deficient in caspase-3. We found that both NMT1 and NMT2 were not cleaved in apoptotic MCF-7 cells at the 8 h time point (**Fig. 3.5A**). In contrast, both enzymes were readily cleaved in

apoptotic MCF-7 cells stably expressing caspase-3 (Kagawa et al., 2001) (**Fig. 3.5B**). The cleavage of the known caspase-3/-7 substrate PARP-1 was also confirmed in both MCF-7 cell lines when apoptosis was induced (**Figs. 3.5 A and B**) (Walsh et al., 2008). Therefore, both NMTs appear to be substrates of caspase-3.

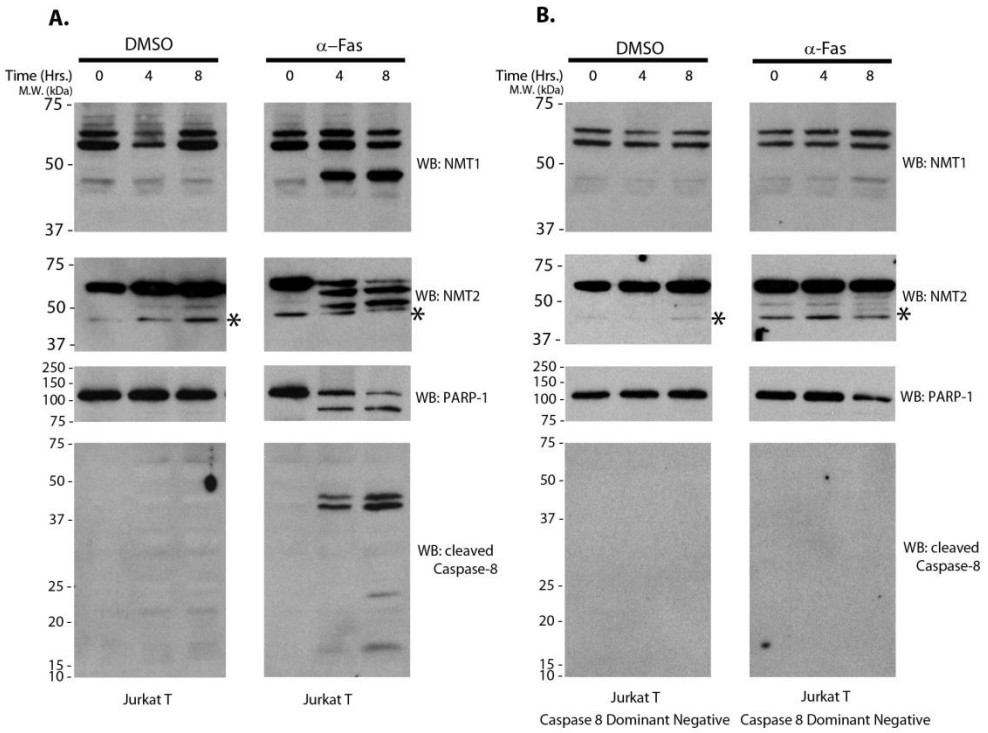

Figure 3.4: NMT1 is cleaved by caspase-8, but not NMT2. Jurkat T cells (**A**) and Jurkat T cells expressing a caspase-8 dominant negative mutant (**B**) were treated with DMSO or anti-Fas (150 ng/mL) and samples were collected at 0, 4 and 8 h time points. Cells were lysed and the presence of NMT1, PARP-1 and cleaved caspase-8 was assessed by western blotting using ECL. * denotes non-specific bands.

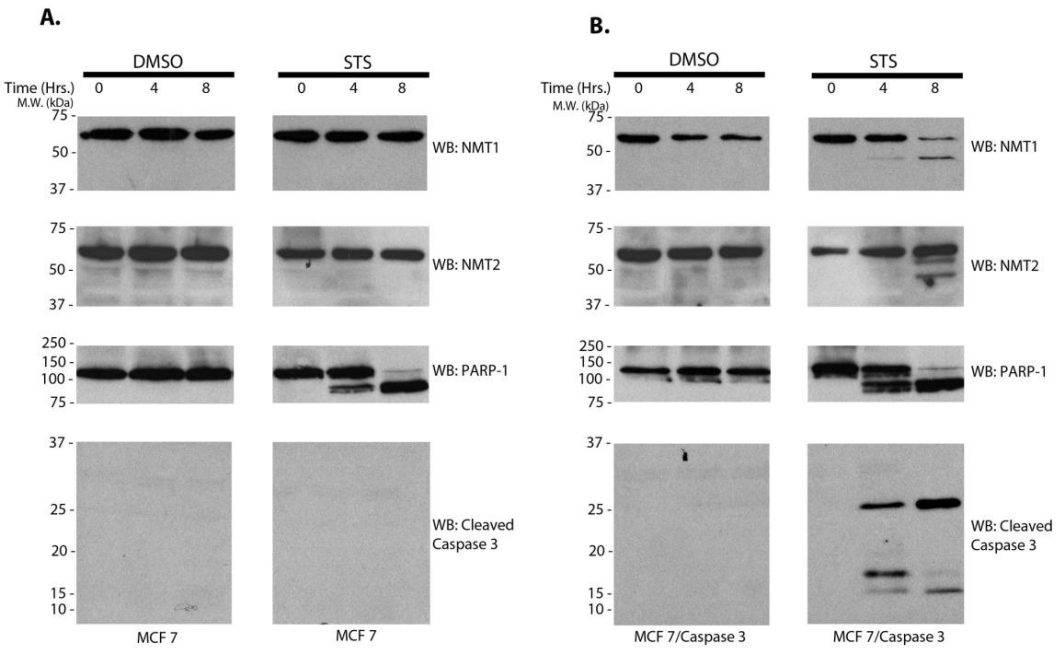

Figure 3.5: Both NMT1 and NMT2 are cleaved by caspase-3. MCF7 (**A**) and MCF7 expressing caspase 3 (MCF7/caspase 3) (**B**) were treated with DMSO or STS (2.5 μM) with cycloheximide (5 μg/mL) and samples were collected at 0, 4 and 8 h time points. Cells were lysed and the presence of NMT2, PARP-1 and cleaved caspase 3 was assessed by western blotting using ECL.

3.2.3 N-terminal sequencing (Edman degradation) reveals caspase cleavage sites of NMTs.

To identify the caspase-cleavage sites, we reconstituted the caspase cleavage of purified recombinant N-terminally tagged His-NMT1 and His-NMT2 (**Figs. 3.14 and 3.15**) with commercially available caspases-3 and -8 *in vitro* and the cleaved fragments were excised and sent for N-terminal sequencing (**Fig. 3.6**). The majority of NMT1 was cleaved by caspase-3 to generate one ~48 kDa fragment, whereas NMT1 cleavage by caspase-8 generated a fragment of the same size and also a larger fragment (~56kDa) (**Fig. 3.6**). Protein sequencing revealed the main caspase-8 (~48kDa) NMT1 cleavage product occurs after Asp (D)-72 (**Fig. 3.7**). Sequencing of the larger ~56 kDa fragment revealed that NMT1 may also be cleaved at Asp (D)-38 (**Fig. 3.7**). Because the cleavage of endogenous NMT1 during apoptosis repeatedly results in one cleavage fragment of ~46 kDa in cells, we presume the non-specific cleavage of His-NMT1 at D-38 by purified caspase-8 *in-vitro* might be non-physiological.

Cleavage of NMT2 by caspase-3 also resulted in 2 cleavage fragments (~54 and ~47 kDa), which correlated with the sizes of the two cleavage fragments observed with the endogenous NMT2 cleavage during apoptosis (~55 and ~46 kDa) (**Fig. 3.6**). When His-NMT2 was incubated with caspase-8 *in vitro*, no NMT2 cleavage was observed (**Fig. 3.6**),

further validating our earlier data that NMT2 is a substrate of caspase-3 and not caspase-8. N-terminal sequencing revealed that NMT2 was cleaved at both D-25 and D-67 sites (**Fig. 3.7**). Interestingly, we found that the cleavage sites for both NMT1 and NMT2 were located in the N-terminus of the enzymes and not in the C-terminal catalytic domain, which suggests that the cleaved enzymes may still be active during apoptosis.

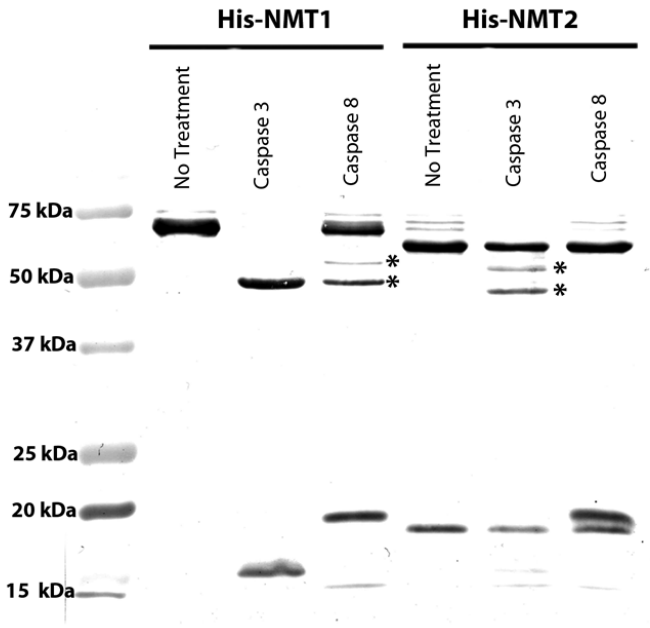

Figure 3.6: Identification of NMT cleavage sites by N-terminal sequencing (Edman degradation). Purified hexahistadine (His)-NMT1 and His-NMT2 (10 μg) was incubated with 1 μg of recombinant human active caspase-3 or -8. The samples were subjected to SDS-PAGE and transferred onto a PVDF membrane. The bands were visualized by coomassie blue staining. The cleavage fragments denoted by (*) were excised from the membrane and subjected to N-terminal sequencing by Edman degradation.

Figure 3.7 : The caspase cleavage sites of NMT1 and NMT2 as identified by Edman degradation are in bold font and the positively charged lysine (K) box is highlighted on the NMT1 and NMT2 amino acid sequences (amino acids 1 to 80).

3.2.4 Mutation of the aspartate residues in NMT caspase cleavage sites into glutamate residues severely abrogates the cleavage of the NMTs.

In order to validate the NMT cleavage sites revealed by N-terminal sequencing, we constructed N-terminally tagged V5-NMT vectors and used the Quickchange® site-directed mutagenesis kit (Stratagene) to create point mutations at the NMT cleavage sites. The engineered D72E mutation in V5-NMT1 abrogated the caspase-cleavage of V5-NMT1 in appropriately transfected HeLa cells induced to undergo apoptosis with STS for 4 h while the WT V5-NMT1 levels were severely diminished in these cells (**Fig. 3.8**). This confirmed D72 as the caspase-cleavage site in NMT1.

Because N-terminal sequencing revealed two caspase cleavage sites (D25 and D67) for NMT2 (**Fig. 3.8**), we mutated both D25 and D67 residues into glutamate (E) residues independently [V5-NMT2 (D25E), V5-NMT2 (D67E)] and together [V5-NMT2 (D25,67E)]. We observed that the cleavage of the V5-NMT2 (D25,67E) double mutant was severely abrogated in appropriately transfected apoptotic HeLa cells while the single mutants [V5-NMT2 (D25E), V5-NMT2 (D67E)] had varying effects (**Fig. 3.8**) and the wild-type V5-NMT2 was mostly cleaved after 5 h after apoptosis induction (**Fig. 3.8**). When comparing the integrity of the single mutants during apoptosis, we observed that V5-NMT2 (D25E) was

reproducibly slightly less cleaved than V5-NMT2 (D67E) (**Fig. 3.8**), suggesting that D25 might be the primary cleavage site of NMT2, whereas D67 may be a secondary cleavage site. Therefore, our mutagenesis studies confirm that NMT2 is cleaved at both D25 and D67 during apoptosis.

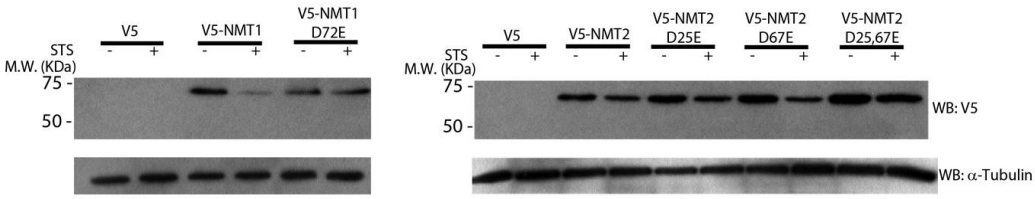

Figure 3.8: Confirmation of NMT cleavage sites by site-directed mutagenesis. HeLa cells transiently expressing the wild-type and mutant V5-NMT constructs were incubated with STS (2.5 μM). Cells transfected with V5-NMT1 or V5-NMT2 constructs were lysed at 4 h and 5 h time points, respectively. Western blotting was performed on the samples using V5 and α-tubulin (loading control) antibodies.

3.2.5 The protein myristoylation profile changes drastically during apoptosis.

Our previously published results demonstrated the existence of numerous post-translationally myristoylated proteins (Martin et al., 2008; Yap et al., 2010). Furthermore, proteomic studies aimed at identifying caspase cleavage sites revealed that caspase cleaved proteins frequently expose new N-terminal glycine residues (Dix et al., 2008; Mahrus et al., 2008). These observations further warranted the investigation of N-myristoylation as a novel type of regulator of apoptosis. To do so, Jurkat T cells were induced to undergo apoptosis using anti-Fas and metabolically labeled for 30 min with ω-alkynyl-myristic acid prior to havesting cells at various time points (0, 1, 2, 4 and 8 h). Cycloheximide was also added to cells to inhibit protein translation as part of the apoptotic stimulus, thereby blocking co-translational myristoylation during apoptosis. Cellular lysates were reacted with azido-biotin using click chemistry and biotinylated-myristoylated proteins were visualized by western blot analysis using NeutrAvidin^{TM}-HRP, as described previously (Yap et al., 2010).

The myristoylation profile at time 0 h correlated with the co-translational myristoylation pattern observed previously in non-apoptotic cells (**Fig. 3.9**) (Martin et al., 2008; Yap et al., 2010). The deliberately low exposure shows only a few myristoylated proteins in the cell lysates. Treatment of the membranes with 0.1M KOH confirmed that ω-alkynyl-

myristic acid is incorporated into proteins via an alkali resistant amide bond, since the alkali treatment removed the label from only a few protein bands. Of note, this alkaline treatment hydrolyzes thioester bonds found in palmitoylated proteins (Armah and Mensa-Wilmot, 1999; Zhao et al., 2000; Vilas et al., 2006). Interestingly, after induction of apoptosis with anti-Fas and cycloheximide for 1h, co-translational myristoylation was drastically reduced presumably as protein translation is inhibited by cycloheximide. This was followed by a drastic change in the cellular content of myristoylated proteins as illustrated by the major differences in electrophoretic myristoylated protein profiles starting at 2 h post-induction of apoptosis and ongoing for the duration of the experiment (**Fig. 3.9**). This result clearly shows that although NMTs are cleaved to various extents during apoptosis (**Fig. 3.10**), myristoylation activity appears to remain in cells up to 8 h after induction of apoptosis.

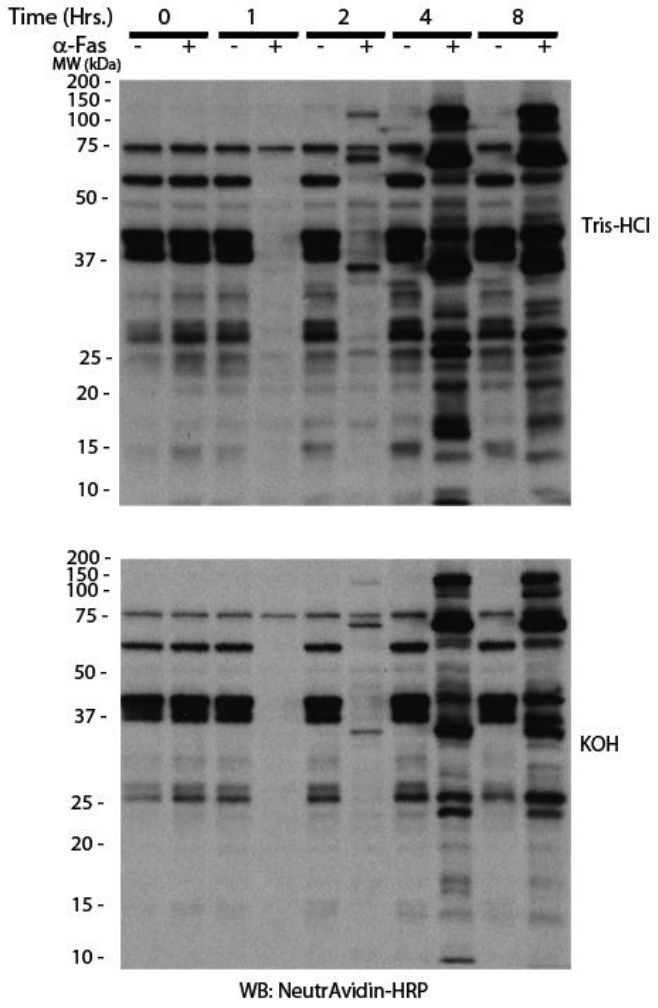

Figure 3.9 : Changes to the myristoylation profile as cells undergo apoptosis. Jurkat cells were metabolically labelled with 25 μM alkynyl-myristate after induction of apoptosis with anti-Fas (150 ng/mL) and cycloheximide (5 μg/ mL). Protein samples were reacted with azido-biotin using click chemistry and visualized by western blotting with NeutrAvidin™-HRP. Prior to the assessment of label incorporation by western blotting, membranes were incubated in 0.1 M Tris-HCl or 0.1 M KOH. *(Contributed by Dr. Erwan Beauchamp, corresponds to figure 5A in Perinpanayagam et al., 2013). Similar results were observed when I repeated this experiment.*

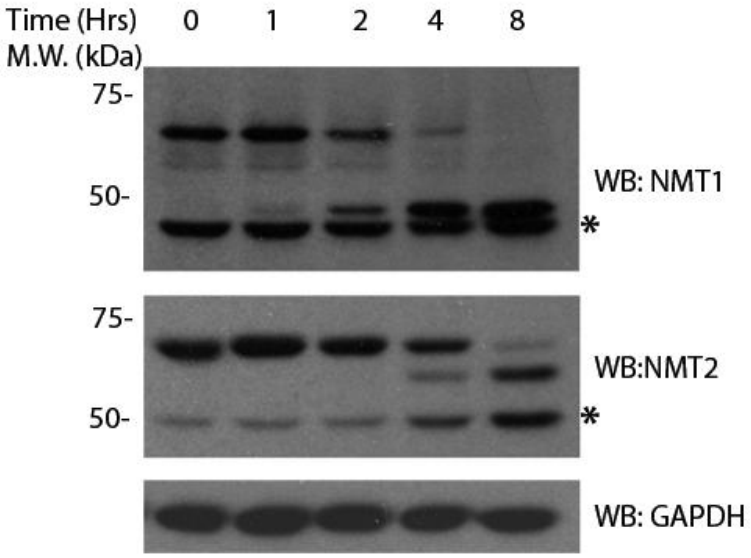

Figure 3.10 : Changes to NMT levels as cells undergo apoptosis. Jurkat cells were metabolically labelled with 25 μM alkynyl-myristate after induction of apoptosis with anti-Fas (150 ng/mL) and cycloheximide (5 μg/ mL) (**Fig. 3.9**). Western blotting was performed on the same samples as in figure **3.9** using antibodies against NMT1, NMT2 and GAPDH. (*) denotes non-specific bands. *(Contributed by Dr. Erwan Beauchamp, corresponds to figure 5B in Perinpanayagam et al., 2013).*

3.2.6 The cleavage of NMTs affects their catalytic activity, but does not abrogate it.

In order to assess whether cleaved NMTs were still catalytically active, we measured the V5-NMT enzymatic activity of transiently transfected cells expressing either V5-NMTs using a filter based-peptide assay (King and Sharma, 1991; Raju and Sharma, 1999) during the onset of apoptosis. This strategy was used because endogenous NMT activity levels were typically too low to be measured accurately. Thus, COS-7 cells transiently transfected with V5-NMT1, V5-NMT2 or empty vector were induced to undergo STS/cycloheximide-mediated apoptosis and used as a source of enzyme. NMT activity was measured at different times of apoptosis using [^{3}H]-myristoyl-CoA and myristoylatable- or non-myristoylatable (G->A) truncated Bid decapeptides were used as substrates (King and Sharma, 1991; Raju and Sharma, 1999). NMT activity was calculated from the amount of radiolabeled peptide that remained bound to the phosphocellulose paper and detected by scintillation counting.

Although the transfected COS-7 cells expressed similar levels of chimeric NMTs (**Fig. 3.11**), those expressing V5-NMT1 showed nearly a 5-fold higher NMT activity than those expressing V5-NMT2 at t=0h (**Fig. 3.12**). The amount of intact V5 -NMTs found in cell lysates decreased over time of apoptosis induction (**Fig. 3.11**) and followed a similar trend as the

endogenous NMTs (**Fig. 3.10**), although nearly all of the over-expressed NMT1 was cleaved after 4h and 8h of apoptosis and all of over-expressed NMT2 after 8h (**Fig. 3.11**). Interestingly, although greater than 90% of V5-NMT1 is cleaved (**Fig. 3.11**) at 4h after apoptotic induction, the NMT activity in those cells remained relatively unchanged up to 8 h after cell death was initiated. Of note, there was a slight trend towards the increase (although not significant) in NMT catalytic activity at t=2h and 4h, in the lysates of COS-7 cells over-expressing NMT1 when compared to activity at t=0h (**Fig. 3.13**). This suggests that cleaved V5-NMT1 is catalytically active during apoptosis when post-translational myristoylation is initiated. However, we observed a significant decrease in NMT activity (20%, $p<0.05$) at 8h after induction of apoptosis when compared to the 0h time point in the cells transfected with V5-NMT1 (**Fig. 3.13**).

The NMT activity of cells expressing V5-NMT2 was not significantly affected from 0h to 4h, until the caspase cleavage of V5-NMT2 resulted in a statistically significant ($p<0.005$) decrease (33% decrease when compared to activity to t=0h) in enzymatic activity after 8 h of apoptosis induction (**Fig. 3.13**). Interestingly, although the NMT2 levels are drastically reduced due to caspase cleavage during apoptosis (**Fig. 3.11**), 66% of NMT2 activity still remains after 8h of apoptosis induction (**Fig. 3.13**), indicating that NMT2 also plays a role in post-translational myristoylation of proteins during apoptosis.

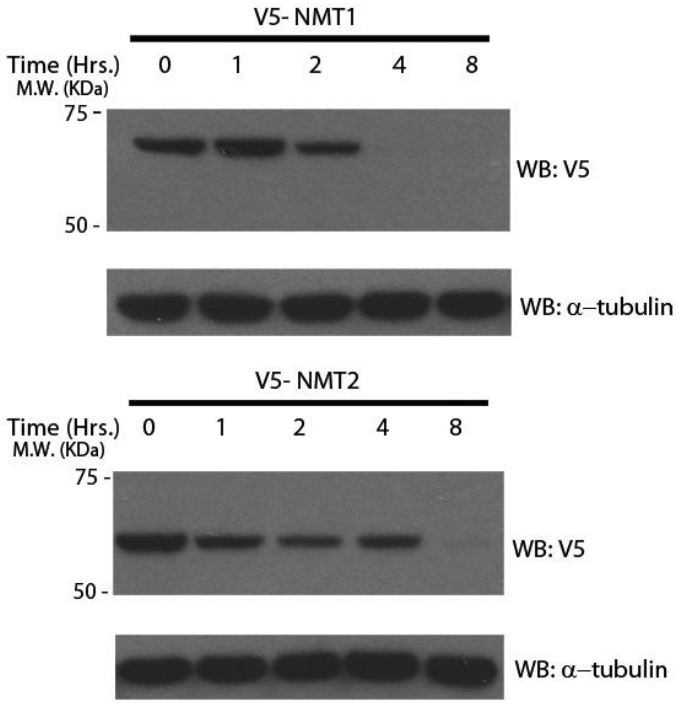

Figure 3.11: Induction of COS7 cells transiently expressing V5-NMT1 and V5-NMT2 to undergo apoptosis with staurosporine and cycloheximide. NMT activity was assayed using a peptide myristoylation assay (**Figs. 3.12 and 3.13**) and western blotting was performed on the same samples using antibodies against V5 and α-tubulin (loading control). *(Contributed by Dr. Erwan Beauchamp, corresponds to figure 5D in Perinpanayagam et al., 2013).*

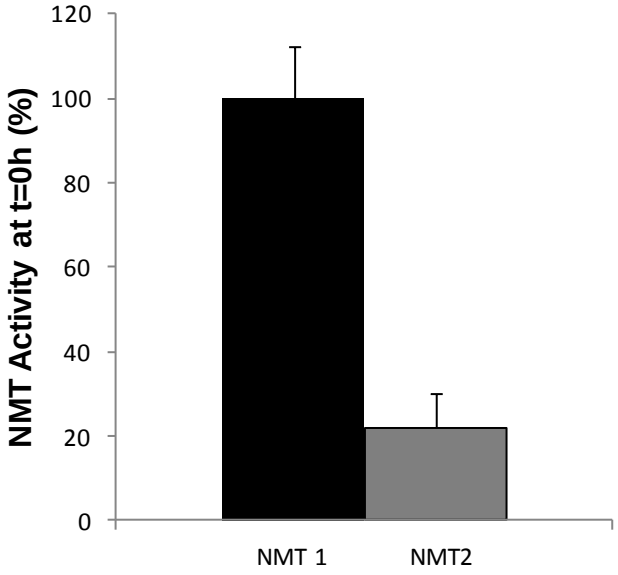

Figure 3.12: Initital NMT activity in the lysates of transiently transfected COS7 cells. COS7 cells transiently expressing V5-NMT1 and V5-NMT2 were incubated with STS (2.5 μM) and cycloheximide (5 μg/mL). NMT activity was assayed using a peptide myristoylation assay as described in materials and methods. N-Myristoyltransferase activity was calculated from the amount of radiolabeled myristoylpeptide produced and detected on phosphocellulose paper (adapted from King *et al.*1991, *Anal Biochem*.). Activity levels were normalized to NMT1 activity at t=0h. NMT1 represents the average of three independent experiments done in duplicates. NMT2 represents the average of four independent experiments done in duplicates. *(Contributed by Dr. Erwan Beauchamp, corresponds to supplementary fig. 1 in Perinpanayagam et al., 2013).*

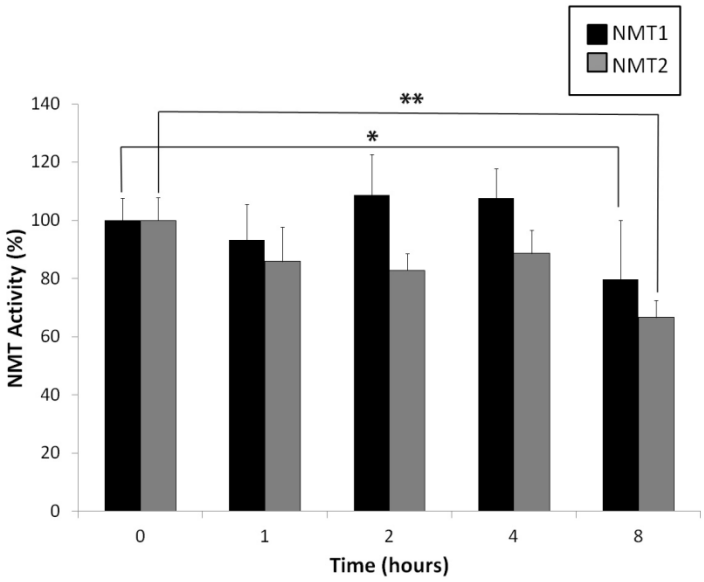

Figure 3.13: NMT activity in COS7 cells transiently expressing V5-NMT1 and V5-NMT2 incubated with staurosporine (2.5 μM) and cycloheximide (5 μg/mL). NMT activity was assayed using a peptide myristoylation assay as described under materials and methods. N-myristoyltransferase activity was calculated from the amount of radiolabeled myristoylpeptide produced and detected on phosphocellulose paper (adapted from King *et al.*1991, *Anal Biochem*.). NMT activity was normalized to 100% at t = 0 h for each NMT. NMT1 represents the average of three independent experiments done in duplicates. NMT2 represents the average of four independent experiments done in duplicates. Differences are denoted by (*) and show statistical significance (* < p=0.05, ** < p=0.005) when compared to the 0 h time point for both NMTs. *(Contributed by Dr. Erwan Beauchamp, corresponds to figure 5C in Perinpanayagam et al., 2013).*

3.2.7 *In-vitro* NMT assay using purified caspase-cleaved truncated NMTs reveal that NMTs are still active after caspase cleavage

Because our previous NMT assay using cell lysates over-expressing V5-NMT1 and V5–NMT2 revealed that caspase cleavage affects but does not abrogate NMT activity (**Fig. 3.13**), we sought to confirm that the caspase truncated human NMTs are catalytically active in an *in vitro* setting. Hence, we generated His-tagged full-length (His-NMT1 and His-NMT2) and caspase truncated (His-73NMT1, His-26NMT2 and His-68NMT2) human NMT vectors and used these vectors for bacterial expression and protein purification (**Fig. 3.14 and 3.15**). Using the filter-based peptide NMT assay (King and Sharma, 1991; Raju and Sharma, 1999), we found that both full-length and caspase cleaved truncated NMT1 and NMT2 were catalytically active when compared to the control in an *in vitro* setting (**Fig. 3.16**). Interestingly, the cleavage of NMT2 appears to enhance its activity as caspase cleaved truncated NMT2 is ~4-fold more active than full-length NMT2 (**Fig 3.16**).

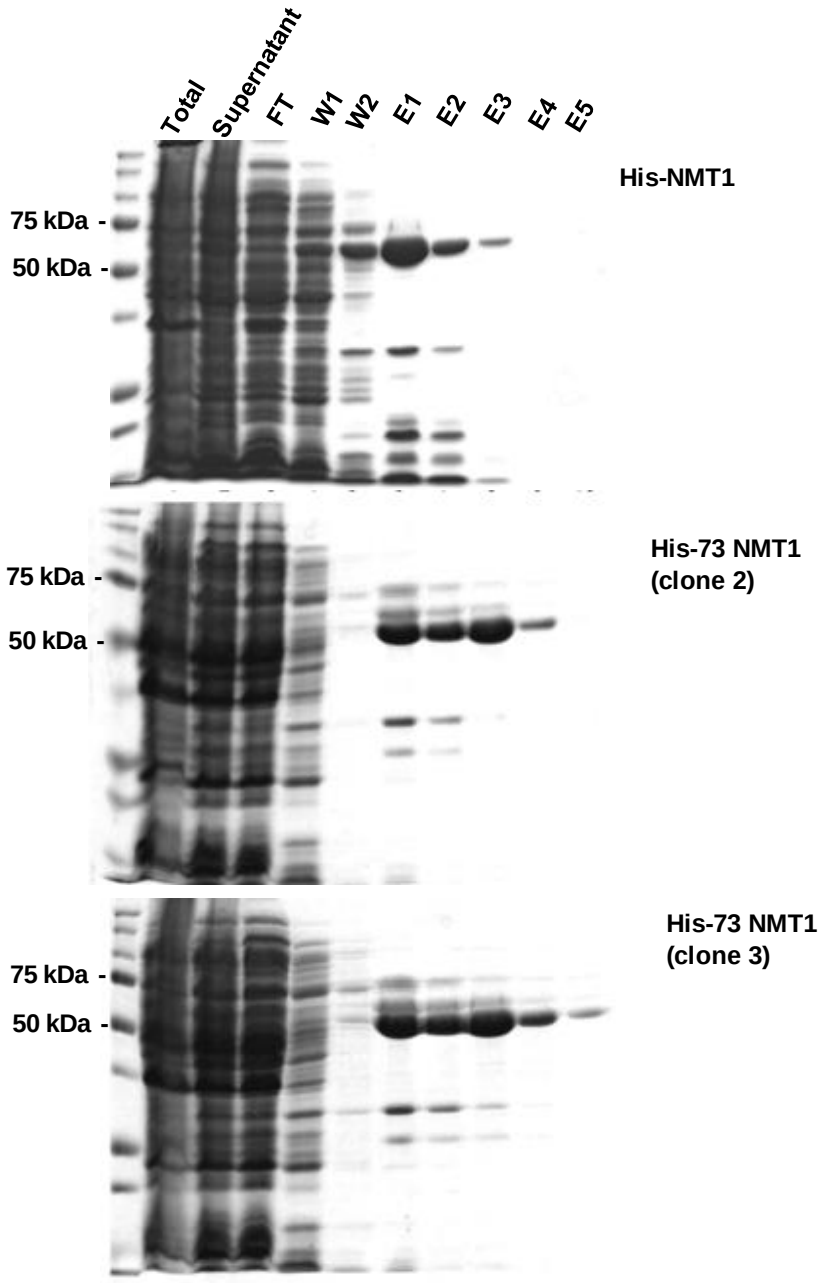

Figure 3.14: Purification of recombinant hexahistidine(His)-tagged full-length and caspase-cleaved hNMT1. Purification was performed using Ni-NTA chromatography (see materials and methods). Purified proteins were visualized by staining gels with coomassie blue gel stain. (FT: flow through, W: wash and E: eluted fractions)

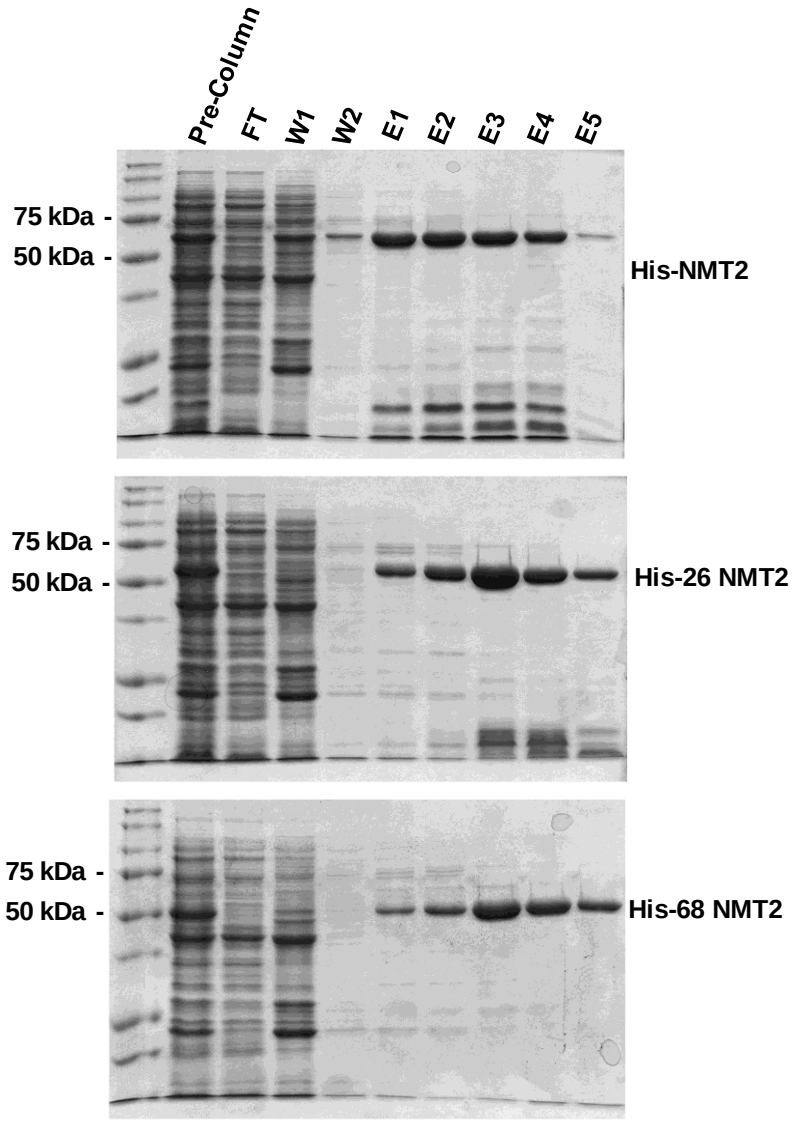

Figure 3.15: Purification of recombinant hexahistidine(His)-tagged full-length and caspase-cleaved hNMT2. Purification was performed using Ni-NTA chromatography (see materials and methods). Purified proteins were visualized by staining gels with coomassie blue gel stain. (FT: flow through, W: wash and E: eluted fractions)

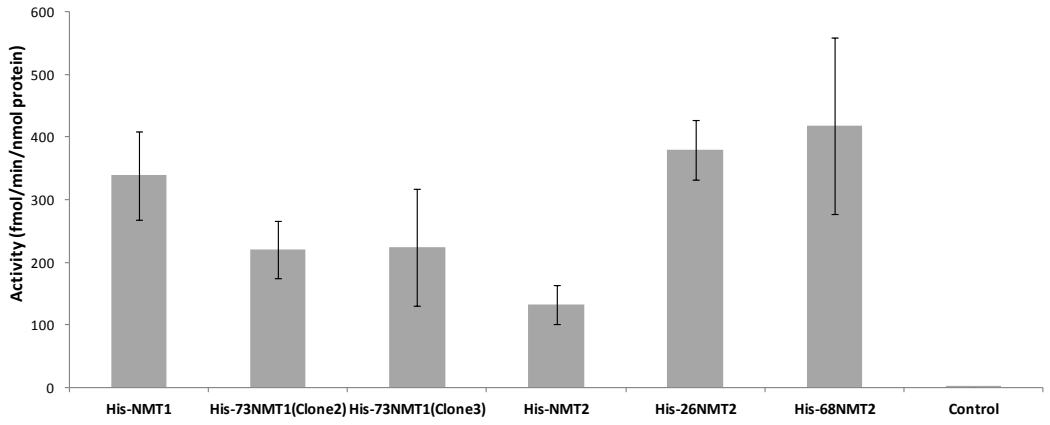

Figure 3.16: NMT activity of purified full length and caspase-cleaved hexahistidine(His)-NMTs was assayed using a peptide myristoylation assay as described under materials and methods. N-Myristoyltransferase activity was calculated from the amount of radiolabeled myristoylpeptide produced and detected on phosphocellulose paper (adapted from King *et al.*1991, *Anal Biochem*.). Each NMT assay was performed in triplicates. Control used is elution 5 from the His-NMT1purification (**Fig. 3.14**).

3.2.8 Caspase-cleaved NMT1 and NMT2 change subcellular localization during apoptosis.

The caspase cleavage of many proteins often results in change in cellular localization (Enari et al., 1998; Zha et al., 2000; Jakobi, 2004; Vilas et al., 2006); therefore, to delineate the localization of the cleaved NMTs during apoptosis we performed subcellular fractionation experiments (**Fig. 3.17**) in normal and apoptotic cells. We found that NMT1 was primarily found localized to the ribosomal/membrane fraction in untreated HeLa cells (63.9% in pellet) (**Fig. 3.18**) and this corroborated with earlier published data showing that NMT1 primarily localized to the ribosome enriched fractions (Glover et al., 1997; Takamune et al., 2010). Interestingly, there was a discernible increase of cleaved caspase-truncated NMT1 in the cytosolic fractions of HeLa cells induced to undergo apoptosis with STS or anti-Fas together with cycloheximide (54% in cytosol in anti-Fas treated cells and 60% in cytosol in STS treated cells) (**Figs. 3.17 and 3.18**). We speculate that the cleaved enzyme localizes to the cytosol because the cleavage of NMT1 at D-72 would remove the lysine (K) cluster (**Fig. 3.7**) which was shown to be important in its localization to the ribosomal fraction (Takamune et al., 2010).

Conversely, the majority of NMT2 (61.7%) localized to the cytosol prior to apoptosis induction (**Figs. 3.17 and 3.18**). However, the larger caspase-cleaved NMT2 fragment (~55 kDa) mainly localized to the

membrane pellet (94.7% in Fas-treated and 80% in STS-treated) in apoptotic cells (**Figs. 3.17 and 3.18**). We postulate that this may be because the cleavage of NMT2 at D-25 (main site) would not remove the K-box (**Fig. 3.7**) that has been shown to be important for the enzyme's localization to the ER- associated ribosomes (Takamune et al., 2010). Of note, we did not observe the presence of the smaller NMT2 cleaved fragment (~46 kDa) during our fractionations, possibly because cells were induced to undergo apoptosis for a maximum of 5 h.

When cells were metabolically labeled with alkynyl-myristate prior to induction of apoptosis or not and subjected to subcellular fractionation, we observed a change in the myristoylation profile after the induction of apoptosis as seen in **figure 3.9** and found out that the post-translationally myristoylated proteins mainly localized to membranes (P100) when compared to the cytosol (S100) (**Fig. 3.19**). This suggests that the addition of a myristoyl moiety to these post-translationally myristoylated proteins appear sufficient to provide stable membrane anchoring.

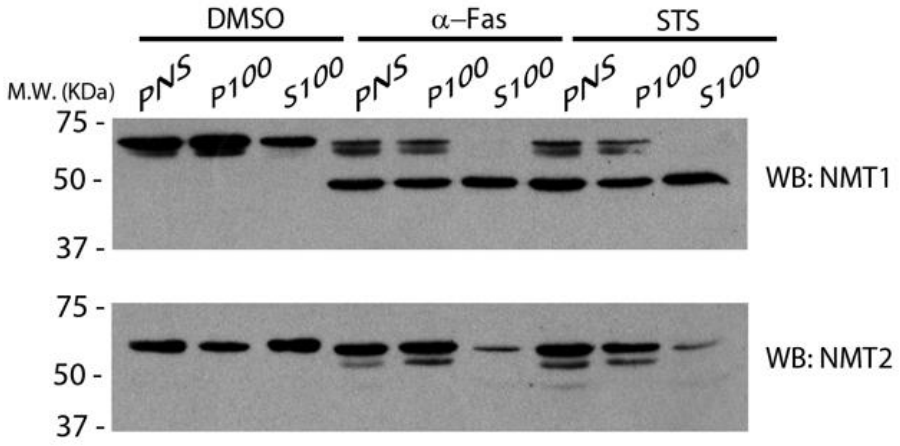

Figure 3.17: Subcellular fractionation of endogenous NMTs in HeLa cells during apoptosis. HeLa cells were treated with DMSO, STS (2.5 μM) or anti-Fas (300 ng/mL) with cycloheximide (5 μg/mL) and samples were collected at the 5 h time point and subjected to subcellular fractionation as described in materials and methods. The same volume of P100 and S100 fractions were subjected to western blotting using NMT1 and NMT2 antibodies.

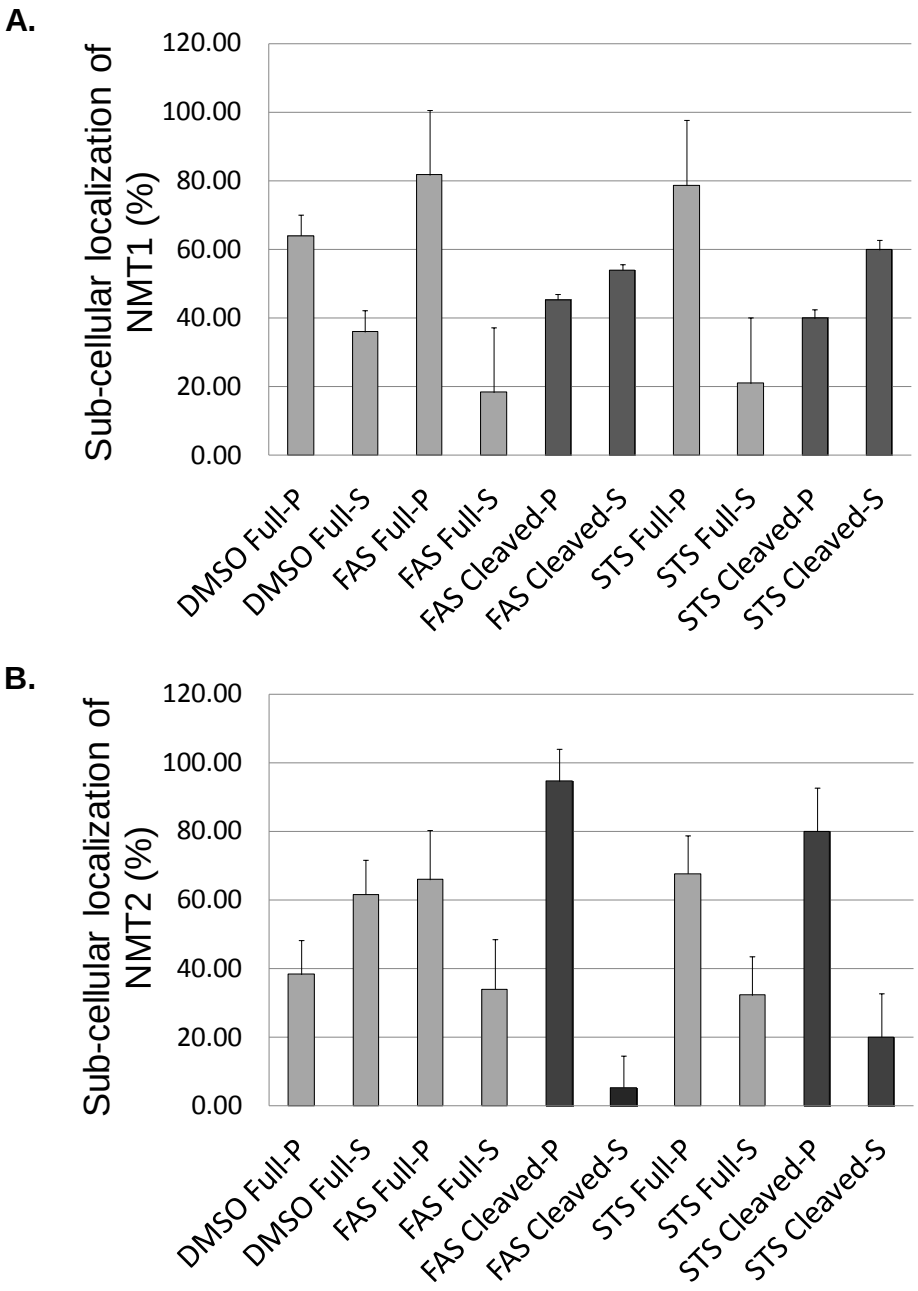

Figure 3.18: Quantification of amount of NMT in different fractions after the subcellular fractionation of endogenous NMTs in HeLa cells during apoptosis. HeLa cells were treated with DMSO, STS (2.5 μM) or anti-Fas (300 ng/mL) with cycloheximide (5 μg/mL) and samples were collected at the 5 h time point and subjected to sub-cellular fractionation (**Fig. 3.17**). The levels of full-length (Full) and cleaved NMT1 (**A**) and NMT2 (**B**) between the P100 (P) and S100 (S) fractions were quantified using Image J (http://rsbweb.nih.gov/ij/). Percentages shown were calculated as levels of each band over total of the two fractions (P100+S100). The above graphs represents the average of three independent experiments.

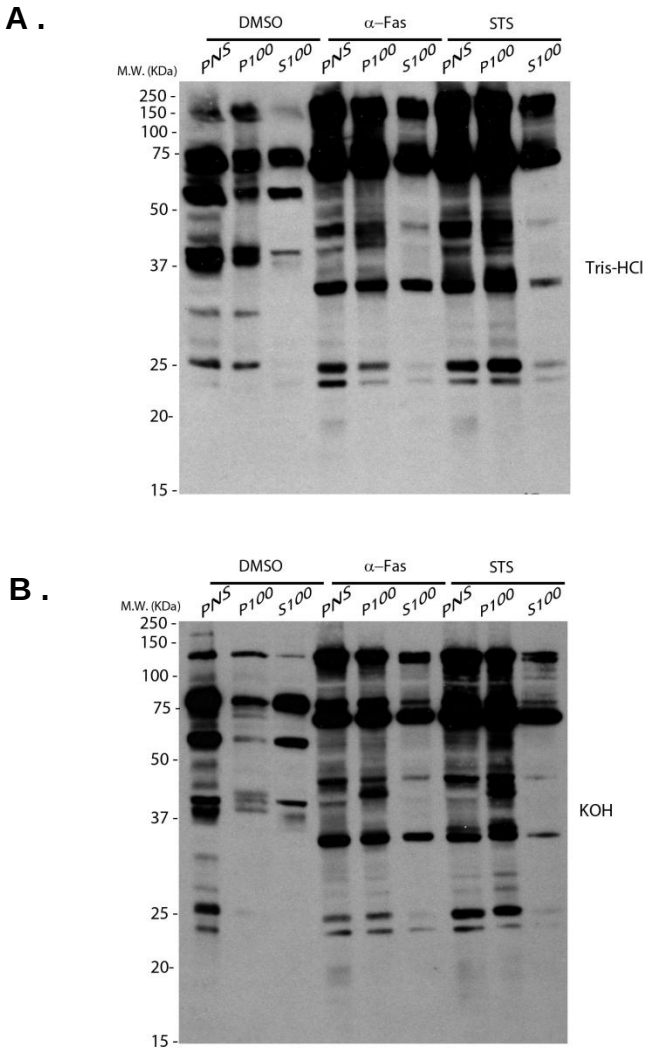

Figure 3.19 : Sub-cellular fractionation of HeLa cells undergoing apoptosis labelled with alkynyl-myristate. Prior to sub-cellular fractionation (**Figs. 3.17 and 3.18**), HeLa cells were metabolically labelled with 25 μM alkynyl-myristate after induction of apoptosis. After fractionation, protein samples were reacted with azido-biotin using click chemistry and visualized by western blotting with NeutrAvidin^{TM}-HRP. Prior to assessment of label incorporation by western blotting membranes were incubated in 0.1 M neutral Tris-HCl (**A**) or 0.1 M KOH (**B**).

3.2.9 Inhibition of NMTs potentiates cell death induced by anti-Fas

Since NMTs are necessary for post-translational myristoylation of proteins during apoptosis and may play an important role in the regulation of programmed cell death (Martin et al., 2011), we sought to investigate how the chemical inhibition of NMTs by 2-hydroxymyristic acid (HMA) would impact the progression of apoptosis. As such, cleavage of PARP-1 occurred 2 h sooner in cells treated with 1mM HMA and anti-Fas as compared to cells treated with 1mM sodium myristate and anti-Fas. A similar trend was also seen in cells exposed to HMA/STS but to a lesser extent than what was seen with anti-Fas. In the presence of HMA/STS, cells exhibited more PARP-1 and PAK2 cleavage at 2 h post induction of apoptosis than in the cells treated with STS or 1mM sodium myristate (**Fig. 3.20**). A similar stimulation of the cleavage of NMT1 and NMT2 was also observed. This indicates that the inhibition of NMTs accelerates the induction of apoptosis in cells. Since the inhibition of NMT potentiated the onset of apoptosis, it appears that NMTs play overall, a pro-survival role in cells.

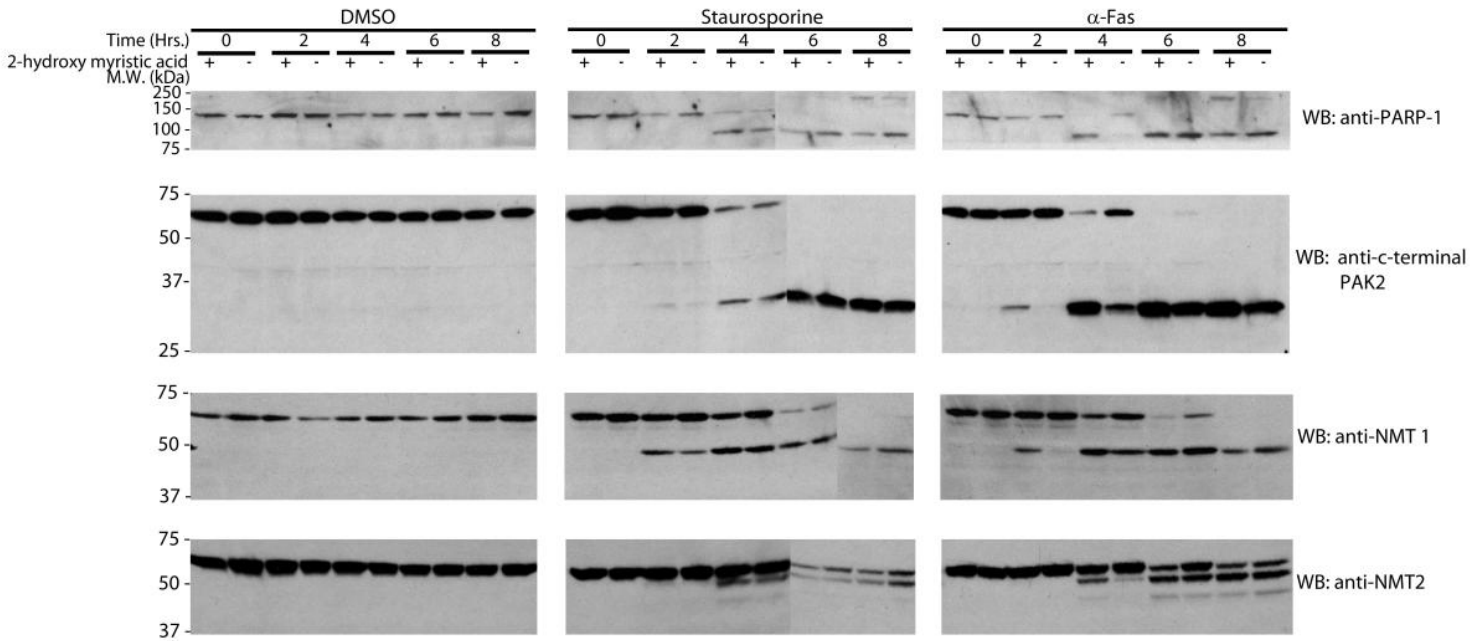
DMSO
Staurosporine
α-Fas
Time (Hrs.)
0
2
4
6
8
2-hydroxy myristic acid
+
-
M.W. (kDa)
250
150
100
75
50
37
25
WB: anti-PARP-1
WB: anti-c-terminal PAK2
WB: anti-NMT 1
WB: anti-NMT2

Figure 3.20: Effect of 2-hydroxymyristic acid (HMA) on the induction of apoptosis. Jurkat T cells were treated with or without HMA (1 mM) and apoptosis was induced with anti-Fas (150 ng/ml) and cycloheximide (5 μg/ml). The control cells were treated with DMSO. Samples were collected at 0, 2, 4, 6 and 8 h time points. Cells were lysed and samples were separated by SDS-PAGE and immunoblotted with antibodies against PARP-1, PAK2, NMT1 and NMT2 (composite gels).

3.3 Discussion

For the first time, we demonstrate that both NMT1 and NMT2 are cleaved by caspases during apoptosis (**Fig. 3.1**). NMT1 cleavage by caspase-3 or -8 precedes the cleavage of NMT2 by caspase-3 during the apoptotic process. Interestingly, the fact that caspase-3 has been shown to co-immunoprecipitate with NMT2 in human normal and tumor colorectal tissue extracts and HT29 cell lysates supports the later observation (Selvakumar et al., 2006). We found that both NMTs were cleaved within the N-terminal domain (after D72 for hNMT1 and after D25 for hNMT2) (**Fig. 3.7**) which is proposed to be involved in ribosome/membrane binding (Glover et al., 1997; Takamune et al., 2010) and not within the catalytic C-terminal domain (Bhatnagar et al., 1998). This cleavage did not greatly affect the catalytic activity of either enzyme during apoptosis until the 8-hour time point (**Fig. 3.13**). In addition, when apoptotic cells were labeled with ω-alkynyl myristic acid in the presence of cycloheximide (**Fig. 3.9**), we observed a major change in the protein myristoylation profile of apoptotic Jurkat T cells which occurred concomitantly with the cleavages of NMTs also suggesting that cleaved NMTs are still catalytically active. This change in myristoylated substrate was likely due to the appearance of new myristoylatable N-termini revealed by the action of caspases and represents post-translationally myristoylated proteins (since these were observed in the presence of cycloheximide, which blocks protein

translation). The fact that both NMTs were found to be cleaved and yet remained catalytically active was unexpected and suggests that the N-terminal portion of these enzymes released by caspase cleavage is not essential for catalysis in both enzymes. Interestingly, several NMTs (e.g. yeast scNMT and *T. brucei* NMTs) do not have the equivalent N-terminal domain removed from hNMT1 and hNMT2 (Bhatnagar et al., 1998; Price et al., 2003), and supports our data showing that this N-terminal domain is dispensable for activity and might rather play a role in the proper localization of NMTs.

Moreover, using His-tagged caspase cleaved truncated NMTs we were able to demonstrate that the cleavage of NMT2 seems to enhance its activity (**Fig. 3.16**). Our results corroborate with the deletion mutagenesis studies done with bovine spleen NMT (416 aa) that showed the C-terminus of the enzyme is essential for activity, whereas up to 52 amino acid residues can be deleted from the N-terminus without affecting NMT function (Raju et al., 1997a). Interestingly, deletion of only 21 amino acids from the N-terminus of NMT resulted in threefold higher NMT activity (Raju et al., 1997a). Hence, we could speculate that the removal of the first 25 or 67 amino acids from human NMT2 (498aa) by the action of caspases, may increase its enzymatic activity by potentially allowing the enzyme to have better access to its substrates.

Our results indeed demonstrate that the cleavage of NMTs resulted in changes in sub-cellular localization through the removal of either a N-

terminal domain containing a polylysine domain (K-domain) in NMT1 or that of a negatively charged domain upstream the K domain of NMT2 (**Figs. 3.17 and 3.18**). The K domain is thought to be involved in ribosome binding and/or membrane binding (Glover et al., 1997; Takamune et al., 2010). We found that the caspase cleavage and potential removal of the polybasic domain of hNMT1 could be responsible for the cytosolic translocation of the caspase-cleaved NMT1 from its primarily membrane-bound state. Conversely, the cleavage of NMT2 at D-25 (main site) by caspases, triggers the mainly cytosolic NMT2 to relocalize to the membrane fraction. In this case, the cleavage removes a total of eight negatively charged amino acids upstream the K-box of NMT2 reducing the negative charge of the N-terminus and potential electrostatic repulsion with negatively charged membranes thereby promoting membrane association.

Consequently, the removal of either the ribosome binding domain (K-box) or the negatively charged N-terminal amino acids might represent important features controlling the proper location of NMTs to ensure efficient post-translational myristoylation of proteins after caspase cleavage. In addition to affecting the location of NMTs, the removal of the N-terminal fragments through the action of caspases might also be required to modulate the NMT structures and alter their substrate specificities to accommodate newly exposed substrate for post-translational myristoylation.

To assess the overall role of NMTs during apoptosis, we used a selective chemical inhibitor of NMTs (HMA), which inhibits myristoylation and not palmitoylation (Paige et al., 1990). We show that inhibition of NMTs stimulated not only the rates of caspase-cleavage of known apoptotic markers PARP-1 and PAK2 but also those of NMT1 and NMT2 during apoptosis, especially in anti-Fas treated cells (**Fig. 3.20**). This suggests that the inhibition of NMTs potentiates cell death and that NMTs play a pro-survival role in cells. This finding is also corroborated by the observations of Ducker *et al.* who showed that the simple act of down regulating the expression of NMT using siRNAs was sufficient to promote apoptosis (Ducker et al., 2005).

Interestingly, the number of caspase cleaved proteins with N-terminally exposed glycine residues encompasses ~17% of all known caspase substrates (Martin et al., 2011). These studies and ours suggest that there are likely many more post-translationally myristoylated proteins that remain to be identified (Mahrus et al., 2008; Martin et al., 2008; Yap et al., 2010). Once identified, these post-translationally myristoylated proteins may reveal important new roles for fine tuning the balance between cell survival and cell death. New detection methods taking advantage of various click chemistries (Martin et al., 2008; Yap et al., 2010; Hang and Linder, 2011) and the TRAMPP methodology (Martin et al., 2012) will enable the characterization of myristoylation during

apoptosis and allow the assessment of its implications in a variety of conditions such as neurodegenerative diseases and cancer.

The fact that apoptosis regulation is often defective in cancer cells that often exhibit low caspase expression levels (Olsson and Zhivotovsky, 2011) might suggest an explanation as to why NMT (NMT1) levels are increased in numerous cancer types, namely brain tumors, gallbladder carcinomas, colon and colorectal cancers (Selvakumar et al., 2007; Kumar et al., 2011). The higher levels of NMT might thus enhance the pro-survival signaling pathways of cancer cells and promote their growth. Thus, our finding that the inhibition of NMTs potentiates the onset of apoptosis also indicates that NMT inhibitors could also potentiate the action of chemotherapeutic agents as well. Such NMT inhibitors may eventually be used as chemotherapeutic agents in combinatorial therapies.

Recently, Patwardhan *et al.* (Patwardhan and Resh, 2010) demonstrated that myristoylation positively regulates the activity of c-Src, a member of the oncogenic Src family kinases, whereas the non-myristoylated c-Src had reduced kinase activity. Src family kinases play critical roles in cell proliferation, survival and invasion during tumor development and are often overexpressed in a variety of cancers (Kim et al., 2009). Therefore, the concomitant overexpression of both c-Src kinases and NMTs might be required to potentiate the full transformative action of Src-related kinases.

In conclusion, our work demonstrates an elegant interplay between the NMTs and caspases during apoptosis whereby caspases not only cleave the proteins that become substrates for NMTs but also the NMTs themselves effecting on their localization and perhaps substrate specificities.

Chapter 4

Development of inhibitors of NMT as a novel means for the personalized medical treatment of Burkitt Lymphoma

4.1 Overview

Lymphomas originate from immune system cells (B or T cells), and account for a ~3% of cancers and cancer related deaths worldwide (Kuppers, 2005). B cell lymphomas are further subdivided into two sub types, namely, Hodgkin's (HLs) and Non-Hodgkin's Lymphomas (NHLs). The origin of NHL is unclear, but some NHL subtypes typically exhibit characteristic reciprocal chromosomal translocations which result in the deregulated constitutive expression of a proto-oncogene (such as c-myc), which is under the control of a strong immunoglobulin promoter (Kuppers, 2005). More recently, Rituximab, a monoclonal antibody directed at CD20 surface antigen, has transformed B cell lymphoma treatment when added to aggressive cytotoxic chemotherapy (Saini et al., 2011). However, these chemotherapies are not only costly but also have significant toxic side-effects, which include immunosuppression, myelosuppression, mucositis, hair loss, nausea, infertility and also have a 40-60% recurrence rate (Kuppers, 2005; Lee et al., 2008; Beveridge et al., 2011). The Leukemia and Lymphoma society (www.lls.org) reports that NHL is the 7th most common cancer in the United States as over 500,000 people in the United States are living with or are in remission from NHL and over 70,000 people are estimated to be diagnosed with NHL in 2012.

Burkitt Lymphoma (BL) is the most widespread form of NHL that is found in children and adolescents in non-endemic areas (40%) (Miles et

al., 2012). Interestingly, endemic BL accounts for up to 74% of childhood malignancies in the African equatorial belt and is often found in areas where malaria (*Plasmodium falciparum*) is holoendemic (van den Bosch, 2004; Kelly and Rickinson, 2007). BL is one of the most aggressive cancers as it has one of the highest proliferative rates of any human cancer with a doubling time 24-48h, hence, BL tumors are often treated with short, high intensity chemotherapy and these treatments typically result in improved prognosis for BL patients (Iversen et al., 1972; Yustein and Dang, 2007; Molyneux et al., 2012). Current BL treatments include aggressive cyclical chemotherapy that is combined with intrathecal prophylaxis (this involves chemotherapeutics to be introduced into the space under the arachnoid membrane, which covers the brain and spinal cord). These combined treatments routinely achieve 80% to 90% response rates (Kenkre and Stock, 2009) and the recent addition of rituximab to BL chemotherapy regimens has also significantly improved the survival rates of BL patients (Kenkre and Stock, 2009; Molyneux et al., 2012). However, administration of the above mentioned aggressive treatments to BL patients unfortunately leads to severe side effects such as neurotoxicities, hematological toxicities and severe mucositis (Yustein and Dang, 2007).

Myristoylation is the irreversible attachment of myristate (C14) on the amino-terminal glycine residue of a protein via an amide bond by N-myristoyltransferase (NMT). Typically, myristoylation occurs in a co-

translational manner on the nascent polypeptide after the initiator methionine has been removed by methionyl aminopeptidase (MetAP). Examples of co-translationally myristoylated proteins include proto-oncogene tyrosine kinases (e.g. Src, Yes and c-Abl) and heterotrimeric G_α proteins (Resh, 2006). Myristoylation is now also known to occur post-translationally during apoptosis and several of these proteins (ct-Bid, ct-actin, ct-gelsolin, ct-PAK2 and ct-PCKε) have now been characterized by our laboratory and others (Zha et al., 2000; Utsumi et al., 2003; Sakurai and Utsumi, 2006; Vilas et al., 2006; Martin et al., 2012). There are two N-myristoyltransferases (NMT1 and NMT2) which catalyze the myristoylation reaction that have been cloned and characterized and they have distinct, but overlapping substrate specificities (Duronio et al., 1992; McIlhinney, 1995; Giang and Cravatt, 1998). Several reports have shown that NMT (NMT1) expression levels are increased in several cancers such as brain tumors, colorectal cancers and gallbladder carcinoma (Magnuson et al., 1995; Raju et al., 1997b; Rajala et al., 2000; Lu et al., 2005; Selvakumar et al., 2007).

Previous studies in our laboratory have demonstrated that both NMTs are cleaved during apoptosis and this cleavage alters the sub-cellular localization of both enzymes (Perinpanayagam et al., 2013). Interestingly, some of the post-translational myristoylated caspase cleaved proteins that have been characterized seem to play either a pro-survival or a pro-apoptotic role during apoptosis. Furthermore, our laboratory has demonstrated the existence of numerous (>15) post-translationally myristoylated proteins that

could be playing various roles during apoptosis (Martin et al., 2008; Yap et al., 2010). Therefore, this suggests once again that post-translational myristoylation of caspase cleaved proteins could be an active regulator of apoptosis and since the regulation of apoptosis is often altered in cancer, that the post-translational myristoylation process that is intimately linked to apoptosis could also be deregulated in cancer.

Therefore, we initiated the search for potential myristoylation "abnormalities" in cancer cells by first querying for variations in NMT expression in cancer cell lines using the microarray data available from the cancer cell line encyclopedia (CCLE) database (Barretina et al., 2012) and second, looking for variations in myristoylated protein content of normal vs. cancer cells (in progress). We first observed that NMT2 mRNA expression levels were down regulated in cell lines derived from many hematological cancers, including BL and diffuse large B cell lymphoma (DLBCL). Next, we confirmed that NMT2 protein expression was also severely reduced in BL cell lines and select B lymphoma tumors from human patients but not in "normal" immortalized B lymphocytes or normal lymph nodes. We further showed that the myristoyl protein content (myristoylome) of BL cell lines Ramos and BL2 to be different from that of normal immortalized B cells.

Hence, we sought to exploit this unique molecular context by using NMT inhibitors to preferentially kill BL cells that only express one NMT (NMT1) in comparison to normal cells, which express two NMTs. We discovered that a pyrazole sulfanomide based NMT inhibitor, selectively killed

BL cells at very low concentrations while sparing “normal” immortalized B lymphocytes. Furthermore, we report that NMT2 down regulation in BL cells is due to low NMT2 mRNA levels, owing to transcriptional down regulation of *NMT2* gene expression by histone deacetylases (HDACs).

4.2 Results

4.2.1 NMT2 mRNA expression is reduced in several hematological neoplasms

Apoptosis is typically deregulated in cancer cells and recent evidence indicates that myristoylation is a potential new regulator of apoptosis [reviewed in (Martin et al., 2011)]. Hence, myristoylation could also be hypothetically deregulated in cancers. When we searched for variations in NMT expression levels in the public microarray cancer cell line encyclopedia (CCLE) database that recapitulates the spectrum of common cancers [made available by the Broad Institute, Massachusetts Institute of Technology (Barretina et al., 2012)], the relative NMT2 mRNA expression levels varied considerably ($\log_2$ transformed data relative range ~3-11, arbitrary units of expression) whereas NMT1 mRNA expression was relatively stable (relative range ~6-9), across the 967 cancer cell lines that were queried (**Fig. 4.1A**). Next, we compiled a list of 50 cancer cell lines with the lowest NMT2 mRNA expression levels and

found that 38 (76%) of those were from human malignant hematological origins (derived from hematopoietic and lymphoid tissues) (**Table 4.1**). Furthermore, a Box and Whisker plot was created to highlight the differences in NMT expression within the cell lines derived from a common type of cancer. We show that three malignant B cell lymphomas; namely, Burkitt, Diffuse Large B-cell (DLBCL) and unspecified B-cell lymphoma had significantly lower amounts (p values <0.001) of NMT2 mRNA expression when compared to NMT2 mRNA expression in all 967 cancer cell lines included in the CCLE database (**Fig. 4.1B**) [*In each case the respective cell type (i.e. BL, DLBCL or unspecified B cell lymphomas) were removed from the 'all cell lines list' when generating p values for each respective cell type*]. In contrast and surprisingly, NMT2 mRNA levels were significantly increased (p value <0.001) in grade IV astrocytomas, a type of brain tumor (**Fig. 4.1B**) [*Grade IV astrocytoma cell lines was removed from the 'all cell lines list' when generating p values for Grade IV astrocytoma cell lines*]. Interestingly NMT2 expression levels were also sporadically reduced in select breast, gastro-intestinal and lung cancer cell lines (**Table 4.1**).

A.

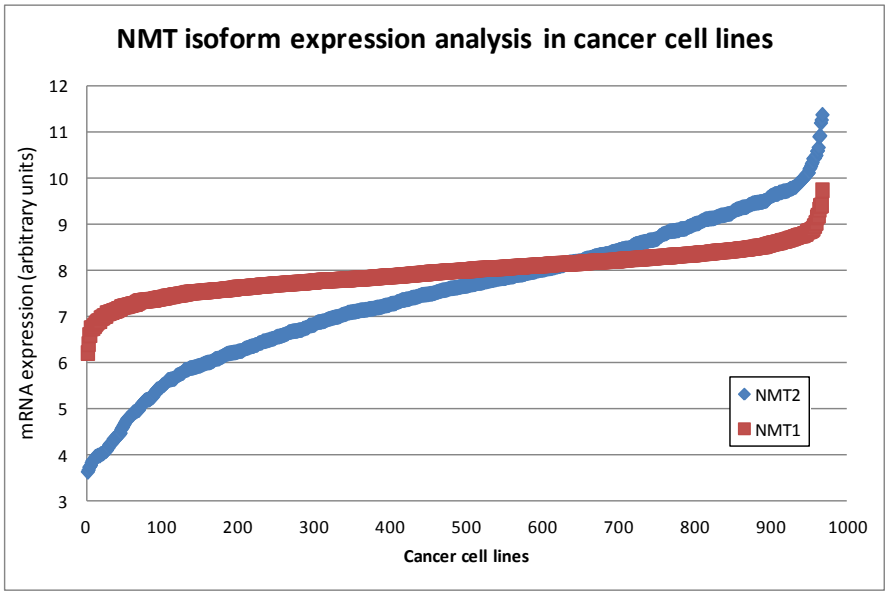

B.

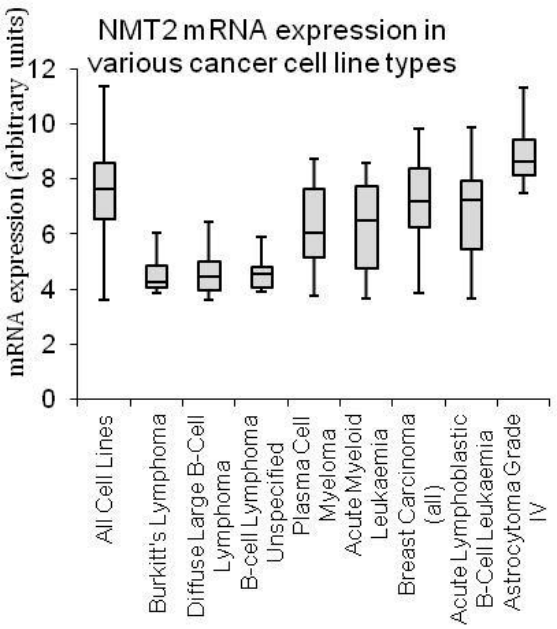

Figure 4.1: NMT2 levels are depleted in various lymphocytic cell lines. A. CCLE database was queried for NMT1 and NMT2 expression and respective NMT levels (log_2 range of expression) were plotted. **B.** Box and Whisker plots of the same cancer cell lines from several cancer subtypes are plotted and compared to all cancer cell lines. Data put together with the assistance of Ryan Heit.

	Histological Subtype	Cell line	NMT2 Expression	Source
Haematopoietic or Lymphoid Source	Acute Myeloid Leukemia	EOL-1	3.6642	DSMZ
	Acute Myeloid Leukemia	GDM-1	3.7673	ATCC
	Acute Myeloid Leukemia	PL-21	4.0117	ATCC
	Acute Myeloid Leukemia	Kasumi-6	4.0205	ATCC
	Acute Myeloid Leukemia	MV-4-11	4.0953	HSRRB
	Acute Myeloid Leukemia	HL-60	4.3381	ATCC
	Acute Myeloid Leukemia	MOLM-13	4.3432	ATCC
	Acute Myeloid Leukemia	KO52	4.4048	DSMZ
	Acute Myeloid Leukemia	OCI-AML2	4.6291	DSMZ
	B Cell Lymphoma Unspecified	MC116	3.9043	ATCC
	B Cell Lymphoma Unspecified	RL	3.9759	ATCC
	B Cell Lymphoma Unspecified	JM1	4.0771	DSMZ
	B Cell Lymphoma Unspecified	NU-DUL-1	4.3577	DSMZ
	B Cell Lymphoma Unspecified	RI-1	4.6862	ATCC
	Blast Phase Chronic Myeloid Leukaemia	EM-2	4.1421	DSMZ
	Burkitt's Lymphoma	NAMALWA	3.8721	DSMZ
	Burkitt's Lymphoma	Daudi	3.9571	DSMZ
	Burkitt's Lymphoma	EB1	3.9797	ATCC
	Burkitt's Lymphoma	SU-DHL-10	3.9798	ATCC
	Burkitt's Lymphoma	BL-41	4.0698	ATCC
	Burkitt's Lymphoma	EB2	4.2023	ATCC
	Burkitt's Lymphoma	GA-10	4.2233	ATCC
	Burkitt's Lymphoma	P3HR-1	4.2434	ATCC
	Burkitt's Lymphoma	BL-70	4.4422	DSMZ
	Diffuse Large B Cell Lymphoma	OCI-LY-19	3.6244	ATCC
	Diffuse Large B Cell Lymphoma	DOHH-2	3.7235	ATCC
	Diffuse Large B Cell Lymphoma	WSU-DLCL2	3.8199	DSMZ
	Diffuse Large B Cell Lymphoma	SU-DHL-5	3.8819	DSMZ
	Diffuse Large B Cell Lymphoma	DB	3.9475	DSMZ
	Diffuse Large B Cell Lymphoma	SU-DHL-8	3.9527	DSMZ
	Diffuse Large B Cell Lymphoma	SU-DHL-6	3.9735	DSMZ
	Diffuse Large B Cell Lymphoma	KARPAS-422	4.4105	DSMZ
	Diffuse Large B Cell Lymphoma	SU-DHL-4	4.4221	DSMZ
	Plasma Cell Myeloma	PCM6	3.7393	ATCC
	Plasma Cell Myeloma	KHM-1B	4.0262	HSRRB
	Plasma Cell Myeloma	HuNS1	4.2789	DSMZ
	Plasma Cell Myeloma	L-363	4.4213	RIKEN
	Plasma Cell Myeloma	RPMI 8226	4.6537	ATCC
	Intestinal Adenocarcinoma	COLO 205	4.2498	ATCC
	Lung Mixed Adenosquamous Carcinoma	HCC-1195	4.3572	KCLB
	Lung Small Cell Carcinoma	NCI-H2029	4.2394	ATCC
	Lung Unspecified	BEN	4.5409	DSMZ
	Oesophagus Squamous Cell Carcinoma	TE-4	4.0083	RIKEN
	Bone Unspecified	SK-N-MC	4.1437	ATCC
	Breast Ductal Carcinoma	UACC-893	3.8595	ATCC
	Breast Ductal Carcinoma	HCC202	4.59	ATCC
	Stomach Diffuse Adenocarcinoma	OCUM-1	4.5727	HSRRB
	Stomach Ductal Carcinoma	HCC1500	4.4632	ATCC
	Thyroid Medullary Carcinoma	TT	4.0649	ATCC
	Urinary Tract Transitional Cell Carcinoma	HT-1376	4.0436	ATCC

Table 4.1: List of the 50 cell lines that expressed the lowest NMT2 mRNA levels (from 967 cancer cell lines in the CCLE database). Data put together with the assistance of Ryan Heit.

4.2.2 NMT2 protein levels are reduced in various BL cell lines

Because we saw that NMT2 mRNA expression was markedly reduced in various cancer cell lines of hematological origin while that of NMT1 mRNA was relatively unchanged, we sought to confirm this observation at the protein level. To do so, we prepared lysates from various lymphocytic cell lines gathered from local investigators and analyzed them for their NMT content. Our results demonstrate that NMT2 protein levels were noticeably reduced in all the Burkitt lymphoma (BL2, Daudi, Ramos and BJAB) cell lines tested when compared to the “normal”, immortalized lymphoblastic B cell lines, IM9 , L0 and VDS (**Fig. 4.2 and 4.3**). It is noteworthy to mention that the HL cell line KMH2 and leukemic T cells (Jurkat T and CEM) expressed both NMTs as it will be used as controls in future experiments. Hence, we identified an alteration in cultured BL cell lines that resulted in the loss of one of two NMTs (NMT2).

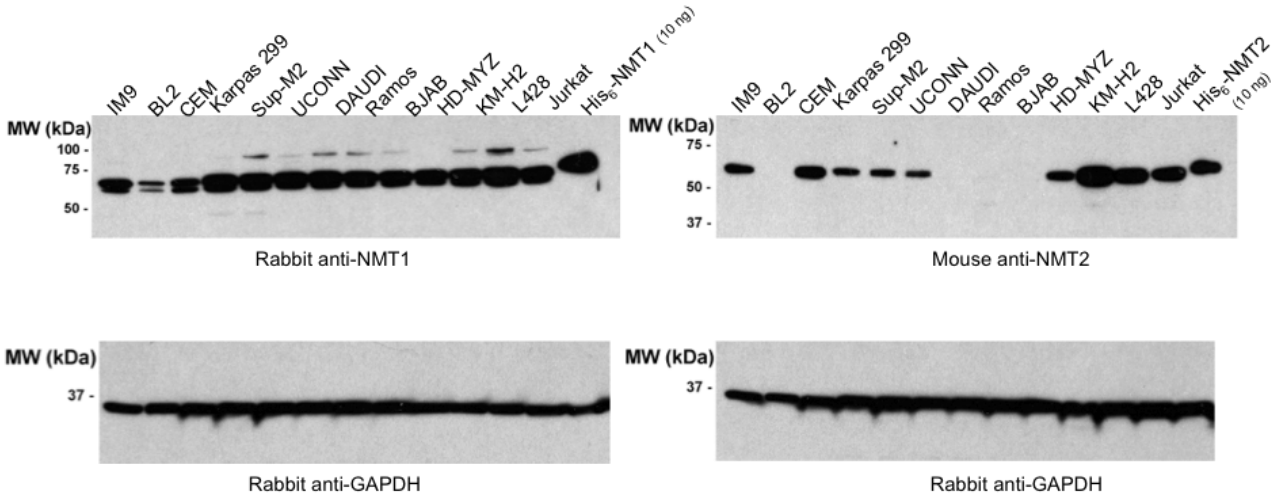

IM9: B lymphoblast
BL2: Burkitt's lymphoma
CEM: T cell leukemia
Karpas 299: T cell lymphoma
Sup-M2: ALCL
UCONN: ALCL
(ALCL: Anaplastic large-cell lymphoma)

DAUDI: Burkitt's lymphoma
Ramos: Burkitt's lymphoma
BJAB: Burkitt's lymphoma
HD-MYZ: Hodgkin lymphoma
KM-H2: Hodgkin lymphoma
L428: Hodgkin lymphoma
Jurkat: T cell leukemia

Figure 4.2: NMT2 levels are depleted in various BL cell lines. Further comparison of the NMT1 and NMT2 levels of various B lymphoma cell lines [anaplastic large cell lymphoma (ALCL), Hodgkin's lymphoma and BL], "normal" immortalized B cell line (IM9) and various T cell leukemia cell lines by western blotting. 10ng Purified His-NMT1 and His-NMT2 were loaded as controls (antibody specificity). [Cell lysates provided by Dr. Robert Ingham (University of Alberta) and western blotting performed by Megan Yap]

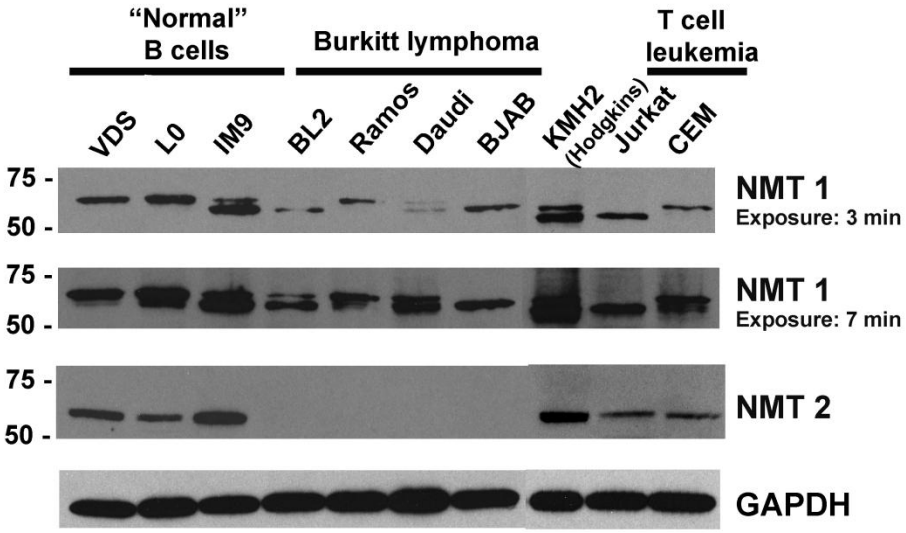

Figure 4.3: Confirmation of the reduction of NMT2 levels in various BL cell lines. Levels of NMT1 and NMT2 assessed by western blotting in immortalized "normal" human B cell lines, various neoplastic BL cell lines and leukemic T cell lines. (composite gels)

4.2.3 Comparison of myristoylation profiles of "normal" immortalized B lymphocytes and malignant BL cells

In order to assess whether the loss of NMT2 expression affected the myristoylated protein proteomes (myristoylomes), we compared the myristoylation profiles of "normal" immortalized B lymphocytes (IM9) and malignant BL cells (Ramos and BL2). To do so, cells were metabolically labelled with 100 μM alkynyl-myristate for 1 hour prior to harvesting them. Protein samples were then reacted with azido-biotin using click chemistry and visualized by western blotting using Neutravidin^{TM}-HRP (Yap et al., 2010). Our results show that the myristoylation profiles of "normal" B lymphocytes and malignant BL cells have extensive similarities (**Fig. 4.4**), but that at least 2 biotinylated-alkyne-myristate labeled proteins present in the "normal" IM9 B lymphocytes appear to be absent in the malignant Ramos and BL2 cells (**Fig. 4.4**). These missing bands could correspond to substrates specifically myristoylated by NMT2.

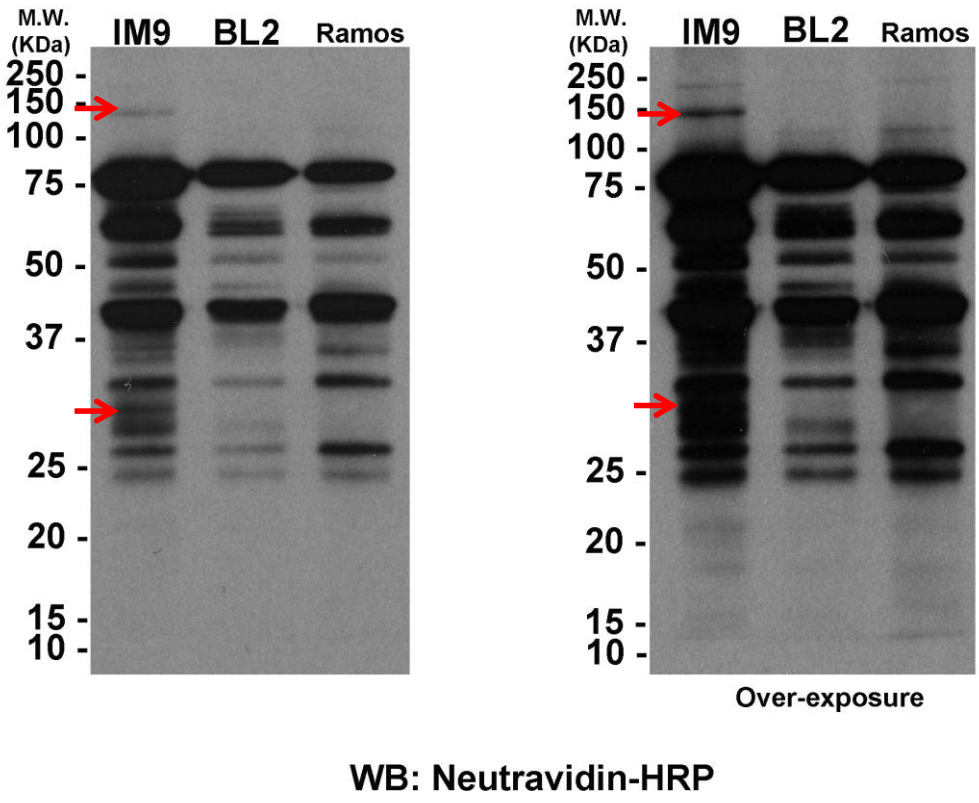

Figure 4.4: Myristoylation profiles of "normal" immortalized B cells and BL cells labeled with alkynyl-myristate. Cells were metabolically labelled with 100 μM alkynyl-myristate for 1 hour prior to harvesting them. Protein samples were reacted with azido-biotin using click chemistry, 25 μg of protein from each cell lysate separated by SDS-PAGE and visualized by western blotting using NeutrAvidin™-HRP. Red arrows indicate biotinylated-alkynyl-myristoylated proteins, which are present in "normal" immortalized B lymphocyte IM9, but seem to be absent in BL cells (BL2 and Ramos).

4.2.4 NMT2 levels are depleted in various B lymphoma tumors

Our western blot analyses suggested that NMT2 protein levels are depleted in BL cell lines (**Figs. 4.2 and 4.3**), we therefore sought to confirm this observation in lysates of human B cell lymphoma tumor tissues. Dr. Raymond Lai (Cross Cancer Institute, Edmonton, AB) provided us with DLBCL and follicular lymphoma (FL) tumors, which were probed for the presence of NMT1 and NMT2 by western blotting. Interestingly, we observed that 4 of 5 DLBCL tumors and 1 of 6 FL tumors had reduced NMT2 levels when compared to "normal" immortalized B cell line IM9 (**Fig. 4.5**). Moreover, we did not observe a noticeable difference in NMT1 levels in the tumors tested. Notably, NMT1 appeared as several bands in some of the tumors tested, which could be indicative of several isoforms of NMT1 being present in the tumor tissues (King and Sharma, 1992). Alternatively, perhaps differences in post-translational modifications (i.e. phosphorylation) could explain the different banding patterns.

To further confirm our results, we also compared NMT levels in formalin-fixed paraffin embedded human B cell lymphoma tumors by immunohistochemistry (IHC) (performed by Cheryl Santos and Dr. W. Dong, Cross Cancer Institute). We observed that NMT1 staining (brown peroxidise stain) in all of the Burkitt and DLBCL tumor tissues tested were similar to the NMT1 staining observed in the normal lymph nodes, indicating that the NMT1 levels of the tumor tissues were relatively similar

to the NMT1 levels of the normal lymph node (**Fig 4.6**). Conversely, we observed that the Burkitt and DLBCL tumors exhibited a negative stain (light blue stain) when compared to the lymph node tissue when immunohistochemistry was performed with a NMT2 antibody (**Fig. 4.7**). Therefore, our results indicate that NMT2 protein levels were severely depleted in specific types of B cell lymphoma tumors, whereas the NMT1 levels were relatively unchanged in normal and cancer tissues. Therefore, the above results obtained with B cell lymphoma tumors recapitulate the phenotypes seen in cultured lymphoma cells (**Fig. 4.2 and 4.3**).

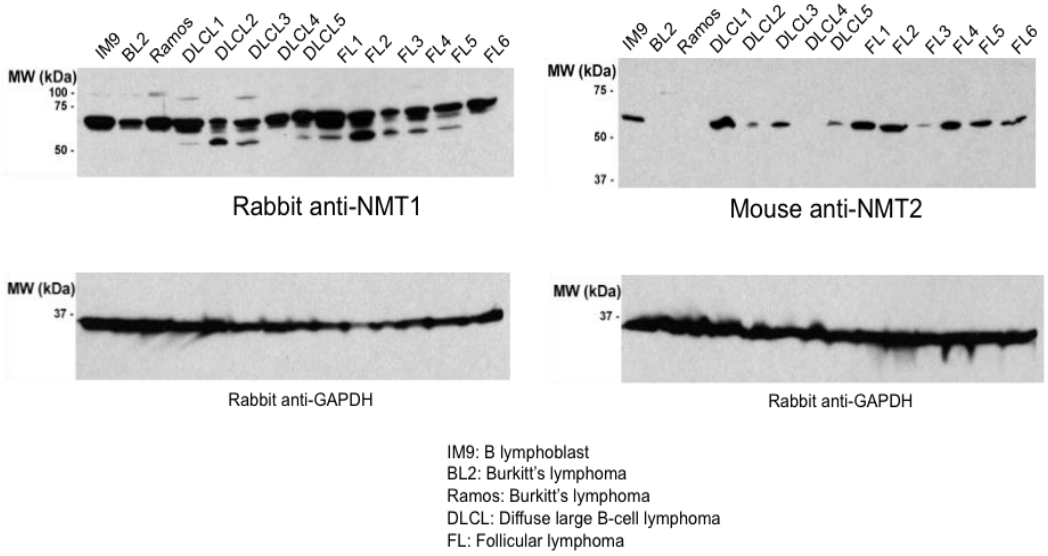

Figure 4.5: NMT2 levels are depleted in various B cell lymphoma tumors. NMT1 and NMT2 levels of various types of human solid lymphoma (Diffuse Large B Cell Lymphoma and Follicular Lymphomas) tumor lysates were compared by western blotting. Lysates were prepared from frozen tumor samples provided by Dr. Raymond Lai (Cross Cancer Institute) and probed by western blotting by Megan Yap. *A highly similar trend was seen in a second blot I performed but because some samples had started to degrade, the blot performed by Megan Yap is presented for clarity.*

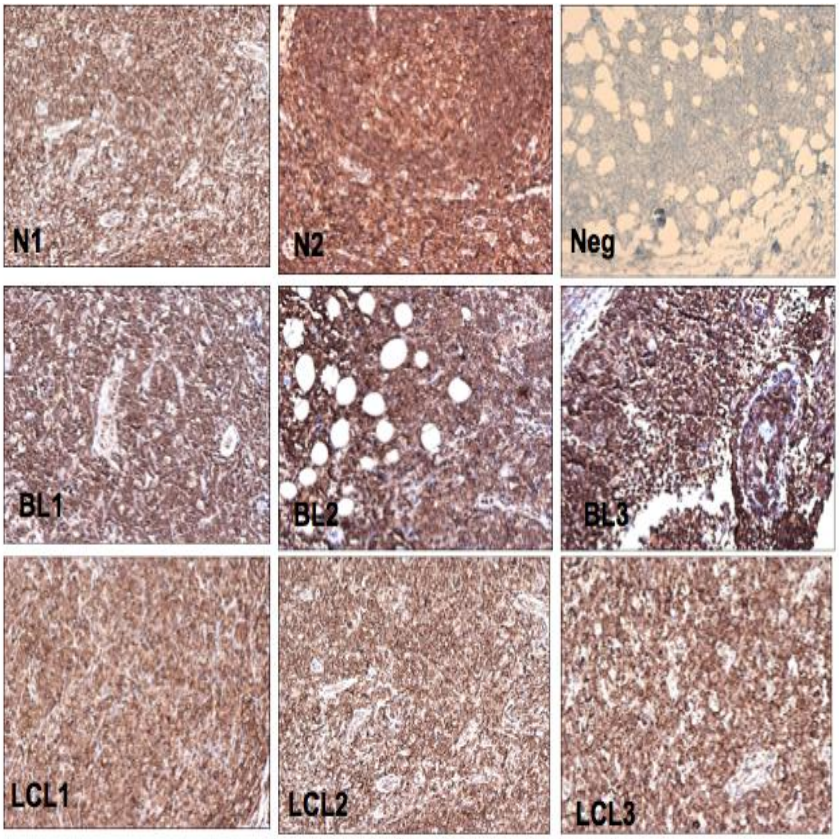

NMT-1 stain. Upper row: N1, N2 normal lymph nodes, Neg negative control. Middle row: three Burkitt lymphoma cases (**BL1-3**). Lower row: three DLBCL (**LCL-1-3**) cases. Both normal lymph nodes and lymphoma show strong stains. No difference is observed.

Figure 4.6: Analysis of NMT1 expression in various BL and DLBCL tumors and normal lymph nodes. NMT1 expression in various solid lymphoma tumors (BL and DLBCL) analyzed by immuno-histochemistry (IHC). *Upper row: N1, N2: normal lymph node, Neg: negative control in which the primary antibody was omitted. Middle row: BL (BL 1-3), Lower row: DLBCL (LCL1-3).* IHC performed by Cheryl Santos (Dr. John Mackey's laboratory, Cross Cancer Institute) and Dr. W. Dong (Cross Cancer Institute)

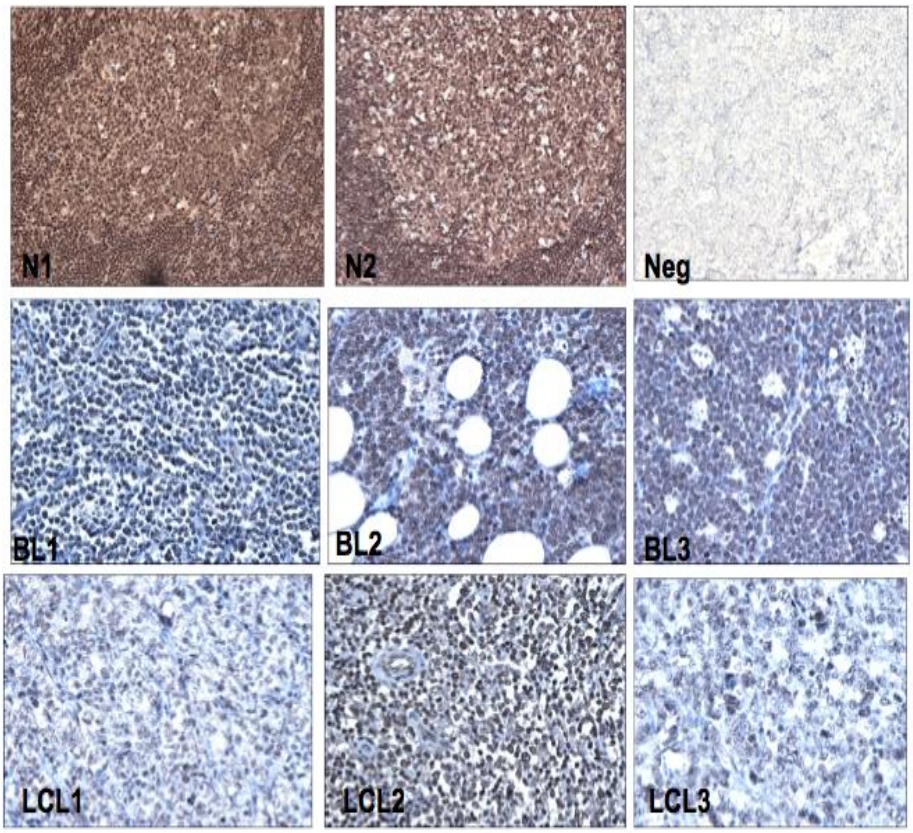

NMT-2 stain. Upper row: N1, N2 normal lymph node, Neg negative control.
Middle row: three Burkitt lymphoma (**BL1-3**); Lower row: three DLBCL (**LCL1-3**). The normal lymph nodes show a strong stain, whereas the Burkitt lymphoma (**BL**) and diffuse large B cell lymphoma (**LCL**) show a weak stain.

Figure 4.7: Analysis of NMT2 expression in various BL and DLBCL tumors and normal lymph nodes. NMT2 expression in various solid lymphoma tumors (BL and DLBCL) analyzed by immuno-histochemistry (IHC). *Upper row: N1, N2: normal lymph node, Neg: negative control in which the primary antibody was omitted. Middle row: BL (BL 1-3), Lower row: DLBCL (LCL1-3).* IHC performed by Cheryl Santos (Dr. John Mackey's laboratory, Cross Cancer Institute) and Dr. W. Dong (Cross Cancer Institute)

4.2.5 Inhibiting the only remaining pro-survival NMT (NMT1) in BL cells results in cell death

Our data so far suggests that BL typically express mainly one NMT (NMT1), while normal B cells and other tissue types express both NMTs (**Figs. 4.2, 4.3, 4.6 and 4.7**). *Therefore, we hypothesized that inhibition of the remaining NMT would deprive the malignant B cells of pro-survival signals and that these would selectively undergo apoptosis*. Hence, we treated "normal" and malignant BL cells with increasing concentrations of the NMT1 inhibitor, tris dibutylbenzinylidene acetone palladium (Tris DBA) (Bhandarkar et al., 2008), monitored cell viability using a trypan blue exclusion assay and the concentration that killed 50% of the cancer cells (EC_{50}) was measured. Incidentally, we demonstrate that Tris DBA selectively killed BL cells lacking NMT2 while leaving immortalized "normal" B cells (L0) apparently intact at 5μM (TrisDBA EC_{50} for BL = ~5 μM) (**Fig. 4.8**). Hence, we established the *proof-of-concept* (initially performed by Dr. Erwan Beauchamp) that NMT inhibitors could be used to selectively kill BL cells expressing only NMT1 while sparing "normal" immortalized B lymphocytes which express both NMTs.

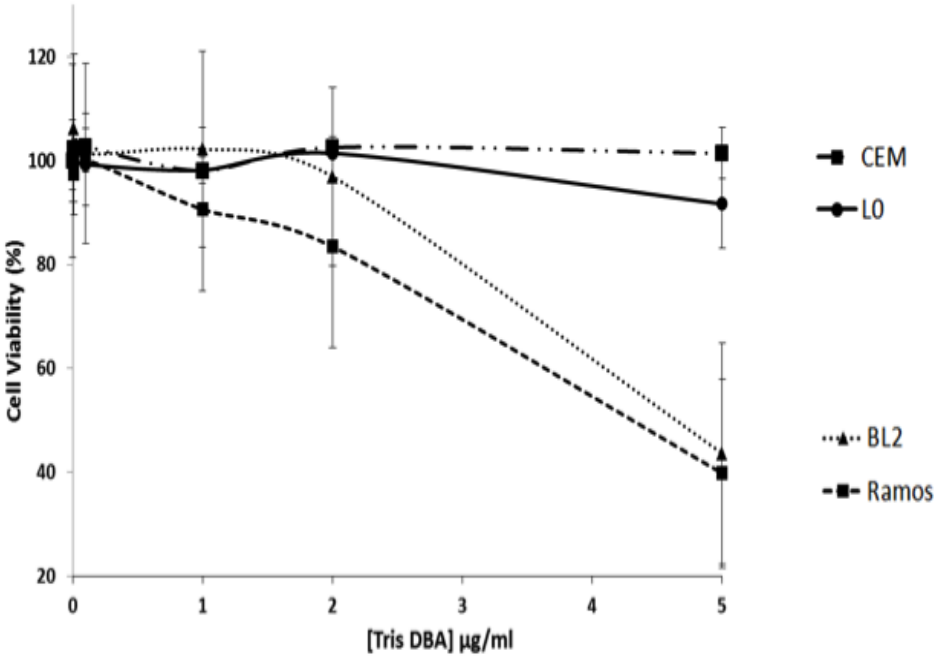

Figure 4.8: Residual viability of various lymphocytic cell lines treated with NMT inhibitor Tris DBA for 24 hours. The residual viability of various cell lines treated with TrisDBA for 24 hours (n=9) was measured by a Trypan blue exclusion assay. (Molecular weight of Tris DBA is 915.72 g mol^{-1}, hence 1 μg is almost equivalent to 1 μM of Tris DBA) (Assay performed by Dr. Erwan Beauchamp).

4.2.6 The pyrazole sulfonamide inhibitor DDD85646 of *Trypanosoma brucei* NMT induces cell death preferentially in BL cells

To assess whether we could take advantage of the loss of NMT2 in select lymphomas, we treated BL cell lines with a highly selective NMT inhibitor, DDD85646 [Inhibitory concentration 50 (IC_{50}) for hNMT *in vitro,* 10 nM]. DDD85646 was originally discovered in a screen for inhibitors of *T. brucei* NMT in search for a treatment of African sleeping sickness (Frearson et al., 2010). Increasing concentrations of DDD85646 were used to treat BL cell lines (BL-2 and Ramos) along with the relevant controls [IM9 ("normal" B lymphocyte) and KMH2 (HL cell line) that expresses both NMTs]. Trypan blue assay was used to measure the cytotoxity of the drug at 24, 48 and 72 hours. Although data were collected at 24h and 48h time points (data not shown), the most noticeable effect of the drug (DDD85646) was observed at the 72h time point.

Our results show that the survival rate, is decreased in the B-lymphoma cell lines used (Ramos: DDD85646 EC_{50}=0.37+/- 0.05 μM and BL2: DDD85646 EC_{50}=0.43+/-0.2 μM) in a DDD85646 concentration dependent manner (**Fig. 4.9**). Interestingly, the survival rates of the control cell lines, IM-9 (DDD85646 EC_{50}=7.08+/-2.32 μM) and KMH2 (DDD85646 EC_{50}=29.6+/-10.6 μM) were much higher (**Fig. 4.9**). This indicates that DDD85646 selectively killed the BL cell lines tested (low EC_{50}) while apparently sparing the "normal" (IM9) and HL (KMH2) cells (much higher

EC_{50}) at the concentration that kills 50% of cancer cells. Therefore we show that DDD85646 has a high selective killing index for cancer cells. *We define selective killing index as the ratio of "normal" immortalized B cell EC_{50} /malignant cell EC_{50},* and the selective killing index for DDD85646 was 16.4 and 19.1 for BL-2 and Ramos cells, respectively.

Next, a less potent analog of the pyrazole sulfonamide NMT inhibitor named DDD73226 was used to treat BL cell lines (BL-2 and Ramos) along with the relevant controls [IM9 ("normal" B lymphocyte) and KMH2 (HL cell line) that expresses both NMTs)] and the cytotoxity of the drug was measured using a trypan blue exclusion assay at 72h (**Fig. 4.10**). No significant changes to cell viability were observed at 24 and 48h (data not shown). Also, we did not observe any significant changes to the viability of IM9, KMH2 and Ramos cells even when cells were treated with DDD73226 at concentrations as high as 100 μM at the 72h time point. Interestingly, there was a slight decrease in cell viability observed in BL2 cells treated with 100 μM DDD73226 at 72 h, when compared to other cells (**Fig 4.10**). This may be because in addition to having severely decreased NMT2 levels, BL2 also has lower NMT1 levels when compared to Ramos and other cell lines (**Figs. 4.2 and 4.3**), and therefore may be more susceptible to the action of even less potent NMT inhibitors.

A.

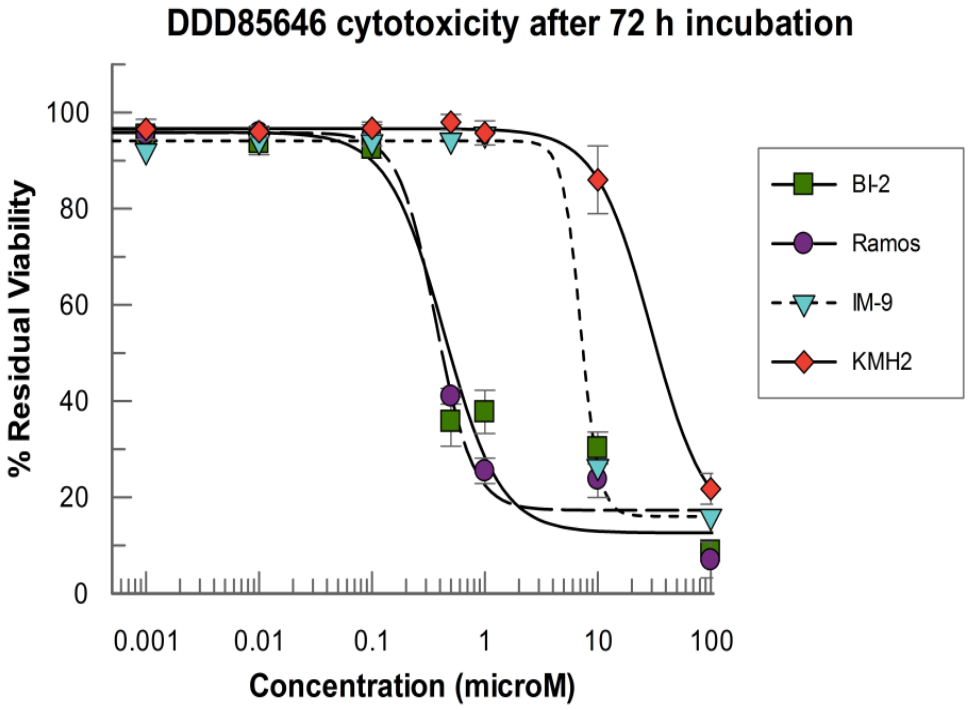

B.

Cell type	EC_{50} (µM)	NMT1	NMT2	Type of cell
Bl-2	0.43 +/- 0.20	Yes	No	Burkitt's lymphoma
Ramos	0.37 +/- 0.05	Yes	No	Burkitt's lymphoma
IM-9	7.08 +/- 2.32	Yes	Yes	Immortalized "normal" B cell
KMH2	29.6 +/- 10.6	Yes	Yes	Hodgkins Lymphoma

Figure 4.9: Residual viability of various B lymphocytic cell lines treated with DDD85646 for 72 hours. A. Cells were treated with increasing concentrations of DDD85646 (n=6) and cell viability was measured using a trypan blue exclusion assay 72h post-treatment. Curves were plotted according to a 4 Parameter Logistic equation on *Grafit (version 6)* (Leatherbarrow, 2009) **B.** Cell type description and EC_{50}.

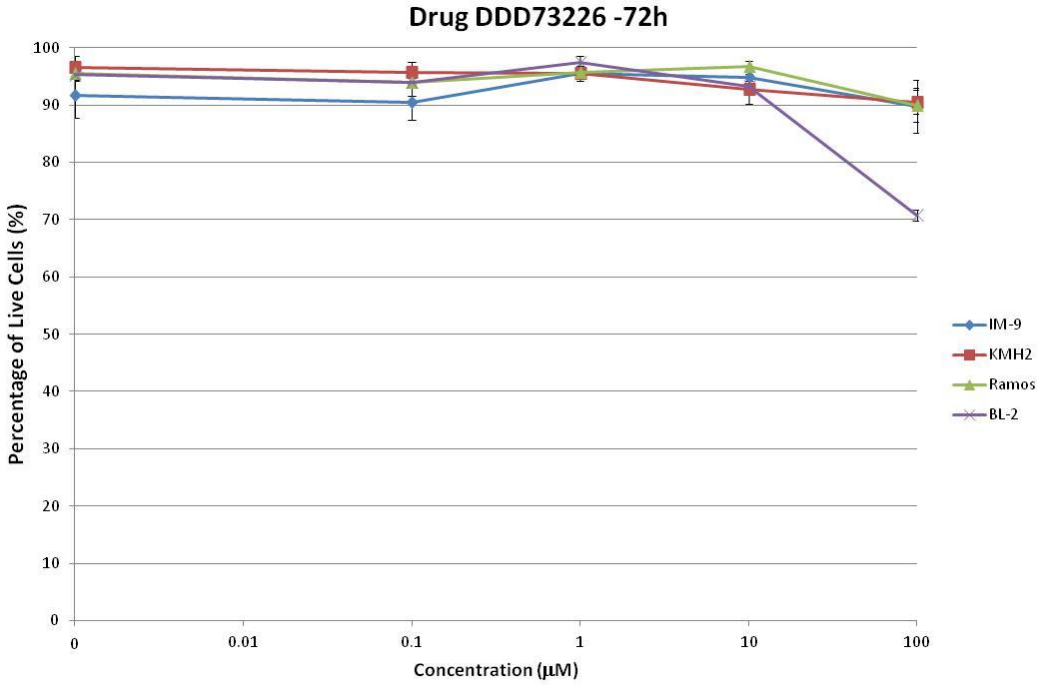

Figure 4.10: Residual viability of various B lymphocytic cell lines treated with DDD73226 for 72 hours. Cells were treated with increasing concentrations of DDD73226 (n=6) and cell viability was measured using a trypan blue exclusion assay 72h post-treatment. The percentage of live cells were calculated and plotted.

4.2.7 Potent pyrazole sulfonamide inhibitor of NMT, DDD86481 induces cell death preferentially in BL cells.

Consequently, a more potent NMT inhibitor, DDD86481 (IC_{50} for hNMT<1nM; Dr. David Gray and Dr. Paul Wyatt, personal communication) was used to treat BL cells and control cell lines [IM9 ("normal" B lymphocyte) and KMH2 (HL cell line) that expresses both NMTs]. Cell viability was measured using the MTS assay at 48h and 72h, although we did not observe a significant change to cell viability at 48h (data not shown), we found that the survival rate of the BL cell lines tested decreased significantly at the 72 h time point (Ramos: DDD86481 EC_{50}=42 nM and BL2: DDD86481 EC_{50}=58 nM) in a DDD86481 concentration dependent manner (**Fig. 4.11**). Interestingly, the survival rates of the control cell lines, IM-9 (DDD86481 EC_{50}=2.2 μM) and KMH2 (DDD86481 EC_{50}=12.6 μM), were noticeably higher (**Fig. 4.11**), indicating that DDD86481 could be used to selectively kill B lymphomas. Importantly, the selective killing index calculated for DDD86481 was 37.9 and 52.3 for BL-2 and Ramos cells, respectively. Excitingly, since DDD86481 was shown to have a lower EC_{50} required to kill BL cells than DDD85646, it may have a better chemotherapeutic potential in the treatment of B-lymphomas.

A.

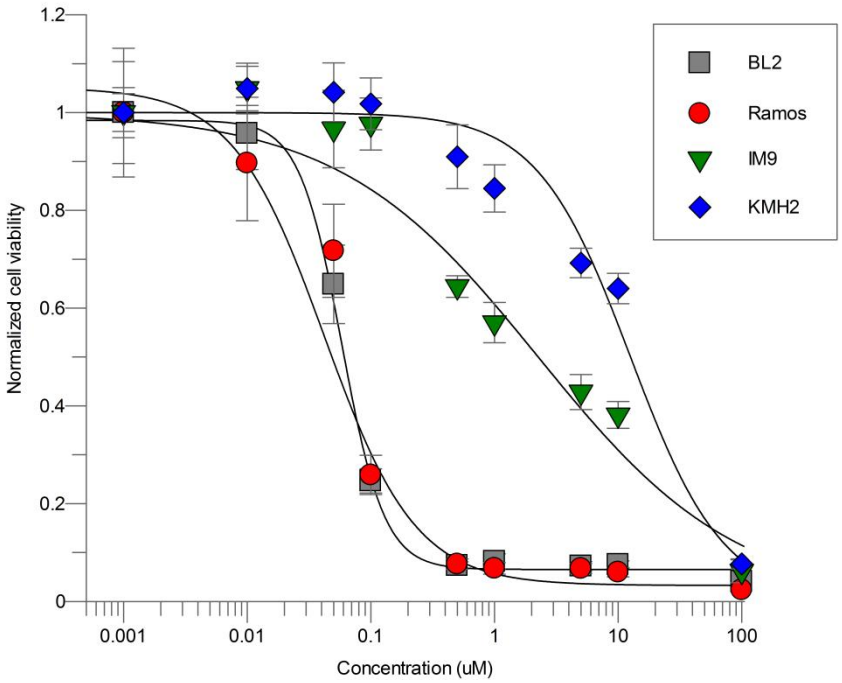

B.

Cell type	EC_{50} (µM)	NMT1	NMT2	Type of cell
Bl-2	0.058	Yes	No	Burkitt's lymphoma
Ramos	0.042	Yes	No	Burkitt's lymphoma
IM-9	2.2	Yes	Yes	Immortalized "normal" B cell
KMH2	12.6	Yes	Yes	Hodgkins Lymphoma

Figure 4.11: Residual viability of various B lymphocytic cell lines treated with DDD86481 for 72 hours. A. Cells were treated with increasing concentrations of DDD86481 (n=6) and cell viability was measured using a MTS assay 72h post-treatment. Curves were plotted according to a 4 Parameter Logistic equation on *Grafit (version 6)* (Leatherbarrow, 2009) **B.** Cell type description and EC_{50}.

4.2.8 Investigating the inhibitory action of DDD86481

In order to gain a better understanding of the effectiveness of DDD86481, we performed a time-course experiment where we labeled IM-9 and BL2 cells with 100 μM alkynyl-myristate for 1h after treatment with DDD86481 (0, 1 and 10 μM) for 0, 1 or 4h. Protein samples were reacted with azido-biotin using click chemistry and visualized by western blotting with NeutrAvidin^{TM}-HRP. We observed that the inhibitory action of DDD86481 was very rapid as we saw nearly complete inhibition of myristoylation in the cells (both IM-9 and BL2) treated with 1 μM DDD86481 after just one hour of treatment (**Figure 4.12**).

Subsequently, we analyzed the minimal dose of DDD86481 that is required to inhibit myristoylation in IM-9, BL2 and Ramos cell lines. Therefore, we treated cells with DDD86481 at 0, 10, 50, 100, 500 and 1000 nM concentrations for 2h with metabolic cell labeling with alkynyl-myristate in the last 1h of treatment. We observed that DDD86481 inhibited myristoylation in a concentration dependent manner in all cell lines tested. Interestingly, BL-2 and Ramos cell lines were more sensitive to the inhibitory action of DDD86481, as a decrease in the incorporation of the alkyne-myristate label into the myristoylated proteins was apparent starting at 50 nM for both BL cell lines when compared to IM-9 where incorporation of alkyne–myristate label only decreased starting at the 100 nM concentration (**Fig. 4.13**). Hence, we conclude once more that the

minimal concentration of NMT inhibitor DDD86481 required to inhibit myristoylation is lower in malignant BL cell lines than in “normal” immortalized B cells therefore corroborating our earlier results (**Fig. 4.11**).

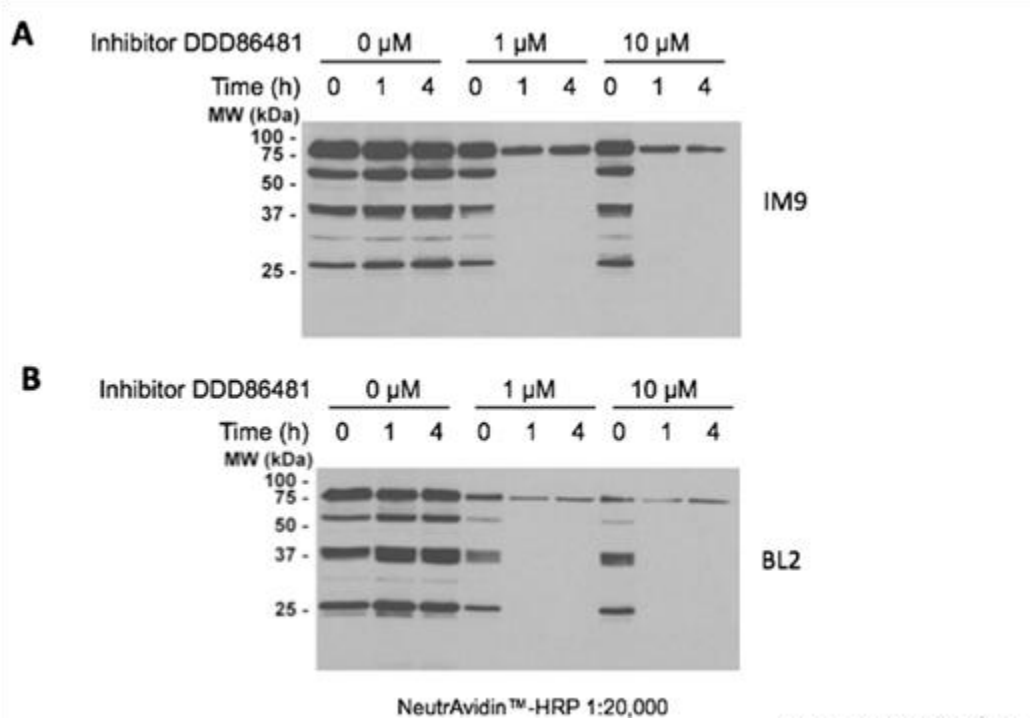

Figure 4.12: Inhibition of myristoylation by DDD86481 in B lymphocytes. Cells were incubated with DDD86481 for 0*, 1 or 4 hours and metabolically labeled for the last hour of treatment with 100µM alkynyl-myristate, solubilized, reacted with azido-biotin using click chemistry and biotinylated-alkynyl-myristoylated proteins were detected with Neutravidin-HRP/ECL. (* at the 0 time point, cells were labeled for 1 hour prior to addition of the drug or vehicle and then solubilized).

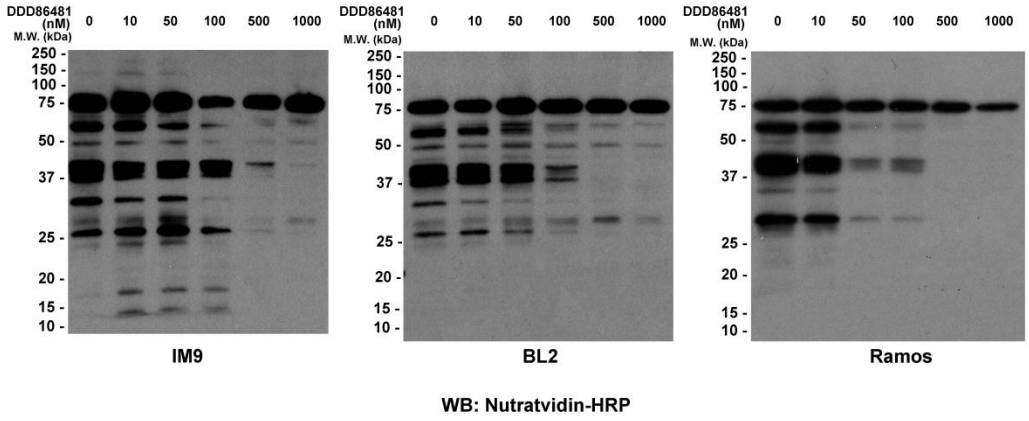

Figure 4.13: Concentration dependent inhibition of myristoylation by DDD86481 in normal and malignant B lymphocytes. Cells were incubated with increasing concentrations of DDD86481 for 2 hours and metabolically labeled for the last hour of treatment with 100μM alkynyl-myristate, solubilized, reacted with azido-biotin using click chemistry and biotinylated-alkynyl-myristoylated proteins were detected with Neutravidin-HRP/ECL.

4.2.9 DDD86481 induces apoptosis in BL cells

In order to investigate the mechanisms leading to cell death upon treatment with DDD86481, we incubated normal and malignant B lymphocytes with increasing concentrations of DDD86481 and monitored the cleavage of poly-ADP-ribose polymerase-1 (PARP-1) and caspase-3 after the 72h time point. We show that both PARP-1 and caspase-3 cleavage occurs in a dose-dependent fashion when BL cell lines were treated with the inhibitor, indicating that these cells undergo apoptosis (**Fig. 4.14**). Interestingly, no PARP-1 or caspase-3 cleavage was observed in the "normal" IM9 cells treated with the inhibitor, although, full-length PARP-1 levels were reduced in IM-9 cells treated with 1000 nM DDD86481 (**Fig. 4.14**). We did observe PARP-1 cleavage in KMH2 (HL) cells at higher concentrations, although it was minimal when compared to PARP-1 cleavage observed in the BL cells (**Fig. 4.14**). Therefore, in comparison, we found that BL cells are more inclined to undergo apoptosis than "normal" B cells when treated with DDD86481.

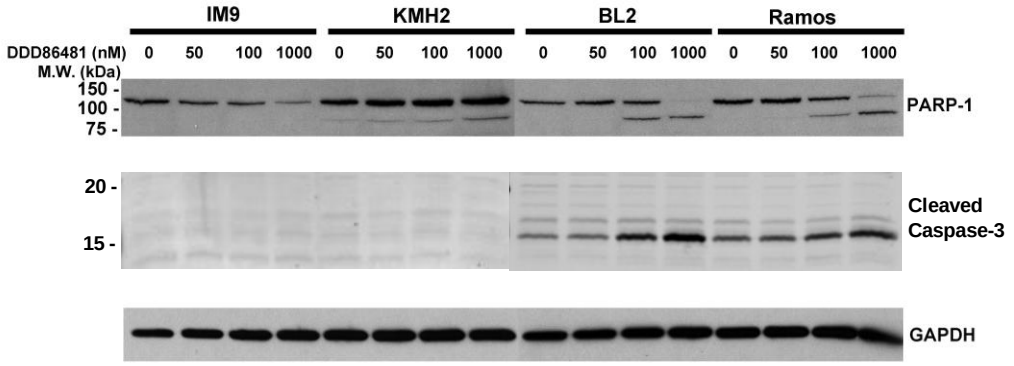

Figure 4.14: DDD86481 induces apoptosis in BL cells. "Normal" immortalized B lymphocytes (IM9), KMH2 (Hodgkin's lymphoma) and BL (BL2 and Ramos) cells were treated with increasing concentrations of DDD86481 for 72 h. Western blotting was performed on cell lysates to monitor the cleavage or PARP-1 and caspase-3 as well as the presence of GAPDH as loading control. (composite gels)

4.2.10 Proteasomal degradation is not the cause of NMT2 depletion in BL cells

Our previous results clearly showed that the potential for DDD86481 as a new chemotherapeutic approach towards the treatment of B cell lymphoma and perhaps other types of cancers (**Fig 4.1**) is linked to the extent of the loss of NMT in malignant BL cells. Considering this, we sought to investigate the common mechanisms that could lead to depletion of NMT2. To investigate whether NMT2's degradation was increased perhaps as a result of a destabilizing mutation or the presence of an unknown factor that could destabilize NMT2 in cancer cells, we treated normal and malignant lymphocytes with the proteasomal degradation inhibitor MG-132 for 5h. Cell lysates were subjected to western blotting to analyze the presence of NMT1, NMT2 and myeloid cell leukemia-1 protein (Mcl-1), which was used as a control to check the effectiveness of MG-132 since it is subject to proteasomal degradation. Our results indicate that the NMT2 levels do not increase in BL cells upon treatment with MG-132, ruling out the possibility of a destabilizing mutation or destabilizing factor present in malignant lymphocytes leading to the degradation of NMT2 (**Fig. 4.15**). As expected, the treatment of cells with MG-132 lead to increased levels of Mcl-1 in all cell types.

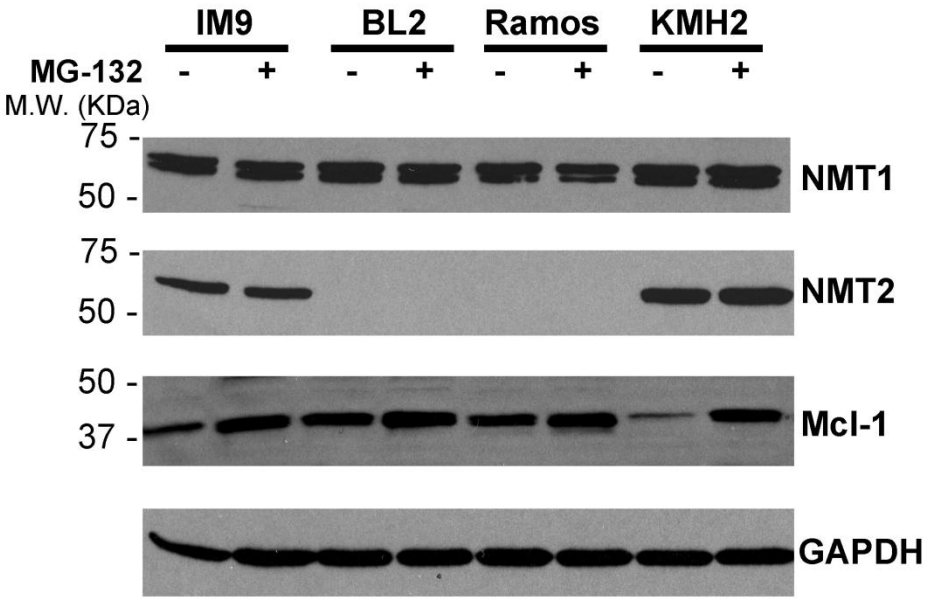

Figure 4.15: Proteasomal inhibitor MG-132 does not increase NMT2 levels in BL cells. "Normal" immortalized B lymphocytes (IM9) and malignant B lymphoma cells [Hodgkin's lymphoma (KMH2) and BL (Ramos, BL2)] treated with 10 μM of proteosomal inhibitor (MG-132) for 5h. Western blotting was performed on cell lysates to monitor levels of NMT1, NMT2, Mcl-1 and GAPDH.

4.2.11 Reduction of NMT2 protein levels in BL cells is due to reduced NMT2 mRNA levels

Since we ruled out the possibility that destabilizing mutation or factor may be responsible for lowering NMT2 levels in BL cells, we investigated whether the NMT2 mRNA levels were altered in the BL cells that exhibited diminished NMT2 levels. To do so, we performed qRT-PCR on total RNA isolated from “normal” and B-lymphoma cell lines using NMT1 and NMT2 probes and 18S probes as an internal control (Taqman® probes, Life Technologies). We show that the relative mRNA expression ratio of NMT1 to NMT2 was severely decreased in the B-cell lymphoma cell lines tested (Ramos, BL2) (**Table 4.2**). Indeed, the qRT-PCR analysis of $mRNA^{NMTs}$ indicated that there were ~25 to ~53 fold reductions in the NMT1 mRNA /NMT2 mRNA ratios in the malignant BL cells when compared to NMT1 mRNA / NMT2 mRNA ratios found in “normal” immortalized L0 or IM-9 B cells, which varied from 0.5 to 3.5, respectively (**Table 4.2**). Hence, the loss of NMT2 seen in our western blot analysis of cell and tumor lysates as well as IHC tests could be attributed to reduced NMT2 mRNA levels.

		mRNA sequence	Δct (ctNMT-ct18S)	NMT mRNA expression normalized to 18S	NMT1/NMT2
Immortalized Normal B cell line	IM9	NMT1	1.25	0.42	3.5
		NMT2	3.12	0.12	
	L0	NMT1	4.02	0.06	0.5
		NMT2	3.06	0.12	
B cell lymphoma cell line	Ramos	NMT1	-1.21	2.31	25.6
		NMT2	3.42	0.09	
	BL2	NMT1	-0.088	1.06	53
		NMT2	5.83	0.02	

Table 4.2: Analysis of NMT1 and NMT2 mRNA expression levels. qRT-PCR was performed with Taqman NMT1 and NMT2 probes using an 18S probe as an internal control. NMT mRNA expression was normalized to 18S mRNA expression and NMT1 expression fold increase over NMT2 expression was calculated (qRT-PCR performed by Ryan Heit)

4.2.12 Reduction of NMT2 levels in BL cells involves the action of histone deacetylases.

Since we showed that the loss of NMT2 in BL cells was due to a reduction of NMT2 mRNA, we sought to assess the possible involvement of gene silencing at the NMT2 locus. The acetylation of the ε-amino group of lysine residues on histones by histone acetylases (HATs) results in the reduction of the positive charge of histones, which relaxes the chromatin conformation and allowing transcription machinery to have better access to DNA (Barneda-Zahonero and Parra, 2012). Therefore, histone acetylation is typically associated with gene activation. Conversely, the removal of acetyl groups from histones by histone deacetylases (HDACs) induces chromatin condensation and results in the transcriptional repression or silencing of genes (Barneda-Zahonero and Parra, 2012).

Therefore, to test whether the reduction in $mRNA^{NMT2}$ was due to chromatin silencing, we treated “normal” B cells (IM9) and malignant BL cells with suberoylanilide hydroxamic acid (SAHA) (also named vorinostat), a class I and class II histone deacetylase inhibitor, for 24 hours and monitored the levels of NMT1 and NMT2 by western blot (**Fig. 4.16**). Excitingly, we found that use of SAHA increased NMT2 levels in BL cells where NMT2 levels are typically depleted, whereas NMT1 levels remained relatively unchanged (**Fig. 4.16**). p21/WAF1, a protein binds to and inhibits the activity of cyclin dependent kinase 1 (CDK1) or

CDK2 complexes, was used as a control to verify the effectiveness of SAHA, which is known to increase the p21/WAF1 gene expression in cells (Gui et al., 2004). IM-9, KMH2 and BL2 cells treated with SAHA contained increased p21/WAF1 levels (**Fig. 4.16**) and over-exposure of the western blot revealed that p21/WAF1 levels were slightily increased in Ramos cells treated with SAHA (unpublished observation). Hence, our results demonstrate that a class I or class II HDAC is responsible for the silencing of the NMT2 gene by deacetylating histones and thereby compacting the NMT2 locus in BL cells.

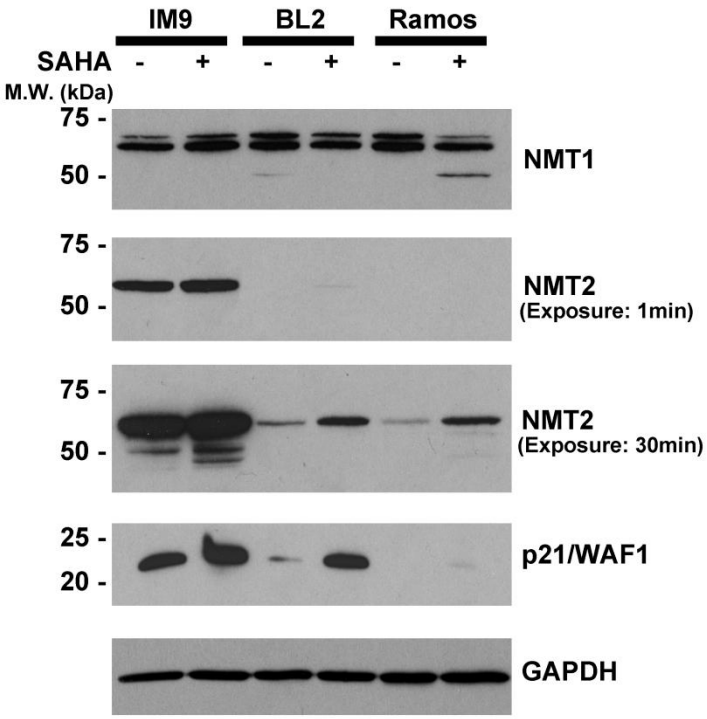

Figure 4.16: Inhibition of histone deacetylase (HDAC) classI/II with SAHA increases NMT2 expression levels in BL cells. "Normal" B cells (IM9) and malignant BL cells (Ramos, BL2) treated with 1 μM SAHA (HDAC class I/II inhibitor) for 24 h. Cells were then lysed, subjected to SDS-PAGE and western blotting was performed with NMT1, NMT2, p21/WAF1 and GAPDH antibodies.

	DDD85646	DDD86481
Structure	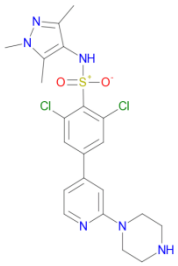	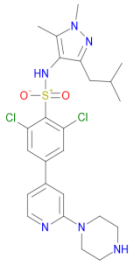
Human NMT (IC_{50})	4nM	< 1 nM

Table 4.3: Comparison of lead pyrazole sulfanomide based NMT inhibitors

4.3 Discussion

Because myristoylation is emerging as a novel regulator of apoptosis (Martin et al., 2011) and NMT expression was shown to be increased in various cancers such as, colonic tumors, colorectal adenocarcinomas, gall bladder carcinomas and brain tumors (Magnuson et al., 1995; Raju et al., 1997b; Rajala et al., 2000; Lu et al., 2005; Selvakumar et al., 2007), we sought to look for potential myristoylation defects in cancer cells. When we analyzed the expression levels of NMT1 and NMT2 mRNA in a publicly available microarray database comprised of 967 cancer cell lines representing a spectrum of common cancers (Barretina et al., 2012), we surprisingly found that several cancer lines were almost devoid of NMT2 mRNA as assessed by microarray. This came as a surprise as this observation went against the dogma NMTs (mainly NMT1) are often over-expressed in cancer (Magnuson et al., 1995; Raju et al., 1997b; Rajala et al., 2000; Lu et al., 2005; Selvakumar et al., 2007; Shrivastav et al., 2009; Kumar et al., 2011). Interestingly, hematological malignancies often exhibited the lowest NMT2 levels (**Table 4.1**), but loss of NMT2 expression was also noted in sporadic cases of breast, gastro-intestinal and lung carcinomas. Of the hematological cancers, BL, DLBCL and unspecified B cell lymphomas had the lowest NMT2 mRNA expression levels (**Fig. 4.1B**). Western blot and immuno-histochemistry analyses confirmed the loss of NMT2 protein in both BL

cell lines as well as BL and DLBCL tumors, thereby confirming our observed loss of NMT2 phenotype *in vivo*.

Having identified a molecular alteration characterized by the loss of one of two NMTs (NMT2) in BL cell lines and tumors, (**Figs. 4.2, 4.3**, **4.6 and 4.7**), we sought to investigate whether this loss could render the corresponding malignant lymphocytes more vulnerable towards NMT inhibitors. We demonstrate that the general inhibitor Tris DBA (EC_{50} for BL cells =~5 μM) and highly potent inhibitors DDD85646 and DDD86481 (EC_{50} for BL cells= ~0.4 μM and ~ 0.05 μM, respectively) (**Figs. 4.9 and 4.11**) selectively killed BL cells at low concentration whilst sparing "normal" immortalized B cells. Furthermore, our lead inhibitor compound DDD86481 is ~8 times more effective than DDD85646 at killing BL cells (structures of the drugs are given in **Table 4.3**). Interestingly, the selective killing indexes of DDD85646 and DDD86481 were ~17 to ~40, respectively, when the EC_{50} of BL cells are compared to the EC_{50} of "normal" immortalized B lymphocytes. Furthermore, this index ranges from ~334 to 636 for DDD86481 when we compare the ratios of the EC_{90} (concentration that kills 90% of cells) for normal cells / EC_{90} of cancer cells; (EC_{90} calculated for IM9, Ramos and BL-2 are 133.5 μM, 0.4 μM and 0.21 μM, respectively). These are truly remarkable numbers when known treatments for BL equally target normal and malignant B cells and have major side effects (Yustein and Dang, 2007; Kenkre and Stock, 2009; Saini et al., 2011). Hence, our results suggests that NMT inhibitors could

exploit NMT2 loss in select B cell lymphomas in order to form the basis for an improved personalized chemotherapeutic treatment of various B cell lymphomas [and eventually perhaps other types of cancers (**Fig. 4.1 and Table 4.1**)] with minimized side effects.

We demonstrated the mechanism of action of DDD86481 was involving the inhibition of myristoylation (**Fig. 4.12, 4.13**) and induction of apoptosis (**Fig. 4.14**). It is noteworthy to mention that DDD86481 preferentially inhibited myristoylation in BL (Ramos and BL2) cells (at lower concentrations) than it did for in IM9 ("normal" immortalized B lymphocyte) cells thereby supporting the EC_{50} data we obtained with our cell viability assay (**Figs. 4.9, 4.11 and 4.13**). Importantly, the two types of BL cells treated with DDD86481 underwent apoptosis as monitored by PARP-1 and caspase-3 cleavages while normal immortalized cells did not and were insensitive to the drug at the effective concentration used (**Fig. 4.14**). Altogether, these data demonstrate the potential of our novel synthetically lethal approach towards the selective killing of malignant BL cells.

Mechanistically, because the proteasomal inhibitor MG-132 failed to rescue NMT2 protein levels in BL cells, we ruled out that a destabilizing mutation or factor was involved in the reduction of NMT2 expression in malignant B cells investigated (**Fig. 4.15**). Rather, we found that the NMT2 loss seen in BL cells corresponded to a reduction in NMT2 mRNA (**Table 4.2**) due to epigenetic chromatin silencing at the NMT2 locus because the

HDAC inhibitor SAHA partially rescued NMT2 expression levels (**Fig 4.16**).

Interestingly, Richter-Larrea et al. demonstrated that the combination of HDAC inhibitor Vorinostat (SAHA) and chemotherapy had an additive effect when treating a xenograft BL mouse model, compared to chemotherapy alone (Richter-Larrea et al., 2010). Interestingly, they also demonstrated that lymphoma chemoresistance was dependent on BIM gene dosage and this phenomenon was reversible on BIM reactivation by genetic manipulation or by histone-deacetylase inhibitors (Richter-Larrea et al., 2010). Interestingly, this may be clinically relevant, as the reactivation of pro-apoptotic Bcl-2 family member Bim in BL cells with *BIM* epigenetic silencing by therapies such as HDAC inhibitors can restore *BIM* expression and reverse chemoresistance, as cells maybe more sensitized to undergo apoptosis (Richter-Larrea et al., 2010). Hence, it is possible that NMT2 upregulation by HDAC inhibitors in BL cells may increase myristoylation of pro-apoptotic post-translationally myristoylated proteins such as ct-Bid (Zha et al., 2000) and ct-PAK2 (Vilas et al., 2006) or that of yet to be identified protein(s) and therefore sensitize BL cells to undergo apoptosis.

Because NMTs are thought of as pro-survival enzymes (Ducker et al., 2005; Yang et al., 2005), how malignant B cell lymphomas such as BL overcome the near total loss of NMT2 represents an important unresolved question. The most parsimonious explanation for this phenomenon would

link the loss of NMT2 expression to the loss of one or more tumor suppressor selectively myristoylated by NMT2. The loss of such myristoylated tumor suppressor(s) would therefore benefit malignant cell growth. Interestingly, there are three known myristoylated tumor suppressors: FUS1 (Uno et al., 2004), Naked 2 (Hu et al., 2010) and BASP1 (Toska et al., 2012). Furthermore the myristoylation of FUS1 was shown to be a crucial determinant for its stability and activity. Whether FUS1 is involved in BL is not known at this point. When we performed a direct comparison of the myristoylomes of normal and malignant (BL) B lymphocytes, we observed at least 2 myristoylated proteins present in "normal" immortalized B lymphocytes (IM9) but absent the BL cell lines (Ramos and BL2) (as indicated by red arrows in **Fig. 4.4**). Whether these two myristoylated proteins are established or novel tumor suppressors or possible pro-apoptotic proteins myristoylated by NMT2 is unknown and this certainly warrants their identification and characterization. Since there are no known substrates that are exclusively myristoylated by either NMTs (Giang and Cravatt, 1998; Wright et al., 2010; Traverso et al., 2013), the identification of substrates selectively myristoylated by NMT2 would be an important premier.

Pharmacologically and economically, the success of DDD86481 as a chemotherapeutic compound will depend on the prevalence of the loss of NMT2 in human cancers as well as the extent of the loss of NMT2, which allows the enhanced cytocidal effects seen on malignant versus

normal cells. Because DDD86481 inhibits both NMTs, an eventual second generation inhibitor selectively directed towards the NMT1 should improve therapeutic potential.

Several NMT inhibitors have been developed as potential therapeutics since myristoylation is essential for the life cycles of various yeast, virus, fungi and cancer cells, but none of these NMT inhibitors have been tested in a clinical setting. Our results suggest that BL cells which are almost devoid of NMT2 are more sensitive to the action of NMT inhibitors and selectively killed with impressive selectivity indices as high as 636, which in principle should minimize non-specific side-effects. Hence, our results certainly warrant the testing of tumoricidal effects of DDD86481 *in vivo* using mouse BL xenograft models [as in (Richter-Larrea et al., 2010)].

Chapter 5

Discussion

5.1 Overview

Apoptosis plays a critical role in development, immunity, growth regulation and ageing. Deregulation of apoptotic pathways is implicated in various diseases, including tumor development and neurodegenerative disorders. The study of apoptosis and its underlying mechanisms is therefore of high clinical relevance. Apoptosis is orchestrated by a cascade of proteases known as caspases, which cleave hundreds of proteins in a highly regulated manner resulting in cell death. Consequently, caspase activity leads to the exposure of novel N-termini susceptible to various post-translational modifications.

Myristoylation is one such post-translational modification which involves the attachment of myristic acid to N-terminal glycine residues of proteins by one of two N-myristoyltransferases (NMT1 and NMT2). Until 2000, myristoylation was thought to be a strictly co-translational modification that occurred when myristic acid was attached to the N-terminal glycine of nascent proteins, following the cleavage of the initiator methionine by MetAP. However, the discovery that pro-apoptotic Bcl-2 family member Bid was post-translationally myristoylated upon caspase cleavage during apoptosis, changed this notion (Zha et al., 2000). Importantly, not only was caspase truncated (ct)-Bid myristoylated, but the post-proteolytic myristoylated Bid also played a pro-apoptotic role, by enhancing the release of cytochrome c (Zha et al., 2000). Subsequently,

several other proteins were also demonstrated to be post-translationally myristoylated by our lab and others; these include ct-Actin, ct-gelsolin, ct-PAK2 and ct-PKCε (Utsumi et al., 2003; Sakurai and Utsumi, 2006; Vilas et al., 2006; Martin et al., 2012). Further characterization of these caspase-cleaved myristoylated proteins revealed that while ct-Bid and ct-PAK2 were pro-apoptotic, both ct-gelsolin and ct-PKCε play an anti-apoptotic role upon post-translational myristoylation (Zha et al., 2000; Utsumi et al., 2003; Sakurai and Utsumi, 2006; Vilas et al., 2006; Martin et al., 2012). In addition, we showed that 15 or more post-translationally myristoylated proteins exist in various cell lines undergoing apoptosis and we have already identified several of these proteins, although their role in apoptosis remain to be investigated (Martin et al., 2008; Yap et al., 2010; Martin et al., 2012). Of note, NMTs have been shown to play a pro-survival role since their knock down by siRNA lead to increased apoptosis (Ducker et al., 2005). Historically, the fact that NMT levels (NMT1) are often elevated in various types of tumours such as colonic tumors, colorectal adenocarcinomas, brain tumors and gall bladder carcinomas is also consistent with this pro-survival role (Magnuson et al., 1995; Raju et al., 1997b; Rajala et al., 2000; Lu et al., 2005). The seemingly paradoxical roles of NMTs as catalysts of co- and post-translational myristoylation of both pro- and anti-apoptotic proteins suggest it could play a key role in the regulation of cell death and perhaps cancer (**Fig. 5.1**).

Since NMTs are emerging as novel regulators of apoptosis, and because the apoptotic process is usually defective in cancer cells, we hypothesized that the co- and post-translational myristoylation processes would be defective in cancer cells. We had anticipated seeing more cases in over-expression of either NMTs in select cancers (but not the loss of either). Possible over-expression of myristoylated anti-apoptotic or pro-survival proteins and loss of expression of myristoylated pro-apoptotic tumor suppressors in cancer cells were also envisaged but remain to be established. In addition, variations in the activities of either or both NMTs could definitely influence the balance between cell death and cell survival (**Fig. 5.1**). Furthermore, how do the NMTs accommodate to the change in substrates as the cell transitions from co- to post-translational myristoylation still remain to be answered. This thesis work aimed at answering some of these questions by characterizing the roles of NMTs especially during apoptosis via their contributions in post-translational myristoylation. Also, we provide the first thorough investigation of the expression of NMTs in cancer cells with surprising findings and applications for the personalized medical treatment of hematological cancers and perhaps other cancer types in the near future.

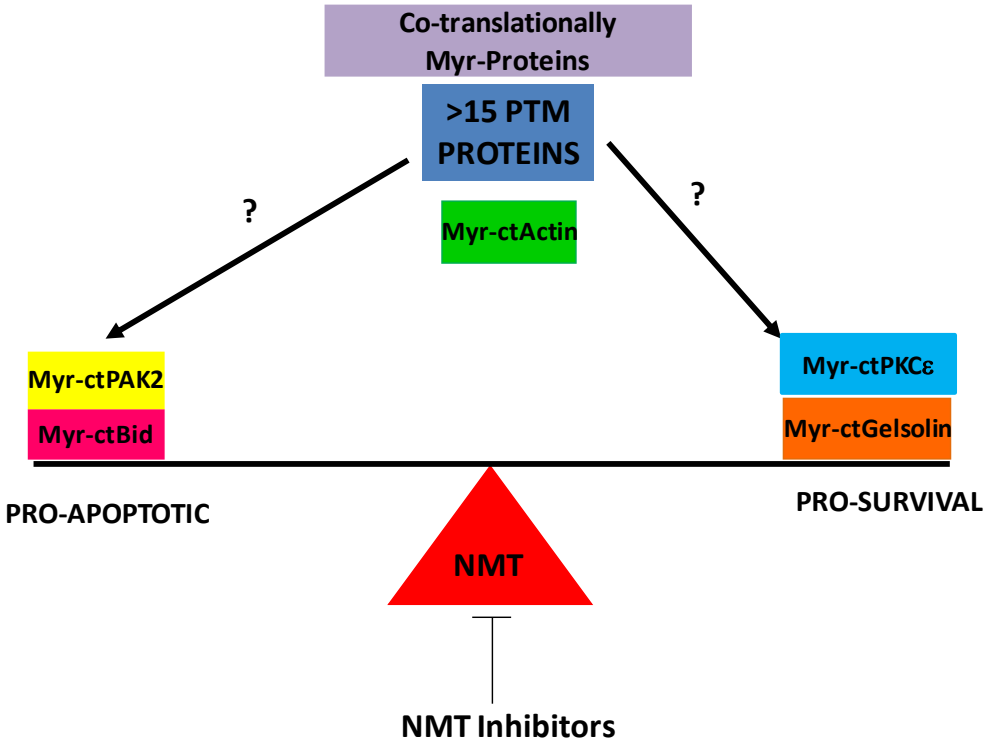

Figure 5.1: The balance between pro- vs. anti-apoptotic signals originating from various co- and post-translationally myristoylated proteins may regulate apoptosis and affect cellular life and death decisions

5.1.1 Characterization of the roles of N-myristoyltransferases in co- and post-translational myristoylation

The main goal of this project was to characterize the roles played by NMTs during apoptosis. Importantly, we report for the first time the surprising observation that NMTs are cleaved by caspases but remain active during apoptosis. More specifically we showed that NMT1 is cleaved by caspases-3/-8 at Asp 72, while NMT2 is cleaved by caspase-3 at two cleavage sites, Asp-25 and Asp-67 (**Fig. 5.2**).

Importantly, we observed a significant change in the protein myristoylation profile when apoptotic Jurkat T cell lysates were labeled with ω-alkynyl myristic acid as the cell transitions from co- to post-translational myristoylation. Because myristoylation is still occurring in the dying cells, this also suggests that caspase-cleaved NMTs are still catalytically active (**Fig. 3.9**). Essentially, these results also suggest that the N-terminal portion released during caspase cleavage is not required for catalytic activity.

In this part of our study we were also able to show that the N-terminal fragments removed by caspase cleavage play an important role in directing NMTs to their specific sub-cellular compartments. Indeed, we were able to demonstrate that the sub-cellular localization of the NMTs changed following their cleavage by caspases during apoptosis. Notably, the mainly membrane bound NMT1 (64%) lost a polybasic stretch of

amino acids and relocalized to the cytosol (>55%), whereas predominantly cytosolic NMT2 (62%) relocalized to membranes after caspase cleavage (>80%), following the removal of negatively charged domain (**Figs. 5.3 and 5.4**). Our results suggests that the removal of either the ribosome and/ or membrane binding domain (K-box) (Glover et al., 1997; Takamune et al., 2010) or the negatively charged N-terminal amino acids of NMT1 and NMT2, respectively, may be responsible for directing NMTs to their proper location during apoptosis and consequently ensure efficient post-translational myristoylation of proteins after their caspase cleavage. We further postulate that the removal of the N-terminal fragments by the action of caspases may also in fact change the NMT structure as to alter their substrate specificities. This change in substrate specificity could allow the cleaved enzymes to accommodate new substrates for post-translational myristoylation. This possibility is also supported by the fact that either caspase cleaved NMT2s (His-26NMT2 and His-67NMT2) display enhanced catalytic activity once their N-termini are removed (**Fig. 3.16)**.

Although NMT has been extensively studied in the context of co-translational myristoylation (Bhatnagar et al., 1999; Resh, 1999; Farazi et al., 2001; Resh, 2006; Wright et al., 2010), we were the first to characterize its role in post-translational myristoylation. Exploring the role of NMT in post-translational myristoylation is important because there are a vast number of proteins, which are subjected to caspase cleavage

during apoptosis, which may be putative candidates for post-translational myristoylation. In fact, ~17% of all known caspase substrates include an exposed N-terminal glycine residue, which is a main component of the consensus sequence that is required for a protein to undergo myristoylation (Martin et al., 2011). Furthermore, the Staudinger ligation and click chemistry labeling methods developed by our lab have been used to demonstrate the existence of a large number (>15) of post-translationally myristoylated proteins, which are yet to be identified and their role in cell death remain to be characterized [Fig. **1.4** (Martin et al., 2008; Yap et al., 2010)]. Hence, the numerous post-translationally myristoylated caspase-cleaved proteins strongly suggests that post-translational myristoylation may in fact have an underappreciated role in executing the apoptotic process. Therefore, it is imperative that we identify these myristoylated proteins and that we gain a better understanding of the regulation and localization of the two enzymes responsible for catalyzing the myristoylation reaction (NMT1 and NMT2) during apoptosis.

Importantly, our finding, which shows that NMT locations change during apoptosis is highly novel, but the fact that the location of the two full length NMTs is different in normal cells was also described in previous publications (Glover et al., 1997; Takamune et al., 2010). Glover et al. also showed that the N-terminal domain NMT1 may be involved in targeting the enzyme to the ribosome where co-translational myristoylation takes place (Glover et al., 1997). Furthermore, it has been suggested that

the divergent N-terminal domains of the two NMT isoenzymes (NMT1 and NMT2) may allow differential cellular localization of the enzymes (Giang and Cravatt, 1998; Farazi et al., 2001; Ducker et al., 2005). This possibility was demonstrated by us and other groups (Glover et al., 1997; Takamune et al., 2010; Perinpanayagam et al., 2013). Additionally, it has been speculated that NMT1 may be responsible for ribosome-based co-translational myristoylation, while NMT2 may be responsible for cytosol-based post-translational myristoylation during apoptosis (Farazi et al., 2001; Ducker et al., 2005).

The possible role for NMT2 during apoptosis is further supported by the fact that it co-immunoprecipitates with caspase-3 in normal and malignant human colorectal tissues and in the colorectal adenocarcinoma cell line HT29 lysates (Selvakumar et al., 2006). In the near future, it would be interesting to investigate if either of the NMTs (NMT1 or NMT2) plays a more predominant role in co- or post-translational myristoylation. This is discussed further in the future directions section of this chapter. This thesis work demonstrated that NMTs are cleaved by caspases during apoptosis and in turn we demonstrated an elegant role for caspases in controlling the rates of substrate production for NMTs and also their post-translational myristoylation efficiency by changing the location of both NMTs during apoptosis (Perinpanayagam et al., 2012).

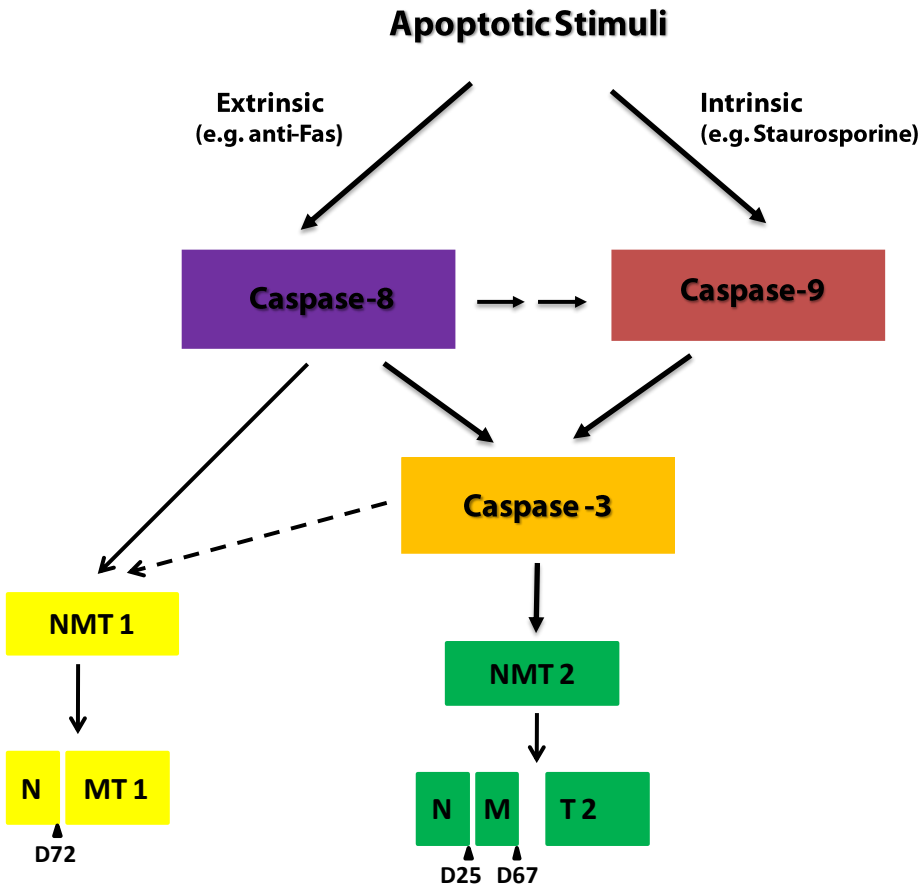

Figure 5.2: Schematic of NMT cleavage by caspases during apoptosis.

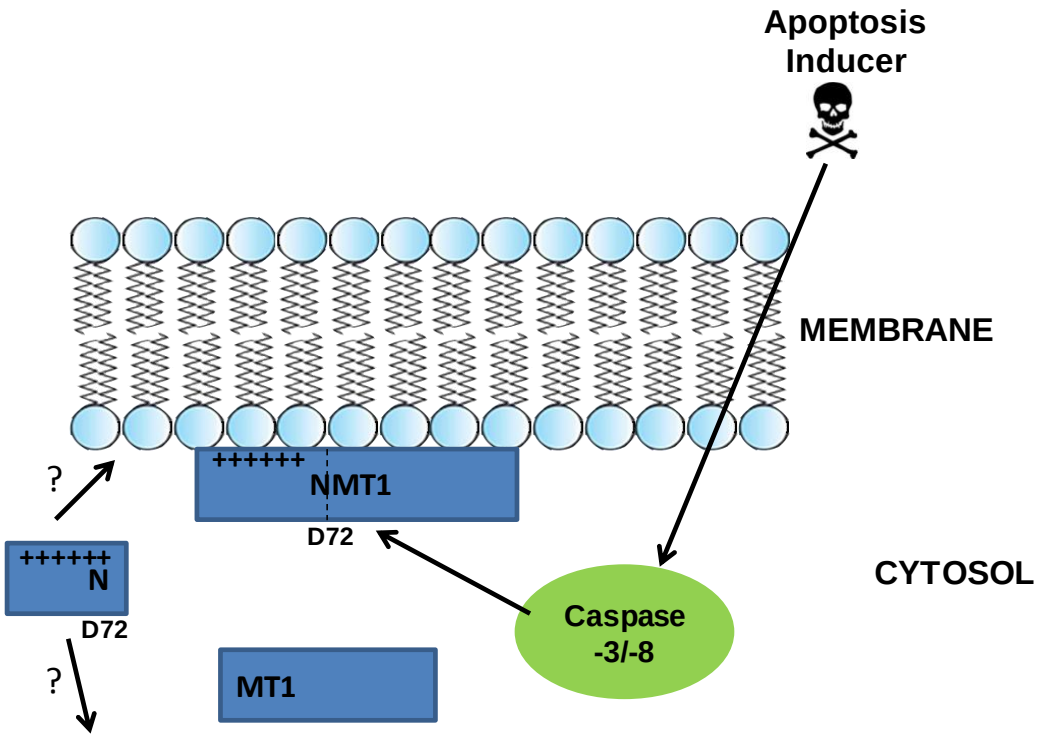

Figure 5.3: NMT1 cleavage during apoptosis relocalizes ct-NMT1 to the cytosol. Predominantly membrane and/or ribosome bound NMT1 is cleaved at Asp(D) 72 by caspase-3/-8 during apoptosis and relocalizes to the cytosol after the positively charged lysine (K) box is removed.

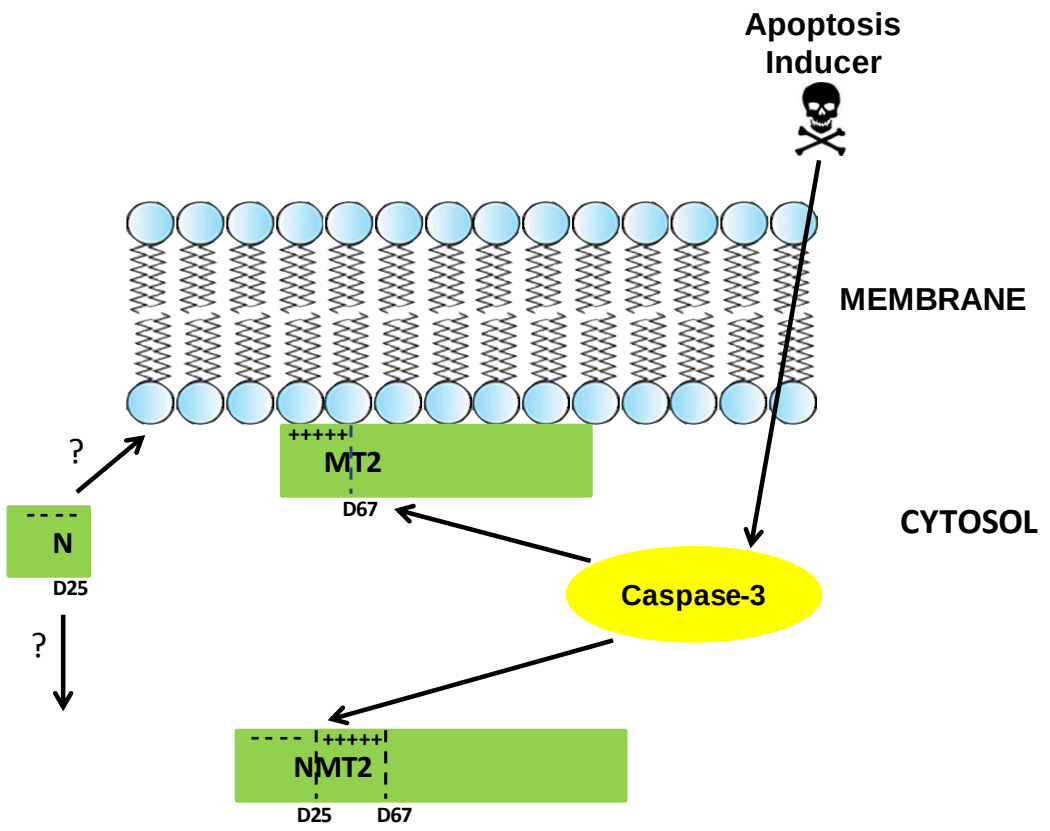

Figure 5.4: NMT2 cleavage during apoptosis relocalizes ct-NMT2 to the membrane. Predominantly cytosolic NMT2 is initially cleaved at Asp(D) 25 by caspase-3 during apoptosis and relocalizes to the membrane after the removal of amino acid sequence containing 8 negatively charged residues upstream of the K box, which could possibly by increase the net positive charge of the N-terminal region and/or reduce the electrostatic repulsion with negatively charged membranes.

5.1.2 Use of NMT inhibitors as a novel personalized medical treatment of Burkitt lymphoma (BL)

Recent evidence indicates that post-translational myristoylation of caspase cleaved proteins have an underappreciated role as an active regulator of cell death (Zha et al., 2000; Utsumi et al., 2003; Sakurai and Utsumi, 2006; Vilas et al., 2006; Martin et al., 2011; Martin et al., 2012; Perinpanayagam et al., 2013). Because of the opposing functions of the characterized post-translational myristoylated proteins during apoptosis and their significant number (>15) (Martin et al., 2008; Yap et al., 2010), myristoylation is emerging as a novel regulator of apoptosis (Martin et al., 2011). We therefore hypothesized that the myristoylation process may be defective in cancers. Our hypothesis was further reinforced by reports stating that NMT (NMT1) levels are elevated in various malignant tumors (i.e.: gall bladder carcinomas, brain tumors, colonic tumors) [reviewed in (Selvakumar et al., 2007)].

Therefore, we investigated possible myristoylation “defects” in cancer by analyzing the NMT expression in cancer cell lines in a publically available microarray data base (CCLE) (Barretina et al., 2012). We found that the expression of NMT1 mRNA levels were relatively stable across the 967 cancer cell lines queried, while NMT2 mRNA levels varied considerably. In depth analysis of these cell lines revealed that NMT2 appeared to be in fact down regulated in various cancers, such as lung, breast and various

hematological cancers (**Table 4.1**). Intriguingly, cell lines derived from various hematological cancers such as BL, DLBCL, and unspecified B cell lymphomas exhibited a statistically significant reduction in NMT2 mRNA expression (p values, < 0.001), when compared to the average NMT2 expression in all of the 967 cancer cell lines investigated. Conversely, cell lines originating from astrocytoma grade IV tumors exhibited increased NMT2 levels (**Fig 4.1B**). Therefore, it is both intriguing and surprising that NMT2 levels vary tremendously across the spectrum of cancer cell lines. Furthermore, the fact that NMT2 expression is reduced in certain cancers goes against the dogma that states that NMTs (NMT1 in particular) are over-expressed in cancer. Indeed, elevated NMT levels have long been postulated to increase tumor growth through their pro-survival roles (Ducker et al., 2005) and through their role in the co-translational myristoylation of many proteins that promote cell growth and maintenance (i.e. c-Src, Gα proteins, Arfs and c-Abl tyrosine kinases) (Chen and Manning, 2001; Hantschel et al., 2003; Patwardhan and Resh, 2010). In addition, NMTs contribute to the post-translational myristoylation of anti-apoptotic caspase-cleaved proteins during apoptosis (i.e.: ct-Gelsolin, ctPKCε) (Sakurai and Utsumi, 2006; Martin et al., 2012) and this may also promote tumor growth.

Further to our microarray analysis, which showed that NMT2 levels appeared down regulated in several hematological cancers, we confirmed the severe NMT2 depletion in several BL cell lines and, BL and DLBCL biopsies by western blotting (WB) and immuno-histochemistry (IHC) (**Figs.**

4.2, 4.3, 4.5, 4.6 and 4.7). Although NMT2 levels were severely depleted in the BL cell lines and most tumors tested, the NMT1 levels in the same cell lines and tumors remained relatively the same as that found in "normal" immortalized B cell lines (IM9, L0 and VDS) and normal lymph nodes tested, respectively. Our finding suggests that there is an as yet unknown but common mechanism at play and by which B cell lymphomas benefit from the loss of NMT2 expression.

Because most cells express two NMTs and BLs express only one NMT (NMT1), we sought to test whether NMT inhibitors would be synthetically lethal to BL and potentially spare normal cells. The concept of synthetic lethality originates from yeast studies and represents an emerging approach for the treatment of cancer (Kaelin, 2005). Briefly, two genes are synthetically lethal if mutation of either alone is compatible with viability, but mutation of both leads to death (Kaelin, 2005). In oncology, synthetic lethality describes situations where a mutation in cancer cells and a drug together cause a cancer cell's death while either the mutation or the drug alone would not result in cell death (Kaelin, 2005). A key example of exploiting synthetic lethality to develop chemotherapeutics to treat cancer is the use of PARP-1 inhibitors to selectively treat replication deficient $BRCA1^{-/-}$ or $BRCA2^{-/-}$ breast cancers (Bryant et al., 2005; Farmer et al., 2005; Ashworth, 2008). At this time, we do not know the identity of the mutation(s) leading to altered NMT2 expression but have ruled out destabilizing mutations in NMT2. We initially tested our hypothesis and

established our first proof-of-concept using a general NMT inhibitor, Tris DBA (Bhandarkar et al., 2008) (**Fig. 4.8**) and then with two highly specific pyrazole sulfonamide based inhibitors DDD85646 and DDD86481 (Frearson et al., 2010) (**Figs. 4.9 and 4.11**). Excitingly, BL cells were selectively killed at extremely low concentrations of DDD86481 (EC_{50}=~50nM) while "normal" immortalized B lymphocytes (IM9) were spared at the same concentrations (EC_{50} for IM9 = 2.2 μM). Hence, DDD86481 was ~40 times more efficient at killing BL cells than B lymphocytes, making this NMT inhibitor an attractive potential chemotherapeutic drug to treat BL (*patent filed*). Furthermore, because NMT2 levels are reduced in many hematological neoplasms and other types of cancers (**Fig. 4.1 and Table 4.1**), we propose that NMT2 may even be used as a biomarker to select individual patients who would benefit from treatment with NMT inhibitors (*patent filed*). Our IHC results (**Figs. 4.6 and 4.7**) confirm that specific NMT antibodies could be used in such a predictive test.

Further studies on the mechanism of action of the NMT inhibitor DDD86481 revealed that DDD86481 not only inhibited myristoylation in BL cells at lower concentrations than in normal cells but that its effect was almost immediate (within 1 hour of treatment) (**Fig. 4.12**). Interestingly, even though the myristoylation of new substrates are inhibited within an hour of treatment with the NMT inhibitor, a noticeable effect on cell viability was only seen 72 h following treatment. Hence, we could speculate that

proteins that are already myristoylated before the addition of DDD86481 are very stable, explaining the long lag phase prior to the action of the drug. In fact, by blocking the N-terminus to the action of peptidase, post-translational modifications such as myristoylation could be increasing the half-lives of some proteins. Alternatively, certain cancer cells could be modulating alternative signaling pathways that promote cell survival until cell viability is finally compromised by the action of the NMT inhibitor.

The genetic ablation of NMT1 alleles is embryonic lethal (Yang et al., 2005), suggesting that there are myristoylatable substrates that cannot be myristoylated by the action of NMT2. Currently, we are unaware of how specific B cell lymphomas such as BL and DLBCL overcome the near total loss of NMT2. We speculate that NMT2 may be responsible for exclusively catalyzing the myristoylation of a putative tumor suppressor whose function would depend on its proper myristoylation. FUS1 (Uno et al., 2004), Naked 2 (Hu et al., 2010) and BASP1 (Toska et al., 2012) are all examples of tumor suppressors that are myristoylated, and FUS1 is known to be functional only upon myristoylation (Uno et al., 2004). Hence, we speculate that increased BL or DLBCL tumor growth may be a result of the loss of such a putative tumor suppressor (**Fig 5.5**). The identity of the tumor suppressor involved is still being investigated. Interestingly, in **figure 4.4** we show that there are several proteins that are myristoylated in “normal” immortalized B cells, but not in NMT2-deficient BL2 and

Ramos cell lines. These represent possible candidate tumor suppressors and therefore warrant their identification.

Excitingly, we report that the loss of NMT2 is not due to a destabilizing mutation since incubation with the proteosomal inhibitor MG-132 did not rescue NMT2 levels (**Fig. 4.15**) rather, the loss of NMT2 protein levels could be reversed by treating BL cells with the HDAC inhibitor, SAHA (vorinostat). Interestingly, HDAC inhibitors are a new class of anti-tumor agents which are currently being explored as epigenetic cancer therapy (Cabanillas, 2011). Both HDAC inhibitors and DNA methyltransferase inhibitors modulate the expression of several genes associated with carcinogenesis and this may result in anti-tumorigenic activity (Cabanillas, 2011). Interestingly, HDACs appear to have a role in lymphomagenesis and several HDAC inhibitors are being explored for treatment of lymphoma. Importantly, the most common oncoprotein over-expressed in NHL tumors (specifically DLBCL) is the transcriptional repressor gene, BCL6 and this mediates aberrant cell survival and proliferation (Parekh et al., 2008). Elevated BCL6 levels (as found in DLBCL), lead to the transcriptional repression of p53, thus interfering with the apoptotic process in the malignant cells and thereby promoting cell survival (Phan and Dalla-Favera, 2004). Importantly, histone acetylation was shown to be required for the down-regulation of BCL6 activity (Bereshchenko et al., 2002). Hence, the inactivation of BCL6 through the use HDAC inhibitors would result in increased expression of p53, and

consequently allow tumor cells to undergo apoptosis, which would be a favorable, anti-tumorigenic effect (Cabanillas, 2011). Recently, clinical trials with various HDAC inhibitors such as vorinostat (SAHA), romidepsin, panobinostat and valproic acid have demonstrated significant promise in the treatment of a range of NHL (Cabanillas, 2011).

Because HDAC inhibitors could re-establish NMT2 levels, we further speculate that this could lead to an increase in the myristoylation of the putative myristoylated tumor suppressor specifically myristoylated by NMT2, and consequently this could cause increased BL cell death (**Fig. 5.5B**). It is also possible that treatment with DDD86481 alone might not suffice to kill cancer cells *in vivo* and it is possible that combinatorial therapy with rituximab or CHOP may potentiate cancer specific cell death. Interestingly, our previous results demonstrating that using an NMT inhibitor (HMA) together with an apoptotic stimulus (α-Fas) potentiated cell death further support this possibility (**Fig. 3.20**).

As indicated by our results, epigenetic silencing of the *NMT2* gene by HDACs is the mechanism responsible for the down-regulation of NMT2 in BL cells. Epigenetics is described as heritable changes present in a cellular phenotype that are independent of alterations to the DNA sequence, such as DNA methylation and histone modification (Dawson and Kouzarides, 2012). Indeed, the relationship between epigenetics and cancer has recently been gaining much attention as a variety of epigenetic processes are responsible for a variety of factors that promote tumor

growth (Dawson and Kouzarides, 2012). Furthermore, epigenetic mechanisms are thought to promote cell proliferation and subsequently influence tumor growth by silencing tumor suppressor genes (Feinberg and Tycko, 2004; Dawson and Kouzarides, 2012). Hence it is feasible that *NMT2 itself* may in turn also be a tumor suppressor that is down-regulated in BL cells by the epigenetic gene silencing to promote cell proliferation (**Fig. 5.5B**).

This thesis work has revealed that BL cells are practically devoid of NMT2 and this unique molecular context confer sensitivity to the action of NMT inhibitors. Interestingly, NMT inhibitors used in this study specifically killed BL cells with remarkable selective killing indices that could spare normal cells *in vivo*. Hence, our lead NMT inhibitor (DDD86481) is promising and could be further developed into a personalized medical treatment of BL and eventually perhaps other cancers devoid of NMT2. Towards this goal, much pre-clinical work remains to establish the efficacy and bio-safety of the compound in animal models and then eventually in humans. Then, we must also establish the prevalence of the loss of NMT2 in various human cancers as well as the levels of depletion of NMT2 required to confer the synthetically lethal effects of our potent NMT inhibitors in cancer cells.

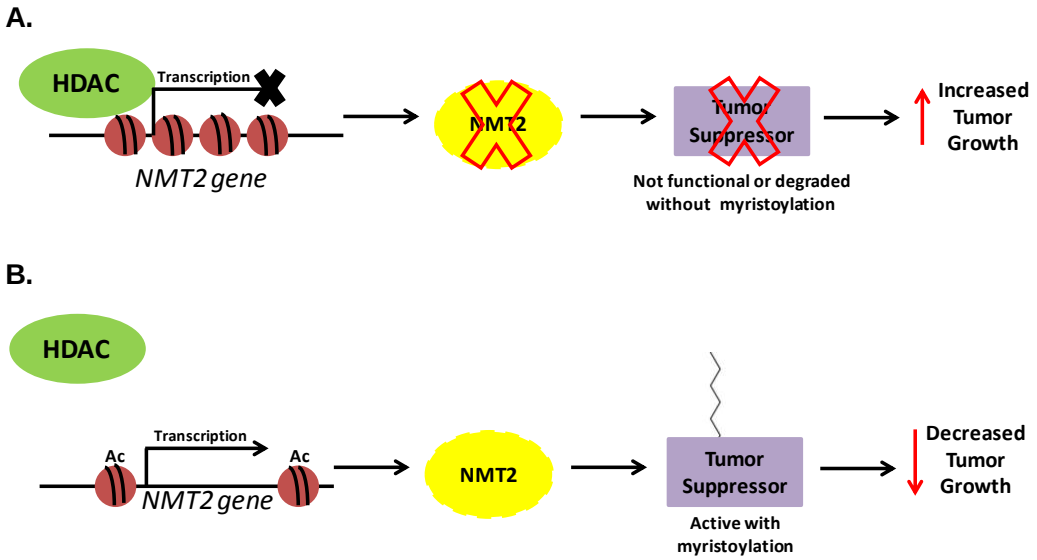

Figure 5.5: Putative model illustrating how loss of NMT2 could benefit BL cells.

5.2 Future Directions

5.2.1 Determining if caspase cleavage of NMTs during apoptosis alters substrate specificity

From analysis of the active sites of both NMTs, it appears that the of the amino acids that make the catalytic pocket appear almost completely conserved and so far no substrates have been identified that are mutually exclusive to either NMT (Giang and Cravatt, 1998; Farazi et al., 2001). These observations suggest that the location of the NMTs might be important in placing either NMTs in the proper cellular context as to encounter the optimal substrates for their activity, whatever these may be. The differential localization of NMTs might therefore control their substrate specificity in normal and dying cells.

To confirm the sub-cellular localization of the caspase cleaved truncated NMTs (ct-NMTs), we have cloned V5-tagged truncated NMTs into pcDNA 3.1 vectors to generate the following vectors; V5-73NMT1, V5-26NMT2 and V5-68NMT2, which lack the amino (N)-terminal amino acids which are lost when cleaved by caspases. In order to confirm the cleaved NMT localization results we obtained with sub-cellular fractionation of apoptotic cell lysates, we intend to transfect mammalian cells with these constructs, along with full length V5-NMT1 and V5-NMT2 and utilize

immunofluoresence microscopy to visualize the sub-cellular localization of these truncated NMTs.

Additionally, His-73NMT1, His-26NMT2 and His-68NMT2 were also subcloned into the bacterial expression vector pET19b and purified by nickel chelating chromatography and we showed that the NMT1 was ~3 fold more active than NMT2, which is consistent with the results observed earlier (**Fig. 3.16**) (Giang and Cravatt, 1998; Frearson et al., 2010). Interestingly, while the specific activity of truncated NMT1 did not differ from the full length enzyme, the activity of both truncated NMT2 proteins increased ~3 to 4 fold when compared to full length NMT2 activity (**Fig. 3.16**), suggesting that NMT2's N-terminal region might contain some regulatory elements, which may have an impact on substrate specificity.

One of the future aims of our study will be to uncover whether caspase-cleavage formally modulates NMT substrate specificity. To investigate this, we will first assess whether either NMT has a preference for co- *vs.* post-translationally myristoylated substrates. To do so, we will perform activity studies on intact His-NMTs and His-ct-NMTs mentioned above using various myristoylatable (G-) or non-myristoylatable (G->A) decapeptides for *co-translationally myristoylated* proteins (i.e. c-Src, Arf1, $G_{\alpha s}$) and *post-translationally myristoylated* proteins (i.e. ct-Bid, ct-PAK2, ct-Gelsolin), using the NMT assay adapted from King *et al.* (King and Sharma, 1991). By varying substrate concentrations, we expect to assess the substrate specificity (approximated by the K_M), the catalytic rates (k_{cat})

and the catalytic efficiency (k_{cat} / K_M) of WT- and ct-NMTs. The results from these experiments might allow us to identify substrates that are preferred by either enzymes.

5.2.2. Validate our pyrazole sulfonamide based lead NMT inhibitor (DDD86481) *in vivo* using a subcutaneous human B cell lymphoma tumor mouse and a patient-derived xenograft mouse model.

Our preliminary results using cell lines *in vitro* have shown great promise in the development of a novel personalized medical treatment of B cell lymphomas with impressive selective killing indices as high as ~636. Prior to the initiation of human clinical trials, a few steps remain. First we must establish our proof-of-principle *in vivo* and then establish the bio-safety of the compound in larger animals (i.e. cat, dog or pig). It is noteworthy to mention that DDD86481 has minimal toxicity to mice up to 100mg/kg (Dr. David Gray and Dr. Paul Wyatt, personal communication).

To establish our proof-of-principle *in vivo*, we intend to use the *In vivo* Pharmacology Services (Jackson Laboratory) to test DDD86481 efficacy against human tumor cells *in vivo* subcutaneous xenograft mouse models using human B cell lymphoma cell lines (e.g. Ramos or BL2) or patient derived B cell lymphoma (deficient in NMT2) xenografts.

In the first experiment, immuno-compromised NOD *scid* mice will be injected with B lymphoma cells (Ramos or BL2 “BL” cells) and tumors

will be allowed to grow. Mice will be treated with DDD86481 at increasing concentrations. The size of tumors will be measured daily. After 21 days of therapy (or moribund), autopsies will be performed to count, extract and weigh the tumors. The mean tumor volume response and Kaplan-Meier survival curves will be plotted as a function of time. The regimen will be varied as to optimize therapeutic efficacy.

In a second experiment, the potency of DDD86481 will be assessed using patient derived xenograft mouse model (PDX). Briefly, NOD *scid* IL2 receptor gamma chain knockout (NSG) mice with established human primary DLBCL lymphoma xenografts (mouse model PDX LY0055) will be subjected to treatment with increasing concentrations of DDD86481 by the Jackson Laboratory *in vivo* Pharmacology Services. Importantly, microarray analysis of PDX LY0055 mouse states that NMT2 levels as being comparable to those of Daudi cells, in which NMT2 could not be detected by WB. Moreover, we expect BL and PDX tumors to both cease growth and also regress upon treatment, because our results show that BL cells with depleted levels of NMT2 readily undergo apoptosis when treated with DDD86481. Because Ramos and BL2 cell lines have been cultured for over 40 years (ATCC; www.atcc.org), we expect that these will require a higher dose of DDD86481 than tumors freshly derived from patients, which have a very low passage number and potentially carry less mutations than cultured BL cells. In addition, one could imagine that the extraction of malignant B

cells from the blood or bone marrow of consented patients, and treating these cells *ex vivo* with DDD86481, may be a more effective method for testing the drug. We think both *in vivo* and *ex vivo* strategies using patient derived cancer cells will yield valuable information and allow us to further establish our proof-of-concept.

5.2.3 Optimize specificity and pharmacokinetic properties of NMT inhibitors through rational drug design and medicinal chemistry

We demonstrated that DDD85646 and especially DDD86481 NMT inhibitors are promising candidates for the treatment of BL. Still, these pyrazole sulfanomide based NMT inhibitors do not discriminate between the human NMT isozymes. Hence, we presume that these NMT inhibitors are effective against B lymphomas that have low total levels of NMT1 and NMT2, **or**, low levels of NMT1 without NMT2. Conceivably, we think that developing a chemotherapeutic drug that kills cancer cells with higher levels of NMT1 with low levels of NMT2 would require preferentially targeting of the NMT1 enzyme. Overall, a second generation of NMT1 specific inhibitors could also improve the therapeutic efficacy of our novel personalized treatment. Hence, we intend to identify NMT inhibitors that are more selective towards NMT1 using structure-based approaches. This would require solving the structure of full length hNMTs since the available structures are generated using truncated NMTs which are missing 108

residue N-terminal domain (Protein Data bank, PDB Id: 3IWE, 3JTK, 3IU1, 3IU2; solved by Dr. Paul Wyatt, University of Dundee, Scotland).

The greatest sequence dissimilarity between the two NMTs is found in the N-terminal region that is removed by the action of caspases during apoptosis (Giang and Cravatt, 1998; Perinpanayagam et al., 2013). Hence, solving the structures of full-length and caspase truncated (ct-) NMTs will give us the opportunity to understand the enzyme mechanism and in turn facilitate the design of NMT1 specific inhibitors. Furthermore, solving the crystal structures of these NMTs alone or NMTs bound to peptides corresponding to the N-termini of pro-survival co-translationally myristoylated c-Src or c-Abl, and the post-translationally myristoylated pro-apoptotic ct-Bid or ct-PAK2 as well as inhibitors (DDD86481) will be fundamental to understanding the process of NMT substrate binding and consequently lead to designing drugs with improved selectivity for NMT1 using rational drug design and medicinal chemistry. Alternatively, identifying drugs that would inhibit NMT1 but not NMT2 (or less so) could be done by through the use of high throughput drug screens performed in parallel with NMT1 and NMT2 on separate plates. Furthermore, assessing whether our lead NMT inhibitors have good pharmacokinetic and toxicology profiles is of great importance. Hence, we plan to investigate the pharmacokinetics of our lead NMT inhibitors by ADME (absorption, distribution, metabolism and elimination) assays early in the drug discovery process (Kassel, 2004).

5.2.4 Comparison of the co- and post-translational myristoylomes of normal and malignant lymphocytes treated with or without DDD86481 to identify putative myristoylated tumor supressors in BL cells

To date, no NMT inhibitor has made it to the clinic. The Identification of this novel target in cancer cells definitely warrants further characterization of the mechanisms of action at play. After characterizing the NMTs, the next step will involve the characterization of the myristoylomes of “normal” (i.e. IM9) and malignant BL cells (i.e. Ramos and BL2). To do so, cultured cells will be induced to undergo apoptosis (to assess post-translational myristoylation) or not and then metabolically labeled with alkynyl-myristate followed by conjugation with biotin-azide using click chemistry as in (Yap et al., 2010). Myristoylomes from normal and malignant cell lines will be compared once biotinylated-alkynyl-myristoylated proteins are identified by mass spectrometry. We expect that these proteomic experiments will yield some candidate proteins with altered myristoylation linked to destablization and protein degradation in the presence of the drug but not in its absence. Comparison of proteins which are myristoylated in “normal” immortalized B cells (IM9) and BL cells, will give indirect insights into the contributions of NMT2 (missing in BL2 and Ramos) to altered cell survival or cell death mechanisms in BL. Consequently, we may be able to identify a potential tumor suppressor,

whose function would depend on its proper myristoylation by NMT2. Importantly, **figure 4.4** already shows that there are several myristoylated proteins missing in the lysates of BL2 and Ramos cells in comparison to that of IM-9 cells. This further justifies the need to characterize the myristoylomes of normal and malignant B cells.

5.3 Significance

In this work, I have demonstrated for the first time that NMTs are regulated by caspases during apoptosis and identified a molecular lesion resulting in the loss of NMT2 expression in BL that render these cells highly susceptible to NMT inhibitors. Hence, this work includes fundamental discoveries important to our understanding of apoptosis, which is often altered in cancer cells, as well translational applications towards the development of a novel personalized medical treatment of BLs with anticipated minimized side-effects. Furthermore, because NMT2 expression levels appear to be detrimentally altered in several other types of cancers (**Fig. 4.1 and Table 4.1**), our novel synthetically lethal personalized treatment using NMT inhibitors might eventually also benefit other types of cancers.

CHAPTER 6

Bibliography

Aitken, A., P. Cohen, S. Santikarn, D.H. Williams, A.G. Calder, A. Smith, and C.B. Klee. 1982. Identification of the NH2-terminal blocking group of calcineurin B as myristic acid. *FEBS Lett*. 150:314-318.

Al Massadi, O., M.H. Tschop, and J. Tong. 2011. Ghrelin acylation and metabolic control. *Peptides*. 32:2301-2308.

Alizadeh, A.A., M.B. Eisen, R.E. Davis, C. Ma, I.S. Lossos, A. Rosenwald, J.C. Boldrick, H. Sabet, T. Tran, X. Yu, J.I. Powell, L. Yang, G.E. Marti, T. Moore, J. Hudson, Jr., L. Lu, D.B. Lewis, R. Tibshirani, G. Sherlock, W.C. Chan, T.C. Greiner, D.D. Weisenburger, J.O. Armitage, R. Warnke, R. Levy, W. Wilson, M.R. Grever, J.C. Byrd, D. Botstein, P.O. Brown, and L.M. Staudt. 2000. Distinct types of diffuse large B-cell lymphoma identified by gene expression profiling. *Nature*. 403:503-511.

Armah, D.A., and K. Mensa-Wilmot. 1999. S-myristoylation of a glycosylphosphatidylinositol-specific phospholipase C in Trypanosoma brucei. *J Biol Chem*. 274:5931-5938.

Ashworth, A. 2008. A synthetic lethal therapeutic approach: poly(ADP) ribose polymerase inhibitors for the treatment of cancers deficient in DNA double-strand break repair. *J Clin Oncol*. 26:3785-3790.

Barneda-Zahonero, B., and M. Parra. 2012. Histone deacetylases and cancer. *Mol Oncol*. 6:579-589.

Barretina, J., G. Caponigro, N. Stransky, K. Venkatesan, A.A. Margolin, S. Kim, C.J. Wilson, J. Lehar, G.V. Kryukov, D. Sonkin, A. Reddy, M. Liu, L. Murray, M.F. Berger, J.E. Monahan, P. Morais, J. Meltzer, A. Korejwa, J. Jane-Valbuena, F.A. Mapa, J. Thibault, E. Bric-Furlong, P. Raman, A. Shipway, I.H. Engels, J. Cheng, G.K. Yu, J. Yu, P. Aspesi, Jr., M. de Silva, K. Jagtap, M.D. Jones, L. Wang, C. Hatton, E. Palescandolo, S. Gupta, S. Mahan, C. Sougnez, R.C. Onofrio, T. Liefeld, L. MacConaill, W. Winckler, M. Reich, N. Li, J.P. Mesirov, S.B. Gabriel, G. Getz, K. Ardlie, V. Chan, V.E. Myer, B.L. Weber, J. Porter, M. Warmuth, P. Finan, J.L. Harris, M. Meyerson, T.R. Golub, M.P. Morrissey, W.R. Sellers, R. Schlegel, and L.A. Garraway. 2012. The Cancer Cell Line Encyclopedia enables predictive modelling of anticancer drug sensitivity. *Nature*. 483:603-607.

Bereshchenko, O.R., W. Gu, and R. Dalla-Favera. 2002. Acetylation inactivates the transcriptional repressor BCL6. *Nat Genet*. 32:606-613.

Berndt, N., A.D. Hamilton, and S.M. Sebti. 2011. Targeting protein prenylation for cancer therapy. *Nat Rev Cancer*. 11:775-791.

Berthiaume, L., S.M. Peseckis, and M.D. Resh. 1995. Synthesis and use of iodo-fatty acid analogs. *Methods Enzymol*. 250:454-466.

Beveridge, R., S. Satram-Hoang, K. Sail, J. Darragh, C. Chen, M. Forsyth, and C. Reyes. 2011. Economic impact of disease progression in follicular non-Hodgkin lymphoma. *Leuk Lymphoma*. 52:2117-2123.

Bhandarkar, S.S., J. Bromberg, C. Carrillo, P. Selvakumar, R.K. Sharma, B.N. Perry, B. Govindarajan, L. Fried, A. Sohn, K. Reddy, and J.L. Arbiser. 2008. Tris (dibenzylideneacetone) dipalladium, a N-myristoyltransferase-1 inhibitor, is effective against melanoma growth in vitro and in vivo. *Clin Cancer Res*. 14:5743-5748.

Bhatnagar, R.S., K. Futterer, T.A. Farazi, S. Korolev, C.L. Murray, E. Jackson-Machelski, G.W. Gokel, J.I. Gordon, and G. Waksman. 1998. Structure of N-myristoyltransferase with bound myristoylCoA and peptide substrate analogs. *Nat Struct Biol*. 5:1091-1097.

Bhatnagar, R.S., K. Futterer, G. Waksman, and J.I. Gordon. 1999. The structure of myristoyl-CoA:protein N-myristoyltransferase. *Biochim Biophys Acta*. 1441:162-172.

Bhatnagar, R.S., E. Jackson-Machelski, C.A. McWherter, and J.I. Gordon. 1994. Isothermal titration calorimetric studies of Saccharomyces cerevisiae myristoyl-CoA:protein N-myristoyltransferase. Determinants of binding energy and catalytic discrimination among acyl-CoA and peptide ligands. *J Biol Chem*. 269:11045-11053.

Boisson, B., C. Giglione, and T. Meinnel. 2003. Unexpected protein families including cell defense components feature in the N-myristoylome of a higher eukaryote. *J Biol Chem*. 278:43418-43429.

Bokoch, G.M. 2003. Biology of the p21-activated kinases. *Annu Rev Biochem*. 72:743-781.

Boutin, J.A. 1997. Myristoylation. *Cell Signal*. 9:15-35.

Bowyer, P.W., E.W. Tate, R.J. Leatherbarrow, A.A. Holder, D.F. Smith, and K.A. Brown. 2008. N-myristoyltransferase: a prospective drug target for protozoan parasites. *ChemMedChem*. 3:402-408.

Brady, G., G.J. MacArthur, and P.J. Farrell. 2007. Epstein-Barr virus and Burkitt lymphoma. *J Clin Pathol*. 60:1397-1402.

Brannigan, J.A., B.A. Smith, Z. Yu, A.M. Brzozowski, M.R. Hodgkinson, A. Maroof, H.P. Price, F. Meier, R.J. Leatherbarrow, E.W. Tate, D.F. Smith, and A.J. Wilkinson. 2010. N-myristoyltransferase from

Leishmania donovani: structural and functional characterisation of a potential drug target for visceral leishmaniasis. *J Mol Biol*. 396:985-999.

Bratton, S.B., and G.M. Cohen. 2001. Apoptotic death sensor: an organelle's alter ego? *Trends Pharmacol Sci*. 22:306-315.

Bryant, H.E., N. Schultz, H.D. Thomas, K.M. Parker, D. Flower, E. Lopez, S. Kyle, M. Meuth, N.J. Curtin, and T. Helleday. 2005. Specific killing of BRCA2-deficient tumours with inhibitors of poly(ADP-ribose) polymerase. *Nature*. 434:913-917.

Bryant, M., and L. Ratner. 1990. Myristoylation-dependent replication and assembly of human immunodeficiency virus 1. *Proc Natl Acad Sci U S A*. 87:523-527.

Buglino, J.A., and M.D. Resh. 2008. Hhat is a palmitoylacyltransferase with specificity for N-palmitoylation of Sonic Hedgehog. *J Biol Chem*. 283:22076-22088.

Buglino, J.A., and M.D. Resh. 2012. Palmitoylation of Hedgehog proteins. *Vitam Horm*. 88:229-252.

Burkitt, D. 1958. A sarcoma involving the jaws in African children. *Br J Surg*. 46:218-223.

Buss, J.E., M.P. Kamps, and B.M. Sefton. 1984. Myristic acid is attached to the transforming protein of Rous sarcoma virus during or immediately after synthesis and is present in both soluble and membrane-bound forms of the protein. *Mol Cell Biol*. 4:2697-2704.

Cabanillas, F. 2011. Non-Hodgkin's lymphoma: the old and the new. *Clin Lymphoma Myeloma Leuk*. 11 Suppl 1:S87-90.

Carr, S.A., K. Biemann, S. Shoji, D.C. Parmelee, and K. Titani. 1982. n-Tetradecanoyl is the NH2-terminal blocking group of the catalytic subunit of cyclic AMP-dependent protein kinase from bovine cardiac muscle. *Proc Natl Acad Sci U S A*. 79:6128-6131.

Charron, G., M.M. Zhang, J.S. Yount, J. Wilson, A.S. Raghavan, E. Shamir, and H.C. Hang. 2009. Robust fluorescent detection of protein fatty-acylation with chemical reporters. *J Am Chem Soc*. 131:4967-4975.

Chen, C.A., and D.R. Manning. 2001. Regulation of G proteins by covalent modification. *Oncogene*. 20:1643-1652.

Chen, Y., and D.J. Klionsky. 2011. The regulation of autophagy - unanswered questions. *J Cell Sci*. 124:161-170.

Cohen, G.M. 1997. Caspases: the executioners of apoptosis. *Biochem J*. 326 (Pt 1):1-16.

Cordeddu, V., E. Di Schiavi, L.A. Pennacchio, A. Ma'ayan, A. Sarkozy, V. Fodale, S. Cecchetti, A. Cardinale, J. Martin, W. Schackwitz, A. Lipzen, G. Zampino, L. Mazzanti, M.C. Digilio, S. Martinelli, E. Flex, F. Lepri, D. Bartholdi, K. Kutsche, G.B. Ferrero, C. Anichini, A. Selicorni, C. Rossi, R. Tenconi, M. Zenker, D. Merlo, B. Dallapiccola, R. Iyengar, P. Bazzicalupo, B.D. Gelb, and M. Tartaglia. 2009. Mutation of SHOC2 promotes aberrant protein N-myristoylation and causes Noonan-like syndrome with loose anagen hair. *Nat Genet*. 41:1022-1026.

Cordo, S.M., N.A. Candurra, and E.B. Damonte. 1999. Myristic acid analogs are inhibitors of Junin virus replication. *Microbes Infect*. 1:609-614.

Cory, A.H., T.C. Owen, J.A. Barltrop, and J.G. Cory. 1991. Use of an aqueous soluble tetrazolium/formazan assay for cell growth assays in culture. *Cancer Commun*. 3:207-212.

Cross, F.R., E.A. Garber, D. Pellman, and H. Hanafusa. 1984. A short sequence in the p60src N terminus is required for p60src myristylation and membrane association and for cell transformation. *Mol Cell Biol*. 4:1834-1842.

Dang, C.V. 1999. c-Myc target genes involved in cell growth, apoptosis, and metabolism. *Mol Cell Biol*. 19:1-11.

Dave, S.S., K. Fu, G.W. Wright, L.T. Lam, P. Kluin, E.J. Boerma, T.C. Greiner, D.D. Weisenburger, A. Rosenwald, G. Ott, H.K. Muller-Hermelink, R.D. Gascoyne, J. Delabie, L.M. Rimsza, R.M. Braziel, T.M. Grogan, E. Campo, E.S. Jaffe, B.J. Dave, W. Sanger, M. Bast, J.M. Vose, J.O. Armitage, J.M. Connors, E.B. Smeland, S. Kvaloy, H. Holte, R.I. Fisher, T.P. Miller, E. Montserrat, W.H. Wilson, M. Bahl, H. Zhao, L. Yang, J. Powell, R. Simon, W.C. Chan, and L.M. Staudt. 2006. Molecular diagnosis of Burkitt's lymphoma. *N Engl J Med*. 354:2431-2442.

Dawson, M.A., and T. Kouzarides. 2012. Cancer epigenetics: from mechanism to therapy. *Cell*. 150:12-27.

Deichaite, I., L.P. Casson, H.P. Ling, and M.D. Resh. 1988. In vitro synthesis of pp60v-src: myristylation in a cell-free system. *Mol Cell Biol*. 8:4295-4301.

Dekker, F.J., O. Rocks, N. Vartak, S. Menninger, C. Hedberg, R. Balamurugan, S. Wetzel, S. Renner, M. Gerauer, B. Scholermann, M. Rusch, J.W. Kramer, D. Rauh, G.W. Coates, L. Brunsveld, P.I. Bastiaens, and H. Waldmann. 2010. Small-molecule inhibition of APT1 affects Ras localization and signaling. *Nat Chem Biol*. 6:449-456.

Devadas, B., S.K. Freeman, M.E. Zupec, H.F. Lu, S.R. Nagarajan, N.S. Kishore, J.K. Lodge, D.W. Kuneman, C.A. McWherter, D.V. Vinjamoori, D.P. Getman, J.I. Gordon, and J.A. Sikorski. 1997. Design and synthesis of novel imidazole-substituted dipeptide amides as potent and selective inhibitors of Candida albicans myristoylCoA:protein N-myristoyltransferase and identification of related tripeptide inhibitors with mechanism-based antifungal activity. *J Med Chem*. 40:2609-2625.

Devadas, B., T. Lu, A. Katoh, N.S. Kishore, A.C. Wade, P.P. Mehta, D.A. Rudnick, M.L. Bryant, S.P. Adams, Q. Li, and et al. 1992. Substrate specificity of Saccharomyces cerevisiae myristoyl-CoA: protein N-myristoyltransferase. Analysis of fatty acid analogs containing carbonyl groups, nitrogen heteroatoms, and nitrogen heterocycles in an in vitro enzyme assay and subsequent identification of inhibitors of human immunodeficiency virus I replication. *J Biol Chem*. 267:7224-7239.

Dix, M.M., G.M. Simon, and B.F. Cravatt. 2008. Global mapping of the topography and magnitude of proteolytic events in apoptosis. *Cell*. 134:679-691.

Draper, J.M., and C.D. Smith. 2009. Palmitoyl acyltransferase assays and inhibitors (Review). *Mol Membr Biol*. 26:5-13.

Ducker, C.E., J.J. Upson, K.J. French, and C.D. Smith. 2005. Two N-myristoyltransferase isozymes play unique roles in protein myristoylation, proliferation, and apoptosis. *Mol Cancer Res*. 3:463-476.

Duronio, R.J., S.I. Reed, and J.I. Gordon. 1992. Mutations of human myristoyl-CoA:protein N-myristoyltransferase cause temperature-sensitive myristic acid auxotrophy in Saccharomyces cerevisiae. *Proc Natl Acad Sci U S A*. 89:4129-4133.

Duronio, R.J., D.A. Towler, R.O. Heuckeroth, and J.I. Gordon. 1989. Disruption of the yeast N-myristoyl transferase gene causes recessive lethality. *Science*. 243:796-800.

Dyda, F., D.C. Klein, and A.B. Hickman. 2000. GCN5-related N-acetyltransferases: a structural overview. *Annu Rev Biophys Biomol Struct*. 29:81-103.

Enari, M., H. Sakahira, H. Yokoyama, K. Okawa, A. Iwamatsu, and S. Nagata. 1998. A caspase-activated DNase that degrades DNA during apoptosis, and its inhibitor ICAD. *Nature*. 391:43-50.

Fadeel, B., and S. Orrenius. 2005. Apoptosis: a basic biological phenomenon with wide-ranging implications in human disease. *J Intern Med*. 258:479-517.

Farazi, T.A., G. Waksman, and J.I. Gordon. 2001. The biology and enzymology of protein N-myristoylation. *J Biol Chem*. 276:39501-39504.

Farmer, H., N. McCabe, C.J. Lord, A.N. Tutt, D.A. Johnson, T.B. Richardson, M. Santarosa, K.J. Dillon, I. Hickson, C. Knights, N.M. Martin, S.P. Jackson, G.C. Smith, and A. Ashworth. 2005. Targeting the DNA repair defect in BRCA mutant cells as a therapeutic strategy. *Nature*. 434:917-921.

Feinberg, A.P., and B. Tycko. 2004. The history of cancer epigenetics. *Nat Rev Cancer*. 4:143-153.

Felsted, R.L., C.J. Glover, and K. Hartman. 1995. Protein N-myristoylation as a chemotherapeutic target for cancer. *J Natl Cancer Inst*. 87:1571-1573.

Ferrara, F., and R. Ravasio. 2008. Cost-effectiveness analysis of the addition of rituximab to CHOP in young patients with good-prognosis diffuse large-B-cell lymphoma. *Clin Drug Investig*. 28:55-65.

Foon, K.A., K. Takeshita, and P.L. Zinzani. 2012. Novel therapies for aggressive B-cell lymphoma. *Adv Hematol*. 2012:302570.

Frearson, J.A., S. Brand, S.P. McElroy, L.A. Cleghorn, O. Smid, L. Stojanovski, H.P. Price, M.L. Guther, L.S. Torrie, D.A. Robinson, I. Hallyburton, C.P. Mpamhanga, J.A. Brannigan, A.J. Wilkinson, M. Hodgkinson, R. Hui, W. Qiu, O.G. Raimi, D.M. van Aalten, R. Brenk, I.H. Gilbert, K.D. Read, A.H. Fairlamb, M.A. Ferguson, D.F. Smith, and P.G. Wyatt. 2010. N-myristoyltransferase inhibitors as new leads to treat sleeping sickness. *Nature*. 464:728-732.

French, K.J., Y. Zhuang, R.S. Schrecengost, J.E. Copper, Z. Xia, and C.D. Smith. 2004. Cyclohexyl-octahydro-pyrrolo[1,2-a]pyrazine-based

inhibitors of human N-myristoyltransferase-1. *J Pharmacol Exp Ther*. 309:340-347.

Frottin, F., A. Martinez, P. Peynot, S. Mitra, R.C. Holz, C. Giglione, and T. Meinnel. 2006. The proteomics of N-terminal methionine cleavage. *Mol Cell Proteomics*. 5:2336-2349.

Fukata, Y., and M. Fukata. 2010. Protein palmitoylation in neuronal development and synaptic plasticity. *Nat Rev Neurosci*. 11:161-175.

Gatto, D., and R. Brink. 2010. The germinal center reaction. *J Allergy Clin Immunol*. 126:898-907; quiz 908-899.

Giang, D.K., and B.F. Cravatt. 1998. A second mammalian N-myristoyltransferase. *J Biol Chem*. 273:6595-6598.

Gisselbrecht, C., B. Glass, N. Mounier, D. Singh Gill, D.C. Linch, M. Trneny, A. Bosly, N. Ketterer, O. Shpilberg, H. Hagberg, D. Ma, J. Briere, C.H. Moskowitz, and N. Schmitz. 2010. Salvage regimens with autologous transplantation for relapsed large B-cell lymphoma in the rituximab era. *J Clin Oncol*. 28:4184-4190.

Glover, C.J., K.D. Hartman, and R.L. Felsted. 1997. Human N-myristoyltransferase amino-terminal domain involved in targeting the enzyme to the ribosomal subcellular fraction. *J Biol Chem*. 272:28680-28689.

Greaves, J., and L.H. Chamberlain. 2011. DHHC palmitoyl transferases: substrate interactions and (patho)physiology. *Trends Biochem Sci*. 36:245-253.

Griffin, T.C., S. Weitzman, H. Weinstein, M. Chang, M. Cairo, R. Hutchison, B. Shiramizu, J. Wiley, D. Woods, M. Barnich, and T.G. Gross. 2009. A study of rituximab and ifosfamide, carboplatin, and etoposide chemotherapy in children with recurrent/refractory B-cell (CD20+) non-Hodgkin lymphoma and mature B-cell acute lymphoblastic leukemia: a report from the Children's Oncology Group. *Pediatr Blood Cancer*. 52:177-181.

Gui, C.Y., L. Ngo, W.S. Xu, V.M. Richon, and P.A. Marks. 2004. Histone deacetylase (HDAC) inhibitor activation of p21WAF1 involves changes in promoter-associated proteins, including HDAC1. *Proc Natl Acad Sci U S A*. 101:1241-1246.

Gutkowska, M., and E. Swiezewska. 2012. Structure, regulation and cellular functions of Rab geranylgeranyl transferase and its cellular partner Rab Escort Protein. *Mol Membr Biol*. 29:243-256.

Hang, H.C., E.J. Geutjes, G. Grotenbreg, A.M. Pollington, M.J. Bijlmakers, and H.L. Ploegh. 2007. Chemical probes for the rapid detection of Fatty-acylated proteins in Mammalian cells. *J Am Chem Soc*. 129:2744-2745.

Hang, H.C., and M.E. Linder. 2011. Exploring protein lipidation with chemical biology. *Chem Rev*. 111:6341-6358.

Hannoush, R.N., and N. Arenas-Ramirez. 2009. Imaging the lipidome: omega-alkynyl fatty acids for detection and cellular visualization of lipid-modified proteins. *ACS Chem Biol*. 4:581-587.

Hannoush, R.N., and J. Sun. 2010. The chemical toolbox for monitoring protein fatty acylation and prenylation. *Nat Chem Biol*. 6:498-506.

Hantschel, O., B. Nagar, S. Guettler, J. Kretzschmar, K. Dorey, J. Kuriyan, and G. Superti-Furga. 2003. A myristoyl/phosphotyrosine switch regulates c-Abl. *Cell*. 112:845-857.

Hao, Z., and T.W. Mak. 2010. Type I and type II pathways of Fas-mediated apoptosis are differentially controlled by XIAP. *J Mol Cell Biol*. 2:63-64.

Harper, D.R., R.L. Gilbert, C. Blunt, and R.A. McIlhinney. 1993. Inhibition of varicella-zoster virus replication by an inhibitor of protein myristoylation. *J Gen Virol*. 74 (Pt 6):1181-1184.

Heal, W.P., B. Jovanovic, S. Bessin, M.H. Wright, A.I. Magee, and E.W. Tate. 2011. Bioorthogonal chemical tagging of protein cholesterylation in living cells. *Chem Commun (Camb)*. 47:4081-4083.

Hedo, J.A., E. Collier, and A. Watkinson. 1987. Myristyl and palmityl acylation of the insulin receptor. *J Biol Chem*. 262:954-957.

Hu, T., C. Li, Z. Cao, T.J. Van Raay, J.G. Smith, K. Willert, L. Solnica-Krezel, and R.J. Coffey. 2010. Myristoylated Naked2 antagonizes Wnt-beta-catenin activity by degrading Dishevelled-1 at the plasma membrane. *J Biol Chem*. 285:13561-13568.

Hudson, L., and F.C. Hay. 1976. Practical Immunology. Blackwell Scientific Publications, Oxford, England. 29-32.

Hummel, M., S. Bentink, H. Berger, W. Klapper, S. Wessendorf, T.F. Barth, H.W. Bernd, S.B. Cogliatti, J. Dierlamm, A.C. Feller, M.L. Hansmann, E. Haralambieva, L. Harder, D. Hasenclever, M. Kuhn, D. Lenze, P. Lichter, J.I. Martin-Subero, P. Moller, H.K. Muller-Hermelink, G. Ott, R.M. Parwaresch, C. Pott, A. Rosenwald, M.

Rosolowski, C. Schwaenen, B. Sturzenhofecker, M. Szczepanowski, H. Trautmann, H.H. Wacker, R. Spang, M. Loeffler, L. Trumper, H. Stein, and R. Siebert. 2006. A biologic definition of Burkitt's lymphoma from transcriptional and genomic profiling. *N Engl J Med*. 354:2419-2430.

Inoue, S., G. Browne, G. Melino, and G.M. Cohen. 2009. Ordering of caspases in cells undergoing apoptosis by the intrinsic pathway. *Cell Death Differ*. 16:1053-1061.

Iversen, U., O.H. Iversen, A.Z. Bluming, J.L. Ziegler, and S. Kyalwasi. 1972. Cell kinetics of African cases of Burkitt lymphoma. A preliminary report. *Eur J Cancer*. 8:305-308.

Jackson, P., and D. Baltimore. 1989. N-terminal mutations activate the leukemogenic potential of the myristoylated form of c-abl. *EMBO J*. 8:449-456.

Jaffe, E.S. 2009. The 2008 WHO classification of lymphomas: implications for clinical practice and translational research. *Hematology Am Soc Hematol Educ Program*:523-531.

Jakobi, R. 2004. Subcellular targeting regulates the function of caspase-activated protein kinases in apoptosis. *Drug Resist Updat*. 7:11-17.

Juo, P., C.J. Kuo, J. Yuan, and J. Blenis. 1998. Essential requirement for caspase-8/FLICE in the initiation of the Fas-induced apoptotic cascade. *Curr Biol*. 8:1001-1008.

Kaelin, W.G., Jr. 2005. The concept of synthetic lethality in the context of anticancer therapy. *Nat Rev Cancer*. 5:689-698.

Kagawa, S., J. Gu, T. Honda, T.J. McDonnell, S.G. Swisher, J.A. Roth, and B. Fang. 2001. Deficiency of caspase-3 in MCF7 cells blocks Bax-mediated nuclear fragmentation but not cell death. *Clin Cancer Res*. 7:1474-1480.

Kamps, M.P., J.E. Buss, and B.M. Sefton. 1985. Mutation of NH2-terminal glycine of p60src prevents both myristoylation and morphological transformation. *Proc Natl Acad Sci U S A*. 82:4625-4628.

Kassel, D.B. 2004. Applications of high-throughput ADME in drug discovery. *Curr Opin Chem Biol*. 8:339-345.

Kelly, G.L., and A.B. Rickinson. 2007. Burkitt lymphoma: revisiting the pathogenesis of a virus-associated malignancy. *Hematology Am Soc Hematol Educ Program*:277-284.

Kenkre, V.P., and W. Stock. 2009. Burkitt lymphoma/leukemia: improving prognosis. *Clin Lymphoma Myeloma*. 9 Suppl 3:S231-238.

Kim, L.C., L. Song, and E.B. Haura. 2009. Src kinases as therapeutic targets for cancer. *Nat Rev Clin Oncol*. 6:587-595.

King, M.J., and R.K. Sharma. 1991. N-myristoyl transferase assay using phosphocellulose paper binding. *Anal Biochem*. 199:149-153.

King, M.J., and R.K. Sharma. 1992. Demonstration of multiple forms of bovine brain myristoyl CoA:protein N-myristoyl transferase. *Mol Cell Biochem*. 113:77-81.

King, M.J., and R.K. Sharma. 1993. Identification, purification and characterization of a membrane-associated N-myristoyltransferase inhibitor protein from bovine brain. *Biochem J*. 291 (Pt 2):635-639.

Kishore, N.S., T.B. Lu, L.J. Knoll, A. Katoh, D.A. Rudnick, P.P. Mehta, B. Devadas, M. Huhn, J.L. Atwood, S.P. Adams, and et al. 1991. The substrate specificity of Saccharomyces cerevisiae myristoyl-CoA:protein N-myristoyltransferase. Analysis of myristic acid analogs containing oxygen, sulfur, double bonds, triple bonds, and/or an aromatic residue. *J Biol Chem*. 266:8835-8855.

Kojima, M., H. Hosoda, Y. Date, M. Nakazato, H. Matsuo, and K. Kangawa. 1999. Ghrelin is a growth-hormone-releasing acylated peptide from stomach. *Nature*. 402:656-660.

Korycka, J., A. Lach, E. Heger, D.M. Boguslawska, M. Wolny, M. Toporkiewicz, K. Augoff, J. Korzeniewski, and A.F. Sikorski. 2012. Human DHHC proteins: a spotlight on the hidden player of palmitoylation. *Eur J Cell Biol*. 91:107-117.

Kumar, S., J.R. Dimmock, and R.K. Sharma. 2011. The Potential Use of N-Myristoyltransferase as a Biomarker in the Early Diagnosis of Colon Cancer. *Cancers (Basel)*. 3:1372-1382.

Kuppers, R. 2005. Mechanisms of B-cell lymphoma pathogenesis. *Nat Rev Cancer*. 5:251-262.

Laemmli, U.K. 1970. Cleavage of structural proteins during the assembly of the head of bacteriophage T4. *Nature*. 227:680-685.

Leatherbarrow, R.J. 2009. Grafit (Version 6). *Erithacus Software Ltd., Horley, United Kingdom*.

Lee, R.C., D. Zou, D.J. Demetrick, L.M. Difrancesco, K. Fassbender, and D. Stewart. 2008. Costs associated with diffuse large B-cell

lymphoma patient treatment in a Canadian integrated cancer care center. *Value Health*. 11:221-230.

Lenz, G., and L.M. Staudt. 2010. Aggressive lymphomas. *N Engl J Med*. 362:1417-1429.

Liang, X., Y. Lu, T.A. Neubert, and M.D. Resh. 2002. Mass spectrometric analysis of GAP-43/neuromodulin reveals the presence of a variety of fatty acylated species. *J Biol Chem*. 277:33032-33040.

Liang, X., Y. Lu, M. Wilkes, T.A. Neubert, and M.D. Resh. 2004. The N-terminal SH4 region of the Src family kinase Fyn is modified by methylation and heterogeneous fatty acylation: role in membrane targeting, cell adhesion, and spreading. *J Biol Chem*. 279:8133-8139.

Lin, H., X. Su, and B. He. 2012. Protein lysine acylation and cysteine succination by intermediates of energy metabolism. *ACS Chem Biol*. 7:947-960.

Liston, P., W.G. Fong, and R.G. Korneluk. 2003. The inhibitors of apoptosis: there is more to life than Bcl2. *Oncogene*. 22:8568-8580.

Liu, M., A.K. Sjogren, C. Karlsson, M.X. Ibrahim, K.M. Andersson, F.J. Olofsson, A.M. Wahlstrom, M. Dalin, H. Yu, Z. Chen, S.H. Yang, S.G. Young, and M.O. Bergo. 2010. Targeting the protein prenyltransferases efficiently reduces tumor development in mice with K-RAS-induced lung cancer. *Proc Natl Acad Sci U S A*. 107:6471-6476.

Lobo, S., W.K. Greentree, M.E. Linder, and R.J. Deschenes. 2002. Identification of a Ras palmitoyltransferase in Saccharomyces cerevisiae. *J Biol Chem*. 277:41268-41273.

Lodge, J.K., E. Jackson-Machelski, D.L. Toffaletti, J.R. Perfect, and J.I. Gordon. 1994a. Targeted gene replacement demonstrates that myristoyl-CoA: protein N-myristoyltransferase is essential for viability of Cryptococcus neoformans. *Proc Natl Acad Sci U S A*. 91:12008-12012.

Lodge, J.K., R.L. Johnson, R.A. Weinberg, and J.I. Gordon. 1994b. Comparison of myristoyl-CoA:protein N-myristoyltransferases from three pathogenic fungi: Cryptococcus neoformans, Histoplasma capsulatum, and Candida albicans. *J Biol Chem*. 269:2996-3009.

Love, C., Z. Sun, D. Jima, G. Li, J. Zhang, R. Miles, K.L. Richards, C.H. Dunphy, W.W. Choi, G. Srivastava, P.L. Lugar, D.A. Rizzieri, A.S. Lagoo, L. Bernal-Mizrachi, K.P. Mann, C.R. Flowers, K.N. Naresh,

A.M. Evens, A. Chadburn, L.I. Gordon, M.B. Czader, J.I. Gill, E.D. Hsi, A. Greenough, A.B. Moffitt, M. McKinney, A. Banerjee, V. Grubor, S. Levy, D.B. Dunson, and S.S. Dave. 2012. The genetic landscape of mutations in Burkitt lymphoma. *Nat Genet*. 44:1321-1325.

Lu, Y., P. Selvakumar, K. Ali, A. Shrivastav, G. Bajaj, L. Resch, R. Griebel, D. Fourney, K. Meguro, and R.K. Sharma. 2005. Expression of N-myristoyltransferase in human brain tumors. *Neurochem Res*. 30:9-13.

Luciano, F., A. Jacquel, P. Colosetti, M. Herrant, S. Cagnol, G. Pages, and P. Auberger. 2003. Phosphorylation of Bim-EL by Erk1/2 on serine 69 promotes its degradation via the proteasome pathway and regulates its proapoptotic function. *Oncogene*. 22:6785-6793.

Magee, T., and M.C. Seabra. 2005. Fatty acylation and prenylation of proteins: what's hot in fat. *Curr Opin Cell Biol*. 17:190-196.

Magnuson, B.A., R.V. Raju, T.N. Moyana, and R.K. Sharma. 1995. Increased N-myristoyltransferase activity observed in rat and human colonic tumors. *J Natl Cancer Inst*. 87:1630-1635.

Mahrus, S., J.C. Trinidad, D.T. Barkan, A. Sali, A.L. Burlingame, and J.A. Wells. 2008. Global sequencing of proteolytic cleavage sites in apoptosis by specific labeling of protein N termini. *Cell*. 134:866-876.

Mann, R.K., and P.A. Beachy. 2004. Novel lipid modifications of secreted protein signals. *Annu Rev Biochem*. 73:891-923.

Martin, B.R., and B.F. Cravatt. 2009. Large-scale profiling of protein palmitoylation in mammalian cells. *Nat Methods*. 6:135-138.

Martin, D.D., C.Y. Ahpin, R.J. Heit, M.A. Perinpanayagam, M.C. Yap, R.A. Veldhoen, I.S. Goping, and L.G. Berthiaume. 2012. Tandem reporter assay for myristoylated proteins post-translationally (TRAMPP) identifies novel substrates for post-translational myristoylation: PKCepsilon, a case study. *FASEB J*. 26:13-28.

Martin, D.D., E. Beauchamp, and L.G. Berthiaume. 2011. Post-translational myristoylation: Fat matters in cellular life and death. *Biochimie*. 93:18-31.

Martin, D.D., G.L. Vilas, J.A. Prescher, G. Rajaiah, J.R. Falck, C.R. Bertozzi, and L.G. Berthiaume. 2008. Rapid detection, discovery, and identification of post-translationally myristoylated proteins

during apoptosis using a bio-orthogonal azidomyristate analog. *FASEB J*. 22:797-806.

Matheson, A.T., M. Yaguchi, and L.P. Visentin. 1975. The conservation of amino acids in the n-terminal position of ribosomal and cytosol proteins from Escherichia coli, Bacillus stearothermophilus, and Halobacterium cutirubrum. *Can J Biochem*. 53:1323-1327.

Maurer-Stroh, S., B. Eisenhaber, and F. Eisenhaber. 2002a. N-terminal N-myristoylation of proteins: prediction of substrate proteins from amino acid sequence. *J Mol Biol*. 317:541-557.

Maurer-Stroh, S., B. Eisenhaber, and F. Eisenhaber. 2002b. N-terminal N-myristoylation of proteins: refinement of the sequence motif and its taxon-specific differences. *J Mol Biol*. 317:523-540.

Maurer-Stroh, S., and F. Eisenhaber. 2005. Refinement and prediction of protein prenylation motifs. *Genome Biol*. 6:R55.

Mayor, S., and H. Riezman. 2004. Sorting GPI-anchored proteins. *Nat Rev Mol Cell Biol*. 5:110-120.

McCabe, J.B., and L.G. Berthiaume. 1999. Functional roles for fatty acylated amino-terminal domains in subcellular localization. *Mol Biol Cell*. 10:3771-3786.

McCabe, J.B., and L.G. Berthiaume. 2001. N-terminal protein acylation confers localization to cholesterol, sphingolipid-enriched membranes but not to lipid rafts/caveolae. *Mol Biol Cell*. 12:3601-3617.

McIlhinney, R.A. 1995. Characterization and cellular localization of human myristoyl-COA: protein N-myristoyltransferase. *Biochem Soc Trans*. 23:549-553.

McIlhinney, R.A., and K. McGlone. 1996. Immunocytochemical characterization and subcellular localization of human myristoyl-CoA: protein N-myristoyltransferase in HeLa cells. *Exp Cell Res*. 223:348-356.

McIlhinney, R.A., K. McGlone, and A.C. Willis. 1993. Purification and partial sequencing of myristoyl-CoA:protein N-myristoyltransferase from bovine brain. *Biochem J*. 290 (Pt 2):405-410.

McLaughlin, S., and A. Aderem. 1995. The myristoyl-electrostatic switch: a modulator of reversible protein-membrane interactions. *Trends Biochem Sci*. 20:272-276.

McTaggart, S.J. 2006. Isoprenylated proteins. *Cell Mol Life Sci*. 63:255-267.

Miles, R.R., S. Arnold, and M.S. Cairo. 2012. Risk factors and treatment of childhood and adolescent Burkitt lymphoma/leukaemia. *Br J Haematol*. 156:730-743.

Mishkind, M. 2001. Morbid myristoylation. *Trends Cell Biol*. 11:191.

Mitchell, D.A., A. Vasudevan, M.E. Linder, and R.J. Deschenes. 2006. Protein palmitoylation by a family of DHHC protein S-acyltransferases. *J Lipid Res*. 47:1118-1127.

Moffitt, K.L., S.L. Martin, and B. Walker. 2010. From sentencing to execution--the processes of apoptosis. *J Pharm Pharmacol*. 62:547-562.

Molyneux, E.M., R. Rochford, B. Griffin, R. Newton, G. Jackson, G. Menon, C.J. Harrison, T. Israels, and S. Bailey. 2012. Burkitt's lymphoma. *Lancet*. 379:1234-1244.

Morgan, M.A., F.O. Onono, H.P. Spielmann, T. Subramanian, M. Scherr, L. Venturini, I. Dallmann, A. Ganser, and C.W. Reuter. 2012. Modulation of anthracycline-induced cytotoxicity by targeting the prenylated proteome in myeloid leukemia cells. *J Mol Med (Berl)*. 90:149-161.

Nagata, S. 2000. Apoptotic DNA fragmentation. *Exp Cell Res*. 256:12-18.

Nimchuk, Z., E. Marois, S. Kjemtrup, R.T. Leister, F. Katagiri, and J.L. Dangl. 2000. Eukaryotic fatty acylation drives plasma membrane targeting and enhances function of several type III effector proteins from Pseudomonas syringae. *Cell*. 101:353-363.

Novelli, G., and M.R. D'Apice. 2012. Protein farnesylation and disease. *J Inherit Metab Dis*. 35:917-926.

Ntwasa, M., S. Aapies, D.A. Schiffmann, and N.J. Gay. 2001. Drosophila embryos lacking N-myristoyltransferase have multiple developmental defects. *Exp Cell Res*. 262:134-144.

Ntwasa, M., M. Egerton, and N.J. Gay. 1997. Sequence and expression of Drosophila myristoyl-CoA: protein N-myristoyl transferase: evidence for proteolytic processing and membrane localisation. *J Cell Sci*. 110 (Pt 2):149-156.

Ohno, Y., A. Kihara, T. Sano, and Y. Igarashi. 2006. Intracellular localization and tissue-specific distribution of human and yeast

DHHC cysteine-rich domain-containing proteins. *Biochim Biophys Acta*. 1761:474-483.

Olsson, M., and B. Zhivotovsky. 2011. Caspases and cancer. *Cell Death Differ*. 18:1441-1449.

Paige, L.A., G.Q. Zheng, S.A. DeFrees, J.M. Cassady, and R.L. Geahlen. 1990. Metabolic activation of 2-substituted derivatives of myristic acid to form potent inhibitors of myristoyl CoA:protein N-myristoyltransferase. *Biochemistry*. 29:10566-10573.

Panethymitaki, C., P.W. Bowyer, H.P. Price, R.J. Leatherbarrow, K.A. Brown, and D.F. Smith. 2006. Characterization and selective inhibition of myristoyl-CoA:protein N-myristoyltransferase from Trypanosoma brucei and Leishmania major. *Biochem J*. 396:277-285.

Parekh, S., G. Prive, and A. Melnick. 2008. Therapeutic targeting of the BCL6 oncogene for diffuse large B-cell lymphomas. *Leuk Lymphoma*. 49:874-882.

Patwardhan, P., and M.D. Resh. 2010. Myristoylation and membrane binding regulate c-Src stability and kinase activity. *Mol Cell Biol*. 30:4094-4107.

Paulick, M.G., and C.R. Bertozzi. 2008. The glycosylphosphatidylinositol anchor: a complex membrane-anchoring structure for proteins. *Biochemistry*. 47:6991-7000.

Peitzsch, R.M., and S. McLaughlin. 1993. Binding of acylated peptides and fatty acids to phospholipid vesicles: pertinence to myristoylated proteins. *Biochemistry*. 32:10436-10443.

Perinpanayagam, M.A., E. Beauchamp, D.D. Martin, J.Y. Sim, M.C. Yap, and L.G. Berthiaume. 2012. Regulation of co- and post-translational myristoylation of proteins during apoptosis: interplay of N-myristoyltransferases and caspases. *FASEB J*.

Perinpanayagam, M.A., E. Beauchamp, D.D. Martin, J.Y. Sim, M.C. Yap, and L.G. Berthiaume. 2013. Regulation of co- and post-translational myristoylation of proteins during apoptosis: interplay of N-myristoyltransferases and caspases. *FASEB J*. 27:811-821.

Peseckis, S.M., I. Deichaite, and M.D. Resh. 1993. Iodinated fatty acids as probes for myristate processing and function. Incorporation into pp60v-src. *J Biol Chem*. 268:5107-5114.

Phan, R.T., and R. Dalla-Favera. 2004. The BCL6 proto-oncogene suppresses p53 expression in germinal-centre B cells. *Nature*. 432:635-639.

Podell, S., and M. Gribskov. 2004. Predicting N-terminal myristoylation sites in plant proteins. *BMC Genomics*. 5:37.

Porter, J.A., K.E. Young, and P.A. Beachy. 1996. Cholesterol modification of hedgehog signaling proteins in animal development. *Science*. 274:255-259.

Price, H.P., M.R. Menon, C. Panethymitaki, D. Goulding, P.G. McKean, and D.F. Smith. 2003. Myristoyl-CoA:protein N-myristoyltransferase, an essential enzyme and potential drug target in kinetoplastid parasites. *J Biol Chem*. 278:7206-7214.

Rajala, R.V., J.M. Radhi, R. Kakkar, R.S. Datla, and R.K. Sharma. 2000. Increased expression of N-myristoyltransferase in gallbladder carcinomas. *Cancer*. 88:1992-1999.

Raju, R.V., J.W. Anderson, R.S. Datla, and R.K. Sharma. 1997a. Molecular cloning and biochemical characterization of bovine spleen myristoyl CoA:protein N-myristoyltransferase. *Arch Biochem Biophys*. 348:134-142.

Raju, R.V., T.N. Moyana, and R.K. Sharma. 1997b. N-Myristoyltransferase overexpression in human colorectal adenocarcinomas. *Exp Cell Res*. 235:145-154.

Raju, R.V., and R.K. Sharma. 1999. Preparation and assay of myristoyl-CoA:protein N-myristoyltransferase. *Methods Mol Biol*. 116:193-211.

Rasti, N., K.I. Falk, D. Donati, B.A. Gyan, B.Q. Goka, M. Troye-Blomberg, B.D. Akanmori, J.A. Kurtzhals, D. Dodoo, R. Consolini, A. Linde, M. Wahlgren, and M.T. Bejarano. 2005. Circulating epstein-barr virus in children living in malaria-endemic areas. *Scand J Immunol*. 61:461-465.

Resh, M.D. 1994. Myristylation and palmitylation of Src family members: the fats of the matter. *Cell*. 76:411-413.

Resh, M.D. 1996. Regulation of cellular signalling by fatty acid acylation and prenylation of signal transduction proteins. *Cell Signal*. 8:403-412.

Resh, M.D. 1999. Fatty acylation of proteins: new insights into membrane targeting of myristoylated and palmitoylated proteins. *Biochim Biophys Acta*. 1451:1-16.

Resh, M.D. 2006. Trafficking and signaling by fatty-acylated and prenylated proteins. *Nat Chem Biol*. 2:584-590.

Richter-Larrea, J.A., E.F. Robles, V. Fresquet, E. Beltran, A.J. Rullan, X. Agirre, M.J. Calasanz, C. Panizo, J.A. Richter, J.M. Hernandez, J. Roman-Gomez, F. Prosper, and J.A. Martinez-Climent. 2010. Reversion of epigenetically mediated BIM silencing overcomes chemoresistance in Burkitt lymphoma. *Blood*. 116:2531-2542.

Rioux, V., E. Beauchamp, F. Pedrono, S. Daval, D. Molle, D. Catheline, and P. Legrand. 2006. Identification and characterization of recombinant and native rat myristoyl-CoA: protein N-myristoyltransferases. *Mol Cell Biochem*. 286:161-170.

Rocks, O., A. Peyker, M. Kahms, P.J. Verveer, C. Koerner, M. Lumbierres, J. Kuhlmann, H. Waldmann, A. Wittinghofer, and P.I. Bastiaens. 2005. An acylation cycle regulates localization and activity of palmitoylated Ras isoforms. *Science*. 307:1746-1752.

Rocque, W.J., C.A. McWherter, D.C. Wood, and J.I. Gordon. 1993. A comparative analysis of the kinetic mechanism and peptide substrate specificity of human and Saccharomyces cerevisiae myristoyl-CoA:protein N-myristoyltransferase. *J Biol Chem*. 268:9964-9971.

Roskoski, R., Jr. 2003. Protein prenylation: a pivotal posttranslational process. *Biochem Biophys Res Commun*. 303:1-7.

Rostovtsev, V.V., L.G. Green, V.V. Fokin, and K.B. Sharpless. 2002. A stepwise huisgen cycloaddition process: copper(I)-catalyzed regioselective "ligation" of azides and terminal alkynes. *Angew Chem Int Ed Engl*. 41:2596-2599.

Rudel, T., and G.M. Bokoch. 1997. Membrane and morphological changes in apoptotic cells regulated by caspase-mediated activation of PAK2. *Science*. 276:1571-1574.

Rudnick, D.A., R.L. Johnson, and J.I. Gordon. 1992a. Studies of the catalytic activities and substrate specificities of Saccharomyces cerevisiae myristoyl-coenzyme A: protein N-myristoyltransferase deletion mutants and human/yeast Nmt chimeras in Escherichia coli and S. cerevisiae. *J Biol Chem*. 267:23852-23861.

Rudnick, D.A., T. Lu, E. Jackson-Machelski, J.C. Hernandez, Q. Li, G.W. Gokel, and J.I. Gordon. 1992b. Analogs of palmitoyl-CoA that are substrates for myristoyl-CoA:protein N-myristoyltransferase. *Proc Natl Acad Sci U S A*. 89:10507-10511.

Rudnick, D.A., C.A. McWherter, W.J. Rocque, P.J. Lennon, D.P. Getman, and J.I. Gordon. 1991. Kinetic and structural evidence for a sequential ordered Bi Bi mechanism of catalysis by Saccharomyces cerevisiae myristoyl-CoA:protein N-myristoyltransferase. *J Biol Chem*. 266:9732-9739.

Ryan, K.E., and C. Chiang. 2012. Hedgehog secretion and signal transduction in vertebrates. *J Biol Chem*. 287:17905-17913.

Saini, K.S., H.A. Azim, Jr., E. Cocorocchio, A. Vanazzi, M.L. Saini, P.R. Raviele, G. Pruneri, and F.A. Peccatori. 2011. Rituximab in Hodgkin lymphoma: is the target always a hit? *Cancer Treat Rev*. 37:385-390.

Sakurai, N., and T. Utsumi. 2006. Posttranslational N-myristoylation is required for the anti-apoptotic activity of human tGelsolin, the C-terminal caspase cleavage product of human gelsolin. *J Biol Chem*. 281:14288-14295.

Schey, K.L., D.B. Gutierrez, Z. Wang, J. Wei, and A.C. Grey. 2010. Novel fatty acid acylation of lens integral membrane protein aquaporin-0. *Biochemistry*. 49:9858-9865.

Seaton, K.E., and C.D. Smith. 2008. N-Myristoyltransferase isozymes exhibit differential specificity for human immunodeficiency virus type 1 Gag and Nef. *J Gen Virol*. 89:288-296.

Sehn, L.H., and J.M. Connors. 2005. Treatment of aggressive non-Hodgkin's lymphoma: a north American perspective. *Oncology (Williston Park)*. 19:26-34.

Selvakumar, P., A. Lakshmikuttyamma, A. Shrivastav, S.B. Das, J.R. Dimmock, and R.K. Sharma. 2007. Potential role of N-myristoyltransferase in cancer. *Prog Lipid Res*. 46:1-36.

Selvakumar, P., E. Smith-Windsor, K. Bonham, and R.K. Sharma. 2006. N-myristoyltransferase 2 expression in human colon cancer: cross-talk between the calpain and caspase system. *FEBS Lett*. 580:2021-2026.

Shawgo, M.E., S.N. Shelton, and J.D. Robertson. 2009. Caspase-9 activation by the apoptosome is not required for fas-mediated apoptosis in type II Jurkat cells. *J Biol Chem*. 284:33447-33455.

Sheng, C., H. Ji, Z. Miao, X. Che, J. Yao, W. Wang, G. Dong, W. Guo, J. Lu, and W. Zhang. 2009. Homology modeling and molecular dynamics simulation of N-myristoyltransferase from protozoan parasites: active site characterization and insights into rational inhibitor design. *J Comput Aided Mol Des*. 23:375-389.

Shrivastav, A., M.K. Pasha, P. Selvakumar, S. Gowda, D.J. Olson, A.R. Ross, J.R. Dimmock, and R.K. Sharma. 2003. Potent inhibitor of N-myristoylation: a novel molecular target for cancer. *Cancer Res*. 63:7975-7978.

Shrivastav, A., S. Varma, A. Senger, R.L. Khandelwal, S. Carlsen, and R.K. Sharma. 2009. Overexpression of Akt/PKB modulates N-myristoyltransferase activity in cancer cells. *J Pathol*. 218:391-398.

Sigal, C.T., W. Zhou, C.A. Buser, S. McLaughlin, and M.D. Resh. 1994. Amino-terminal basic residues of Src mediate membrane binding through electrostatic interaction with acidic phospholipids. *Proc Natl Acad Sci U S A*. 91:12253-12257.

Sikorski, J.A., B. Devadas, M.E. Zupec, S.K. Freeman, D.L. Brown, H.F. Lu, S. Nagarajan, P.P. Mehta, A.C. Wade, N.S. Kishore, M.L. Bryant, D.P. Getman, C.A. McWherter, and J.I. Gordon. 1997. Selective peptidic and peptidomimetic inhibitors of Candida albicans myristoylCoA: protein N-myristoyltransferase: a new approach to antifungal therapy. *Biopolymers*. 43:43-71.

Silverman, L., and M.D. Resh. 1992. Lysine residues form an integral component of a novel NH2-terminal membrane targeting motif for myristylated pp60v-src. *J Cell Biol*. 119:415-425.

Sjogren, A.K., K.M. Andersson, O. Khan, F.J. Olofsson, C. Karlsson, and M.O. Bergo. 2011. Inactivating GGTase-I reduces disease phenotypes in a mouse model of K-RAS-induced myeloproliferative disease. *Leukemia*. 25:186-189.

Smotrys, J.E., and M.E. Linder. 2004. Palmitoylation of intracellular signaling proteins: regulation and function. *Annu Rev Biochem*. 73:559-587.

Solary, E., B. Eymin, N. Droin, and M. Haugg. 1998. Proteases, proteolysis, and apoptosis. *Cell Biol Toxicol*. 14:121-132.

Sperandio, S., I. de Belle, and D.E. Bredesen. 2000. An alternative, nonapoptotic form of programmed cell death. *Proc Natl Acad Sci U S A*. 97:14376-14381.

Stevenson, F.T., S.L. Bursten, C. Fanton, R.M. Locksley, and D.H. Lovett. 1993. The 31-kDa precursor of interleukin 1 alpha is myristoylated on specific lysines within the 16-kDa N-terminal propiece. *Proc Natl Acad Sci U S A*. 90:7245-7249.

Stevenson, F.T., S.L. Bursten, R.M. Locksley, and D.H. Lovett. 1992. Myristyl acylation of the tumor necrosis factor alpha precursor on specific lysine residues. *J Exp Med*. 176:1053-1062.

Sugii, M., R. Okada, H. Matsuno, and S. Miyano. 2007. Performance improvement in protein N-myristoyl classification by BONSAI with insignificant indexing symbol. *Genome Inform*. 18:277-286.

Suzuki, T., K. Moriya, K. Nagatoshi, Y. Ota, T. Ezure, E. Ando, S. Tsunasawa, and T. Utsumi. 2010. Strategy for comprehensive identification of human N-myristoylated proteins using an insect cell-free protein synthesis system. *Proteomics*. 10:1780-1793.

Takada, R., Y. Satomi, T. Kurata, N. Ueno, S. Norioka, H. Kondoh, T. Takao, and S. Takada. 2006. Monounsaturated fatty acid modification of Wnt protein: its role in Wnt secretion. *Dev Cell*. 11:791-801.

Takamune, N., T. Kuroe, N. Tanada, S. Shoji, and S. Misumi. 2010. Suppression of human immunodeficiency virus type-1 production by coexpression of catalytic-region-deleted N-myristoyltransferase mutants. *Biol Pharm Bull*. 33:2018-2023.

Tate, E.W., A.S. Bell, M.D. Rackham, and M.H. Wright. 2013. N-Myristoyltransferase as a potential drug target in malaria and leishmaniasis. *Parasitology*:1-13.

Tomatis, V.M., A. Trenchi, G.A. Gomez, and J.L. Daniotti. 2010. Acyl-protein thioesterase 2 catalyzes the deacylation of peripheral membrane-associated GAP-43. *PLoS One*. 5:e15045.

Toska, E., H.A. Campbell, J. Shandilya, S.J. Goodfellow, P. Shore, K.F. Medler, and S.G. Roberts. 2012. Repression of transcription by WT1-BASP1 requires the myristoylation of BASP1 and the PIP2-dependent recruitment of histone deacetylase. *Cell Rep*. 2:462-469.

Towler, D., and L. Glaser. 1986. Protein fatty acid acylation: enzymatic synthesis of an N-myristoylglycyl peptide. *Proc Natl Acad Sci U S A*. 83:2812-2816.

Towler, D.A., S.P. Adams, S.R. Eubanks, D.S. Towery, E. Jackson-Machelski, L. Glaser, and J.I. Gordon. 1987a. Purification and

characterization of yeast myristoyl CoA:protein N-myristoyltransferase. *Proc Natl Acad Sci U S A*. 84:2708-2712.

Towler, D.A., S.R. Eubanks, D.S. Towery, S.P. Adams, and L. Glaser. 1987b. Amino-terminal processing of proteins by N-myristoylation. Substrate specificity of N-myristoyl transferase. *J Biol Chem*. 262:1030-1036.

Traverso, J.A., C. Giglione, and T. Meinnel. 2013. High-throughput profiling of N-myristoylation substrate specificity across species including pathogens. *Proteomics*. 13:25-36.

Tsai, Y.H., X. Liu, and P.H. Seeberger. 2012. Chemical biology of glycosylphosphatidylinositol anchors. *Angew Chem Int Ed Engl*. 51:11438-11456.

Turnay, J., E. Lecona, S. Fernandez-Lizarbe, A. Guzman-Aranguez, M.P. Fernandez, N. Olmo, and M.A. Lizarbe. 2005. Structure-function relationship in annexin A13, the founder member of the vertebrate family of annexins. *Biochem J*. 389:899-911.

Uno, F., J. Sasaki, M. Nishizaki, G. Carboni, K. Xu, E.N. Atkinson, M. Kondo, J.D. Minna, J.A. Roth, and L. Ji. 2004. Myristoylation of the fus1 protein is required for tumor suppression in human lung cancer cells. *Cancer Res*. 64:2969-2976.

Utsumi, T., K. Nakano, T. Funakoshi, Y. Kayano, S. Nakao, N. Sakurai, H. Iwata, and R. Ishisaka. 2004. Vertical-scanning mutagenesis of amino acids in a model N-myristoylation motif reveals the major amino-terminal sequence requirements for protein N-myristoylation. *Eur J Biochem*. 271:863-874.

Utsumi, T., N. Sakurai, K. Nakano, and R. Ishisaka. 2003. C-terminal 15 kDa fragment of cytoskeletal actin is posttranslationally N-myristoylated upon caspase-mediated cleavage and targeted to mitochondria. *FEBS Lett*. 539:37-44.

van den Bosch, C.A. 2004. Is endemic Burkitt's lymphoma an alliance between three infections and a tumour promoter? *Lancet Oncol*. 5:738-746.

Vilas, G.L., M.M. Corvi, G.J. Plummer, A.M. Seime, G.R. Lambkin, and L.G. Berthiaume. 2006. Posttranslational myristoylation of caspase-activated p21-activated protein kinase 2 (PAK2) potentiates late apoptotic events. *Proc Natl Acad Sci U S A*. 103:6542-6547.

Walsh, J.G., S.P. Cullen, C. Sheridan, A.U. Luthi, C. Gerner, and S.J. Martin. 2008. Executioner caspase-3 and caspase-7 are

functionally distinct proteases. *Proc Natl Acad Sci U S A*. 105:12815-12819.

Wang, Q., T.R. Chan, R. Hilgraf, V.V. Fokin, K.B. Sharpless, and M.G. Finn. 2003. Bioconjugation by copper(I)-catalyzed azide-alkyne [3 + 2] cycloaddition. *J Am Chem Soc*. 125:3192-3193.

Webb, Y., L. Hermida-Matsumoto, and M.D. Resh. 2000. Inhibition of protein palmitoylation, raft localization, and T cell signaling by 2-bromopalmitate and polyunsaturated fatty acids. *J Biol Chem*. 275:261-270.

Weinberg, R.A., C.A. McWherter, S.K. Freeman, D.C. Wood, J.I. Gordon, and S.C. Lee. 1995. Genetic studies reveal that myristoylCoA:protein N-myristoyltransferase is an essential enzyme in Candida albicans. *Mol Microbiol*. 16:241-250.

Weston, S.A., R. Camble, J. Colls, G. Rosenbrock, I. Taylor, M. Egerton, A.D. Tucker, A. Tunnicliffe, A. Mistry, F. Mancia, E. de la Fortelle, J. Irwin, G. Bricogne, and R.A. Pauptit. 1998. Crystal structure of the anti-fungal target N-myristoyl transferase. *Nat Struct Biol*. 5:213-221.

Wilcox, C., J.S. Hu, and E.N. Olson. 1987. Acylation of proteins with myristic acid occurs cotranslationally. *Science*. 238:1275-1278.

Wright, M.H., W.P. Heal, D.J. Mann, and E.W. Tate. 2010. Protein myristoylation in health and disease. *J Chem Biol*. 3:19-35.

Wu, J., Y. Tao, M. Zhang, M.H. Howard, S. Gutteridge, and J. Ding. 2007. Crystal structures of Saccharomyces cerevisiae N-myristoyltransferase with bound myristoyl-CoA and inhibitors reveal the functional roles of the N-terminal region. *J Biol Chem*. 282:22185-22194.

Wu, W., P. Liu, and J. Li. 2012. Necroptosis: an emerging form of programmed cell death. *Crit Rev Oncol Hematol*. 82:249-258.

Yang, J., M.S. Brown, G. Liang, N.V. Grishin, and J.L. Goldstein. 2008. Identification of the acyltransferase that octanoylates ghrelin, an appetite-stimulating peptide hormone. *Cell*. 132:387-396.

Yang, S.H., A. Shrivastav, C. Kosinski, R.K. Sharma, M.H. Chen, L.G. Berthiaume, L.L. Peters, P.T. Chuang, S.G. Young, and M.O. Bergo. 2005. N-myristoyltransferase 1 is essential in early mouse development. *J Biol Chem*. 280:18990-18995.

Yap, M.C., M.A. Kostiuk, D.D. Martin, M.A. Perinpanayagam, P.G. Hak, A. Siddam, J.R. Majjigapu, G. Rajaiah, B.O. Keller, J.A. Prescher, P. Wu, C.R. Bertozzi, J.R. Falck, and L.G. Berthiaume. 2010. Rapid and selective detection of fatty acylated proteins using omega-alkynyl-fatty acids and click chemistry. *J Lipid Res*. 51:1566-1580.

Youle, R.J., and A. Strasser. 2008. The BCL-2 protein family: opposing activities that mediate cell death. *Nat Rev Mol Cell Biol*. 9:47-59.

Yustein, J.T., and C.V. Dang. 2007. Biology and treatment of Burkitt's lymphoma. *Curr Opin Hematol*. 14:375-381.

Zha, J., S. Weiler, K.J. Oh, M.C. Wei, and S.J. Korsmeyer. 2000. Posttranslational N-myristoylation of BID as a molecular switch for targeting mitochondria and apoptosis. *Science*. 290:1761-1765.

Zhang, F.L., and P.J. Casey. 1996. Protein prenylation: molecular mechanisms and functional consequences. *Annu Rev Biochem*. 65:241-269.

Zhao, Y., J.B. McCabe, J. Vance, and L.G. Berthiaume. 2000. Palmitoylation of apolipoprotein B is required for proper intracellular sorting and transport of cholesteroyl esters and triglycerides. *Mol Biol Cell*. 11:721-734.

Zverina, E.A., C.L. Lamphear, E.N. Wright, and C.A. Fierke. 2012. Recent advances in protein prenyltransferases: substrate identification, regulation, and disease interventions. *Curr Opin Chem Biol*. 16:544-552.